The Role of Tissue Kallikrein in *Helicobacter pylori*-associated Gastric Disease

by

Strinivasen Naidoo

Submitted in partial fulfilment of
the requirements for the degree of

Master of Technology

in the
Department of Biological Sciences
M.L. Sultan Technikon
Durban
South Africa
1999

ABSTRACT

Today, the number one income-generating drugs are remedies prescribed for gastric disorders, in particular dyspepsia. These clinical conditions have a multi-faceted aetiology and pathology of dysfunction. One likely causal factor is the entero-pathogen *Helicobacter pylori.* It has been shown to be more than just a commensal related to gastric diseases like dyspepsia (80-90% incidence) and duodenal ulcer sufferers (100% incidence), with a total estimated world-wide population infection of 50%. The current therapy offered to dyspepsia sufferers is a triple regimen of an anti-bacterial, an H^+ proton-pump inhibitor, and bismuth colloidal salts.

There has been a clear need for the elucidation of the inflammatory events associated with the initiation, maintenance, and healing of gastric diseases. This study was proposed to examine the role of the inflammatory regulators, tissue kallikrein and the vaso-active kinins in the cellular pathology of gastric disorders and disease. In particular, the aim was to examine whether *Helicobacter pylori* regulated the turnover of tissue kallikrein in the patho-biology of kinin-induced gastric inflammation.

As a first step, the proposed hypothesis of the cellular localisation and the gastric secretion of tissue kallikrein, was tested in experiments involving gastric biopsy tissue and lavage aspirates obtained from patients with dyspepsia (n = 23). The tissue biopsies from the antrum and body of the stomach were histologically classified into four broad groups ranging from non-*Helicobacter pylori*-infected and non-inflamed (group 1), to atrophy and metaplasia with very mild infection (group 4). The gastric tissue was subjected to (1) localisation of tissue kallikrein by immuno-precipitation and immuno-fluorescence and (2) extraction and measurement of tissue kallikrein amidase activity. Tissue kallikrein determination by ELISA and amidase assay was also performed on the lavage fluid.

An insight into the physiological role of tissue kallikrein and released kinins was sought by immuno-localisation of tissue kallikrein in specific cells and their cellular orientation in gastric mucosa, and it was found that increased inflammation coincided with increased *helicobacter* presence, which corresponded to increased kallikrein, and when quantified by digital image analysis, was primarily confined to the parietal cells in both antral and body

mucosal regions. It is of major significance that kallikrein was excreted almost exclusively from the acid-producing cells of the stomach. The quantification of immuno-reactive kallikrein by ELISA showed increased presence in the inflammation-associated lavage fluid, while the functional enzymic capacity of the lavage kallikrein depicted a similar profile. Results also showed gastric tissue depletion of kallikrein with increasing severity of disease. Atrophy signalled a drop in kallikrein levels and disappearance of the bacterium. The synthesis and storage of kallikrein was reduced to baseline levels when chronicity of the disease evolved into metaplasia. In the regenerating cells of the superficial mucosal regions induction of tissue kallikrein synthesis was observed.

This study demonstrates that tissue kallikrein levels are enhanced in a linear manner with increasing colonisation of the gastric mucosa by *Helicobacter pylori.* These results also draws attention as to whether tissue kallikrein simulates a gastro-protective role in the absence of bacterial infection and the ensuing inflammation. Is this a mutational role inherited by *Helicobacter pylori* to increase the acidity of the gastric juice, or is the response that of the tissue to create an adverse environment against *Helicobacter pylori*? Another issue highlighted is whether Hp bacterial infection is an initiator of inflammation, co-regulator or independent factor in gastritis.

It would be premature to singularly propose an effective, conclusive remedy for *Helicobacter pylori*-induced gastritis, but the need for a kinin antagonist definitely exists within the realm of successful, single application type multi-therapy.

PREFACE

The experiments in this thesis were conducted under the direct supervision of Professor K.D. Bhoola, in the Department of Clinical and Experimental Pharmacology, University of Natal Medical School, Durban, during the period of January 1996 to December 1998. No work represented in this dissertation has been submitted to any other tertiary institution, either in part or full. The opinions and views expressed in this dissertation are those of the author, and do not necessarily reflect those of the M.L. Sultan Technikon.

S. Naidoo

ACKNOWLEDGEMENTS

The author wishes to express his sincere gratitude to the following individuals for their assistance in the preparation of this dissertation:

Professor K.D. Bhoola, supervisor, Research Professor, Department of Clinical and Experimental Pharmacology, University of Natal Medical School, for his expert guidance and constructive criticism.

Dr. B. Odhav, supervisor, Department of Biological Sciences, M.L. Sultan Technikon for her help and encouragment during the preparation of this work.

Dr. R.L. Bhoola, Specialist Physician, City Hospital, for the collection of the patient samples.

Dr. R. Ramsaroop, Pathologist, University of Natal Medical School, for her excellent histological examination of the patient sample tissue, and her suggestions.

Mrs C. Snyman, for her technical expertise in use of the confocal microscope and her preparation of the fluorescent image analysis results.

Mrs A. Naicker, Imaging and Optics Unit, University of Natal Medical School, for her expert use of the digital imaging and analysis system.

Mr S. Khedun, Department of Clinical and Experimental Pharmacology, University of Natal Medical School, for his helpful advice and the preparation of the statistical data of results.

The nursing staff, Outpatients Department, City hospital, for their help in the collection of the patient samples.

The Kinin Research Team , Department of Clinical and Experimental Pharmacology, University of Natal Medical School, for their invaluable scientific input.

DEDICATION

I dedicate this work to my family, who have always encouraged me to better myself. I thank my support system - my wife Anita, for her belief in me, and the conviction that success is always attainable, regardless of how daunting the prospect may initially appear to be.

PUBLICATIONS AND PRESENTATIONS

Naidoo, S., Ramsaroop, R., Bhoola, R. and Bhoola, K.D. 1997. The evaluation of tissue kallikrein in *Helicobacter pylori*-associated gastric ulcer disease. Immunopharmacology **36**: 263-269.

Bhoola, R., Ramsaroop, R., Naidoo, S., Müller-Esterl, W. and Bhoola, K.D. 1997. Kinin receptor status in normal and inflamed gastric mucosa. Immunopharmacology. **36**: 161-165.

Naidoo, S., Ramsaroop, R., Bhoola, R. and Bhoola, K.D. 1999. Correlation of kinin-generating activity of tissue kallikrein to *Helicobacter pylori*-associated gastric infection. Immunopharmacology. *in press.*

TABLE OF CONTENTS

page

LIST OF FIGURES

CHAPTER 1

LIST OF TABLES

CHAPTER 1

CHAPTER 2

CHAPTER 2

CHAPTER 4

CHAPTER 3

LIST OF PLATES

CHAPTER 1

CHAPTER 3

ABBREVIATIONS

NS	normal saline
RT	room temperature
Hp	*Helicobacter pylori*
rTK	recombinant tissue kallikrein
PBS	phosphate buffered saline
ICC	immunocytochemistry
HUK	human urinary kallikrein
PAP	peroxidase anti-peroxidase
EDTA	ethylenediaminetetraacetic acid
mg	milligrams
ng	nanograms
ug	micrograms
um	micromoles
FITC	fluoresceinisothiocyanate
EtoH	ethanol
MeOH	methanol
H_2O_2	hydrogen peroxide
NaCl	sodium chloride
ATPase	adenosine triphosphatase
v/v	volume per volume
M	molar
BSA	bovine serum albumin
kD	kilodalton
bp	basepair
SBTI	soya bean trypsin inhibitor
IgG	immunoglobulin G
H&E	haemotoxylin and eosin
dH_2O	distilled water
xg	times the force of gravity
NSAID	non-steroidal anti-inflammatory drug

E. coli	*Eschericia coli*
CagA	cytotoxin-associated gene A
VacA	vacuolating associated gene A
TNF-α	tumour necrosis factor alpha
IL	interleukin
INF-γ	interferron gamma
ROM	reactive oxygen metabolite
PGE_2	prostaglandin E_2
MALT	mucosal-associated lymphoid tissue

CHAPTER 1

INTRODUCTION

INTRODUCTION

This study was designed to investigate components of an inflammatory system within a specific morphological area, the human stomach. In order to elucidate the pathophysiology of gastric inflammatory disease, the physiology of the stomach has to be understood, in addition to a detailed knowledge of the inflammatory process. To this end, the first part of chapter 1 illustrates the physiology, form and function of the human stomach, which is then expanded to encompass gastric diseases, while the latter part of this chapter deals with the kallikrein-kinin system. This system is strongly implicated in initial inflammatory responses associated with disease processes.

1.1 The Gastrointestinal Tract

The digestive tube is an elongated muscular body extending from the oesophagus to the lower intestinal tract. It consists of four distinct layers, namely, the mucosa, the submucosa, the muscularis and the serosa (adventitia). The distinct nature and thickness of these layers, alluding to particular functional requirements, are specific to each region. In general, the stomach serves three principle purposes (1) a reservoir for food until it can be passaged into the duodenum, (2) maceration and partial digestion of this food, and (3) emptying into the small intestine at a rate suitable for proper digestion by the intestine (Guyton 1992).

1.1.1 Physiology of the Stomach

To understand mechanics of the stomach, this histologically complex organ has to be eviscerated along the lines of the mechanisms of its functions. The stomach can be characterised by histologically distinct areas (refer to figure 1). The entrance to the stomach is turnstiled by the gastroesophageal or cardiac sphincter, whereas the pyloric sphincter is found in operation at the junction between the stomach and the beginning of the small intestine. The cardia extends from the lower end of the oesophagus for a variable distance into upper stomach. The bulk area of the stomach is the body, and the pylorus covers an area approximately halfway down the lesser curvature (the size of the pylorus is gender-associated). The digestive juices of the stomach are secreted by the gastric glands that cover almost the entire wall of the body (figure 2). These glands open up onto the luminal surface as pits or foveolae. The gastric mucosae housing these glands can be zoned into three regions, namely, the superficial zone consisting of surface mucous cells/goblet cells (mucous contained in small vacuoles) with invaginous downgrowths (pits, foveolae, crypts), the neck zone composed mostly of immature stem cells and some neck mucous cells, and the deep zone composed almost entirely of glands.

The gastric epithelium secretes dilute (approximately 0.16N) hydrochloric acid, digestive enzymes like pepsin, renin, gastric lipase and mucus (mainly in the form of neutral mucins). Glandular exudates are produced by the oxyntic/gastric glands (found in abundance in the body area), which secrete hydrochloric acid, pepsinogen (pepsin precursor), intrinsic factor (glycoprotein that metabolises vitamin B_{12} by binding to it and making it absorbable), and mucus; and the pyloric glands (located in the antral stomach region) that secrete gastrin, some pepsin, but mainly mucous (Guyton 1992).

1.1.1.1 Parietal cells

These are the acid-producing cells that are scattered throughout the gastric mucosae. They are characteristically large pyramidal cells, located in the glands such that their bases extrude into the lamina propria. They have vast microvilli-lined invaginations called canaliculi that extend extensively throughout the cell (Plates 1a and 1b). These acid-producing cells possess abundant carbonic anhydrase, which is thought to be the source of H^+ for hydrochloric acid. CO_2 diffuses across the blood capillary-basement membrane junction and carbonic anhydrase catalyses the production of carbonic acid from the reaction of water and carbon dioxide (Figure 3). The H^+ ions are transported into the lumen of the canaliculi. Chloride ions (react with H^+) may also be transported into the canaliculi from the lamina propria capillaries (Stevens and Lowe 1997).

1.1.1.2 Chief / Oxyntic (Zymogenic) cells

These cells are situated in the lower parts of the fundic glands and span the mucosa from the basal lamina to the lumen (Leeson and Leeson 1981). They resemble the exocrine cells of the pancreas and salivary gland, in that they are pyramidal, have large basal nuclei, contain eosinophilic refractile cytoplasmic granules and have rich rough endoplasmic reticuli (Plate 2). The low electron-dense cytoplasmic granules contain the inactive precursor of pepsin, pepsinogen, which, when exocytosed into the gastric lumen, is activated to pepsin by gastric acid.

Figure 1: Diagrammatical sketch of the human stomach, showing the various anatomical regions and delineations

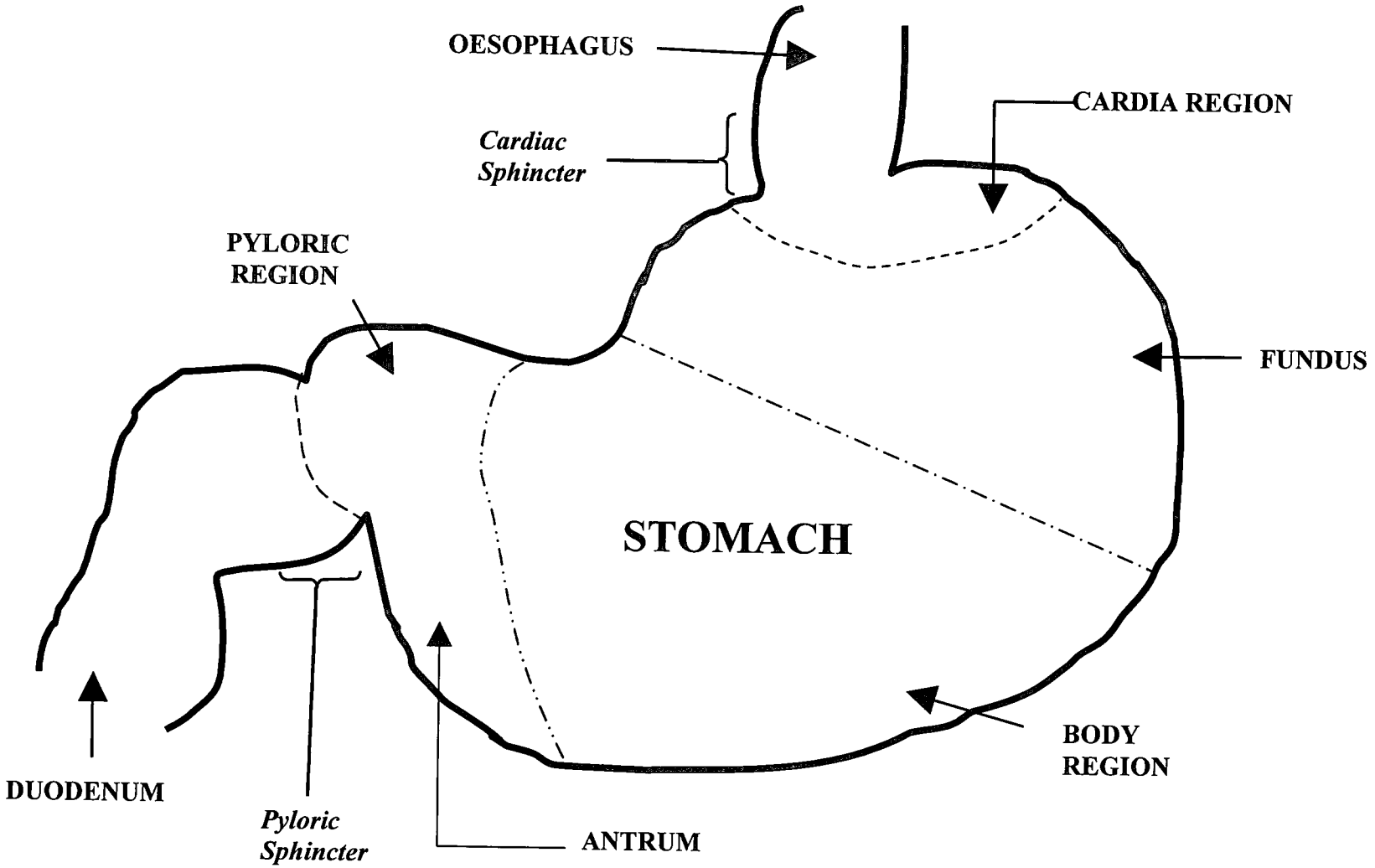
OESOPHAGUS
CARDIA REGION
Cardiac Sphincter
PYLORIC REGION
FUNDUS
STOMACH
DUODENUM
Pyloric Sphincter
ANTRUM
BODY REGION

Plate 1a: Photo-micrograph of an electron microscopy image of a gastric parietal cell showing the mitocondria (M) of the cell, and the micro-vesicles (MV) containing highly fragmented gastric acid (HCl) entering the lumen of the gastric glands.

Plate 1b: This photomicrograph of an electron microscopy image shows the canaliculi (C) tubular connective system, the nucleus (N), and the mitocondria of the gastric parietal cell.

Figure 2: Electron microscopy photo-micrograph of a gastric chief / oxyntic cell showing zymogen granules (ZG) containing the precursor pepsinogen, which when released into the lumen is activated to the protease pepsin; the mitocondria (M) and the nucleus (N).

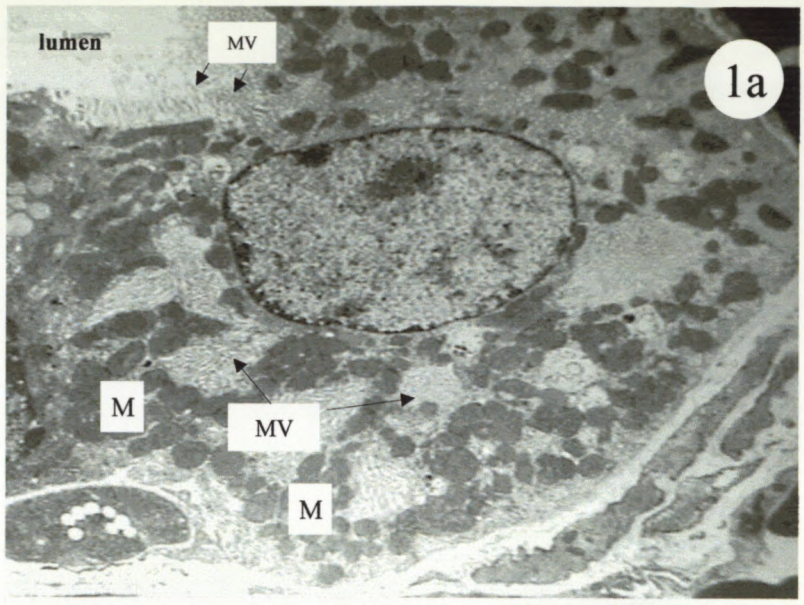
lumen
MV
1a
M
MV
M

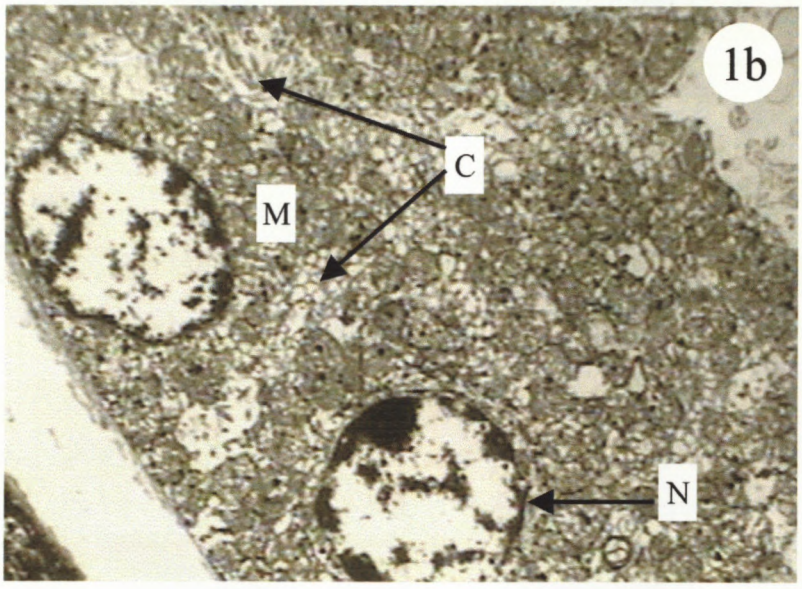
1b
C
M
N

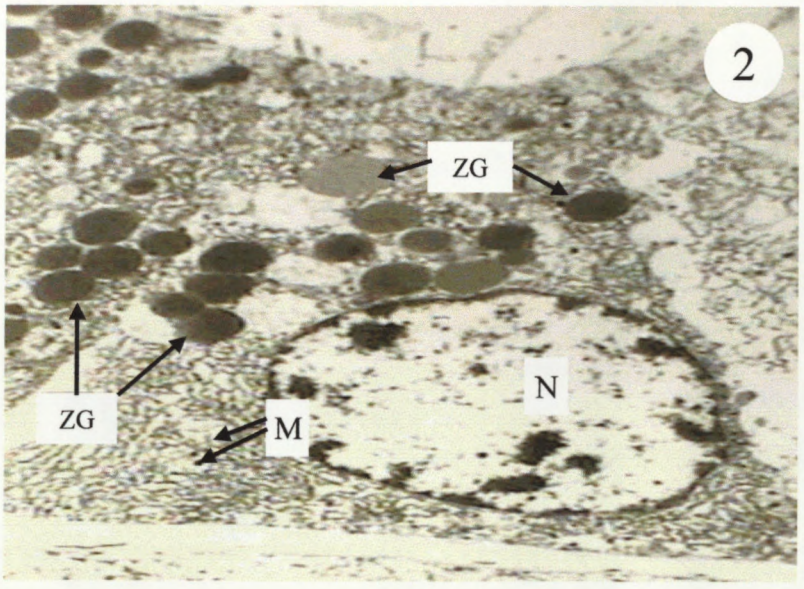
2
ZG
N
ZG
M

Figure 2: Diagram depicting the body (A) and the antral (B) mucosal regions of the human stomach together with the various populations of the glandular cells.

A . BODY

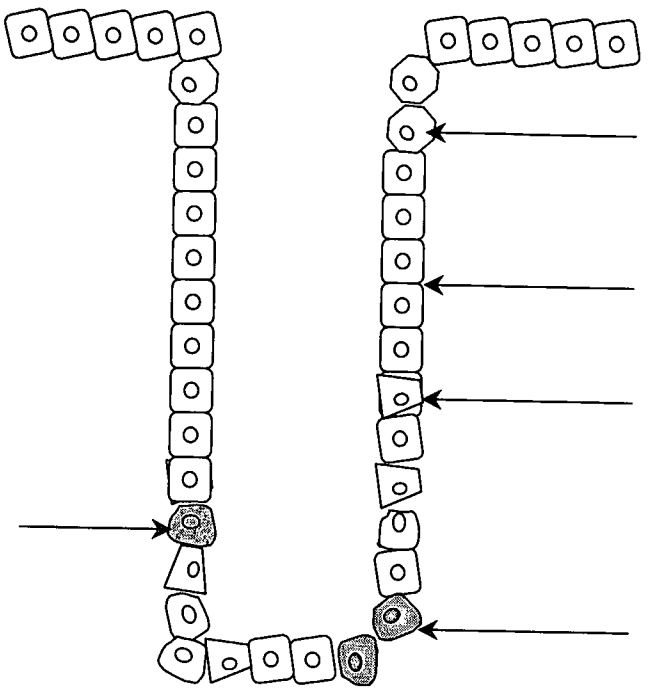

B . ANTRUM

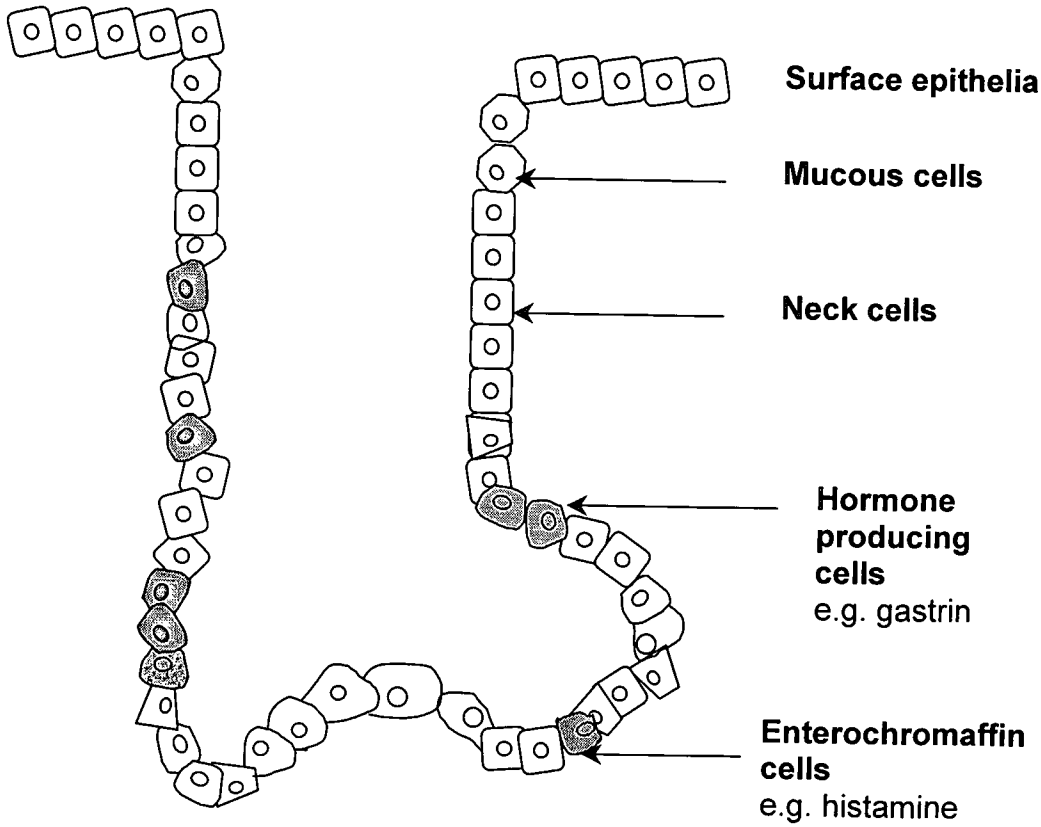

1.1.1.3 Endocrine cells

These cells are also known as *enterochromaffin* cells, and are usually small, round, epithelially based mucosal cells. They contain membrane-bound neurosecretory granules in their cytoplasm. They store and secrete histamine, serotonin, somatostatin, and vasoactive intestinal polypeptide (VIP) in the cardia, body and antrum. Gastrin- and bombesin-secreting endocrine cells are mainly concentrated in the neck regions of the pyloric mucosa

1.1.1.4 The Gastrin-Somatostatin Feedback System

Gastric acid secretion is regulated in the periphery by the interplay between three major endocrine cell types: the enterochromaffin-like (ECL) cell, the gastrin-secreting G cell, and the somatostatin-secreting D cell (Sachs et al 1997). Gastric acid regulation is dependant upon neural, endocrine and paracrine events that either upregulate or downregulate acid secretion by the parietal cell. During normal physiological events, gastrins are the major stimulants of acid secretion in the stomach. Upon secretion of gastrin, usually induced by a meal, the enzyme circulates through the blood and acts on parietal cells located in the upper portion of the body of the stomach to secrete acid (see Figure 4). Stomach acid thereafter flows to the antrum, and stimulates D cells to secrete somatostatin. The D cells are in close juxtaposition to the G cells, and the somatostatin secreted has an inhibitory action on the G cells. Upregulation of ECL cells is regulated by the activation of cholecystokinin (CCK) β receptors by gastrin. The histamine released from ECL cells binds to H2 receptors on the parietal cells, and stimulates acid secretion (Sawada and Dickinson, 1997). Somatostatin inhibits ECL cell-

signalling pathways, while stimulation of ECL cells opens chloride and calcium ion channels, which allow for the formation of HCl by the 'gastric acid ATPase pump'. The functional integration of these three cell types creates a highly sensitive negative feedback system for gastric acid secretion

1.2.1 Pathophysiology of gastric diseases

1.2.1.1 Gastritis

Gastritis can be simply defined as inflammation of the stomach occurring either as an acute or chronic disorder. The criteria for defining these pathologies are subjective, and often under controversy because of a lack of precision in the diagnosis.

1.2.1.2 Acute or haemorrhagic or erosive gastritis

Acute or haemorrhagic or erosive gastritis comprises focal necrosis of the mucosa in an otherwise normal stomach (Farber 1995). Necrosis is accompanied by inflammation usually of a transient nature, and the mucosal erosion (sloughing-off of the superficial mucosal epithelium) may extend into the deeper tissues to form ulcers and acute haemorrhagia. Depending on the severity of the injury, the mucosal response varies from vasodilatation and oedema of the lamina propria, to erosion and gastrointestinal bleeding. Erosion is characterised by the partial loss of the mucosa, whereas an ulcer is loss of the full thickness (Underwood 1996). The pathogenesis of erosive gastritis, although not yet clearly understood, has

been attributed to a number of possible aetiologies, notably, the heavy use of aspirin and other non-steroidal anti-inflammatory drugs (NSAID's), excessive alcohol consumption, cigarette smoking, treatment with chemotherapeutic drugs, systemic infections, ischaemia and shock, gastric irradiation, mechanical trauma, reflux of bilious material following distal gastrectomy, and severe stress (Kumar et al. 1997). Fortunately most lesions are transient, and often regeneration after 24 to 48 hours allows the erosion to heal and disappear.

1.2.1.3 Non-erosive gastritis

Non-erosive gastritis refers to chronic inflammatory conditions of the stomach ranging from a mild superficial status to severe atrophy of the mucosa and epithelial metaplasia. Chronic gastritis is noted for the distinct causal subgroups in the stomach (e.g., antrum and body).

1.2.1.4 Histological differentiation, and clinical features

The uncommon, *type A*, or *autoimmune gastritis*, or *diffuse corporal atrophic gastritis* is referred to a chronic, diffuse inflammatory disease of the body and fundus, which is often associated with pernicious anaemia (Farber 1995). Pernicious anaemia refers to a deficiency of intrinsic factor that results from the malabsorption of vitamin B_{12} due to gland destruction and mucosal atrophy. This condition is characterised by the presence of auto-antibodies directed against the gastric gland parietal cell components and intrinsic

Figure 3: Diagram showing the gastric parietal cell and the mechanism of gastric acid production from blood, and the cellular process and finally into the gastric lumen by exocytosis. The different components of the system shown are HCl (hydrochloric acid, highly fragmented), Cl^- (chloride ions), H^+ (hydronium ions), K^+ (potassium ions), CO_2 (carbon dioxide), HCO_3^+ (bicarbonate ions), and H_2O (water molecules).

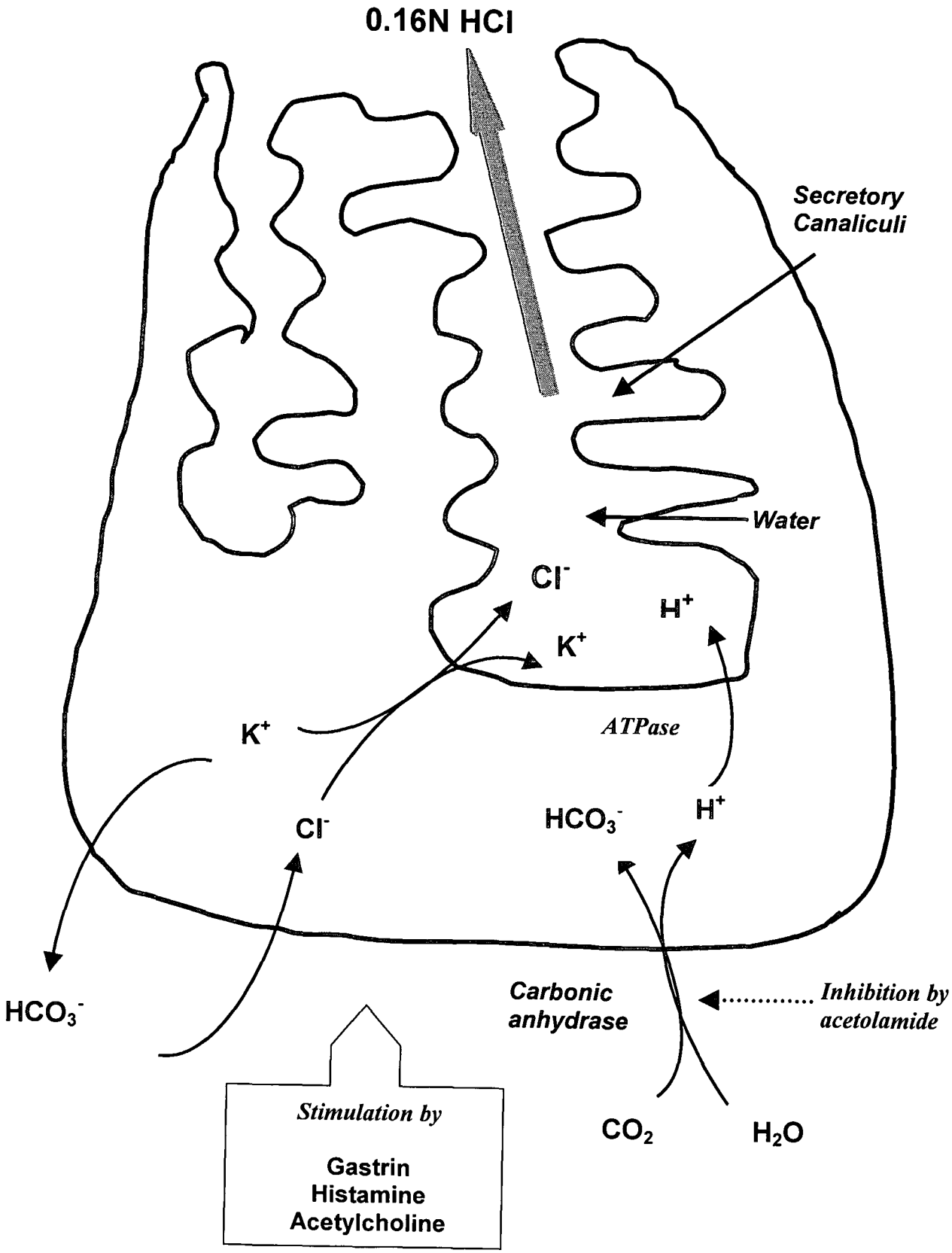
0.16N HCl
Secretory Canaliculi
Water
Cl⁻
H⁺
K⁺
K⁺
ATPase
Cl⁻
HCO₃⁻
H⁺
HCO₃⁻
Carbonic anhydrase
..... Inhibition by acetolamide
Stimulation by
Gastrin
Histamine
Acetylcholine
CO₂
H₂O

Figure 4: Diagram depicting the gastrin-somatostatin feedback mechanism of acid production in the human stomach highlighting the peripheral interplay between the gastrin G cells and the somatostatin D cells. Gastrin, induced hormonally or by a meal stimulus, circulates through the blood and acts on parietal cells located in the upper portion of the body of the stomach to secrete acid. Stomach acid thereafter flows to the antrum and stimulates D cells to secrete somatostatin. The D cells lie close to the G cells, and the somatostatin secreted has an inhibitory action on the G cells

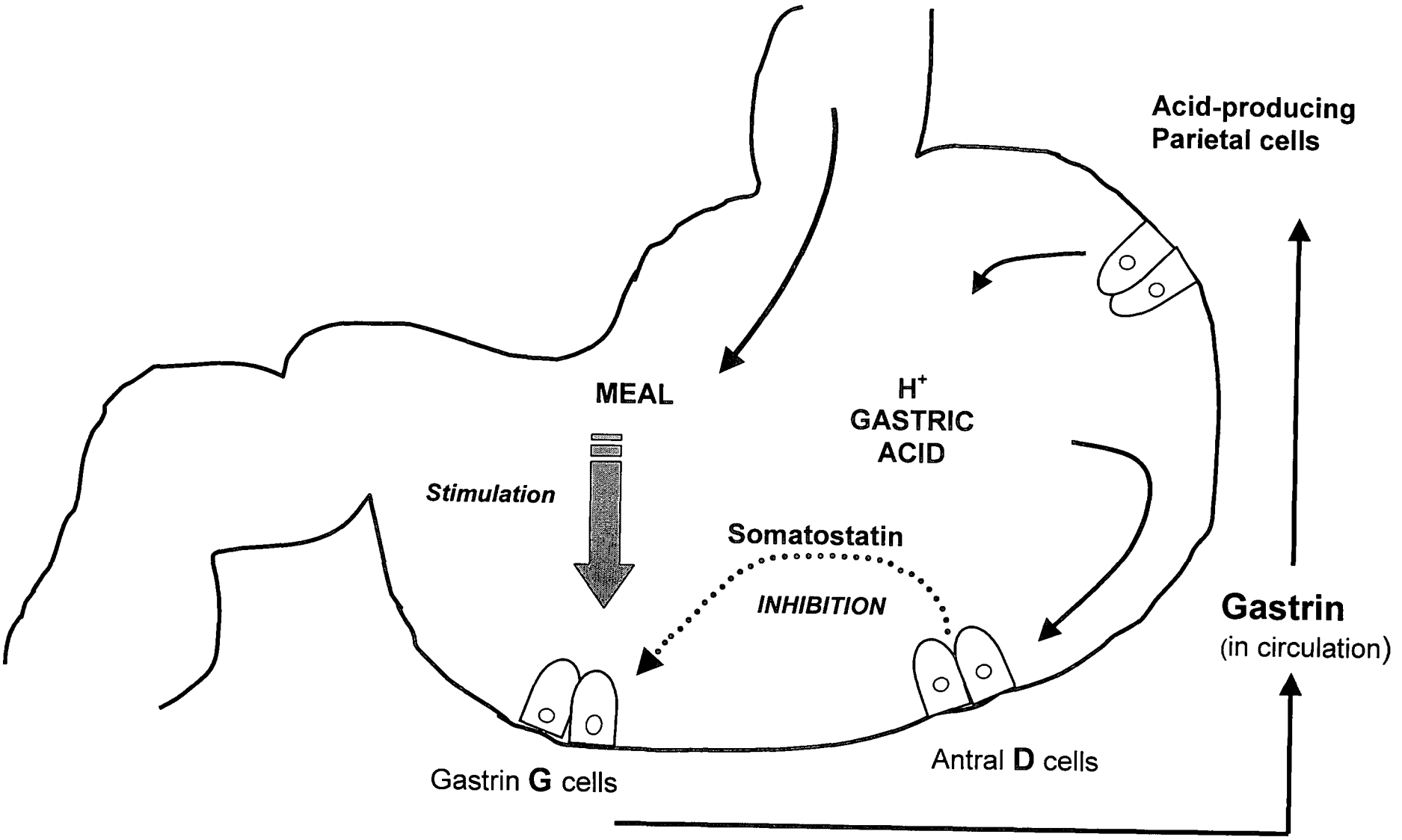
Acid-producing
Parietal cells
MEAL
H+
GASTRIC
ACID
Stimulation
Somatostatin
INHIBITION
Gastrin
(in circulation)
Gastrin G cells
Antral D cells

factor. Most cases of chronic gastritis are unrelated to autoimmunity (Cotran et al. 1994).

Type B, or *chronic idiopathic gastritis*, or *chronic gastritis,* is by definition of varied aetiology. It typically involves the antrum and adjacent areas of the body (Farber 1995). This disease is typified by distinct features. Regardless of the histological distribution, the inflammatory changes consist of a lymphocytic and plasma cell infiltrate in the lamina propria, occasioned by the presence of neutrophilic attack in the neck region of the mucosal pits. Inflammation may be accompanied by the loss of glandular features and atrophy. Chronic gastritis is not associated with autoimmune disease mechanisms, but it does result in hypochlorhydria (reduced acid production). The complete absence of gastric acid secretion and pernicious anaemia are rare. Type B gastritis is more common than Type A, and is perhaps four times more frequent in Caucasians than in other race groups. In fact, it has been reported that chronic idiopathic gastritis is prevalent in over 50% of the western population (based on histological indicators) (Kumar et al. 1997).

This type of stomach disorder is age and geographically parallel to that of gastric carcinoma, and is believed to be a precursor of such cancers. In asymptomatic Japanese men and women older than 60 years of age, there has been a 90% incidence reported. About half the populations of Finland, Italy and Hungary have been reported to show evidence of chronic gastritis.

It is now generally accepted that bacterial infection appears to be one of the major cause of chronic gastritis for which *Helicobacter pylori* (Hp) has been implicated (Hanson et al. 1993; Miller et al. 1991; Peek and Blaser 1996). The role of this pathogen in gastric diseases is discussed in detail in section 1.3. The pathological and histological indicators of chronic gastritis, with respect to grading, are discussed in detail in chapter 3 of this dissertation.

Intestinal metaplasia refers to the replacement of gastric epithelia with metaplasic columnar absorptive cells and mucous goblet cells of intestinal phenotype (usually small intestine). The mucosa of the fundus and the body may also exhibit the simpler glandular structures typical of the antral-pyloric junction regions.

There also exists other minor forms of gastritis, namely, *lymphotic gastritis* which features the presence of large amounts of mature lymphocytes within the epithelium and whose proliferation and link to Hp is uncertain; *eosinophilic gastritis* which is thought to be a dietary antigen allergenic inflammatory response, characterised by the presence of eosinophils in the inflammatory cell infiltrate; and *granulomatous gastritis* which features epitheloid cell granulomas and is thought to be part of Crohn's disease or sarcoidosis.

1.2.2 Ulcers

Ulcers can be defined as a breach of the mucosa of the alimentary tract that extends through the muscularis mucosa into the submucosa or deeper (Kumar et al. 1997). Erosions differ from ulcers in that there is loss of the superficial epithelium of the mucosa and the healing may take place within days as compared to ulcers, which can take much

longer. The most prevalent form of ulcer concerned with the duodenum and stomach is termed *peptic ulcers*, and they usually are chronic in nature. This pathology occurs as the result of a breach in the mucosa of the stomach and small intestine, and is produced by the mucolytic action of acid and pepsin (Underwood. 1996). The histology of such an ulcer indicates a round, 'punched out' crater usually 2 to 4 cm in diameter with clear-cut edges that overhang. The favoured sites are the lesser curvature of the stomach, and the posterior and anterior walls of the first portion of the duodenum. The location of the ulcer is a direct function of the extent of gastritis and with antral gastritis being most common; the lesions are often observed along the margin of the inflamed area and the acid-secreting mucosa of the corpus. The actual histological appearance varies with the degree of chronicity, activity and rate of healing. Complications include perforation of the mucosal wall leading to peritonitis; penetration, whereby the ulcer extends into an adjacent organ such as the liver or pancreas; and haemorrhage from an eroded blood vessel at the base of the ulcer. Peptic ulcers usually heal by epithelial regeneration and progressive fibrosis, to reconstruct the mucosa. Later, central narrowing of the stomach, caused by the shrinkage/ cicatrisation of the fibrous tissue may cause the so-called *hour glass* deformation. Peptic ulcers are notoriously chronic and recurrent, and if left untreated can take up to 15 years to heal.

Most peptic ulcer sufferers have some form of epigastric pain, which is reported to be most intense during sleep and a few hours following a meal. Classically, the pain may be relieved by alkalis or food, but there are many exceptions. Some of the symptoms include nausea, vomiting, bloating, belching, and anaemia, with life-threatening bleeding being the most serious and occurring in up to one third of sufferers.

The pathogenesis of peptic ulcers can be linked to a variety of factors that include environmental (NSAID's, especially aspirin; smoking), genetic (hereditary, blood group antigens, pepsinogen secretion), physiological (hyperacidity, accelerated gastric emptying, pH, impaired mucosal defence, hyperpepsinogenemia), and bacterial (*Helicobacter pylori*, discussed in section 1.3).

Acute gastric ulcers are focally developed acute mucosal defects and appear stress related, hence the term *stress* ulcers. Usually these are multiple lesions in the stomach and occasionally the duodenum, and range from superficial epithelial erosion to lesions involving the entire mucosa. The shallow erosions are extensions of erosive gastritis (discussed earlier in section 1.2.1.1) whereas the deeper lesions have a totally different pathobiology and are not precursors of chronic peptic ulcers. Stress ulcers are most commonly encountered in individuals with shock, extensive burns (Curling's ulcers), severe trauma (including major surgery, sepsis or grave illness), central nervous system trauma and brain surgery (raising of the intercranial pressure, commonly referred to as Cushing's ulcers). Acute stress ulcers are usually circular and small about 1 cm in diameter. Unlike chronic peptic ulcers they may be found anywhere in the stomach and man be in single or multiple form, characterised by a dark brown base that is so stained due to the acid digestion of extruded blood (Cotran et al. 1994). These types of acute gastric ulcers are of limited clinical consequence or life threatening. The removal of the underlying causative factor can lead to complete recovery of the gastric mucosa.

1.2.3 Carcinoma

Gastric cancer is the sixth most common cause of cancer deaths in the United States, and has a notably high rate of incidence in Japan, Colombia, China, Finland and Chile. Although the incidence of gastric carcinoma has been on the decline in recent decades, it still remains the second most fatal malignancy (after lung cancer). In many countries gastric cancer remains the most common form of cancer.

Among the malignant tumours of the stomach the most common (90-95%) is carcinoma, next is lymphoma (4%), followed by carcinoids (3%) and malignant spindle-cell tumours (2%) (Citran et al. 1994). Carcinomas of the stomach are almost exclusively *adenocarcinomas* resulting from abnormalities of the mucus-secreting epithelial cells. Gastric cancer exhibits two distinct morphological forms denoted '*intestinal*' and '*diffuse*', as defined by Lauren (1965). Intestinal carcinomas are thought to arise from gastric mucous cells that have undergone intestinal metaplasia as a result of chronic gastritis. Diffuse-type gastric carcinomas are thought to arise *de novo* from native gastric mucous cells and are not associated with chronic gastritis. Pathogenic factors include diet (nitrates found in food and water, smoked and pickled food, excessive salt intake), genetic (poorly defined), gender/sex (uncommon in persons under 30 years, 2:1 male predominance after age 50 with chronic gastritis), and *Helicobacter pylori* infection (discussed in section 2.1.1.1).

The favoured location is the lesser curvature of the antro-pyloric region, with 50 -60% of carcinomas found in the antrum and pylorus, 25% in the cardia, and the remainder in the body and fundus. The early stages of gastric carcinoma present as lesions to mucosa and

submucosa, whereas the advanced form is neoplasmic and extends well below the submucosa into the muscular wall. Carcinomas are classified on the basis of their depth of invasion, macroscopic growth pattern and histologic subtype.

1.3 Implications of *Helicobacter pylori*

1.3.1 Bacteriology

Organs with acid-secreting epithelia (stomach-like) have existed for more than 300 millions years, and helicobacter or related bacteria have been found to colonise the gastrointestinal tract of many animals including non-human primates. If *Helicobacter pylori* (Hp) is an ancient organism, it is probably not very harmful to humans judging from the non-selection of virulent strains which would have caused substantial mortality before the end of the reproductive cycle of the host. Indeed, despite immune recognition, the ubiquity and persistence of the infection, no loss of fertility of the host and the genetic diversity of Hp tends to suggest that microbial parasitism has been fashioned into commensulism and then symbiosis (Blaser 1997).

The first reported observation of bacteria residing in the hostile gastric environment (namely for microbials) was made by Rappin (1881) while working with canines and felines. The distinctive spiral morphology was further noted a decade later by Bizzozero (1893), and Salomon (1896) later published reports on the transmission of canine gastric spirals. In 1939 Doenges reported that nearly 50% of human stomachs investigated, from accident victims, were found to be infected with spiral organisms. Freedburg and Barron (1940) identified a bacterium in up to 37% of endoscopic specimens examined by them.

At this point interest in gastrointestinal micro-flora waned. It was only rekindled in 1975 when Steer published electron micrographs of spiral bacteria in gastritis; which he could not culture. However, Steer and Collin-Jones (1975) did demonstrate gram-negative bacilli in 80% of gastric ulcer patients. The final significant proof of involvement of spiral bacteria in the pathobiology of the gastritis was made when Helicobacter pylori was isolated and cultured at the Royal Perth Hospital, Australia in 1982 (Marshall and Warren 1984). This result was achieved through the fortuitous mistake of leaving a bacterial culture to incubate over an extended period. Originally thought to be of the *Campylobacter* genus due to its morphology and culture conditions, this new organism was later reclassified as *Helicobacter pyloridis* (Goodwin and Worsley 1993). The genus already has at least twelve species (Stark et al. 1995), of which two, Hp (causes 99% of human helicobacter infection) and *Helicobacter heilmanii* (acquired from canines or felines) account for all human infections. Initial sceptiscm suggesting that the bacterium was an opportunistic pathogen attracted by changes in the gastric mucosa caused by inflammation and ulceration, has now been superseded by overwhelming evidence and conviction that *Helicobacter pylori* (Hp) is indeed a major bacterial pathogen directly related as a causal factor, rather than a mere commensal, in chronic gastritis and peptic ulcer disease (Goodwin et al. 1987, Graham et al. 1988, Hanson et al. 1993, Miller et al. 1991, Peek and Blaser 1996).

1.3.2 Pathogenic Determinants and Colonising Factors

It is important to distinguish between those properties of *Helicobacter pylori* that are required for initial infection and those necessary for the conversion of the acute phase infection to a chronic one. In fact, the initial inflammatory response and infection correlate

closely with factors such as motility, adhesion, urease production, and other-enzyme synthesis may induce the initial inflammatory response and infection, and perpetuation.

The study of Hp colonisation gained importance only after the initial ingestion studies by Barry Marshall (Marshall and Warren 1984) that produced histological abnormalities, characterised by inflammatory cell invasion on antral biopsy specimens. Direct evidence that Hp colonised normal gastric mucosa and that histological changes associated with infection was obtained by Morris and Nicholson. (1987), and this proved that Hp is at least a cause of superficial chronic gastritis.

Structure and morphology Hp is a gram-negative, spiral, assacharolytic, non-spore bearing, micro-aerophilic, motile, urease-, catalase- and oxidase-positive bacillis [Blaser 1990, Ishihara et al. 1997, Halter et al. 1992) (refer to Plate 3a)]. It is about 2.5 to 5 um long and 0.5 - 1.0 μm wide with a slight curve along its length of about 1.5 wavelengths when grown in culture media (Stark et al. 1995). At the end of the cell there are four to six lophotricate-sheathed flagella, some of which end in a terminal bulb. These flagella are up to 2.5 um long with a sheath 30 nm wide enclosing a 15 nm wide filament. Hp is distinguished from campylobacter and other helicobacters by a divergent 16s rRNA sequence, a distinctive fatty acid profile, and the absence of the respiratory quinone TPQ-6 (Collins 1992). Genetic studies of Hp have shown the genome to be small (about 1.7 million base pairs, whereas *E. coli* is 4.6 Mbp). Also of note is that Hp has fewer regulatory genes than even *E. coli.* These regulators are responsible for the "on-off" switch of certain gene expressions as the bacterium encounters a new environment (Lee 1998). Such evidence suggests that Hp lives only in the human stomach and is able to manipulate the biological pathways it requires to live in this forbidding environment. There has also

been discovered a number of hypervariable regions that encode for the antigenic determinants found on the cell-surface of the parasite. Continual altering of presenting antigens would account for the skilful evasion of the host immune system.

Motility Motility is essential for many of the gut pathogens, such *as V. Cholerae* and the *Salmonella spp.*, and seems to be especially more so in the spiral shaped mucus colonisers. This was revealed by the more pronounced spiral shape of free-moving bacteria in the mucus rather than adherent Hp seen in biopsy specimens (Hazell et al. 1996). The flagellum sheath of Hp is continuous with the outer cell wall. It has been suggested that this sheath forms a protective barrier for the flagella core-protein contents against the acidic gastric juices, since low pH found in the stomach would lead to rapid protein dissociation and denaturation. The active flagella of the bacterium probably are responsible for navigation through the stomach mucosae (Stark et al. 1995). It has been proven that aflagellate non-motile Hp mutants will not colonise gastric epithelia in gnotobiotic porcine models (Eaton et al. 1989). The ability to move rapidly through the gastric mucus would have the added advantage of Hp being able to escape the acidic luminal contents. The spiral shape of Hp (Plate 3a) also contributes significantly to the movement through flowing mucus and it is thought that chemotactic stimuli, probably released by eukaryotic cells, would favour movement toward optimal nutrition and a minimal hostile environment (Newell 1991).

Adherence Colonisation of the stomach is seen as an essential factor in the causation of gastritis and ulcerogenesis (Slomiany et al. 1994). In this way the host mucosal surface is exposed to larger concentrations of bacterial endotoxins. Adherence is also an entry point for organisms into epithelial structures (Hemalatha et al. 1991). Hp has a very specific

association with gastric-type epithelium, and this was shown by the colonisation of gastric metaplastic cells while adjacent duodenal cells remained bacterial free. Conversely, areas of intestinal metaplasia (common in chronic atrophic gastritis) were not colonised. Replacement of gastric epithelium by surface structures that are less susceptible to injury represents a defence mechanism (Halter et al. 1992).

Ultrastructural studies demonstrate bacterial attachment to gastric epithelia involves the formation of *'adherence pedestals/pedicles'* (Hemalatha et al. 1991, Collins 1992). Histological examination reveal that these pedestals are seen to adhere to the apical membranes of the gastric epithelial cells similar to those seen with *E. coli* (Plate 3b). It has also been suggested that attachment involves certain surface-associated adhesion molecules, details of which are still uncertain (Slomiany et al. 1994). These adhesion/s would be similar to other pathogenic bacterial adhesins with respect to the properties of their colonising antigens. One of the first candidates identified was *N-acetylneuraminyllactose-binding fibrillar haemagglutinin* which shows haemaglutinin activity towards human and animal erythrocytes (Emody et al. 1988). Lingwood et al (1989) have also reported that an antral glycolipid receptor *phospatidylethanolamine* binds Hp, whereas the Piotrowski group (1992) have shown Hp to bind laminin (component of basement membrane). Cell culture studies on human gastric epithelial cell lines characterise a surface-expressed haemagglutinin, which is expressed by Hp as a fibrillar adhesin (Evans et al. 1988a). Research also shows that Hp recognises specific acidic glycosphingolipids on cells surfaces. Data on the distribution of sulfated and sialylated glycolipids indicate predominance in the antral mucosa compared to the fundus. This supports evidence that Hp prefers colonising antral rather than fundic regions (Slomiany and Slomiany 1991). Surprisingly enough, only about 3% of bacteria are seen adhering via

a pedicle, while loose attachment via fimbriae can occur. This suggests that pathogenesis may not involve attachment, although the rapid turnover of gastric epithelial cells would dislodge even firmly attached bacteria.

Urease Urease (*urea amidohydrolase* E.C. 3.5.1.5) catalyses the hydrolysis of urea to yield ammonia and carbamate, the latter spontaneously hydrolysing to yield another molecule of ammonia and carbonic acid (Mobley et al. 1991). Subsequently the ammonia equlibrates with water to form ammonia hydroxide and this contributes to an increase in pH. Analysis of purified Hp urease reveals that it is a multimeric enzyme composed of two different subunits *UreA* (31 kD) and *UreB* (66 kD), while the native form is about 600 kD (Megraud 1994). Both subunits are required for activity, and UreA has been shown to contain a nickel ion (Stark et al. 1995). Hp urease is the most studied of all Hp enzymes and all gastric helicobacters isolated so far have a similar enzyme (Dunn et al. 1991, Eaton et al. 1991) suggesting an important role in colonisation. The location of Hp urease appears to vary from strain to strain with the enzyme being located on the cell surface (Hawtin et al. 1990), the cell membrane and cytoplasm (Bode et al. 1993). It is found within 50% of the bacterium and is associated with two pH optima (4.0 and 7.5) (Dunn et al. 1990). It comprises 6% of the total proteins produced by Hp (Newell 1991, Stark et al. 1995). Urease is thought to play a central role in pathogenesis of Hp. Generation of ammonia enables the organism to survive in an acidic environment. Ammonia has lysomotropic activity and may produce extremely cytotoxic effects within gastric epithelium (Smoot et al. 1990).

Plate 3a: Scanning electron microscopy photo-micrograph of a *Helicobacter pylori* bacillis. Shown are the curved shape, the lophotricate-sheated flagella used for motility through the mucous of the stomach, the bulbous nodular ends of the flagella, and the continuous cell body.

Plate 3b: Scanning electron microscopy image of *Helicobacter pylori* infested gastric tissue. Evident are the adherence of the bacterium to epithelial cell surfaces (by the formation of 'pedestals') and the presence of free-swimming bacteria. Also shown are some of the bacteria destroying cell membranes, invading the intercellular junctions between adjacent cells and infiltrating the tissue.

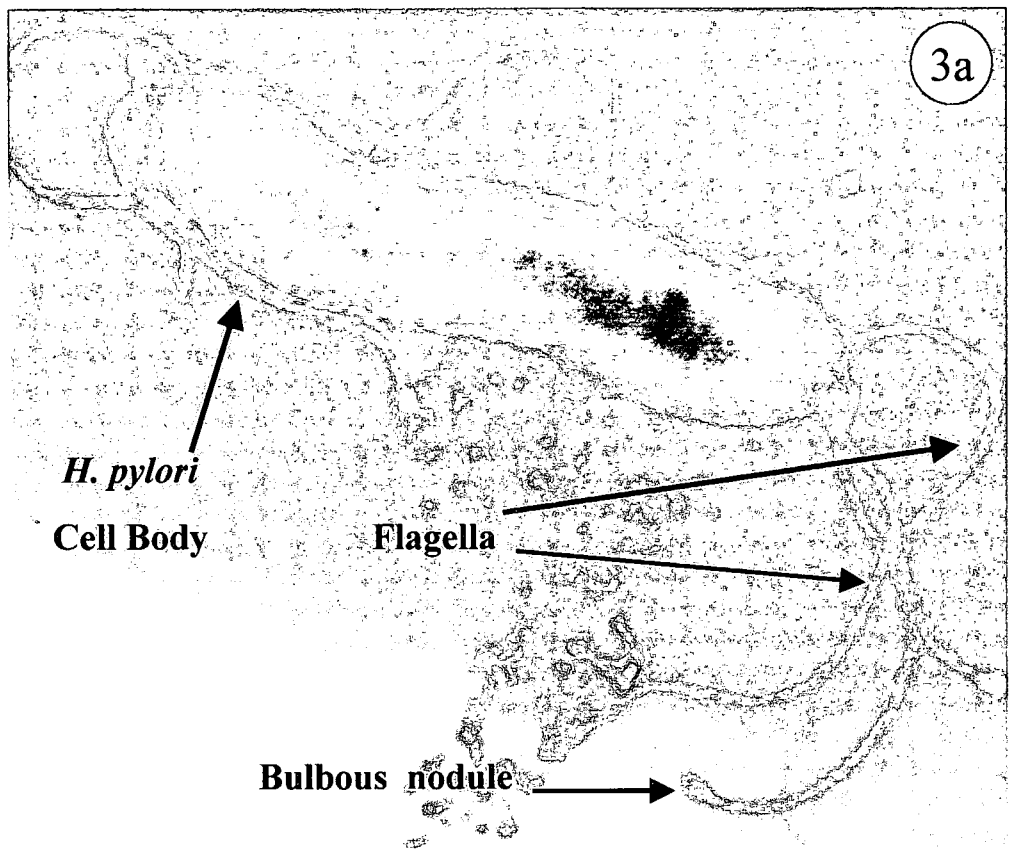
3a
H. pylori
Cell Body
Flagella
Bulbous nodule

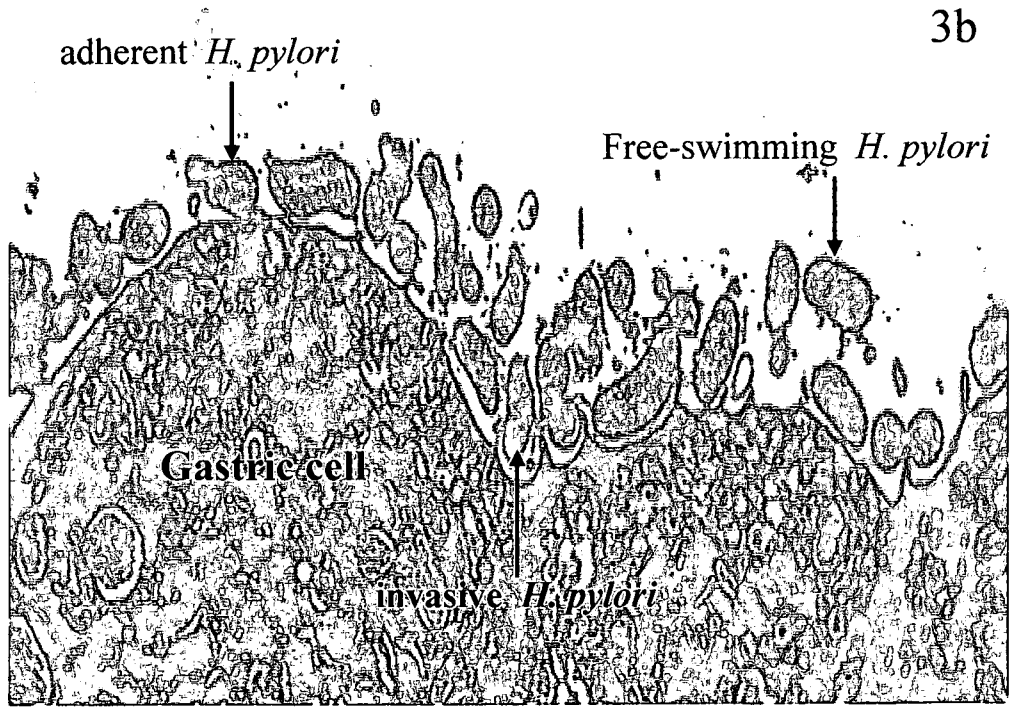
3b
adherent H. pylori
Free-swimming H. pylori
Gastric cell
invasive H. pylori

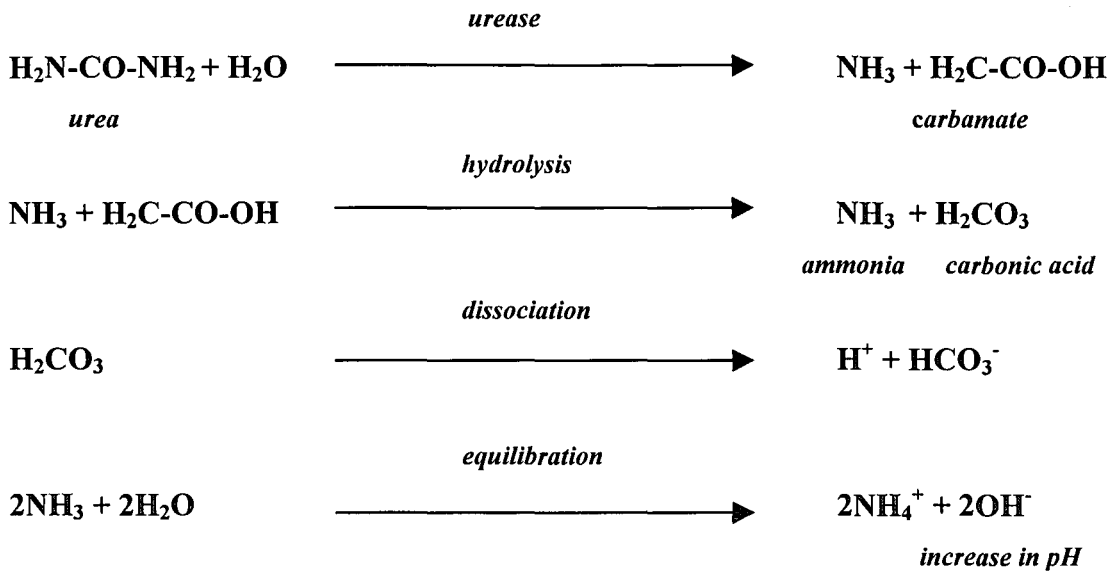

In addition, it causes intracellular vacuolisation (Xu et al. 1990). Ammonia produced by urease action inhibits the consumption of oxygen in gastric mucosal cells, decreases energy charges and ATP levels in the gastric mucosa, and may therefore cause acute mucosal injury by impairing energy metabolism (Kawano et al. 1993). It has also been suggested that, like *Clostridium difficile* toxin, there may be an alteration in cytoskeletal structures, although no direct evidence for this exists (Segal et al. 1992). Purified Hp urease has also been identified as an activator of leukocytes (Mai et al. 1992). Urease is produced constitutively in Hp, although the reason for this is not known (Mobley et al. 1989). It seems that in addition to a possible nutritional role it may have a protective function especially during the initial stages of infection where the production of 'ammonium clouds' around the organism protects it from the harsh luminal acid (Dunn 1993). Conclusive evidence of the importance of urease in colonisation was demonstrated by the failure of urease-negative mutants to colonise the gastrum of gnotobiotic piglets (Eaton et al. 1991), and the introduction of urease inhibitors at the time of infection prevented colonisation (Ferrero and Lee 1991).

Cytotoxins Certain strains of Hp are known to produce cytotoxic effects i*n vitro.* In human and gnotobiotic piglets the action of vacuolating cytopathic effects has produced intracytoplasmatic vacuoles (Tricottet et al. 1986, Eaton et al. 1989). Serological studies have not established a definite link between cytotoxins and formation of ulcers in individuals with or without Hp infection (Leunk et al. 1990). It has also been discovered that the cytotoxin in impure extracts can be inhibited by eukaryotic vacuolar ATPase inhibitors, and biafilomycins A1, B1, C1 and D. The action of cytotoxin is potentiated by ATPase inhibitors, oubain and digoxin (Papini et al. 1993). Associated with the cytotoxin is the protein CagA; and the majority of Hp strains that express CagA also have the CagA gene. The CagA gene product varies between different strains from 105 to 140 kD. Perez-Perez (1996) has found that CagA-positive strains colonise with increased density, are associated with higher interleukin-8 (IL-8) secretion, have higher levels of inflammation, express more Lewis antigens, and have a more significant interaction with the gastric epithelia than CagA-negative strains.

Other factors such as phospolipase, lipopolysaccharide, lipase, esterases and deaminases have also been implicated, to a lesser extent, in the virulence of the pathogenicity of Hp strains.

Immunological responses Unlike the small and large intestine, the normal stomach contains few inflammatory cells. Plasma cells are rare, and the occasional lymphocyte, macrophage or eosinophil may be found. Thus, Hp infection provokes an inflammatory response directed entirely towards itself (Riddell et al. 1991). Inflammation is characterised by the orderly recruitment and deployment of specific subsets of leukocytes to sites of infection. The accumulation of immune cells, the most common feature of

inflammation, occurs when leukocytes migrate towards the site of infection and attach to the endothelial cells lining the micro-vessels in these tissues. The initial immune response is by neutrophils, which initiate a rapid, nonspecific phagocytic response; followed by the monocytes and T and B cells, which are activated to produce protective and inflammatory molecules.

Infiltration by neutrophils is a typical feature of Hp- associated chronic gastritis. Polymorphs are seen in the lamina propria and they infiltrate the epithelium of the mucosal surface. Given that Hp flourishes on the surface epithelium and rarely penetrates deeply into the gastric pits, it is interesting to note that the superficial infiltration of neutrophils is not greater in number than in the deeper epithelium of the gastric pits, in the isthmus region, and in the adjacent lamina propria and capillary channels. Nevertheless, these regions of infiltration are important since it is the generative zone of immature stem cells that either migrate upwards to the surface, or down into the specialised endocrine cells. The destruction of this underlying area, if inflammation progresses to completion, results in glandular destruction and atrophy. The presence of neutrophils is seen to be a response to Hp antigens, promoted by an increase in adhesion molecules that bind to the vascular endothelium (Dixon 1994). Hatz et al. (1992) recently suggested that factors produced by Hp may stimulate leukocyte accumulation, or may direct epithelial cells to secrete lipid mediators such as leukotrene 4, interleukin 8 (IL-8), C5a, and platelet-activating factor (PGF) (figure 5). They suggest that these substances attract granulocytes or stimulate local T cell response, or even both. Tumor necrosis factor-alpha (TNF-α) has been demonstrated in individuals with Hp-associated gastritis (Crabtree et al. 1991). Formylated peptides, released by Hp, are chemotactic for granulocytes and stimulate the release of oxygen-derived free radicals and proteases from granulosa cells (Wallace, 1991).

Monocyte activation has been demonstrated through the activation of monocyte HLA-DR and IL-2 receptors. Epithelial cells express class II major histocompatibility complexes that are responsible for directing presenting antigens on cell surfaces. Increases in the T cell count occur, and there is also an increase of CD2, CD3, CD5, CD6, and CD8 (Engstrand et al. 1989, Kirchner et al. 1990). Hp also produces other potentially immunological compounds including urease (discussed in section 1.3.2), LPS, a 62 K heat shock protein, the 87 KD vacuolating cytotoxin (VacA) and the 128 KD cytotoxin-associated protein (CagA) (Xiang et al. 1993). Monocytes take up these antigens in the lamina propria resulting in the production of TNF-α, and interleukins 1 and 6 (Crabtree et al. 1991). TNF-α promotes adhesion of leukocytes to endothelial cells and attracts leukocytes to sites of infection (Figure 5). IL-1 and 6 stimulate T helper cells and these produce several cytokines including IL-5, -6 and -8, and interferron-gamma (INF-γ). (Van Deuren et al. 1992). IL-8 is a chemotaxin for polymorphs, while IL-6 stimulates the differentiation of B cells into specific plasma cells. INF-γ stimulates HLA-DR to become antigen presenting on gastric cells. Evans et al (1992) has reported that the 62 K heat shock protein to be 80% analogous to the *E. coli* GroEL heat shock protein and 75% analogous to human chaperonin. Since other HSP60 proteins have been associated with induction of chronic inflammation, it is entirely possible that the Hp 62 K protein is also involved in chronic inflammation of the stomach associated with Hp infection (Kaufman 1990).

Other inflammatory mediators produced by activated monocytes and polymorphs include prostaglandin (PGE_2), leucotrienes, proteases and reactive oxygen metabolites (ROM). These protease and ROM's are likely to cause tissue damage, especially where there is a relative deficiency of antioxidants like vitamin C and E (Phull et al. 1993).

Effect of Hp acid secretion and gastric disease Low pH is responsible for the bactericidal properties of gastric juice. Lack of bacteria in the stomach after fasting and the relative diminution of bacterial content are both related to the acidity of the gastric juice (Stockbruegger et al. 1982). The effect of Hp and acid is an interesting one since the organism itself is killed by pH less than 4 (Tompkins 1989). This organism is also associated with elevated levels of serum gastrin, which has an effect on acid secretion. When Hp infects the stomach the negative feedback system is compromised (see section 1.1.1.5). The effect is thought to principally be directed towards the somatostatin-secreting D cells, which means gastrin release would not be appropriately inhibited. Although initial Hp infection is associated with hyposecretion and gastritis, chronic infection leads to moderate hypersecretion (McGowan et al. 1996). In some patients the bacterial load is high and this correlates with increased levels of gastrin that results in greater acid secretion during infection. The gastrin and acid levels seem to return to normal upon eradication of Hp (Freston 1994). In the pathophysiology of ulcer disease, it seems that both Hp and increased acid levels may be present. It has also been postulated that genetic heterogeneity is responsible, in part, for hyperacidity. Interesting to note is that Hp infected individuals without duodenal ulcers have the same abnormalities seen with ulcer patients after Hp eradication. Hp infected, non-ulcer patients do not, however, have elevated serum gastrin and acid levels after eradication. This could mean that Hp infected patients who develop ulcers may have other factor that increase their gastrin-stimulated acid secretion (El-Omar et al. 1995). In fact, current theory holds that there are two pathways to ulcer disease- hyperacidity and Hp infection- and both interact with one another. This may be highlighted in patients who produce excessive acid, but are not infected with Hp until, after mucosal injury due to acidity.

Figure 5: Diagram showing the immunological response to *Helicobacter pylori.* Neutrophils initiate a rapid, nonspecific phagocytic response; followed by the monocytes and T and B cells, which are activated to produce protective and inflammatory molecules. Bacterial lipopolysaccharides (LPS) stimulate leukocyte chemotaxis and direct epithelial cells to secrete lipid mediators such as leukotrene 4, interleukin 8 (IL-8), C5a, and platelet-activating factor (PGF)

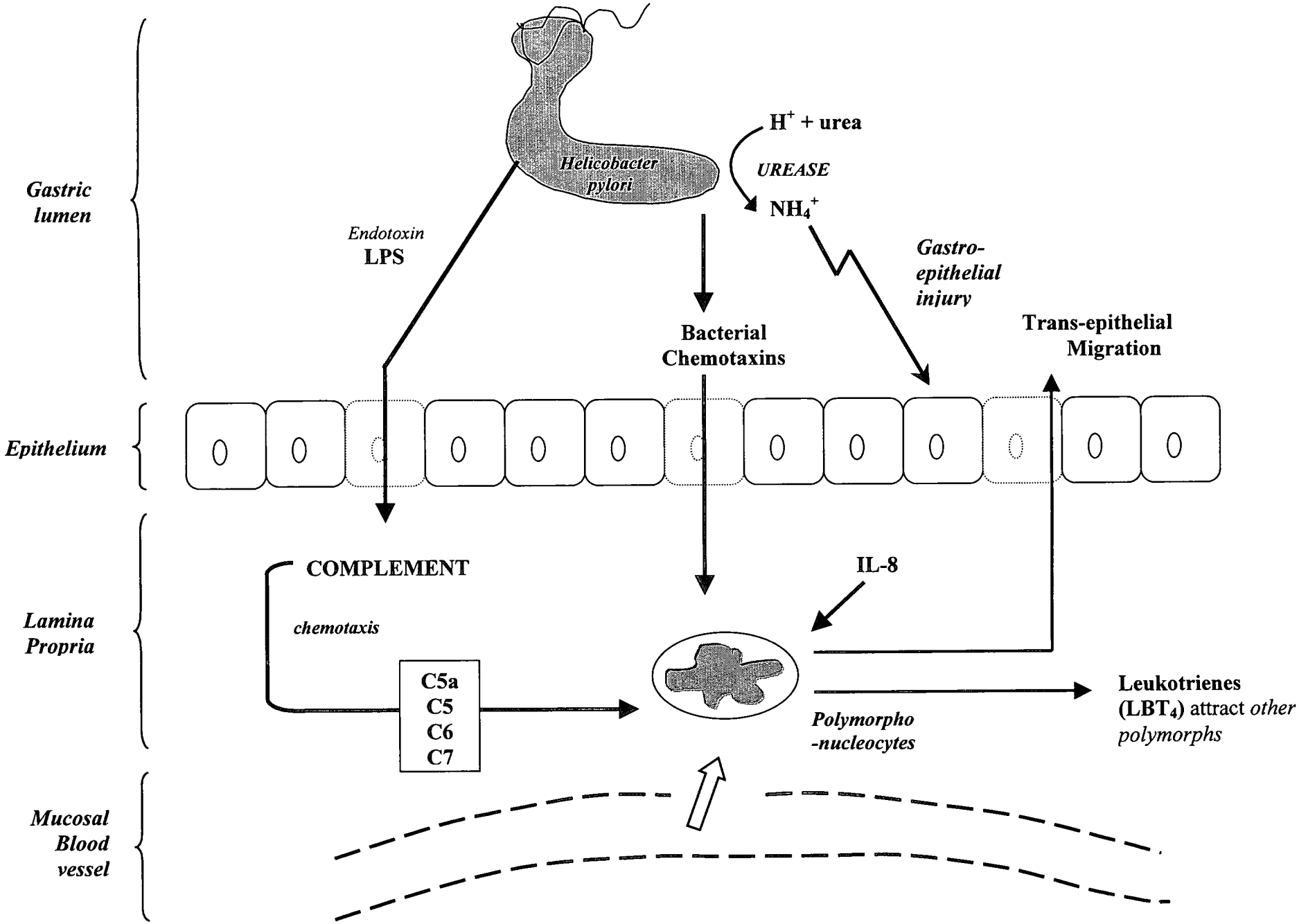
Gastric lumen
Epithelium
Lamina Propria
Mucosal Blood vessel
Helicobacter pylori
H+ + urea
UREASE
NH4+
Endotoxin
LPS
Gastro-epithelial injury
Bacterial Chemotaxins
Trans-epithelial Migration
COMPLEMENT
chemotaxis
C5a
C5
C6
C7
IL-8
Polymorpho -nucleocytes
Leukotrienes (LBT4) attract other polymorphs

1.3.3 Epidemiology

Prevalence The rate of acquisition of Hp infections varies greatly between developing and developed countries. In addition there are also differences between ethnic groups in a country. These variations can be attributed to socio-economic factors, cultural background and genetic predisposition when defining acquisition and transmission. (Megraud 1991)

It has been ascertained that Hp infection usually occurs in childhood and early adulthood. As many as 50% of the world's population is infected but many remain asymptomatic (Goodwin et al. 1997). These infections can remain in the stomachs for decades, and finally leads to glandular atropy and intestinal metaplasia. In developed nations, approximately 95% of patients with duodenal ulcer have Hp, and the prevalence of infection associated with gastritis is between 20% and 40% (Malfertheiner 1996, Collins 1992). Hp infection has been linked to 95% of Mucosal-Associated Lymphoid Tissue (MALT) tumours and complicated ulcer diseases. In the United States, studies conducted on asymptomatic individuals revealed that Hp infection increased with age at a rate of 1% per year, and was twice as frequent in Blacks (66%) and Hispanics (65%), than compared with Caucasians (26%) (Malaty et al. 1994). Even though variables such as socio-economic status, age, alcohol and tobacco consumption, education, income, and housing were factored in, the difference remained. Genetic predisposition was ruled out, since Hispanics are not a race. It was concluded that the differences could be due to economic status (overcrowded living conditions) during childhood, regardless of present status. This highlights the prevalence of infection during childhood, for example, children between the ages of 5 and 10 years in Saudi Arabia show a 40% infection, while those between 3 and

10 years in India show a 60% infection rate (Al-Moagel et al. 1990). In another study relating alcohol, tobacco and coffee consumption to Hp infection, it was found that there was no significant relationship between smoking and infection, while consumption of coffee was associated with increased active Hp infection. Oddly enough, imbibing alcohol was found to have a protective role for the gastric mucosa, and this relationship was dose-dependant. A possible explanation for this is the anti-microbial effect of ethanol (Brenner et al. 1997). Other serological studies have consistently identified socio-economic factors in childhood as major risk factors (Mendall et al. 1992). Current opinion is that there is a rapid, variable Hp acquisition phase early in life, followed by a consistent phase throughout adulthood.

Transmission The latest evidence suggests that man is the reservoir of Hp infection. The mode of transmission is not clearly understood, but is a critical factor for health care authorities trying to limit the spread of infection. What is known is that any method that introduces the organism into the stomach is a facilitating factor in infection. The possible modes of transmission may be faecal-oral, oral-oral, or a common source (for example, water supply). Several studies have highlighted that infection clusters within family groups and this shows person to person transmission (Malaty et al. 1991, Mitchell et al. 1987).

Genetic susceptibility Although it is impossible to separate environmental influences from genetic factors, evidence for a genetic component predisposing to gastric diseases has been found in studies that showed an increased risk of duodenal ulcers in those individuals with hyperpepsinogaemia (Fraser et al. 1992). These results become more important since it has been found that elevated serum pepsinogen I is a feature of Hp infection (Graham et

al. 1990). An interesting finding among genetically identical twins in Sweden, who were separated at birth, showed that Hp infection was largely due to genetic factors, although rearing environments was also significant (Malaty et al. 1992).

1.4 The Kallikrein Kinin system

1.4.1 Chronological Overview

The first discovery of note regarding the enzyme kallikrein was chronicled almost a century ago when two French investigators, Abelous and Bardier (1909), while searching for the toxic principle underlying uraemia, reported on a urinary fraction that lowered blood pressure, as well as a fraction that increased it when injected intravenously into an anaesthetised dog. They called the hypotensive agent urohypotensine. A decade later Pribram and Herrnheiser (1920) observed the vasodepressor effect of a partially purified substance from human urine on rabbit blood pressure. In 1926, the Munich surgeon Frey, working on post-operative reflex anuria, noticed a hypotensive response and increase in heart rate due to human urine injected into dogs. Frey and Kraut (1928) were then able to show that this urinary substance (named F-stoff: Frey-stoff) was a high molecular weight, thermolabile, non-dialyzable macromolecule. These early pioneers, seeking the source of this substance, found similar substances in the blood, and in large amounts in pancreatic extracts (Kraut et al. 1930a) leading to the designation of this substance as "kallikrein", since they believed that it was secreted into the circulation by the pancreas, k*allikreas* being the Greek synonym for pancreas. Furthermore, since they regarded kallikrein as a vascular circulating hormone, they called it *Kreislaufhormon.*

In 1933, Frey and Werle found that pancreatic kallikrein was secreted in a pharmacologically inactive pre-form. These kallikreinogens could be activated by pH change, organic solvents (Werle, 1934; Werle, 1936), and by enzymes such as pepsin and trypsin (Kraut et al. 1933). A significant discovery made by Werle and colleagues (1937) showed that when kallikrein was incubated with serum for a few minutes, it had a potent smooth muscle-contracting action on the dog intestine that could not be explained as being the actions of kallikrein alone. They deduced the serum-treated kallikrein formation of an active compound that was dialysable, thermostable, and contracted the guinea pig ileum from an inactive precursor (kininogen) in plasma. They called it *Substanz Dk* or *Darmkontrahierenderstoff* (intestine-contracting substance). It was also noted that the spasmolytic activity of this mixture on the perfused guinea pig ileum gradually increased and then disappeared slowly. Later Werle and Berek (1948) suggested Substanz Dk be renamed *kallidin* and it's precursor (substrate for kallikrein) *kallidinogen.* At about the same time Rocha e Silva and colleagues (1949) demonstrated the formation of a hypotensive and smooth muscle -stimulating factor when dog plasma pseudo-globulins were incubated with optimal doses of snake venom (*Borthrops jararaca*) or trypsin. This new, pharmacologically active compound caused a slow, delayed contraction of the guinea pig ileum; and it was appropriately called in Greek nomenclature *bradykinin* (brady meaning slow and kinin meaning movement). Later, the adoption of the name "kinin" (Schachter and Thain 1954) prompted scientists to call any enzyme (kallikreins, snake venom, trypsin, bacterial proteases, etc) that releases kinins from an inactive precursor (substrate - kininogen) to be called kininogenase. A number of pharmacologically similar peptides have since been discovered in insect venoms, like the first non-mammalian kinin in wasp venom (Jaques and Schachter 1954). It was this pioneering work that helped start to put the initial pieces of the kallikrein-kinin biological jigsaw together.

1.4.2 The Kallikreins

Kallikreins belong to a sub-group of the serine-protease family and may be responsible for the post-translational processing of protein precursors. These enzymes are further subdivided into plasma and glandular (commonly termed tissue) kallikreins. Distribution of the kallikreins, either in an active and/or inactive but activatable form, range from various glandular cells and neutrophils to urine and other biological fluids (Bhoola et al. 1992a). These kininogenases are two distinct entities that differ from each other with respect to their respective molecular weights, isoelectric points, substrate specificity's, immunological profiles, and the type of bioactive peptide released; with tissue kallikrein being able to process low molecular weight kininogen (LK) to produce kallidin (lysyl bradykinin, lys-BK), and plasma kallikrein liberating bradykinin (BK) from high molecular weight kininogen (HK) (figure 6).

1.4.2.1 Tissue Kallikrein

The true mammalian tissue kallikrein (EC.3.4.21.35), encoded by the gene KLK1, has been classified a member of a subdivision of serine proteases able to release kinins by hydrolytic activity on one methionyl and one arginyl bond on the physiological substrate kininogen, thereby liberating the decapeptide kallidin. The human KLK genes, namely. KLK1, KLK2 and KLK3 are found on chromosome 19q (Evans et al. 1988b), forming a gene cluster of about 60 kilobases. Tissue kallikreins are encoded by a multigene (KLK) family in several species (Murray et al. 1990). These comprise five exons and four introns with the genomic arrangement being highly conserved in all species studied thus far (Lin et

al. 1993). The tissue kallikrein human gene family appears to consist of four distinct genes: kallikrein and an unidentified partial gene sequence, prostate-specific antigen, and a characterised but unidentified gene termed hGK-1 (MacDonald et al. 1988). With the serine protease family, catalytic activity structurally resides in a highly conserved triad of amino acids assembled in the correct configuration (Neurath 1989). The active site that is necessary for serine proteolytic activity of this gene family member is His^{-41}, Asp^{-96}, Ser^{-189} (Bode et al. 1983). Differences in this catalytic triad are responsible for cleavage specificity of true kallikreins. Members of this serine protease sub-family also show differences in translation and regulation at hormonal level. Tissue kallikrein, processing at basic amino acids (trypsin-like), can also cleave arginyl esters, and is sometimes referred to as an 'arginyl esterase' (Fiedler 1979). Tissue kallikrein is a 27 to 45 Kd acidic glycoprotein with an isoelectric point ranging from 3.5 to 4.4 (Pisano 1975). It is synthesised bound to a 17-amino acid signal peptide, and an Ala^{-8}-Ala^{-7} peptide bond is cleaved to release the proenzyme. With the release of the signal peptide, inactive prokallikrein has a very short inactivation peptide of seven amino acids (MacDonald et al. 1988). The activation of the kallikrein is similar to that of other serine proteases, such as chymotrypsin, to expose the active site after alteration of the three-dimensional structure (Kraut 1971). Therefore, certain serine proteases, or enzymes that act on the amino terminus of the hydrophobic amino acids can activate prokallikrein. *In vitro,* Girolami and co-workers (1985) reported the activation of prokallikrein by trypsin, and Takada et al (1986) showed that a bacterial metalloprotease, thermolysin could also hydrolyse the Arg-Ile bond at the amino terminus of the activation peptide. Plasmin (Yamada and Erdos 1982) and plasma kallikrein

(Takada et al. 1985) have also been reported to activate purified prokallikrein *in vitro*. Although the *in vitro* activation mechanisms are known, the intracellular kinetics and processing of prokallikrein are undefined as yet. Inactive prokallikrein has been found in the pancreas (Frey et al. 1950), colon, (Frey et al. 1968), pituitary gland (Powers 1986), submandibular glands, kidney connecting tubules, glands of the trachea, nasal mucosa, prostate epithelia and anterior pituitary gland (Bhoola et al. 1992b), to name a few.

The primary known biochemical action of tissue kallikrein (figure 6) is the highly selective cleavage of the circulating plasma protein kininogen at two peptide bonds to release the vasoactive and spasmogenic decapeptide lys-bradykinin (kallidin). LK (M_r 50Kd in human plasma) and HK (M_r 120Kd) which are both probably hepatic-derived, appear to be substrates for tissue kallikrein (Carretero and Scicli 1980). The processing of other prohormones and inert enzymes have also been proposed as a function of tissue kallikrein (Mason et al. 1983).

1.4.2.2 Plasma Kallikrein

The zymogen, plasma kallikrein (EC 3.4.21.34) is encoded by a single gene of about 22 kilobases and is located on chromosome 4q34-q35 (Beaubien et al. 1991). The Factor XI (Fletcher Factor) gene shows remarkably similar structural organisation to plasma kallikrein, and both plasma kallikrein and Fletcher Factor seem to have arisen from common gene duplication. Animal models (murine) have shown the plasma kallikrein gene to consist of 15 exons, the first two coding for the signal peptide, the next eight coding for the heavy chain, with the last five

exons coding for the light chain and the protease portion that is similar in function and structure to tissue kallikrein. The carboxyl terminus contains the catalytic triad of His^{-415}, Asp^{-464}, and Ser^{-559} (Van der Graaf et al. 1982). There are about 75%-conserved sequences between human, rat and mouse plasma kallikreins (Seidah et al. 1990). The plasma kallilkrein precursor 'prekallikrein' is a γ-globulin zymogen, synthesised in the hepatocytes and secreted into the blood as an inactive form where it circulates as a heterodimer complex bound to its substrate H-kininogen (Mandle et al. 1976). Prekallikrein is a single chain glycoprotein (pI 8.9), and, two forms (88 and 85 Kd) have been isolated from human plasma (Mandle and Kaplan 1977). Activated Factor XII (Hageman Factor) is required to convert prekallikrein to plasma kallikrein by limited proteolysis on a single Arg^{371}-Ile^{372} to form a disulphide-linked two-chain molecule (36 Kd light chain and 52 Kd heavy chain). Plasma kallikrein liberates bradykinin from H-kininogen resulting in the cleavage of Lys-Arg and Arg-Ser bonds (figure 6). Although not the physiological substrate for plasma kallikrein, L-kininogen will form bradykinin in the presence of neutrophil elastase (Sato and Nagasawa 1988). Plasma kallikrein plays a role in the early phases of intrinsic blood clotting cascade system, the fibrinolytic system and the production of bradykinin (Chung et al. 1986). It has a wide variety of substrates that include Factor XII, high molecular weight kininogen, plasminogen, C3 and prorenin, and is required for normal rate of coagulation *in vitro* (Colman et al. 1985). It may be also responsible for the pathophysiological polymorphonuclear chemotaxis that accompanies inflammation (Kaplan et al. 1972).

Figure 6: Schematic profile of the kallikrein-kinin system showing the activation of tissue pro-kallikrein, by various extraneous factors, to active kallikrein. The cleavage sites of kallikrein on its physiological substrate is demonstrated, as well as its conversion to derivatives to form kinin. Also shown are the cleavage sites on the vaso-peptide that are susceptible to protease degradation.

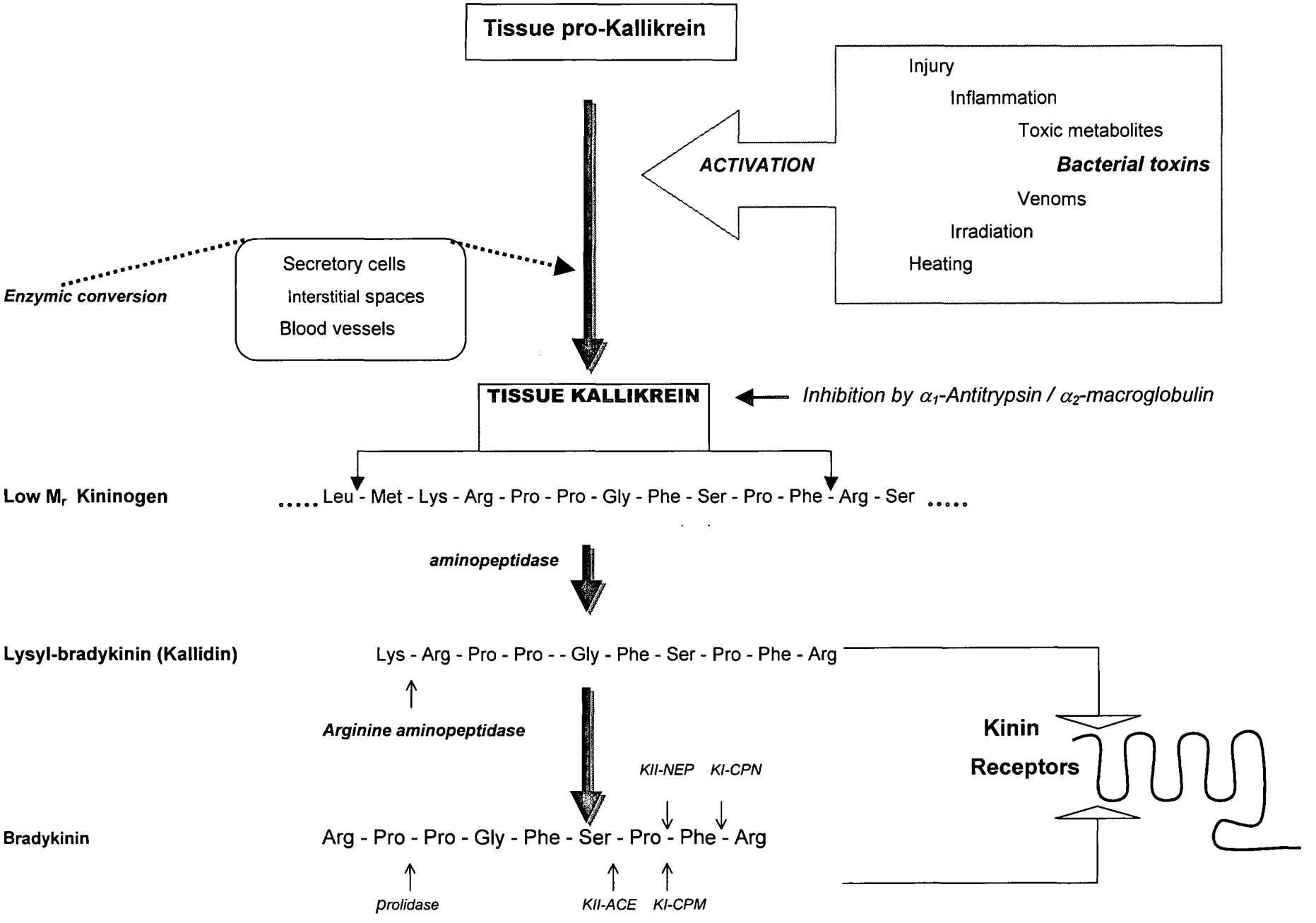
Tissue pro-Kallikrein
Injury
Inflammation
Toxic metabolites
ACTIVATION
Bacterial toxins
Venoms
Irradiation
Heating
Enzymic conversion
Secretory cells
Interstitial spaces
Blood vessels
TISSUE KALLIKREIN
Inhibition by α1-Antitrypsin / α2-macroglobulin
Low Mr Kininogen
..... Leu - Met - Lys - Arg - Pro - Pro - Gly - Phe - Ser - Pro - Phe - Arg - Ser .....
aminopeptidase
Lysyl-bradykinin (Kallidin)
Lys - Arg - Pro - Pro - - Gly - Phe - Ser - Pro - Phe - Arg
Arginine aminopeptidase
KII-NEP
KI-CPN
Kinin
Receptors
Bradykinin
Arg - Pro - Pro - Gly - Phe - Ser - Pro - Phe - Arg
prolidase
KII-ACE
KI-CPM

The contact activation process begins with Hageman factor binding to a macromolecular anionic surface, which leads to the activation of plasma prekallikrein (Revak et al. 1977). Plasma kallikrein then reciprocates to activate Hageman Factor. The rates of the reactions are greatly amplified by the presence of H-kininogen, which behaves as a co-factor (Griffin and Cochrane 1976). The plasma protease inhibitors, C1 inhibitor and α-2 macroglobulin accounts for over 90% of the inhibitory potency for kallikrein in normal plasma (Schapira et al. 1982). The complex set of reactions involving coagulation factors, co-factors, pro-hormones substrates and products are shown in Figure 6.

1.4.3. Kinins

Kinins are the vasoactive peptides that signal the biological effects of the kallikrein-kinin system. Although trypsin, uropepsin and plasmin have kininogenase activity, the two most potent kininogenases are plasma and tissue kallikreins. They generate kinins, in various tissues and biological fluids, by enzymic action. Plasma kallikrein acts on H-kininogen (produced in hepatocytes and the brain) to produce the nonapeptide bradykinin, and tissue/glandular kallikrein (various glands and circulation) releases the decapeptide kallidin (lys-bradykinin) from L-kininogen (Fiedler, 1979), which is rapidly converted to bradykinin by the action of an arginine aminopeptidase (Guimaraes et al. 1973). Kinins in plasma range from 10 to 5000 pg/ml (Carretero and Scicli 1988). Elliot and colleagues, in 1960, proposed the first amino acid sequence for bradykinin, but it was incorrect by one proline residue. The disclosure, and the first chemical sequence

Table 1: Properties and functions of the human kallikeins

	PLASMA KALLIKREIN	TISSUE /GLANDULAR KALLIKREIN
Molecular Weight	90 kD to 100 kD	24 kD to 44 kD
Substrate	➢ H- kininogen ➢ Hageman Factor ➢ Pro-Collagenase	➢ H- and L-kininogen ➢ Pro-Renin ➢ Pro-Collagenase ➢ Prolactin
Kinin Released	Bradykinin	Lysyl-bradykinin*
Inhibitors	SBTI C_1 Esterase Inhibitor α_2- Macroglobulin	α_1-Antitrypsin Kallistatin
Functions	➢ Coagulation ➢ Fibrinolysis ➢ Inflammation ➢ Complement activation ➢ Blood pressure homeostasis	➢ Regulation of organ blood flow ➢ Inflammation ➢ Water and electrolyte excretion ➢ Blood pressure homeostasis

kD : kilodaltons

SBTI : soyabean trypsin inhibitor.

* Only rat glandular kallikrein releases bradykinin.

of the correct amino acid composition for bradykinin (BK, Arg-Pro-Pro-Gly-Phe-Ser-Pro-Phe-Arg) came a year later from the peptide synthesis work of Boissonas and his colleagues (1960). Other mammalian kinin analogues include Hyp^3-lys bradykinin, with T-kinin and Met-T-kinin having so far only been described in the plasma and pouch fluid of rats following carrageenan-induced inflammation (Sakamoto et al. 1987). Tissue kallikrein releases bradykinin, and not kallidin, from both forms of kininogen in the rat model (Okamoto and Greenbaum 1983). Also of note is that T-kininogen is only hydrolysed by large amounts of trypsin, but not by kallikrein, to release T-kinin (for trypsin releasable kinin). Kinins have also been characterised in wasp venom (Schachter and Thain 1954), hornet venom (Bhoola and Schacter 1960). Mammalian kinins exhibit a highly conserved structure, and there is a remarkable degree of homology between the insect, reptile and amphibian kinins. In the circulation, kinins are rapidly inactivated by kininases resulting in estimated half-lives of kallidin and bradykinin being less than 30 seconds. However, in tissue fluids the half-life is believed to be much longer. In the nervous system bradykinin is involved in the central regulation of blood pressure, nociception and diuresis, and it increases neuronal excitability (Nitcsch et al. 1998). Other biological activities displayed by kinins include the ability to lower systemic blood pressure, increase capillary permeability, produce natriuresis, stimulate pain and sensitise nerve fibres to noxious stimuli, and mimic coryza elicited by rhinovirus (Ward 1991), exaggeration of sensory signalling that produce allodynia (painful responses to stimuli not normally painful) and hyperalgesia (Rang and Urban 1995). Kinins are the most potent pain-producing autocoids, and have also been implicated in releasing neurotransmitters like Substance P from nerve terminals, stimulating cytokine synthesis, activating phospholipase A_2 to form lipid mediators like prostaglandins and leukotrienes, releasing endothelium-derived relaxing factor (EDRF, nitric oxide) from endothelial cells thereby

causing endothelial cell contraction (Rodell et al. 1995). At the cellular level they promote glucose and chloride transport and stimulate osteoclast activity (Bhoola et al. 1992b). Both bradykinin and kallidin have similar pharmacological potency in increasing vascular permeability (leading to local oedema) and vasodilatation. Vasodilatation, increased microvascular permeability, and pain production overshadow the smooth muscle contracting actions of kinins (Table 1). Hence kinins are considered to signal the first-line onset of inflammation

1.4.4 Kinin Receptors

Kinins express their pharmacological effects by activating specific kinin receptors situated on the surface membranes of many cell types. Two major subtypes of the kinin receptor, designated B1 and B2, were proposed by Regoli and Barabé (1980). To characterise and subsequently classify these receptors, selective antagonists, gene cloning, and protein expression was used for structure-activity studies to establish the relative order of agonist potency, differences in activity profile, affinity of competitive antagonists, and signal transduction pathways. The B1 receptor agonists order of potency in isolated tissues are: desArg^9-BK > Tyr-(Me)^8 -BK> BK; and those of the B2 receptor are: Tyr(Me)^8 -BK> BK> desArg^9-BK (Hall and Morton 1997a). Initial studies focussed on the relative potencies of kinin agonists on smooth muscle tissue. For example, for the kinin metabolite desArg^9- BK, a thousand-fold excess of the bradykinin was needed to be potently equivalent in contracting the rabbit aorta [B1 mediation] (Regoli et al. 1977). The affinity of B1 receptors for kinin and kinin analogues differ markedly from that of B2 receptors. The effects of BK and lys-BK are mediated by the B2 receptors while those of the metabolites desArg^9-BK and lys-desArg^9-BK are mediated by the B1 receptor (Marceau

1995). Both these kinin receptor types belong to a superfamily of G-protein coupled rhodopsin-like receptors. They consist of a transmembrane-spanning regions with three extracellular and four intracellular linked unique regions. The sequence homology of the receptors is approximately 36%. Kinin is thought to bind to these G-protein coupled receptors thereby activating phospholipase C or phospholipase A_2, which increases the synthesis of inisitol triphosphate or arachidonic acid (Mahan and Burch 1990).

B1 receptors do not seem to be normally expressed, but *de novo* synthesis was achieved in vitro by Regoli and co-workers (1978). The B1 receptor appears to signal via phosphatidylinisitol hydrolysis in smooth muscle (Butt et al. 1995). In response to tissue injury and noxious stimuli (lipopolysaccharide in rabbit, Regoli et al. 1980), the B1 receptor appears be constitutively expressed in smooth muscle cells and fibroblasts (Bhoola et al. 1992b; Figueroa et al. 1995). Stimulation of B1 receptors on macrophages by kinin degradation product desArg^9-BK causes the release of IL-1 (interleukin) and TNF (tumour necrosis factor) (Tiffany and Burch 1989). In various preparations B1 has been implicated in the cardiovascular system (Chahine at al. 1993), urinary tract (Marceau 1995), intestinal tract (Brown et al. 1992), cultured cells (Cahill et al. 1988), embryonic calvarium bones (Ljunggren and Lerner 1990), and tracheal smooth muscle (Marsh and Hill 1994). *In vivo* mediation includes the effect on blood pressure (Tokamasu et al. 1995), persistant hyperalgesia (Perkins et al. 1993), and plasma extravasation (Cruwys et al. 1994).

Most of the actions of kinins are mediated by the B2 receptor (this receptor subtype does not respond to the B1 agonists). Initially, it was found that B2 receptors could be located

on intestinal epithelia, fibroblasts and primary brain cultures (Robert and Gulick 1989); and on a neuronal; blastoma cell line (Snider and Richelson 1984).

The 'smooth muscle' form is weakly activated by [β-(2-thienyl)-alanine, D-Phe]-bradykinin whereas the neuronal form is fully activated by [β-(2-thienyl)-alanine, D-Phe]-bradykinin (McEachern et al. 1991). B2 receptors have been cloned from rat, mouse and human (McIntyre et al. 1993). Northern blot analysis has found the B2 mRNA to be most abundant in the human kidney, with significant levels also in the uterus, ileum, heart, lung, testis and brain (Hess et al. 1992).

Recent work by Farmer and colleagues (1988) has produced controversial evidence for a B3 kinin receptor that may be implicated in bradykinin induced pulmonary bronchoconstriction. The different range of actions produced by the B1 receptor and the B2 receptor subtypes may be explained by the interaction of each receptor/subtype to a specific G-protein coupled second messenger system. Also, kinin produced by different hormones, enzymes and other kininogenases may produce different affinities in the receptor sensitivity.

1.4.5 Kininogen

The primary physiological substrate for kallikreins are kininogens. Three types of kininogens have so far been described, the largest being a H-kininogen form found in blood, a L-kininogen form found in different tissues and blood (Worthy et al. 1990), and T-kininogen unique to the rat. T-kinogen acts as an acute phase protein associated with inflammation in the rat (Müller-Esterl 1989). Initially believed to be exclusive precursors

for kinins, kininogens have been discovered to perform a variety of other biological functions. These include the potent inhibition of cysteine proteinases [such as papain, cathepsins and calpain] (Müller-Esterl 1986).

Mammalian kininogens (HK and LK) are products of a single gene (Takagaki et al. 1985). This single kininogen gene (K gene), consisting of 11 exons of approximately 27 kilobases, codes for bovine and human kininogens (Kitamura et al. 1985). The nine exons located at the 5' terminus transcribe unique sequences common to both mammalian kininogen forms. Kinin mRNA is coded for by exon 10 and includes the first twelve amino acids after the carboxy-terminal bradykinin sequence. Exon 11 codes for the light chain (4 kD) of LK. The full exon 10 codes for the light chain (56 kD) of HK. The two kininogens differ in their size, structure and susceptibility to plasma and tissue kallikrein (Kerbiriou et al. 1980). Separate mRNA's have been identified for each kininogen. LK is a 50-68 kD β-globulin (409 amino acids, plasma concentration 2.4 um, isoelectric point 4.7) while HK is a 88-120 kD α-globulin (626 amino acids, plasma concentration 0.67 um, isoelectric point 4.3) (Schmaier et al. 1986a). Both kininogens are single chain glycoproteins and possess an amino-terminus heavy chain, a carboxy-terminus light chain, with a central kinin moeity sandwiched in-between, linked to both terminii by single disulphide bonds (Kellerman et al. 1987). The different regions of the kininogen molecule are separated into domains linked by serine protease-sensitive divisions (Vogel et al. 1988). These domains are characterised by distinct biological activities (figure 7). Although the individual domains possess separate functions, the molecule as a whole is involved in several biological processes. HK is predicted to have six domains, whereas LK and T-kininogen has five domains (Salvesen et al. 1986).

Figure 7: Structure domains of (A) H-kininogen (six 'apple' domains), and (B) L-kininogen (five 'apple domains); showing (✵) putative reaction sites, (⟠) potential disulphide loops, (⧖) carbohydrate attachment, (⊕) histidine-rich region, (⇂) cleavage site for kallikrein. For the heavy chain of both H-kininogen (HK) and L-kininogen (LK) D1, D2 and D3 are inhibitor domains for cysteine proteinases, while D4 is the kinin domain. The D5 domain of HK is a histidine-rich region and the light chain of HK expresses a binding site for plasma prekallikrein and clotting factor XI. For LK and its light chain the function of the D5 domain has not yet been determined.

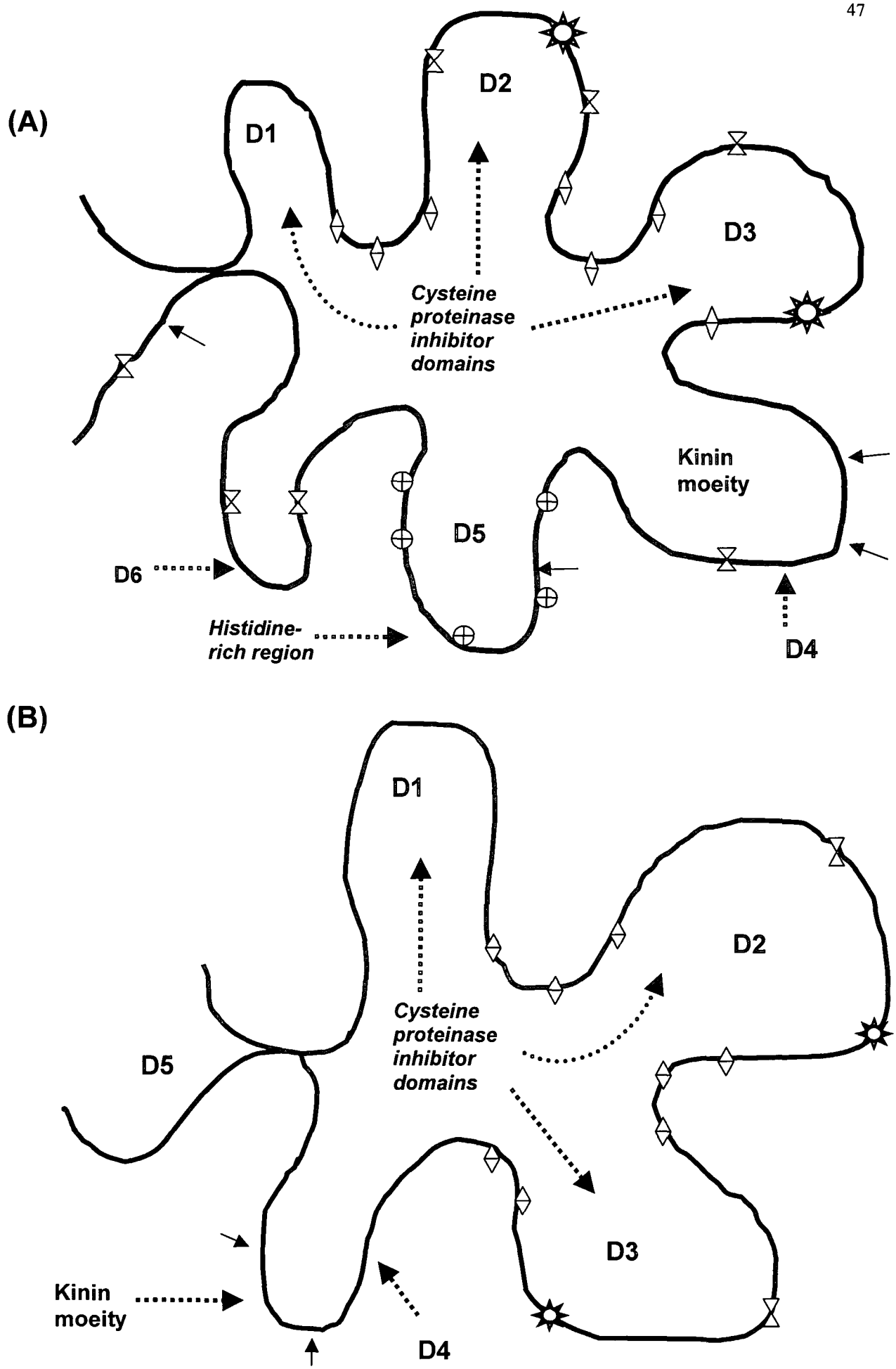
(A)
D1
D2
D3
Cysteine proteinase inhibitor domains
Kinin moeity
D5
D6
Histidine-rich region
D4
(B)
D1
D2
Cysteine proteinase inhibitor domains
D5
D3
Kinin moeity
D4

The human liver is identified as being the primary source of both HK and LK cDNA (Takagaki et al. 1985), along with human umbilical cord endothelial cells (HK sites of localisation and synthesis) (Schmaier et al. 1988). The key functions of kininogens, in addition to being natural substrates for kallikrein, are effected via kinins. In association with Hageman factor and prekallikrein, kininogen triggers the contact activation cascade. Kininogens also inhibit α-thrombin-induced platelet aggregation and endothelium activation (Hasan et al. 1995). Upon cleavage of the kinin moiety the cysteine proteinase inhibitory mechanism of the heavy chain becomes activated. This bioregulatory function inhibits thiol proteinases such as cathepsins B, H, and L, ficin, papain, and calpains I and II (Schmaier et al. 1986b). In addition, the antithrombin and fibrinolytic functions of the various domains are shown in figure 7.

1.4.6 Inhibitors, analogues and antagonists

Inhibitors of kallikrein: The actions of proteases are regulated, in part, by the presence of specific inhibitors. The diversity of the kallikreins was first noted with respect to their inhibitors (Eisen 1975). The first observation of kallikrein inhibition was made by Kraut et al. (1930a) when it was thought that trypsin, which originally released BK in serum plasma, was also responsible for kallikrein inhibition. It has since been established that kallikrein inhibitors in plasma, serum and other biological fluids are high molecular weight proteins able to occlude or bind catalyic sites of kallikrein (Worthy et al. 1990). Aprotinin (trasylol) is an *in vitro* inhibitor of kallikrein, and amino acid substitution has lead to the synthesis of [Val 15] aprotinin, which selectively binds plasma kallikrein and neutrophil elastase (Wenzel et al. 1986). In plasma there are three main kallikrein

inhibitors, namely α-1 antitrypsin, α-2 macroglobulin and C1 esterase inhibitor (Worthy et al. 1990). Kallikrein inhibitors have also been discovered in many bovine organs, including the lung, pancreas, lymph nodes and kidney (Bhoola et al. 1992b). These inhibitor compounds have been shown to inhibit proteins less than 20 kD. Chao and co-workers (1990) recently described a new kallikrein inhibitor found in the rat liver; and human liver, lung and salivary glands that inhibits active tissue kallikrein, neutrophil elastase and chymotrypsin, but not inhibit inactive/inactivated tissue kallikrein, plasma kallikrein, urokinase or collagenase.

Hydrolysis of kinins : Despite their considerable intrinsic potency, the duration of the biological actions of kinins are affected by their enzymatic hydrolysis. They are rapidly degraded in vivo ($t_{1/2}$ < 1 min in plasma), and endogenous circulating levels are even more difficult to measure (Ward, 1991, Rodell et al. 1995). In vivo and in vitro cleavage of kinins are due to the actions of proteases that belong to zinc-metallo-peptidases (Skidgel 1993), serine proteases, astacin-like metallopeptidases (Bond and Beynon 1995), and catheptic protease (Greenbaum and Sherman 1962) families. The kininase I family includes carboxypeptidase N (KI-CPN) and the cell membrane bound carboxypeptidase M (KI-CPM). Kininase I enzymes releases Arg^9 from the carboxy terrminus of BK and lys-BK (Bhoola et al. 1992b). Kininase II, identical to angiotensin-I converting enzyme (KII-ACE), and its family member neutral endopeptidase (KII-NEP) liberate the Phe^8-Arg^9 dipeptide from the kinin moeity. KII-ACE, subsequently, can cleave the remaining carboxy terminus Ser^6-Pro^7.

Kinin antagonists : Due to the pro-inflammatory effects of kinins, particular interest has been shown to the introduction of specific antagonists. Marceau et al (1983) reported

the synthesis of an analogue $Arg^9[Leu^8]$-BK that antagonised the action of $desArg^9$-BK. Stewart and Vavrek (1987) demonstrated that the replacement of Pro^7 on the BK molecule with an aromatic D amino acid conferred antagonistic ability on BK agonists and incidentally rendered more protection against carboxy-terminii peptidases. This single amino acid modification seemed to have converted agonistic behaviour. Several hundred analogues of the BK nonapeptide have since been synthesised and have given mixed results due to their antagonistic behaviour towards other agonists. NPC-567 proved ineffective in humans. Icatibant (HOE-140) is a B2 antagonist more potent than NPC-567 and displays greater resistance to degradation. NPC-17761 is an analogue of HOE-140 and CP-0127 has been fashioned as a bi-kinin-like peptide. In animals BK antagonists have been shown to block kinin-induced hypotensive shock, BK- as well as non-specific-stimulus-induced pain, nasal-allergies, and carageenan-and thermally-induced oedema (Rodell et al. 1995). Current research works toward development of compounds that would selectively affect specific actions of kinins.

1.5 Kallikrein-kinin system in the gastrointestinal tract

The elucidated role of the KKS in the gut is relatively uncertain. The localisation of tissue kallikrein in the gastro-intestinal cells has been reported by Schachter et al (1983) using cross-reacting salivary gland kallikrein antibody. In these studies tissue kallikrein was immunolocalised in goblet cells in the colon of human, rats and felines. Woodbury et al. (1978) was able to localise serine proteases in the intestinal goblet cells as well as in atypical mast cells in the lamina propria of the small intestine.

Kallikrein activity has also been noted in the rat and human gastric mucosa (Uchida et al. 1980, Uetsuji et al. 1982). It has been previously suggested that kallikrein and kininogenase (kallikrein-like) activity was a function of the exocrine pathways (Fuller and Funder 1986), but the localisation of tissue kallikrein mRNA in the rat gastrointestinal tract (Fuller et al. 1989) clearly indicates the synthesis of TK in the corpus of the stomach, and not from submaxillary or pancreatic sources. This, however, does not rule out the possibility that some of the kallikrein secretion, especially in the upper regions, may be derived from the circulation. Schachter and co-workers (1986) proposed that kallikrein may play a role in the processing of mucoprotein peptide segments. They also suggested that abnormalities in kallikrein function could contribute to cystic fibrosis. It is possible that kinins plays a role in the transport of electrolytes or various molecules (Schachter 1980), and in the regulation of local blood flow in the gastrointestinal tract (Overlack et al. 1983).

1.6 Hypothesis

***Helicobacter pylori* infection upregulates the expression of tissue kallikrein in gastric tissue, and by formation of kinins is involved in the pathogenesis of gastritis.**

1.7 Aims of the Project

To investigate the role of tissue kallikrein in *Helicobacter pylori*-associated gastritis through:

- measurement of tissue kallikrein in gastric lavage fluid by amidolytic microassay and enzyme-linked immunosorbent assays (ELISA)

- measurement of tissue kallikrein gastric tissue extracts by amidolytic microassay and enzyme-linked immunosorbent assays (ELISA)
- histochemical localisation of immuno-reactive tissue kallikrein, in the gastric antrum and fundus, in study individuals with dyspepsia, acute peptic ulcers and chronic gastritis associated with Hp infection.

CHAPTER 2

METHODS

METHODS

2.1 Sample collection

2.1.1 Ethical approval and Patient/Guardian Consent

Ethical permission for this study was obtained from the Ethics Committee of the Medical School, University of Natal. Permission for the collection of post-mortem tissue samples was obtained from Professor J. B. Botha, Head - Department of Forensic Medicine, University of Natal. Control stomach tissue was collected at autopsy with the co-operation of the attending forensic surgeon.

Biopsies of stomach tissue were collected by Dr. R.L. Bhoola, Consultant Specialist physician, under endoscopic examination, with the co-operation of staff at City Hospital, Durban and Maxwell Medical Centre, Durban. All patients were informed, either by us or the endoscopist caring for the patient, that a small piece of their tissue being removed would be used for both diagnosis and research into gastric disease. Written informed consent was obtained from all patients (refer to Appendix 1 at end of thesis for copy of patient consent form).

2.1.2 Post-mortem stomach tissue

Control stomach tissue was collected from individuals that had died in, or soon after arrival at hospital, or were declared dead on arrival at hospitals in the Durban area, as a result of trauma not involving the gastrointestinal tract or sudden unexplained death. The corpses had

been refrigerated immediately and had been maintained at 4°C in the hospital or state morgue, prior to removal of tissue.

At post-mortem, performed within 24 hours of death, histologically-undiagnosed, visually *normal* stomach tissue was removed and washed in cold sterile normal saline (physiological saline; 0.9% NaCl, Sabax) at 4°C to remove excess blood, before being divided into approximately 1 cm^3 wedges. This divided tissue was then suspended in 5% formal saline (41% formaldehyde/ 0.9% NaCl, 1:8 v/v) for 48 h at room temperature (RT).

2.1.3 Antral and Pyloric Punch Biopsies

Two sets of antral and pyloric punch-biopsies (Olympus Gastroscope, Japan) were taken from each patient undergoing routine clinical examination for suspected dyspepsia (n=24), by a medically qualified endoscopist. All relevant personal and clinical details together with all medications that had been administered were recorded. One set of antral and pyloric tissue-biopsy specimens was immersed in 5% formal saline, later to be processed and used for light and fluorescent microscopy. The other set of biopsies (antral and pyloric) was immersed in 2 ml 0.2 M Tris-Cl pH 8.2, at 4°C. This set of antral and pyloric tissue was then stored at -20°C, until processed and assayed for TK amidase enzymic assay (see section 2.5.2), and quantification by TK ELISA (see section 2.5.3).

2.1.4 Collection of Antral aspirates

While undergoing endoscopy, 20 ml of cold physiological (0.9% NaCl) saline, maintained at 4°C, was infused into the stomach of each patient, and the subsequent gastric washings

(lavage) aspirated into gastric traps containing 200 ul 0.2 M Tris-Cl, pH 8.2 at 4°C. These stomach washings were frozen and maintained at -20°C, until assayed for TK by the amidase assay (see section 2.5.2) and immuno-reactive TK by ELISA (see section 2.5.3).

2.2 Sample Processing and Extract Preparation

2.2.1 Preparation of tissue extracts

The frozen biopsy tissue (stored in 0.2 M Tris-Cl, pH 8.2) was thawed to 4°C, and then homogenised on ice, using a rotary homogeniser (Polytron PT 1200, Kinematica AG, Switzerland), at 15 second bursts interspersed with 30 second intervals, three times. To obtain a liquid viscosity, 0.5 ml cold physiological saline fractions were added as required. The homogenate was centrifuged at 3500 x g (Heraeus Megafuge 1.0 R, Germany) at 4°C for 20 min to remove unhomogenised tissue and cellular debris. The supernatants were carefully aspirated with a Pasteur pipette and transferred to a 1.5 ml eppendorf tube. For supernatants less than 1 ml, the pellets were resuspended in 0.5 ml cold physiological saline, homogenised and centrifuged as above. This second supernatant was then aspirated and added to the first. The pooled supernatant was centrifuged at 12700 x g (Heraeus Biofuge 13 R, Germany) at 4°C for 20 min, to remove fine particulate matter. The cellular pellets were then discarded. For both the measurement of total protein and the determination of the amidolytic/enzymic activity of TK (as ng TK/ug protein), 400 ul of supernatant was removed. The remainder of the supernate was used to perform TK immuno-assays (ELISA) as described in section 2.5.3.

2.2.2 Tissue processing: fixation and wax embedding for light microscopy

Formalin-fixed tissue samples from sections 2.1.2 and 2.1.3 were orientated and set in plastic tissue cassettes. The tissue samples were then processed by routine fixation and embedding techniques. Briefly, the tissue samples were dehydrated using absolute ethanol and xylene, and then embedded in paraffin-wax under sterile conditions, in an automatic tissue processor (Shandon, UK). These wax-embedded samples were used for both light microscopy and fluorescent microscopy. The automated fixation, dehydration, clearing, infiltration and embedding was carried out by the Department of Histopathology, University of Natal (see Annexe A, table 2.2.2)

2.2.3 Histology

2.2.3.1 Haematoxylin and Eosin (H&E) staining of wax-embedded tissue

Ultra-thin (3 um) sections of the wax-embedded tissue (see section 2.2.2) was cut on a rotary microtome (Jung RM2035, Leica, Germany) and floated onto poly-L-lysine (10% in distilled water v/v; Sigma, St. Louis) coated glass slides (LASEC, SA). The slides were allowed to air-dry and then stained with haematoxylin and eosin (H&E) to confirm the presence/absence of disease in post-mortem stomach, to determine the histological diagnosis in surgical samples, and to ensure that tissue processing was optimal. The following staining method was performed at room temperature (RT)

Protocol: The tissue was dewaxed in xylene (analytical grade; Saarchem, SA) twice for 5 min, then rehydrated through a series of increasingly dilute ethanolic

solutions (100%, 90%, 70% v/v in distilled water) for 1 min each, and finally into distilled water for 5 min. The slides were then immersed in Mayer's Haematoxylin (Sigma, St. Louis) for 5 min at RT, washed under running tap water for 5 min to intensify the stain, immersed in eosin (Sigma, St. Louis) for 2 min at RT, and then rinsed in 95 % ethanol (v/v in distilled water; Saarchem, SA) for 30 s. The stained tissue slides were then dehydrated in absolute ethanol (analytical grade; Saarchem, SA) twice for 1 min each at RT, and finally into xylene (analytical grade; Saarchem, SA). These were then mounted onto glass coverslips using a permanent mountant (Entellen, Merck). For detailed tabulated procedure, see Annexe A, table 2.2.3.1.

2.2.3.2 Giemsa staining of gastric tissue

Three um sections adhered onto poly-L-lysine- coated (Sigma, St. Louis) glass slides were stained with Giemsa stain (Sigma, St. Louis) to confirm the presence of *Helicobacter pylori* (Hp) bacteria. Giemsa staining was therefore used as a histological indicator of Hp presence (Laine et al., 1997). The following modified staining method was used.

Protocol: The tissue was dewaxed in xylene (analytical grade; Saarchem, SA) twice for 5 min, then rehydrated through a series of increasingly dilute ethanolic solutions (100%, 90%, 70%, v/v in distilled water) for 1 min each, and finally into distilled water for 5 min, all performed at RT. Next, the tissue sections were incubated with 40% Giemsa (Sigma, St. Louis, in distilled water v/v) for 1 h at 60^0C. The sections were then differentiated with 1% acetic acid (analytical grade;

Saarchem, SA; in distilled water v/v) for a few sec, and then rapidly dehydrated into xylene. Sections were mounted with a permanent mountant (Entellen, Merck).

For detailed tabulated method, see Annexe A, table 2.2.3.2

2.3 Sample storage

2.3.1 Tissue extracts

50 ul of 40 mM Tris-Cl, pH 8.0 (TK cocktail, see section on buffers and reagents) was added (for the purposes of molecular stability) to 400 ul of the extracts (see extracts prepared in sections 2.1.4 and 2.2.1), and stored at -20°C, to be used for the determination of total TK by ELISA.

2.3.2 Wax-embedded tissue

The wax-embedded tissue samples (see section 2.2.2) were stored at RT for future microscopic and immunohistochemical analysis.

2.4 Anti-tissue kallikrein antibodies

A polyclonal anti-TK antibody was raised in rabbit and goat host animals. Antibody generation was directed against recombinant tissue kallikrein (rTK) generated in *E.coli* transfected with human TK cDNA. Dr. Michael Kemme kindly supplied this rTK (Institute for Biochemistry, Technical University of Darmstadt, Darmstadt, Germany). The lyophilised

rTK protein was reconstituted in sterile physiological saline at a concentration of 1 ug/ul and frozen in 50 ul aliquots, maintained at -20°C.

2.4.1 Generation of a polyclonal goat anti-human rTK antibody

A single healthy adult goat host, housed at the Animal Farm facility in Durban, was used to raise polyclonal antibodies to rTK (ethical permission was obtained from the University of Durban-Westville Ethics Committee). All procedures were performed under ketamine (100 mg/ml) anaesthesia at a dose of 2-3 mg/kg body weight by intra-muscular-injection (IMI). 10 ml of blood was removed from the animal by venupuncture prior to inoculation. The goat was initially immunised by a single intra-muscular injection (IMI), with 100 ug of rTK dissolved in 25 ul 0.01M phosphate buffered saline (PBS) pH 7.2 and conjugated to 125 ul TiterMax^{TM} adjuvent. Thereafter, a booster programme using similar doses of conjugated antigen was initiated at four-week intervals over a 4-month period. Two days before each booster injection and weekly after the final booster 10 ml of venous blood, removed from the animal by venupuncture, was used to determine cross-reactivity, specificity and antibody titre. A standard single site ELISA using human urinary kallikrein (HUK, Calbiochem, USA), as described in section 2.4.4.1, was performed to determined the antibody titre. This titre initially increased from 1:50 and reached a plateau at 1:1600 following the final booster injection. At a final bleed, 200 ml of venous blood was removed from the animal. This whole blood was allowed to clot at RT, centrifuged at 1000 x g for 20min at RT, and the serum collected was stored at -20°C. Collection of blood was performed under such conditions so as to cause the animal no duress and as little discomfort as possible.

2.4.2 Generation of rabbit anti-human rTK antibody

Two healthy free-range adult rabbits were used to raise polyclonal antibodies to rTK. The animals were obtained from, and housed at the Biomedical Resource Centre, University of Durban-Westville, Durban (ethical permission was obtained from the University of Durban-Westville Ethics Committee) where all procedures were performed under ketamine (100 mg/ml) anaesthesia at a dose of 2-3 mg/kg body weight IMI. 2 ml of blood was removed from an ear vein of each rabbit prior to inoculation. For the initial inoculation three aliquots of antigen (150 ug) were pooled and conjugated to 150 ul TiterMax™ adjuvent. The rabbits were then initially immunised with 75 ul conjugated antigen by IMI into each hind limb. For the first booster injection, administered three weeks later, two aliquots of antigen were pooled (100 µg), conjugated to 100 ul TiterMax™ adjuvent, and 50 ul were injected into each hind limb. For the remainder of the booster programme one aliquot (50 ug) of rTK, dissolved in 50 ul 0.01M PBS pH 7.2, was conjugated to 100 ul TiterMax™ adjuvent, and 100 µl conjugate injected into a hind limb of each animal. Subsequent similar booster injections were rotated between limbs and administered at four-week intervals over a 4-month period. Two days before each booster injection, and weekly after the final booster, 2 ml of blood, removed from an ear vein, was used to determine cross-reactivity, specificity and sero-conversion. The antibody titre was determined by a standard single site ELISA using HUK (Calbiochem, USA) as described in section 2.4.4.1. When the antibody titre increased from 1:50 and finally plateaued at an optimum of 1:800 after the final booster injection, the animal was exsanguinated by cardiac puncture. The whole blood removed at each bleed was allowed to clot at RT, centrifuged at 1000 x g

(Heraeus Megafuge 1.0R, Germany) for 20 min at RT, and the serum collected was stored at -20°C.

2.4.3 Isolation and purification of Immunoglobulin G (IgG) from rabbit and goat serum

The isolation and characterisation of the anti-TK IgG was performed according to the method described by Johnstone and Thorpe (1982). The serum proteins were double precipitated with Na_2SO_4 (analytical grade; Saarchem, SA) and centrifuged at 3000xg (Heraeus Megafuge 1.0 R, Germany). The total protein precipitate was reconstituted up to 30% of the original volume with distilled water and dialysed against 0.07 M sodium phosphate buffer (pH 6.3) for 24 h at 4^0C. Isolation of IgG was performed using a diethylaminoethyl sephadex (DEAE A-25; Sigma, St. Louis) ion exchanger column with 0.02 M sodium phosphate (pH 8.0) as the equilibrating buffer. The IgG was eluted with 0.07 M sodium phosphate buffer (pH 6.3), and 1 ml fractions were collected at RT. Those fractions showing the highest absorbance at 280 nm (Shimadzu UV-1601, Japan) were pooled and the absorbance measured again. The detailed stepwise isolation of IgG is was follows.

Protocol: The serum was allowed to thaw to RT, and warmed to 25^0C in a water bath (Tecator, UK). Anhydrous sodium sulphate (analytical grade; Saarchem, SA) was added to make an 18% (w/v) solution at 25°C with frequent stirring. The solution was then centrifuged at 25°C at 3000 x g (Heraeus Megafuge 1.0 R, Germany) for 30 min. The supernatant was discarded, the protein precipitate volume was noted and then dissolved in warm H_2O up to half the original volume at 25^0C. Anhydrous sodium sulphate (analytical

grade; Saarchem, SA) was added to make a 14% (w/v) solution at 25^{0}C for 30 min, with frequent stirring. This solution was then centrifuged at 25°C at 3000 x g (Heraeus Megafuge 1.0 R, Germany) for 30 min. The supernatant was discarded and the protein precipitate redissolved in warm distilled water up to one third the starting volume and dialysed against 0.07 M phosphate buffer (pH 6.3) overnight at 4^{0}C to remove excess salt ions. Diethylaminoethyl sephadex (DEAE A-25, Sigma, St. Louis) ion exchanger was allowed to swell overnight at 4^{0}C in 0.02 M sodium phosphate (pH 8.0). A column was set up and the ion exchanger equilibrated with 50 column volumes of 0.02 M sodium phosphate (pH 8.0). The dialysate (protein solution) was run through the column at a rate of 1ml per minute with 10 column-volumes of 0.02 M sodium phosphate (pH 8.0), and then the IgG eluted with 0.07 M sodium phosphate buffer (pH 6.3) eluting buffer. 1 ml fractions were collected and the absorbance (Shimadzu UV-1601, Japan) of each measured at 280 nm against a blank using the eluting buffer. Fractions were collected until protein concentrations dropped to values less than 0.01 mg/ml. The fractions with the highest absorbances were pooled, and the pooled fraction absorbance measured at 280 nm (for detailed tabulated methods, see Annexe A, table 2.4.3).

For the goat anti-serum, the fractions with the highest absorbance at 280 nm were pooled and the collective protein concentration was 1.11 g/l. For the rabbit anti-serum the protein concentration of the pooled fractions with the highest absorbance at 280 nm, was 0.7 g/l. These IgG's were then characterised on a 7% sodium dodecyl-sulphate polyacrylamide gel (SDS-PAGE) against IgG molecular weight markers (Sigma, St. Louis MW SDS 70, Sigma, St. Louis) to verify their purity and 30 ul aliquots were stored and maintained at -20^{0}C.

2.4.4 Quality control

The purity, immuno-specificity and sensitivity of the antibodies were verified by a single site ELISA using HUK (Calbiochem, USA), Western blot (protein immuno-blotting), positive control tissue and pre-adsorption with rTK in immunocytochemical (ICC) studies, as well as the use of control urine in an ELISA which demonstrated the reproducibility of the results obtained with these antibodies.

2.4.4.1 Titre determination

The stepwise determination of the anti-rTK antibody titre in rabbit and goat serum by a standard single site ELISA using HUK (Calbiochem, USA) was as follows.

Protocol: An aliquot of HUK (1200 ng/ml physiological saline stored at -20^{0}C) was thawed at 4^{0}C and diluted in coating buffer (Na_2CO_3/$NaHCO_3$, pH 9.6). An ELISA microtitre plate (Corning, USA) was coated 100 ul/well with 5 ug/ml HUK and allowed to incubate overnight at 4^{0}C. The plate was washed 3 times for 3 min each with 0.05% Tween 20 (analytical grade; Saarchem, SA)/0.01M PBS, pH 7.2 at RT. All wells were then blocked twice with 200 ul milk blocker (5% Elite/5% BSA) for 30 min each time at RT, with a 0.05% Tween 20 (analytical grade; Saarchem, SA)/ 0.01M PBS, pH 7.2 wash step in-between for 3 min thrice. Serial dilutions of the anti-serum (1/200; 1/400; 1/800; 1/1600 and 1/3200) were made up in 0.01M PBS/0.01% BSA (v/v). Each dilution (100 ul) was added in triplicate to the plate and incubated for 1 h at 37^{0}C in a shaking water bath (Tecator, UK). Blank wells were filled with 100 ul 0.01M PBS/0.1% BSA. The

plate was then washed 3 times for 3 min each with 0.01M PBS pH 7.2/0.05% Tween 20 (analytical grade; Saarchem, SA) at RT. Next, each well was loaded with 100 ul of alkaline phosphatase conjugated anti-goat or anti-rabbit IgG (Sigma, St. Louis), diluted 1/250 in 0.01M PBS/0.01% BSA (v/v), and the plate incubated for 1 h at 37^0C in a shaking water bath (Tecator, UK). The plate was then washed 3 times for 3 min each with 0.05% Tween 20 (analytical grade; Saarchem, SA)/ 0.01M PBS, pH 7.2 at RT. Finally, to facilitate chromogenic colour development, the plate was loaded 100 ul/well with 1mg/ml phosphatase substrate (pNPP; Sigma, St. Louis) and absorbances read at 405 nm on a Biorad Microplate Reader 3550 (Biorad, UK) utilising Biorad Microplate Manager software, until readings peaked at 1.0-1.5 absorbance units.

2.4.4.2 Western blotting

Goat anti-human and rabbit anti-human tissue kallikrein antibodies were characterised on SDS-PAGE and Western-blot transfer, for specificity and purity as follows (refer to Plate 3c):

Electrophoresis: Recombinant tissue pro-kallikrein (to which the above-mentioned antibodies) were directed, was run on a 10% sodium-dodecyl-sulfate polyacrylamide electrophoresis gel. Preparation of the 10% resolving gel and 5% stacking gel were prepared according to the method of Sambrook et al. (1989). 4ug of a 2.1 mg/ml rTK protein was added to 10ul of sample loading buffer (10% SDS, 1% bromophenol blue, 5% ß-mercaptoethanol, 1% glycerol, 0.5M tris-Cl, pH 6.8), boiled at 95 ^{0}C for 5 min, and immediately plunged into ice. Low range

molecular weight markers (Biorad; lysozyme 14.4 kD, trypsin inhibitor 21.5 kD, carbonic anhydrase 31 kD, ovalbumin 45 kD serum albumin 66.2 kD, phosphorylase B 97.4 kD) was also added to sample loading buffer and boiled. 10ul of denatured protein and denatured molecular weight markers was loaded onto the SDS gel and electrophoresed at 160 mV for one hour using a discontinuous buffer system (0.4M glycine, 0.02M SDS, 0.12M Tris-Cl pH 8.3) on a Biorad Mini-Protean® Electrophoresis Cell (Biorad, California) using a Biorad Powerpac 3000 power source.

Controls for the electropheretic run was 1 mg/ml BSA and 1mg/ml human IgG (similar concentration and denaturing conditions as per rTK)
On completion of the run (taken when the dye front had reached within 1cm of the base of the gel), the gel was removed from the gel apparatus.

Western blotting: The gel was equlibrated in transfer buffer (10% methanol, 0.025M Tris-Cl, 0.192M glycine, pH 8.3) for 15 min, as was filter blotting paper (Whatman, cut to the same size as the gel), 0.2 μm Biorad nitrocellulose membrane and Biorad fibre pads. The gel sandwich was assembled according to the Biorad Mini Trans-Blot® Electrophoretic Transfer Cell instruction manual (Biorad, California), and protein transfer was performed for two hours at 90 mA.

Immunoblotting: Upon completion of the protein transfer, the membrane was incubated with 0.1% Ponceau S/ 5% acetic acid (Sigma, St. Louis) for 10min at RT. The membrane was then washed in dH_2O and the protein bands visible were marked in pencil. The membrane was blocked with 5% milk blocker (0.01%

antifoam A, 0.02 azide, 5% milk protein, 0.01M PBS, pH 7.4) overnight at 4^0C. Next the membrane was incubated with goat anti-human tissue kallikrein IgG (isolated in section 2.4.3) (1/1000 in 5% milk blocking reagent) for 2 h at RT on a platform shaker. The membrane was then washed in PBS (3X10min/RT), blocked with 5% milk blocker for 30 min/RT, and incubated with 1/1000 (in 5% milk blocker) anti-goat IgG alkaline phosphatase conjugate (Sigma, St. Louis) for 1 h at RT. The membrane was again washed in PBS (3X10min/RT), blocked with 5% milk blocker for 30 min/RT, and then washed in detection buffer (0.1M Tris-Cl (pH 9.5), 0.05M $MgCl_2$, 0.1M NaCl) for 10 min. A 0.375 mg/ml NBT (nitro blue tetrazolium chloride)/ 0.188 mg/ml BCIP (5-bromo-4-chloro-3-indoyl-phosphate) chromogen solution was used to develop the membrane for a few minutes in the dark at RT. When sufficient colour development showed visible immunoprobed protein bands the reaction was quenched with dH_2O.

2.4.4.3 Positive tissue and method controls for immunocytochemistry (ICC)

Human salivary gland tissue was used a positive control tissue to demonstrate localisation, upon previous evidence of TK abundance in such tissue (Schachter et al. 1978, Simson and Condon 1988). Samples of fresh control human salivary gland were collected at post-mortem, fixed in 5% formalin and embedded in paraffin-wax, as outlined in section 2.1.2. During each immuno-labelling run, this tissue, demonstrating the presence of TK in the ducts of the human salivary gland, served as an appropriate method control for the labelling procedure.

Plate 3c Photo micrograph representing the western blot immuno-detection of recombinant tissue kallikrein with goat anti-human tissue kallikrein IgG by 10% polyacrylamide gel electrophoresis (PAGE), protein blotting by wet tranfer (0.45 um nitrocellulose membrane), and immunodetection. Lane 1 represents the molecular weight markers (sizes of the different protein bands in Kd) stained with India ink (Pelikan Fount, Germany). Lane 2 represents the recombinant TK as stained by India ink. Lane 3 represents the recombinant TK immuno-stained with goat anti-human tissue kallikrein.

MWM: Molecular weight markers

rTK: recombinant tissue kallikrein

kD: kilodaltons

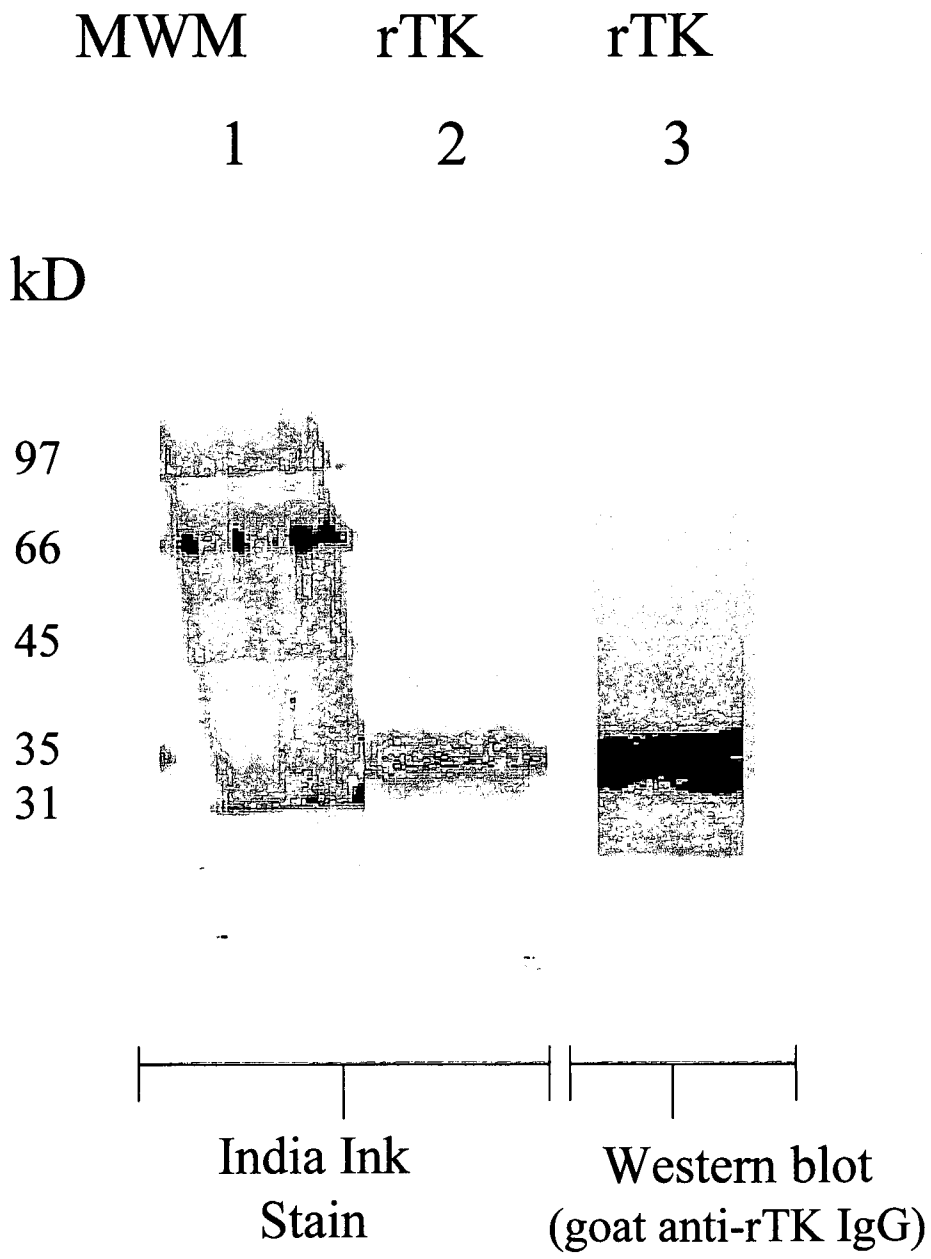
MWM
rTK
rTK
1
2
3
kD
97
66
45
35
31
India Ink
Stain
Western blot
(goat anti-rTK IgG)

Plate 3d: Photo micrograph representing the western blot immuno-detection of recombinant tissue kallikrein with rabbit anti-human tissue kallikrein IgG by 10% polyacrylamide gel electrophoresis (PAGE), protein blotting by wet tranfer (0.45 um nitrocellulose membrane), and immunodetection. Lane 1 represents the molecular weight markers (sizes of the different protein bands in Kd) stained with India ink (Pelikan Fount, Germany). Lane 2 represents the recombinant TK as stained by India ink. Lane 3 represents plasma kallikrein, used as a method control. Lane 4 represents the recombinant TK immuno-stained with rabbit anti-human tissue kallikrein.

MWM: molecular weight marker

rTK: recombinant tissue kallikrein

PK: plasma kallikrein

kD: kilodaltons

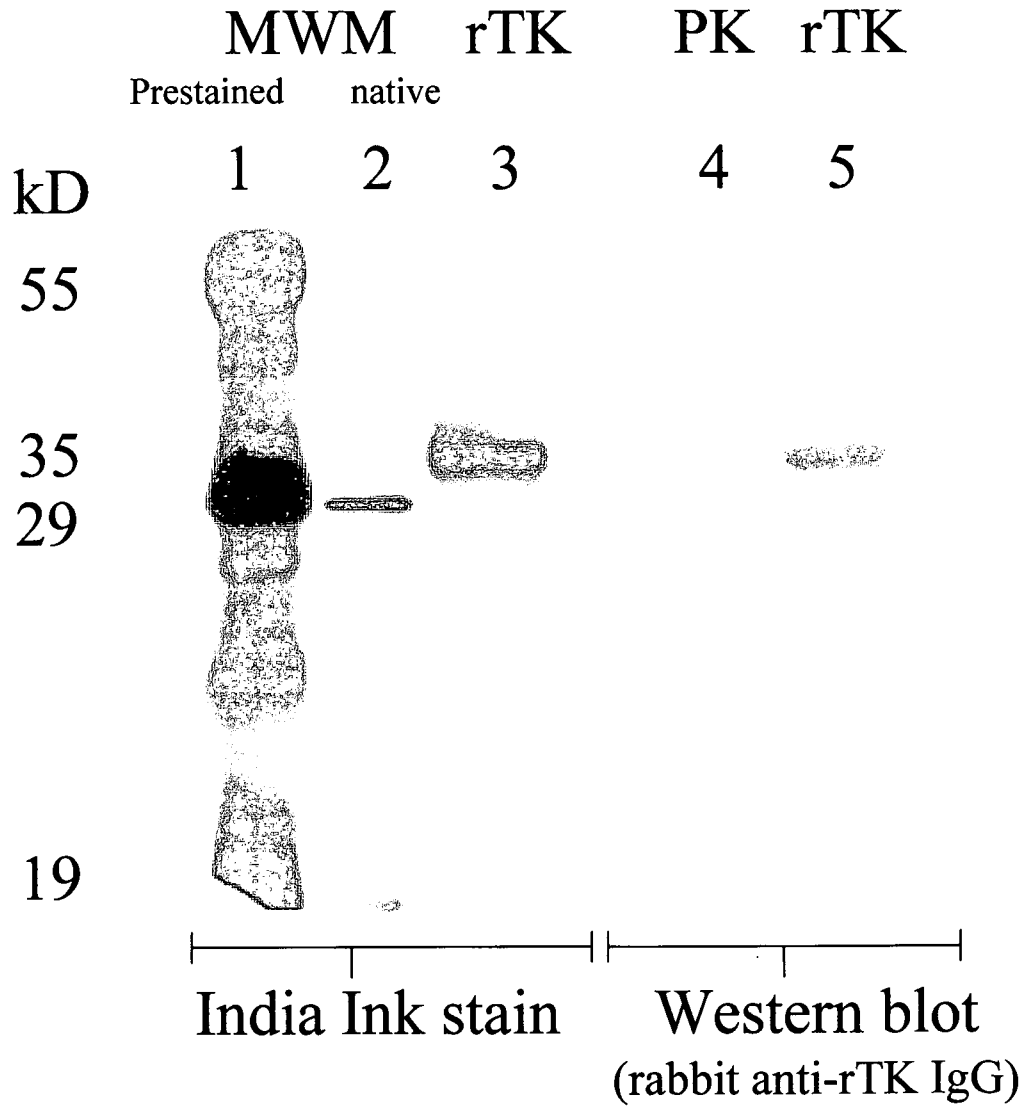
MWM
Prestained
rTK
native
PK
rTK
kD
1
2
3
4
5
55
35
29
19
India Ink stain
Western blot
(rabbit anti-rTK IgG)

2.4.4.4 Negative method controls for ICC

The absence of positive specific immuno-labelling following pre-adsorption of the primary antibody with an excess of rTK demonstrated the specificity of the antibody utilised. The goat anti-human rTK antibody was diluted 1:500 with 0.01M phosphate buffer (pH 7.2) and added to a 2 mg/ml stock solution of rTK to yield a final concentration of 1 mg/ml antigen (rTK). This antibody-antigen conjugate was incubated overnight at 4°C to allow maximum formation of antigen-antibody complexes. Following centrifugation (2200 x g, 4°C, Heraeus Biofuge 1.3 R, Germany) the supernatant was used instead of the primary antibody in the immunocytochemistry experiments described in section 2.5.4.

2.4.4.5 Controls for amidase micro-assay and TK ELISA

A large volume (approximately 2 l) of pooled control human urine (from normal healthy volunteers), was collected in bacitracin (99.6units/ml; Sigma, St. Louis). 1 ml aliquots were stored in 50 ul of 40 mM Tris-Cl (pH 8.0) at -20°C. Serial dilutions of this urine were included as controls for both the TK Amidolytic assay and TK ELISA. These results were then used to calculate both the intra and inter assay coefficients of variation of both the assays.

One set of plain urine samples, stored at -20°C, without any buffer, was used to measure total protein by Bradford Protein Determination (Bradford, 1976).

2.5 Tissue kallikrein measurements

2.5.1 Assays for tissue kallikrein

For the tissue extracts (see section 2.2.1), the presence of enzymatically active TK was determined by an amidolytic assay, while total immuno-reactive TK was measured by ELISA. The localisation of TK in tissue samples was demonstrated by immuno-histochemistry (ICC).

Commercially purified human urinary tissue kallikrein (HUK, Calbiochem, USA) was used to validate both the amidolytic assay and ELISA. These results were used to calculate both the intra- and inter-assay coefficients of variation for both assays.

2.5.2 Enzymic assay (amidolytic micro-assay)

This end-point chromogenic assay was used to measure functionally active TK in biological samples, as well as in extracts prepared from the gastric samples (see section 2.3.1), using a microtitre plate. The amount of functionally active TK was measured by assessing the amidolytic activity of the enzyme TK on a selective, synthetic substrate, H-D-Val-Leu-Arg-pNA (S2266; Kabivitrum, Sweden) (Amundson 1979) in the presence of soybean trypsin inhibitor (SBTI; Sigma, St. Louis) and ethylenediaminetetraacetic acid (EDTA; Sigma, St.Louis) as modified by Figueroa et al. (1989) and further developed as an end-point assay in a microtitre plate by Rahman et al. (1994). In this amidase assay, the enzymic activity of TK on H-D-Val-LeuArg-pNA releases para-nitroaniline (pNA), which has a peak absorbance at 405 nm. A standard curve was set up using commercially available

purified human urinary kallikrein, HUK (Calbiochem, USA) from which the concentration of TK in the sample extracts were calculated using Biorad Microplate Manager software (Biorad, UK). Following the measurement of total protein in an aliquot of the extract, using the Bradford Protein Determination method (Bradford 1976), the enzymic activity of TK was expressed as ng TK/ug protein. Control urine from section 2.4.4.5 was included in each assay run to determine inter-assay coefficients of variation. During each assay, 2 sets of plates were processed simultaneously, one being the measure of basal activity of TK at zero time, and the other measuring the enzymic activity of TK after a 3 h substrate incubation. The method is as follows.

Protocol: For the standard curve 600 ul of 400 ng/ml HUK standard, stored at -20°C as 1200 ng/ml aliquots, was prepared in amidase buffer (0.2 M Tris-Cl, pH 8.2). 300 ul of this standard was serially diluted to 6.25 ng/ml in amidase buffer. 50 ul (in triplicate) of each standard dilution was added to two 96-well tissue culture plates (Corning Cell Wells™, Corning, USA) designated *blank* and *substrate* plates. For the control curve, pooled urine (from section 2.4.4.5) was serially diluted down to 1/64 in amidase buffer (0.2 M Tris-Cl, pH 8.2) and 50 ul of each dilution (in triplicate) was added to both plates. 50 ul of each sample (from section 2.3.1) was loaded (in triplicate) onto each plate. Next, 50 ul of assay buffer (60 mg/ml SBTI, 75 mg/ml EDTA in amidase buffer) was added to each well in both plates. To the *blank* plate 50 ul of dH_20 was added to each well, and the absorbance of this plate read at 405 nm on a Biorad Microplate Reader 3550 at RT. To the *substrate* plate 50 ul of substrate S2266 (1.5 mM in deionised distilled water, as per manufacturer's instructions) was added to each well, and the plate incubated for 3 h at 37^0C. The absorbance of this *substrate* plate was then read at 405 nm on a Biorad Microplate Reader 3550 at RT.

To determine the amidolytic activity of TK, the blank absorbance values were subtracted from the standards, controls and samples, on each plate. Then, the values of each standard, control and sample from the *blank* plate (zero activity) were subtracted from the *substrate* plate (enzymic activity). The net enzymic activity of the HUK standards was used to set up a plot of absorbance versus HUK concentration using Biorad Microplate Manager software (Biorad, UK). The concentration of the TK activity of the samples (in ng TK/ml sample) was extrapolated from this graph (see Annexe A table 2.5.2a).

2.5.2.1 Bradford protein determination

An aliquot of each sample was used for protein determination (in triplicate) using the Bradford micro assay (Bradford, 1976). The net enzymic activity of TK was thus expressed as a ratio of the amidolytic activity and the protein concentration (ng TK/ug protein).

Protocol: To determine the protein concentration, a 1mg/ml protein standard, bovine serum albumin (BSA, fraction V, Boehringer Mannheim, Germany) was made up in distilled water. This was serially diluted down to 0.016 mg/ml in distilled water. 30 ul of each standard was added (in triplicate) to wells of a tissue culture microtitre plate (Corning Cell Wells™, Corning, USA). For blanks, 30 ul of distilled water was added (in triplicate) to the plate. 30 ul of sample was also added (in triplicate) to the tissue culture plate. Next, 300 ul of Biorad Protein Assay Reagent (diluted 1:5 in distilled water; Biorad, UK) was added to each well containing standard, blank and sample, and the absorbance read at 595 nm on a Biorad Microplate reader 3550 (Biorad, UK). The mean blank absorbances were

subtracted from each standard and sample absorbance. A standard curve plot of absorbance versus protein concentration was set up using the Biorad Microplate Manager software and the protein concentrations of each sample were extrapolated from this.

2.5.3 TK ELISA

The basic principle of the ELISA is to use an enzyme label to quantify the binding of an analyte, using a solid-phase system for the separation of bound and free portions.

First described by Engvall and Perlman (1971) to indirectly measure antibodies using antiglobulins as indicators, it has undergone continuous modification and refinement, including the use of the avidin-biotin binding system (Kendall et al. 1983, Bayer and Wilchik 1974). Although the ELISA is reported to be almost equal to RIA (radioimmuno assay) and IFA (immunofluorescent assay) it has the advantage of being non-isotopic, safe, flexible, convenient and fast (Voller et al. 1978). The utilisation of an indirect, non-competitive assay 'sandwiches' the analyte between two macromolecules, one of which is linked to an enzyme label (Nilsson 1990). In this heterogeneous enzyme immuno-assay, the amount of antigen attached is indicated by an enzyme-labelled immunoglobulin and enzyme substrate system whereby the amount of substrate by-product is colorimetrically determined.

An aliquot of the sample extract/filtrate (section 2.3.1) was used to measure the total TK by a basic sandwich ELISA using goat anti-human rTK IgG and rabbit anti-human rTK IgG from sections 2.4.1 and 2.4.2 respectively. A third antibody, anti-rabbit IgG (Sigma, St. Louis), conjugated to the enzyme alkaline phosphatase, interacts with the rabbit anti-human rTK IgG. The conjugated alkaline phosphatase then cleaves the chromogenic substrate disodium p-

nitrophenyl phosphate (pNPP) to produce a yellow colour that has peak absorbance at 405 nm.

Protocol: A 96 well, flat-bottomed polystyrene ELISA plate (Corning, USA) was loaded 100 ul/well with primary antibody, goat anti-human rTK IgG (30 ng/ml goat anti-human rTK IgG in coating buffer) and incubated at 4^0C overnight. The wells were then washed with 200 ul 0.01M PBS/0.5%Tween three times for three min each at RT. The wells were incubated with 200 ul 5% milk blocker twice for 30 min each at RT, with a 0.01M PBS/0.5%Tween wash in-between. Next, a 1200 ng/ ml aliquot of HUK (Calbiochem, USA), stored at -20^0C, was thawed at 4^0C and then serially diluted from 40 ng/ml to 0.625 ng/ ml in 0.01M PBS (pH 7.2), and 100 ul of each standard (in triplicate) added to the wells. Blank wells (in triplicate) were filled with 100 ul of 0.01M PBS (pH 7.2) and control wells were filled (in triplicate) with 100 ul/well pool urine (see section 2.4.4.5) diluted 1/8 to 1/512 in 0.01M PBS (pH 7.2). 100 ul of sample (in triplicate) was also loaded onto the plate. The plate was then incubated at 37^0C for 1 h in a shaking water bath (Tecator, UK). The wells were then washed with 200 ul 0.01M PBS/0.5% Tween three times for three min each at RT. Next, 100 ul of 25 ng/ml secondary antibody rabbit anti-human rTK IgG (in 0.01M PBS, pH 7.2) was loaded into every well and the plate incubated at 37^0C for 1 h in a shaking water bath (Tecator, UK). The wells were then washed with 200 ul 0.01M PBS/0.5% Tween three times for three min each at RT. Finally, the wells were all loaded with 100 ul of a 1 mg/ml chromogenic pNPP substrate (Sigma, St. Louis, 1 tablet in 5 ml of $MgCl_2$/diethanolamine, pH 9.6 substrate buffer) and the colour was allowed to develop until the highest absorbances peaked at 1 to 1.5 absorbance units. Readings were taken at RT with a Biorad Microplate Reader 3550 (Biorad, UK) using Biorad Microplate Manager software. The mean blank absorbance was subtracted

from the standards, controls and samples, and a curve of absorbance versus HUK concentration was plotted. The concentrations of the samples were extrapolated from this graph (see Annexe A table 2.5.3)

2.5.4 Immunolocalisation of TK

3 micron sections of the wax-embedded tissue (section 2.2.2) were adhered onto adhesive coated (poly-L-lysine; Sigma, St. Louis) slides and used for the detection of immuno-reactive TK by standard histochemistry techniques, using polyclonal goat anti-human rTK IgG (see section 2.4.3) as the primary antibody and conjugated antibodies containing either a fluorescent probe visualised by confocal microscopy, or the peroxidase-antiperoxidase (PAP) immuno-enzyme complex and diaminobenzidine as the chromogen visualised by light microscopy. The following detailed methods are modifications of the method described by Figueroa et al. (1989)

2.5.4.1 Localisation of TK by immuno-precipitation

Protocol: The three-micron thin sections of the wax-embedded tissue sections (section 2.2.2) on glass slides were heated on a heating block (Clifton, UK) at 60°C (to melt the wax) for 5 min. The peroxidase-anti-peroxidase (PAP) method required dewaxing the tissue sections in analytical grade xylene (analytical grade; Saarchem, SA) twice for 10 min each, rehydration with graded ethanolic solutions (100%, 90%, 70% and 50% in distilled water, v/v) and distilled water as the final rehydrant. When the tissue was approximately 50% rehydrated, it was immersed in absolute methanol (analytical grade; Saarchem, SA) for 20 min to quench

endogenous tissue-peroxidase activity. The tissue was then boiled in a metal-salt solution, 0.1M sodium citrate, pH 6.0 (analytical grade; Saarchem, SA) at 80°C for 10 min (antigen retrieval) (Shi 1991) in a conventional microwave oven (R-4A52; Sharp Corp., Japan). The tissue in the boiling solution was allowed to cool down to RT (approximately 20 - 25 min). The tissue-sections were then further blocked with 10% H_2O_2 (analytical grade; Saarchem, SA)/90% absolute methanol (v/v) for 20 min to quench endogenous peroxidases. Incubation with the primary antibody, polyclonal goat anti-human rTK IgG [diluted 1:1000 with 0.01 M phosphate buffer (pH 7.2)/1% BSA] was performed at 4°C for 18 h in a humidified chamber. Then, the tissue was treated with a peroxidase-anti-peroxidase (PAP) strepavidin-biotin conjugating system (LSAB K0690; Dako, USA) for 20 min. each. This entailed incubating the tissue with a universal (goat, rabbit, mouse) IgG-biotin link for 20 min at RT in a humidified chamber. Next, the tissue sections were covered with a strepavidin-peroxidase conjugate for 20 min at RT in a humidified chamber. The labelled antibody bound to the PAP immuno-enzyme complex was visualised by incubating the sections, in the dark, for 5 to 7 min with liquid diaminobenzidine (DAB) precipitant (DAB K3465; Dako, USA). The sections were counterstained with Mayers Haematoxylin (Sigma, St. Louis,) for 3 min and intensified under running tap water for 5 min. Sections were then dehydrated by a reversal of the dehydration process from distilled water, through the increasingly concentrated ethanolic solutions into xylene, and finally mounted with a permanent medium (Entellen, Merck). Results were viewed by conventional light microscopy under a Nikon photo-microscope (Nikon Optiphot; Nikon, Japan)

All incubations were carried out in a humidifying chamber. Between incubations the sections were washed thoroughly by submerging the slides in PBS [0.01 M phosphate buffer (pH 7.2) containing 0,0027 M potassium chloride, 0.137 M sodium chloride; Sigma, St. Louis] for 5 min.

Controls for this procedure involved replacing the primary antibody with goat non-immune serum diluted in 0.01 M phosphate buffer (pH 7.2)/1% BSA. Method controls were 1^0 antibody replaced with buffer. All dilutions made up in 0.01 M PBS/1% BSA (pH 7.2). Tissue sections were not allowed to dry out at any time during the labelling process. The labelled slides were stored in the dark. For a detailed tabulated method, see Annexe A, table 2.5.4.1

2.5.4.2 Localisation of TK by immuno-florescence

Antigen enhancement: This required heating, dewaxing and rehydrating three-micron thin wax-embedded sections with increasingly dilute alcohol solutions (100%, 90%, 70% and 50%), with distilled water as the final rehydrant (as described for immunoprecipitation, section 2.5.4.1) The tissue was then boiled in 0.1 M sodium citrate (pH 6.0) at 80°C for 10 min (antigen retrieval) in a microwave oven (R-4A52, Sharp Corp., Japan), and allowed to cool down to RT (approximately 15 - 20 min).

Protocol: Fc receptors in the tissue and other non-specific sites were blocked with 1% human IgG (Sigma, St. Louis) for 10 min at RT. The tissue sections

were then incubated with the specific goat anti-human rTK IgG diluted 1:1000 with 0.01M phosphate buffer (pH 7.2)/ 1% BSA, at 4°C, under humid conditions, for 18 h. Finally, the bound TK-primary-antibody-complex was conjugated to a fluorescein labelled [fluorescein isothiocyanate (FITC), 525 nm emission; Sigma, St. Louis] rabbit anti-goat IgG for 30 min at RT. The labelled tissue slides were then mounted onto glass coverslips with an aqueous mountant (90% glycerol/10% PBS, v/v) and the edges of the coverslips sealed with commercial fingernail varnish. All washing steps, after each incubation, were carried out in 0.01 M phosphate buffered saline (pH 7.2) (Sigma, St. Louis). Fluorescent emission was analysed using the Leica TD4 confocal microscopy system (Leica, Germany). Method controls were 1^0 antibody replaced with buffer. All dilutions were made up in 0.01 M PBS/1% BSA. Tissue sections were not allowed to dry out at any stage and labelled slides were stored in the dark. For the detailed tabulated method see Annexe A, table 2.5.4.2

Annexe A

Table 2.2.2 Fixation, Dehydration and Embedding schedule for light microscopy

STEP	SOLUTION	TEMP	TIME
1.	Fixation - 5% formal saline	24°C	1 h
2.	Fixation - 5% formal saline	24°C	1 h
3.	Dehydration - absolute ethanol	24°C	1 h
4.	Dehydration - absolute ethanol	24°C	1 h
5.	Dehydration - absolute ethanol	24°C	1 h
6.	Dehydration - absolute ethanol	35°C	1 h
7.	Dehydration - absolute ethanol	35°C	1 h
8.	Dehydration - absolute ethanol	35°C	1 h
9.	Dehydration - absolute ethanol	35°C	1 h
10.	Clearing - xylene	35°C	1 h
11.	Clearing - xylene	35°C	1 h
12.	Vacuum infiltration 1 - paraffin wax	60°C	1 h
13.	Vacuum infiltration 2 - paraffin wax	60°C	1 h
14.	Embedding - paraffin wax	20°C	20 min

Table 2.2.3.1 H&E Staining of wax-embedded tissue

STEP	SOLUTION	TIME
1.	Dewax - Xylene	2 x 5 min
2.	Rehydrate - Absolute ethanol	2 x 1 min
3.	Rehydrate - 90% ethanol	1 min
4.	Rehydrate - 70% ethanol	1 min
5.	Rehydrate - water	1 min
6.	Haemotoxylin - immerse slides in Mayer's Haemotoxylin (Sigma, St. Louis)	5 min
7.	Blue - rinse slides in running tap water	5 min
8.	Eosin - immerse slides in Eosin (Sigma, St. Louis)	2 min
9.	Rinse - by quickly immersing slides in 95% ethanol	30 s
10.	Dehydrate - Absolute ethanol	2 x 1 min
11.	Dehydrate - Xylene	1 min
12.	Mount - maintain in xylene until mounting in Entellen (Merck)	

Table 2.2.3.2 Giemsa staining of wax-embedded tissue

STEP	SOLUTION	TEMP.	Time
1	Dewax tissue in xylene (analytical grade; Saarchem, SA)	RT	2 x 3 min
2	Rehydrate - 100% EtOH (analytical grade; Saarchem, SA)	RT	2 x 5 min
3	Rehydrate - 90% ethanol	RT	1 min
4	Rehydrate - 70% ethanol	RT	1 min
5	Rehydrate - water	RT	1 min
6	Stain with Giemsa (40% in dH_20)	60^0C	1 h
7	Wash in 0.01M PBS (pH 7.2)	RT	5 min
8	Differentiate with 1% acetic acid (in dH_20, analytical grade; Saarchem, SA)	RT	5-10 s
9	Wash in 0.01M PBS (pH 7.2)	RT	5 min
10	Rapidly dehydrate 70 % ethanol	RT	30 s
11	Dehydrate 90 % ethanol	RT	30 s
12	Mount with permanent mountant (Entellen, Merck)	RT	

Table 2.4.3 Isolation anti-tissue kallikrein IgG from Anti-serum

STEP	SOLUTION	TEMP.	TIME
1.	Warm serum in water bath	25°C	15 min
2.	Add anhydrous sodium sulphate to make a 18% (w/v) solution, stir to dissolve and incubate	25^0C	30 min
3.	Centrifuge at 3000xg	25^0C	30 min
4.	Discard supernatant, note volume of protein precipitate and redissolve in warm H_2O up to half the original volume	25^0C	
5.	Add anhydrous sodium sulphate to make a 14% (w/v) solution, stir and incubate	25^0C	30 min
6.	Centrifuge at 3000xg	25^0C	30 min
7.	Discard supernatant, redissolve precipitate in warm water up to one third of starting volume and dialyse against 0.07 M phosphate buffer (pH 6.3)	4^0C	ON
8.	Equilibrate ion exchanger (DEAE-cellulose) with the 0.02 M phosphate buffer (pH 8.0)	4^0C	ON
9.	Pack hydrated ion exchanger into a polypropylene column and wash with 50 column volumes 0.02 M phosphate buffer (pH 8.0) at a flow rate 1 ml/min	RT	
10.	Load - dialysate	RT	
11.	Elute - with 0.07 M phosphate buffer (pH 6.3), collect 1 ml fractions	RT	
12.	Measure absorbance at 280 nm	RT	
13.	Pool fractions with highest absorbance, store at -20^0C		

Table 2.4.4.1 Titre determination for anti-rTK antibody in rabbit and goat serum

STEP	SOLUTION	TEMP.	TIME
1.	Dilute HUK (stored at -20°C in aliquots of 1200 ng/400 ul physiological saline) in 4ml coating buffer [Na_2CO_3/$NaHCO_3$, (pH 9.6)] to obtain 5 ug HUK/ml coating buffer	4^0C	
2.	Coat ELISA plate (Corning) by adding 100ul of diluted HUK to each well	4^0C	ON
3.	Wash plate with 0.1 M PBS/Tween	RT	3x3min
4.	Block plate twice with 5%Elite/5%BSA	RT	2x30min
5.	Dilute serum 1/200; 1/400; 1/800; 1/1600 and 1/3200 with 0.1 M PBS/0.1% BSA	4^0C	
6.	Load 100ul of diluted serum (triplicate). Blanks are wells filled with 100 ul 0.1 M PBS/0.1% BSA	37^0C	60 min
7.	Wash plate with 0.1 M PBS/Tween	RT	3x3min
8.	Load 100ul of alkaline phosphatase conjugated anti-goat or anti-rabbit IgG diluted 1/250 in 0.1M PBS/0.1% BSA	37^0C	60 min
9.	Wash plate with 0.1 M PBS/Tween	RT	3x3min
10.	Load plate with 100 ul 1mg/ml phosphatase substrate (pNPP, Sigma, St. Louis) and read 405 nm, until absorbance readings peak at 1.0-1.5 units.	RT	

Table 2.5.2a Enzymic / amidolytic micro-assay for TK

STEP	SOLUTION	TEMP.	TIME
1.	HUK standards - prepare 600 ul of 400 ng/ml HUK from a 1200 ng/ml aliquot stored at -20°C using amidase buffer [0.2 M Tris-Cl (pH 8.2)]. Use 300 ul of this and double diluted down to 6.25 ng/ml in amidase buffer. Add 50 ul of each dilution in triplicate to two 96-well tissue culture plates (Corning Cell Wells™ 25860, Corning, New York)	RT	
2.	Blank - add 50 ul amidase buffer (triplicate) to the two microtitre plates	RT	
3.	Controls - add 50 ul control urine, from section 2.4.4.5 serially diluted to 1:64 (with amidase buffer), in triplicate to both plates	RT	
4.	Samples - add 50 ul extract (section 2.2.1 and 2.1.4) in triplicate to the remaining wells	RT	
5.	Assay buffer - add 50 ul assay buffer (60 mg/ml SBTI, 75 mg/ml EDTA in amidase buffer) to each well of both plates	RT	
6.	Incubate	37°C	30 min
7.	Zero activity - add 50 ul distilled water to each of the wells of one plate and read absorbance at 405 nm on the Biorad Microplate Reader 3550.	RT	
8.	Enzymic activity - add 50 ul S-2266 (1.5 mM in deionised distilled water) to each well of the second plate and incubate	37°C	3 h
9.	Read absorbance at 405 nm after 3 h	RT	
10.	Calculation - for each plate subtract the absorbance of the blanks from the absorbance of the standards, controls and samples. Then subtract the zero activity absorbance from the enzymic activity and use this value to plot absorbance versus concentration of HUK standards. Read concentration of samples from this graph.		

Figure 8 Graph representing the standard curve of human urinary kallikrein (HUK) for the tissue kallikrein amidase micro-assay. The curve-fit formula used to extrapolate the concentrations of TK in the samples measured by the amidase micro-assay, from this graph is:

$$\textit{concentration of sample} = \frac{(\textit{absorbance of sample measured} + 0.001227)}{0.0002}$$

Standard curve of amidase micro-assay for human urinary kallikrein (HUK)

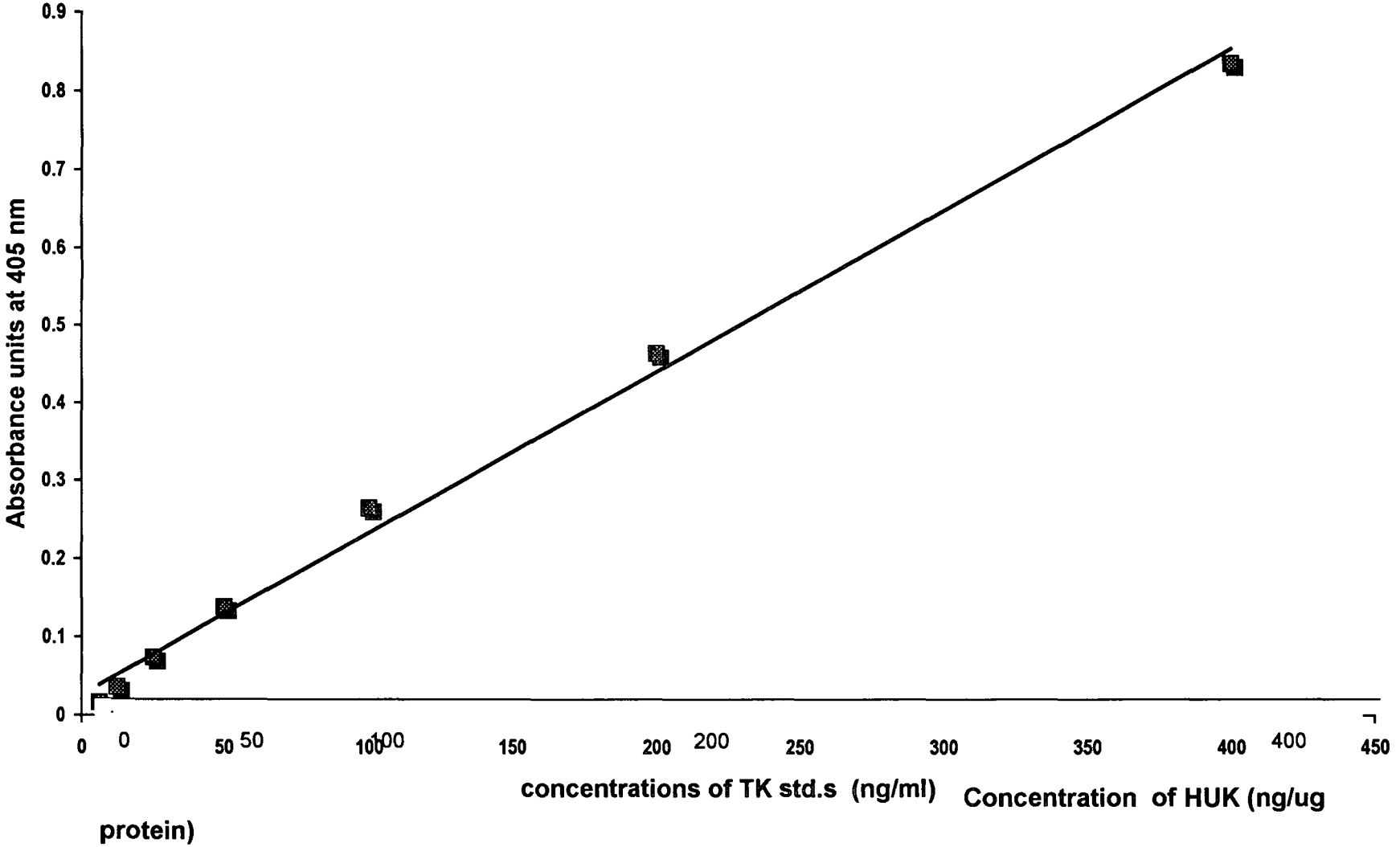

Table 2.5.2 b Measurement of total protein (Bradford 1976)

STEP	SOLUTION	TEMP.	TIME
1.	Protein standard - 100 ml of 1mg/ml Bovine Serum Albumin (BSA, Fraction V, Boehringer) was prepared and stored in 1 ml aliquots at -20C. A single 1 ml aliquot of this standard was serially diluted with distilled water from 1000ug/ml to 16 ug/ml. 30 ul of each dilution was added to a microassay plate, in triplicate.	RT	
2.	Blank - 30 ul distilled water was added to 3 wells of the plate	RT	
3.	Samples - were added in triplicate to the plate	RT	
4.	Biorad Protein Assay Reagent (Biorad, UK) - was diluted 1/5 in distilled water and 300 ul was added to each well of the plate	RT	
5.	Read absorbance at 595 nm.	RT	
6.	Calculation- subtract the absorbance of the blanks from the absorbance of the standards and samples. Plot absorbance versus concentration of BSA standards. Read protein concentration of samples from this graph.	RT	
7.	TK enzymic activity is expressed as ng TK/ug protein	RT	

Figure 9 Graph representing the standard curve of bovine serum albumin (BSA) protein standards for the Bradford protein assay. The curve fit formula used to extrapolate protein concentrations of samples, from this graph is:

$$\textit{concentration of sample} = \frac{(\textit{absorbance of sample measured} + 0.021262)}{0.0027}$$

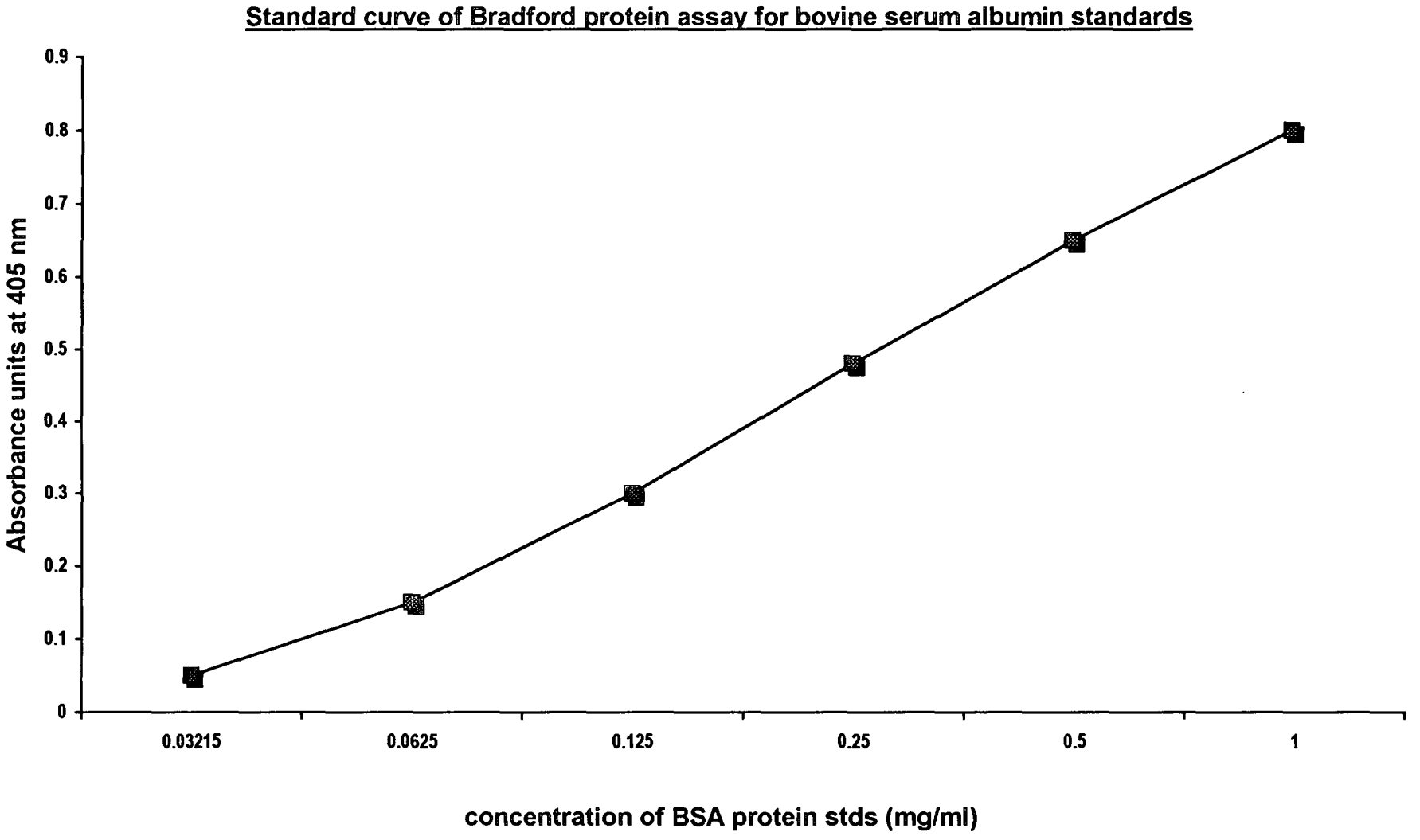
Standard curve of Bradford protein assay for bovine serum albumin standards
Absorbance units at 405 nm
0.9
0.8
0.7
0.6
0.5
0.4
0.3
0.2
0.1
0
0.03215
0.0625
0.125
0.25
0.5
1
concentration of BSA protein stds (mg/ml)

Table 2.5.3 TK ELISA

STEP	SOLUTION	TEMP	TIME
1.	Primary antibody - Coat the ELISA plate (Corning) with 100 ul of 30 ng/ml Goat anti-human rTK IgG in coating buffer	4^0C	ON
2.	Wash the plate with 0.01M PBS/0.5%Tween	RT	3x3min
3.	Block 1 - add 200 ul of 5% milk blocker to each well	RT	30 min
4.	Wash the plate with 0.01M PBS/0.5%Tween	RT	3x3min
5.	Block 2 - add 200 ul of 5% milk blocker to each well	RT	30 min
6.	Wash the plate with 0.01M PBS/0.5%Tween	RT	3x3min
7.	Standards - a 1200 ng/ml aliquot of HUK standard stored at -20°C was double diluted 40 ng/ml to 0.625ng/ml, and 100 ul of each dilution was added in triplicate		
8.	Blanks - 100 ul 0.01M PBS (pH 7.2) was added to 3 wells		
9.	Controls -control urine from section 2.4.4.5 was serially diluted from 1/8 to 1/512 in 0.01M PBS (pH7.2), and 100 ul of each dilution added in triplicate. Also, known samples are rerun to test for inter-assay variation		
10.	Sample - 100 ul of sample was loaded onto the remaining wells of the plate in triplicate		
11.	Incubate	37^0C	60 min
12.	Wash the plate with 0.01 M PBS/0.5%Tween	RT	3x3min
13.	Secondary antibody - add 100 ul of 25 ng/ml rabbit anti-human rTK to each well and incubate	37^0C	60 min
14.	Wash the plate with 0.01 M PBS/0.5%Tween	RT	3x3min
15.	100 ul of anti-rabbit IgG (Sigma, St. Louis) diluted 1:250 with 0.01 M PBS was added to each well and incubated	37^0C	60 min
16.	Wash the plate with 0.01 M PBS/0.5%Tween	RT	3x3min
17.	Chromogen - 100 ul of 1 mg/ml pNPP substrate was added to each well (1 tablet in 5 ml of substrate buffer) and allow colour to develop	37^0C	0-60 min
18.	Calculation - subtract the absorbance of the blanks from the absorbance of the standards, controls and samples.		

Plot absorbance versus concentration of HUK standards.

Read TK concentration of samples and controls from this graph.

Figure 10 Graph representing the standard curve of human urinary kallikrein (HUK) for the enzyme-linked immunosorbent assay (ELISA). The curve fit formula used to extrapolate concentrations of TK in the samples measured, from this graph is:

$$\textit{concentration of sample} = \frac{(\textit{absorbance of sample measured} - 0.0299851)}{0.0084}$$

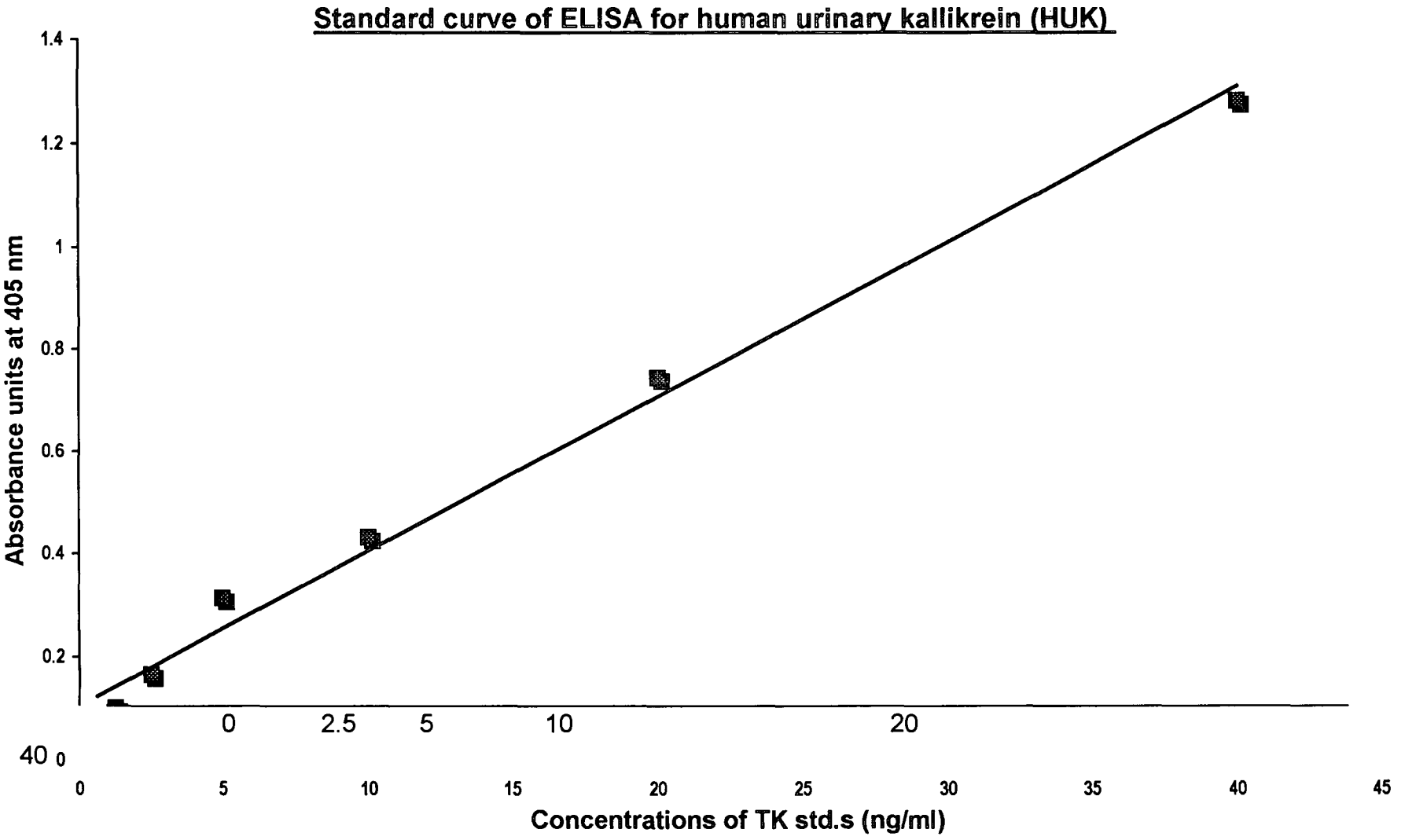
Standard curve of ELISA for human urinary kallikrein (HUK)
Absorbance units at 405 nm
1.4
1.2
1
0.8
0.6
0.4
0.2
0
2.5
5
10
20
40 0
0
5
10
15
20
25
30
35
40
45
Concentrations of TK std.s (ng/ml)

Table 2.5.4.1 Immunocytochemical localisation of TK by immunoprecipitation

STEP	SOLUTION	TEMP	TIME
1.	Dewax - Xylene (analytical grade; Saarchem, SA)	RT	2x10 min
2.	Rehydrate - 100% EtOH (analytical grade; Saarchem, SA)	RT	2x5 min
3.	Quench endogenous peroxidase - 100% MeOH (analytical grade; Saarchem, SA)	RT	1x20 min
4.	Rehydrate - 90% EtOH (in distilled water, v/v; analytical grade; Saarchem, SA)	RT	2x4 min
5.	Rehydrate - 70% EtOH (in distilled water, v/v analytical grade; Saarchem, SA)	RT	1x3 min
6.	Rehydrate - distilled water	RT	1x5 min
7.	Antigen retrieval in 0.1 M Sodium-Citrate (pH 6.0) in microwave. Then allow to cool to RT for ± 20min	Boil	3 min high & 5 min low
8.	Wash - 0.01 M PBS (pH 7.2)	RT	
9.	Block endogenous peroxidase - 10% H_2O_2/ 90% MeOH	RT	20 min
10.	Wash - 0.01 M PBS (pH 7.2)	RT	5 min
11.	Block non-specific binding sites - 1% non-immune goat serum in buffered physiological saline		20 min
12.	Wash - 0.01 M PBS (pH 7.2)	RT	5 min
13.	1^0 Ab - goat anti-human rTK IgG diluted 1:1000 with 0.01 M Phosphate buffer (pH 7.2) [0.1 M PBS/1%BSA]	4°C	18 h
14.	Wash - 0.01 M PBS (pH 7.2)	RT	5 min
15.	Incubate with anti-goat IgG Biotin link (Dako K0690)	RT	20 min
16.	Wash - 0.01M PBS (pH 7.2)	RT	
17.	2^0 Ab - Strepavidin-peroxidase (Dako K0690)	RT	20 min
18.	Wash - 0.01M PBS (pH 7.2)	RT	5 min
19.	Chromogen - liquid DAB (Dako, K3465)	RT	2-5 min
20.	Counterstain - Mayers' Heamatoxylin (Sigma, St. Louis)	RT	3-5 min
21.	Intensify - Wash in tap H_2O		5 min
22.	Dehydrate - 70% EtOH (in distilled water, v/v)	RT	1 min
23.	Dehydrate - 90% EtOH (in distilled water, v/v)	RT	1 min
24.	Dehydrate - 100% EtOH (analytical grade; Saarchem, SA)	RT	1 min

25.	Dehydrate - Xylene (analytical grade; Saarchem, SA)	RT	1 min
26.	Mount - Entellen (Merck)		

Table 2.5.4.2 Immunocytochemical localisation of TK by immuno-fluorescence

STEP	SOLUTION	TEMP	TIME
1.	Dewax - Xylene (analytical grade; Saarchem, SA)	RT	2 x 10 min
2.	Rehydrate - 100% EtOH (analytical grade; Saarchem, SA)	RT	2 x 5 min
3.	Rehydrate - 90% EtOH (in distilled water, v/v)	RT	2 x 4 min
4.	Rehydrate - 70% EtOH (in distilled water, v/v)	RT	1 x 3 min
5.	Rehydrate - distilled water	RT	1 x 5 min
6.	Antigen retrieval - 0.1 M Sodium Citrate (pH 6.0) in microwave. Then allow to cool to RT for ± 20min	Boil at 80^0C	3 min high & 5 min low
7.	Wash - 0.01M PBS pH 7.2	RT	
8.	Block non-specific binding sites - 1% Human IgG	RT	2 min
9.	Wash - 0.01 M PBS (pH 7.2)	RT	5 min
10.	1^0 Ab - goat anti-human rTK IgG diluted 1:1000 with 0.01 M Phosphate buffer (pH 7.2) [0.1 M PBS/1%BSA]	4°C	18 h
11.	Wash - 0.01 M PBS (pH 7.2)	RT	5 min
12.	2^0 Ab - FITC conjugated anti-goat IgG (Sigma, St. Louis) (1/32 dilution in 0.01 M PBS/1%BSA)	RT	30 min
13.	Wash - 0.01 M PBS (pH 7.2)	RT	5 min
14.	Mount - 10% PBS/90% glycerol	RT	

CHAPTER 3

RESULTS

INTRODUCTION

The aims of this study address the question of the role of the serine protease, tissue kallikrein and the vasoactive kinins in the cellular pathology of gastric disorders and disease. In particular, it examines the causative role of the enteropathogen *Helicobacter pylori* in kinin-induced gastric inflammation. In order to examine this hypothesis, it was first necessary to make measurements of the gastric exudates and tissue extracts by enzyme-linked-immunosorbent assay to determine the amount of immuno-reactive tissue kallikrein, and by amidolytic assay to evaluate enzymic activity. An insight into the physiological role of tissue kallikrein and released kinins was sought by immuno-localisation of tissue kallikrein in specific cells and their cellular orientation in gastric mucosa. Therefore, the following chapter deals, in detail, with the results of the experiments performed.

3.1 Patients

3.1.1 Demographics

The patients selected for this study were males and non-pregnant females between 18 and 75 years old who had not exhibited any severe form of renal, respiratory or cardiovascular abnormality. Other exclusion criteria were those patients who had undergone recent oesophageal or gastric surgery. Included in this group for omission were those with ulcer complications like pyloric stenosis, perforations and arterial bleeding. The final exclusions were based on the use of NSAID's (non-steroidal anti-inflammatory drugs), and antibiotics

or drugs such as alluprinol, digoxin, theophyllin and warfarin (refer to Appendix1 for a copy of the patient consent form handed to all patients involved in this study).

Twenty three (n=23) patients were examined, with 8 of them being males and 15 being females (see Table 3). The mean age of the males was 42 years in the range 31 to 63 years. The female group mean age was 39 ranging between 56 and 24 years old. The majority (n=13) of the patients (male and female) came from the Indian ethnic group with a significant number also being Black female (n=6). It is, perhaps, important to note that both patient gender sets belonged to the adult-age group (24 - 63 years). From every patient examined, two sets of biopsy specimens were taken from each of the antral and pyloric regions of the stomach. In addition, gastric lavage fluid from the stomach was aspirated with 0.09% sterile saline, and urine was collected from each patient at time of endoscopy and examination. Table 3 shows the general patient demographics

3.1.2 Statistical analysis of results

The data analysed was from results of tissue kallikrein measurement by ELISA, tissue kallikrein amidase enzymic activity by amidase microassay, and tissue kallikrein immuno-localisation image analysis. Results were analysed using an *analysis of variance* to compare the four histological groups (see section 3.1.3). For comparison of 'parity' between different groups an *unpaired t-test* was employed. *Single Descriptive statistics* (column type) was used to evaluate data relating to each individual group, and presented as *mean, median,* and *standard error.* Due to the variability in the analysis of the measurement of tissue kallikrein for the histological groups, factors such as *range* were also used. For inter- and intra-group comparisons between the various histological and

regional groups, a t-test of equal variance was used with 95% confidence intervals (95% C.I.). A p value <0.05 was selected as an indicator of statistical significance.

3.1.3 Confocal microscopy and fluorescent image analysis

Confocal scanning laser microscopy is a powerful imaging technique in which the staining intensity of fluorescently-labelled cells is viewed. An important tool of the confocal microscope is that it has the capability to section through tissue optically. This feature was used to determine the middle plane of the labelled gastric cell, of which an image representative of the whole cell was then generated. Confocal images were typically recorded at a pixel density of 225 x 225 pixels. For the image analysis process, the colour spectrum (as indicated by the graphic fluorescent images of plates 21 to 28) was converted to a grey scale ranging from 0 to 256 units, which was further divided into 8 equal phases with each phase having a lower and upper threshold value on the grey scale.

The amount of immuno-reactive tissue kallikrein was determined by the analysis of computer generated confocal images. Using the Analysis 2.1 Pro system (Soft-Imaging Software GmbH, 1996, Germany) the regions of interest (ROI) on each image were selected. This information was used to calculate the number of pixels falling within each phase, as well as the area analysed. This data, exported to Microsoft Excel™ (Office 97, Windows 95, Microsoft Corp., USA) was used to calculate the mean intensity of immuno-labelling per phase in (n) number of cells applying the unit pixel/um^2.

Table 3 Demographics of sample patient population (n=23)

* Gender	n	Mean age (years)	Median age (years)	Range (years)	Ethnic groups			
					I	W	C	B
Male	8	41.63	38.5	31 - 63	4	1	1	2
Female	15	38.69	38	24 - 56	9	—	—	6

*
Males and non-pregnant females selected were between 18 and 75 years old

I = Indians
W = Whites
C = Coloureds
B = Blacks

3.1.4 Light microscopy and image analysis

DAB immuno-stained tissue slides were viewed with a Nikon Optiphot microscope (Nikon, Japan) which was interphased to a 3 CCD digital camera system (Sony Corp., Japan). The quantitative image analyser used to determine the labelling intensity of the DAB immuno-localisation of TK was the Kontorn Elektronic KS 300 (Zeiss GmbH, Germany), running on Windows 95™, (Microsoft Corp., USA). The digital images captured, were processed and converted to grey images ranging in grey density from 0 to 255. The areas of TK-DAB labelling were segmented. This involved the immuno-positive areas being separated from their environments on the basis of their grey values (set up of threshold factor), thereby creating a binary image for quantification. The grey values in this image represent the intensity of the label over the entire area of possible x-y co-ordinates. A coloured contour was superimposed on the binary image to complement previous threshold areas. This image was then masked onto the original image of the chosen areas. The median maximal density of immuno-localisation was then calculated as pixels per unit area

3.1.5 Histological grading of gastritis based on H&E staining

Wax-embedded tissue sections were subjected to Haemotoxylin and Eosin (H&E) as well as Giemsa staining to histologically verify the presence and grade of disease type, and to detect the presence of Helicobacter *pylori* (Hp) bacteria, respectively. The gastric pathologies were categorised into non-inflamed, non-Hp infected (group 1, served as a control group, plate 4a,b), mild Hp infection and mild inflammation (group 2, plate 4c,d), moderate chronic infection with moderate to severe inflammation (group 3, plate 4e,f) and

severe chronic gastritis with very mild Hp infection (group 4g). In addition to this, the presence of Hp was visually scored as (+), (++) and (+++) to indicate the degree of infection. Refer to Table 4 for the histological presentation of the groups

Group 1 Classification was on the basis of minimal presence of inflammatory cells being seen in the gastric tissue; and that the cellular integrity and form of the gastric tissue structure was not compromised (Plates 4a, plate 4b).

Group 2 There were more inflammatory cells present compared to group 1; and slight focal regeneration, if any at all. Very few Hp organisms could be seen either free in the lumen or sequestered on the tissue (Plate 4c, Plate 4d).

Group 3 This group showed a dramatic increase in the inflammatory cell activity

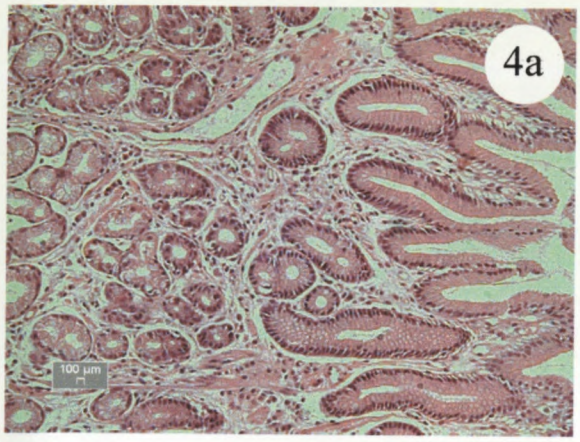
4a
100 µm

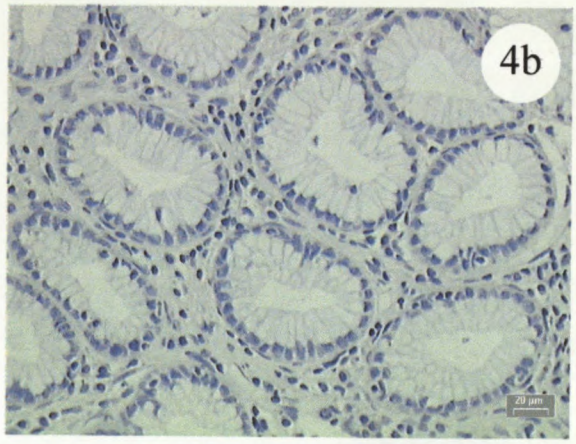
4b
20 µm

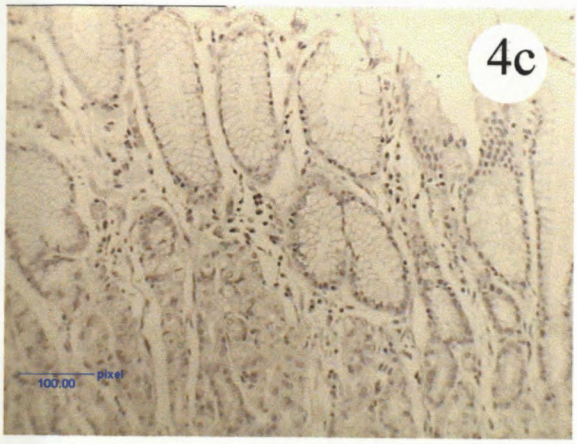
4c
100.00 pixel

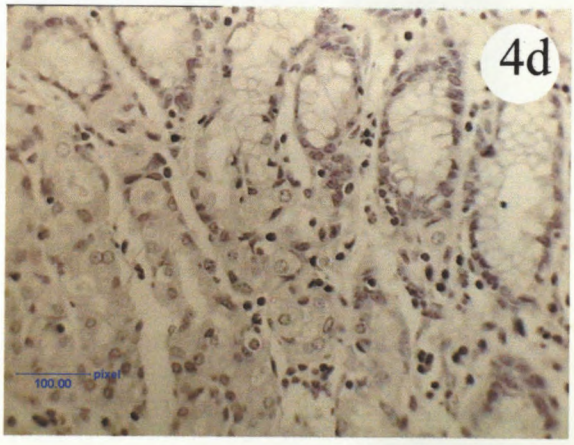
4d
100.00 pixel

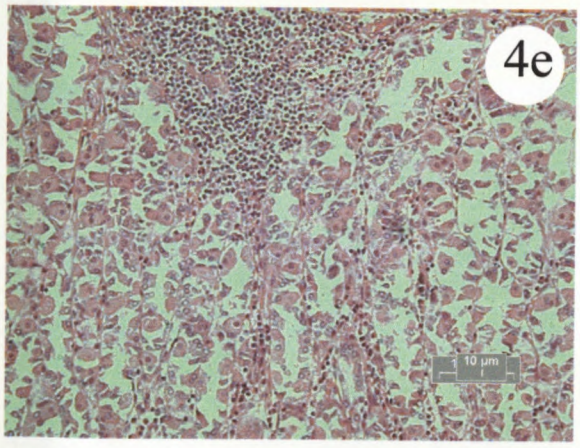
4e
10 µm

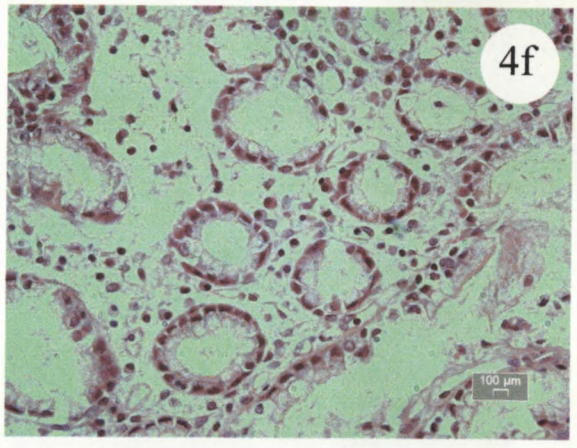
4f
100 µm

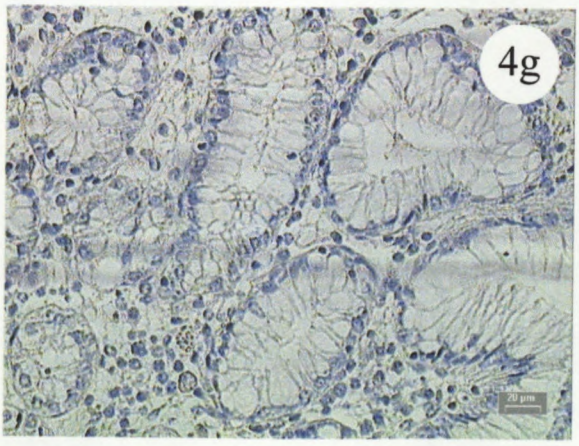
4g
20 µm

(Plate 4e, Plate 4f) extending into the glands; congestion of lamina propria; active regeneration with stratification of nuclei, increased mitotic activity, and hyperchromatism. The presence of polymorphonucleocytes was suggestive of gland destruction as seen by the loss of glandular epithelia. Such 'active' gastritis results in fibrosis of the glands during the latter stages of inflammation.

Group 4 This group showed showing chronic inflammatory cell infiltration into glandular structures; flattening of the epithelia and metaplasia (Plate 4g). The long-standing inflammation resulted in loss of glandular morphology and atrophy of the gastric mucosa. .

Metaplasia This feature was evident when complex mucin cells were replaced by a more simple type of mucous-secreting epithelial cell type that was found lining the glands. This was also termed *foveolar metaplasia* for the tissue in group 3. None of the biopsy specimens exhibited the more severe type of metaplasia - *intestinal metaplasia.* See Plate 6 for a histological presentation of metaplasia on H&E stained antral gastric tissue.

Table 4 outlines the histological criteria on which the groups were graded.

3.1.5.1 Group 1

Histological examination, by H&E, of group 1 antrum (normal control group) revealed the presence of a small number of inflammatory cells in the lamina propria (refer to plate 7a). These inflammatory cells were invariably found in histologically 'normal' tissues and represented basal profiles. The surface epithelia

Plate 5a: Photo-micrograph (X1000) of a Giemsa-stained section of antrum from histological group 3 showing chronic *Helicobacter pylori* infection. Evident in the tissue is the presence of the curved bacteria (circles with pointing arrows) free in the lumen of this gastric gland or attached to the mucous cells lining the glands. This image also shows the inflammatory cells (neutrophils, IC) infiltrating the cellular bi-membrane of the gland from the lamina propria (LP), and is therefore a well-defined model of cryptitis.

Plate 5b: Photo-micrograph (X1000) of an H&E-stained section of antrum from a mildly infected group 2 patient. The presence of a few *Helicobacter pylori*, is shown by circles with pointing arrows, in the gland lumen or attached to the mucous cells. In the lamina propria (LP) there are a number of inflammatory cells indicating 'active' inflammation.

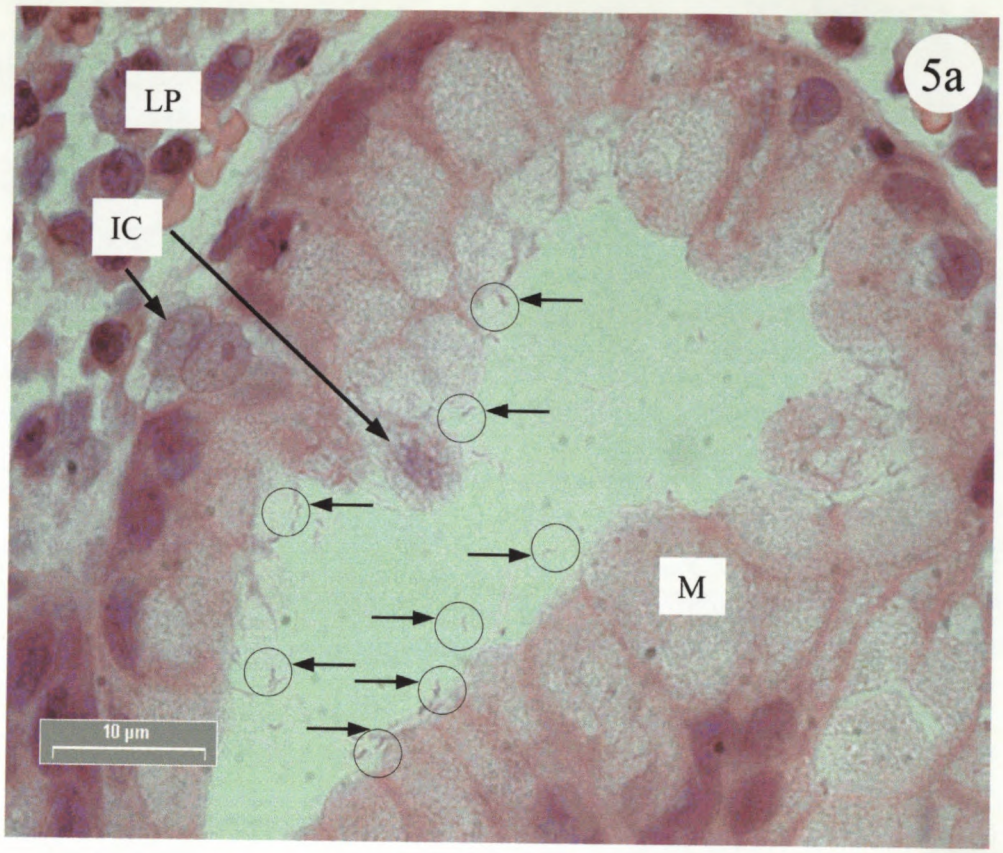
5a
LP
IC
M
10 µm

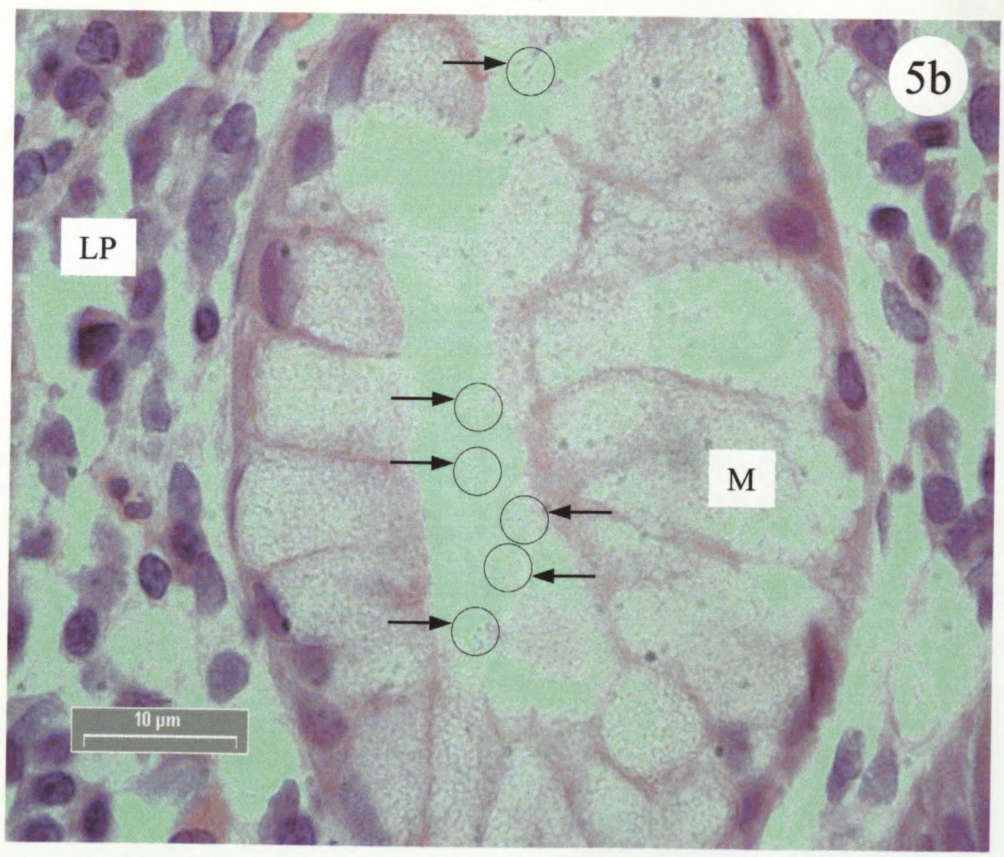
5b
LP
M
10 µm

Plate 6: Photo-micrograph (X1000) showing H&E-stained section of gastric tissue that had undergone metaplasia. Note the metaplasic cells (MC) that are of a simple cell-type profile with large clear cytoplasm, and which have replaced the mucous secreting glandular cells. There are numerous inflammatory cells in the connective tissue lamina propria (LP). Also shown is a gland that is undergoing destruction and atrophy (AG) and has been infiltrated by inflammatory cells that are deposited in the lumen of the gland.

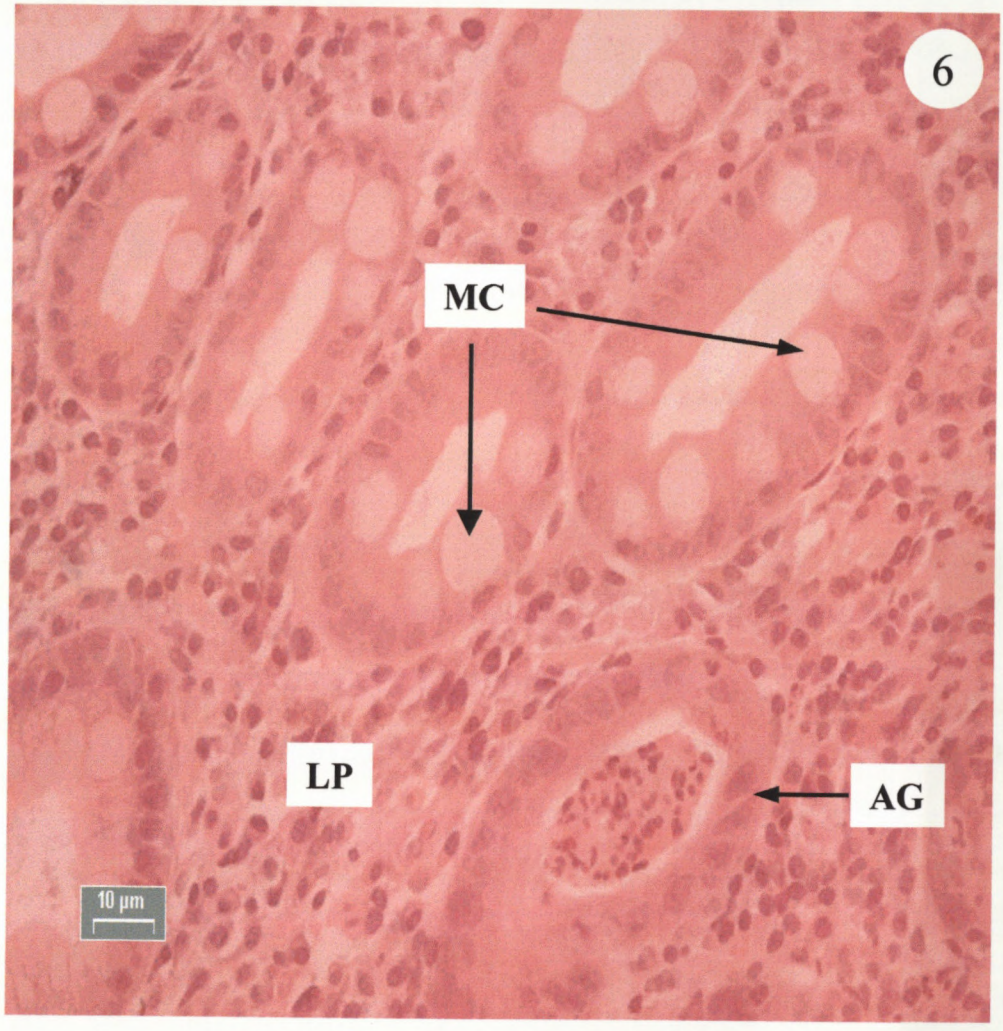
6
MC
LP
AG
10 µm

were found to still retain their tall columnar architecture and there was evidence of mucus production within the secretory glands and on the luminal surface. Plate 7b shows that the structural integrity of the glands was still maintained with secretory cell nuclei basally located. The glandular and superficial structures appeared normal and there were no regenerative features. There was no metaplasia or dysplasia evident. There also appeared to be no *Helicobacter pylori* present within the tissue or free-swimming in the lumen.

3.1.5.2 Group 2

Plate 9a (X200) shows an H&E-stained section of an antral tissue section from group 2. As indicated by the arrows, there were polymorphonucleocytes infiltrating the lamina propria. There was also a small number of inflammatory cells beginning to extend into the superficial glandular structures. Most of the glandular structures still retained their mucus-secreting cells and appear to be structurally intact. There was no evidence of metaplasia. Plate 9b (X400) shows inflammatory cells present between the glands in the lamina propria. pathology attributed to this group was indicative of mild chronic inflammation. There were small numbers of *Helicobacter pylori* on the luminal surface and surface epithelia. Overall, this group displayed slight focal regeneration and no glandular atrophy.

Table 4 Histological grading of patient groups

GROUP	¢GRADE OF GASTRITIS	§*H PYLORI* PRESENCE
1	***NON INFLAMED*** o Minimal numbers of inflammatory cells present o Structural integrity and form of cellular structures not compromised	-
2	***MILD INFLAMMATION*** o some inflammatory cells are present within lamina propria o Slight focal regeneration of the glands	+
3	***MODERATE INFLAMMATION*** o Marked increase in the number of inflammatory cells o Activity of the neutrophils extends into the glands o Congestion of the lamina propria by polymorphonucleocytes o Active regeneration with stratification of nuclei, o Increased mitosis o Hyperchromatism	++
4	***SEVERE INFLAMMATION*** o Chronic inflammatory cell infiltration into the glandular structures o Flattening of epithelia o Regeneration o Metaplasia o Atrophy	+++

¢ Histology based on examination of H&E stained tissue.

§ Grading done visually on Giemsa-stained sections, and subjective to the number of Hp organisms seen on the surface epithelia and in the lamina propria

\+ Mild infection with few Hp present, ++ moderate infection, +++ severe infection with large numbers of Hp present

3.1.5.3 Group 3

Plate 12a (X200) shows an H&E section of group 3. There is a significant increase in the number of inflammatory cells present in the antral tissue, and there is massive infiltration into the lamina propria (shown by arrows) from the submucosa region towards the superficial surface. This group was categorised as moderate to severe chronic active gastritis. There was clear histological evidence of glandular destruction (plate 11a), while plate 12b (X400) shows infiltration of inflammatory cells into the glands (arrow). Plate 12b also shows, at greater magnification, the destruction of individual glands. There was no mucus production. This group (plate 5a, X1000) also showed evidence of colonisation by Hp. The superficial glands showed marked regenerative activity. Epithelial cells showed hyperchromatic nuclei with increased mitosis.

3.1.5.4 Group 4

This group was classified as severe chronic gastritis with destruction of glands, and characteristic of replacement of gastric tissue with simple intestinal metaplasic structures. Plate 17 (X400) shows almost complete loss of cytoplasmic contents of mucous cells, and these cells are indicative of a simple type of differentiating epithelia. The number of inflammatory cells seen were not as great as compared to group 3. This group was not designated as having active inflammation, since there was reduction in granulocyte activity. Glandular atrophy (not shown but similar to that seen in plate 12b) was evident with features of foveolar metaplasia also presenting. There was flattening of the tall columnar

epithelia, and areas of gland-like regeneration. Hp was virtually non-existent in group 4 gastric tissue

3.1.6 Histology of *Helicobacter pylori* infection based on H&E and Giemsa staining

Mild infection: Plate 5b (X1000) is a photo-micrograph depicting an H&E stained tissue section of superficial antral gland. As can be seen (circles with arrows) there are a small number of curved Hp bacilli free within the lumen of the gland. There are also a few organisms that are adherent to the cell surfaces. Tissue sections showing this degree of inflammation and Hp infection were placed into group 2.

Chronic infection: Plate 5a is a Giemsa-stained photo-micrograph section of antral tissue from a group 3 patient. There are a large number of Hp organisms in the lumen of the superficial gland (rings with arrows pointing); and others are seen adhering to the cell surfaces and found at the junction between the cell membranes. Tissue with type of histological presentation were placed in group 3.

3.2 Assays for tissue kallikrein

3.2.1 Amidase assay

3.2.1.1 Descriptive statistics of TK amidase assay of gastric lavage fluid

Group 1 represented a control group since there was no inflammation and no Hp present. Therefore, the mean amidase activity value of group 1 (73.21 ngTK/ug protein ± 69.36) represented the basal TK activity for the control group. Results in Table 5 shows that as the disease state progressed from control to chronic there was an almost 50% increase in TK enzymic values, as is evident from the values from group 1 (73.21 ngTK/ug protein ± 70) to group 3 (130.71 ngTK/ug protein ± 65.29, (p = 0.6±177). In contrast, the severely damaged mucosa with a loss of secretory glandular cells did not show such a marked increase in the amount of active TK (112.05 ngTK/ ug protein ± 14.11)

3.2.1.2 Antral and pyloric tissue extracts

In type B gastritis, the inflamed area is restricted to the antrum of the human stomach. Results from Table 5 indicate a slight increase in the antral TK amidase activity as progression occurs from control group 1 to mild infection of group 2 (3.29 ngTK/ug protein ± 2.55 to 3.47 ngTK/ug protein ± 2.49, p = 0.96 ± 9.8). Unfortunately the enzymic activity of the moderate to severely infected groups could not be ascertained since they were below the detection limits of the TK amidase microassay (group 3 and group 4). However, there was a clear increase

between the group 1 body to group 2 body (2.27 ngTK/ml protein ± 1.55 to 3.19 ng TK/ ug protein ± 2.92, $p = 0.85 \pm 10.40$). It may be considered discrepant that the highest measured amidase activity (compared to the rest of the groups) occurs in the severely diseased body regions of group 4, when a trend of increasing activity (as the disease progresses) indicates otherwise.

3.2.1.3 Intergroup comparison of TK amidase activity of gastric tissue extracts

Table 6 represents an inter-group comparison by *t-test* of *equal variance* of the gastric tissue extracts for the TK amidase activity assay. Antral regions of the histological group were matched against each other for statistical significance. In addition, the body regions of the groups were also matched against each other. For the antral comparisons, no statistical significance could be found between any of the groups (all p values were > 0.05). Similarly, for the body region, no statistical significance in comparison could be found.

3.2.1.4 Intergroup comparison of TK amidase activity of gastric lavage fluid.

Table 7 shows the inter-group comparison, using a *t-test* of *equal variance*, of gastric lavage fluid for TK amidase assay. There appears to be no comparison of statistical significance between any groups, that is, all p values were > 0.05.

Table 5 **Single descriptive statistics (column type) of the various histological groups for tissue kallikrein amidase assay**

Group		TK Amidase Activity of [a]Gastric Lavage Fluid (ng TK/ug protein)				TK Amidase Activity of Gastric tissue Extracts (ngTK/ug protein)			
		Mean	Median	Range	SEM (±)	Mean	Median	Range	SEM (±)
Group 1	antrum	73.21	5.85	9.43-290.56	69.36	3.29	1.55	0.34-8.66	2.55
	body					2.27	1.57	0.08-5.31	1.55
Group 2	antrum	62.74	17.77	.48-243.52	34.06	3.47	0.17	0.13-19.86	2.49
	body					3.19	0.085	0.21-23.79	2.92
Group 3	antrum	130.71	0	3.09-436.90	65.29	*	*	*	*
	body					*	*	*	*
Group 4	antrum	112.05	125.31	82.91-127.91	14.11	*	*	*	*
	body					5.39	5.38	0.015-10.78	5.38

[a] Mean, median and range given in ng tissue kallikrein/ug protein
SEM standard error of mean
* enzymic activity is below the detection limit of the micro-assay

3.2.1.5 Comparison of TK amidase assay of gastric lavage fluid and gastric biopsy tissue extracts.

Table 8 represents a comparative *t-test* of *equal variance* between tissue kallikrein amidase activity of gastric lavage fluid and tissue kallikrein amidase activity of gastric tissue extracts. There appears to be no significant difference between the TK enzymic activity of the gastric lavage fluid and tissue extracts in group 1. In fact, the p value comparison factor shows no significance in the baseline activity series of the control group. A comparative difference does, however, exist between TK activity in group 2 lavage fluid and group 2 tissue extracts ($p = 0.02 \pm 108.53$). Therefore the mildly inflamed group of lavage fluid and tissue extracts show significant differences of equal variance. It can also be gauged from table 6 that a statistically significant ($p = 0.02 \pm 270.76$) difference exist between the TK activity of the lavage fluid and tissue extracts in group 3. The greatest significance factor was obtained for group 4 lavage fluid versus group 4 tissue extracts ($p = 0.0003 \pm 140.77$).

3.2.2 Tissue kallikrein enzyme-linked-immunosorbent-assay

3.2.2.1 Descriptive statistics for TK ELISA for gastric lavage fluid

Table 9 represents the single descriptive statistics of TK ELISA measurement of the gastric lavage fluid. The TK content of group 1 lavage fluid could not be measured by this ELISA, since it would appear that the amount of TK fell below the detection limits of the assay (refer to chapter 2 for the standard curve of the

TK ELISA). This would indicate a very low basal level of Kallikrein in the control group (normal, non-inflamed and non-Hp infected). There is a dramatic increase in the amount of tissue kallikrein measured in the lavage fluid as the disease progresses from mild (group 1: 3.08 ngTK/ug protein ± 3.08) to the moderately inflamed group (group 2: 27 ngTK/ug protein ± 15.63) to the severe group (group 4: 64.16 ngTK/ug protein ± 34.97).

3.2.3 Comparison of TK ELISA versus TK amidase assay of gastric lavage fluid

Table 10 represents a comparison between TK ELISA of lavage fluid and TK amidase assay of lavage fluid using a *comparative t-test* of *equal variance*. Group 1 TK ELISA compared to group 1 TK amidase assay shows no statistical significance (p = 0.27 ± 71.05). Similar comparisons between groups show no statistical significance in comparison, where $p < 0.05$ for statistical significance

Table 6 **Intergroup comparison using *t-test* with *equal variance* of gastric tissue extracts for tissue kallikrein amidase assay**

group		versus Group 1		versus Group 2		versus Group 3	
	region	***Antrum***	***Body***	***Antrum***	***Body***	***Antrum***	***Body***
Group 2	***Antrum***	0.96 ± 9.8					
	Body		0.85 ± 10.40				
Group 3	***Antrum***	0.18 ± 8.78		0.36 ± 11.51			
	Body		0.14 ± 5.60		0.47 ± 12.62		
Group 4	***Antrum***	0.39 ± 13.78		0.53 ± 15.47		*	
	Body		0.54 ± 11.15		0.74 ± 12.72		0.18 ± 3.77

* Raw data values for these groups were not statistically valid
Results of comparison are presented as $p \pm 95$ % confidence interval

Table 7 **Intergroup comparison using *t-test* with *equal variance* of gastric lavage fluid for tissue kallikrein amidase assay**

Tissue Kallikrein Functional Assay	**versus Group 1** (*p* ±95% C.I.)	**versus Group 2** (*p* ±95% C.I.)	**versus Group 3** (*p* ±95% C.I.)	**versus Group 4** (*p* ±95% C.I.)
Group 1 (*p* ±95% C.I).		0.88±161.61	0.6±177.45	0.66±174.3
Group 2 (*p* ±95% C.I.)	*		0.37±89.99	0.42±82.01

p value < 0.05 is not considered to be statistically significant
* : Raw data obtained not statistically viable
95% C.I. : 95% confidence interval

Table 8 ***Comparative t test* with *equal variance* of tissue kallikrein amidase assay of gastric lavage fluid versus gastric tissue biopsy extracts**

TK Amidase Assay	***p* value**	**95% C.I. (maximum)**	TK Amidase Assay
Group 1 *lavage fluid*	0.24	196.94	**Group 1** *gastric tissue extracts*
Group 2 *lavage fluid*	0.02	108.53	**Group 2** *gastric tissue extracts*
Group 3 *lavage fluid*	0.06	270.76	**Group 3** *gastric tissue extracts*
Group 4 *lavage fluid*	0.0003	140.77	**Group 4** *gastric tissue extracts*

A p value < 0.05 is considered to statistically non-significant

95% C.I. = 95% confidence interval

Table 9 ***Single descriptive statistics*** **(column type) of the various histological groups for tissue kallikrein ELISA of gastric lavage fluid**

group	[a]**mean** *(ng TK/ml)*	[a]**median** *(ng TK/ml)*	[a]**range** *(ng TK/ml)*	[a]**sem (±)** *(ng TK/ml)*
Group 1 lavage fluid	*	*	*	*
Group 2 lavage fluid	3.08	0	0.09-24.70	3.08
Group 3 lavage fluid	27.00	0	0.23-99.76	15.63
Group 4 lavage fluid	64.16	72.13	1.33-121.67	34.97

[a] : Mean, median and range given in ng tissue kallikrein/ml of lavage fluid
SEM : standard error of mean
* : value below the detection limit of the assay.

Table 10 **Inter-group comparison by t-test with *equal variance* of gastric lavage fluid for tissue kallikrein ELISA**

Tissue Kallikrein ELISA	***p* value**	**95% CI (Maximum)**	Tissue Kallikrein Amidase Assay
Group 1 gastric lavage	0.27	71.05	**Group 1** gastric lavage
Group 2 gastric lavage	0.10	13.68	**Group 2** gastric lavage
Group 3 gastric lavage	0.14	40.2	**Group 3** gastric lavage
Group 4 gastric lavage	0.27	56.80	**Group 4** gastric lavage

p value < 0.05 is considered to be non-significant
95% C.I. = 95% confidence interval

3.3 Immunocytochemistry

3.3.1 Immuno precipitation and light microscopy

3.3.1.1 TK immuno-localisation using 3,3'-diaminobenzidine (DAB)

For immunocytochemistry, using DAB as the chromogenic substrate, a brown precipitate is formed. That is, the immuno-localisation of an antibody-labelled target protein is specifically and exclusively indicated by brown colour in the tissue, as is demonstrated in the following results.

3.3.1.1.1 DAB staining in group 1

Plate 8a (x200) demonstrates TK immuno-labelling in the normal antrum. There is diffuse labelling in the glandular structures (indicated by arrows). The glands exhibit particularly distinct labelling in the parietal cells, identified by their large pyramidal structure and basal nuclei. There are a few inflammatory cells present (normal feature) and these do not show any presence of TK. Overall, in the normal antral tissue labelled (other results not shown) TK labelling was found predominantly in the parietal cells, but not in the epithelia.

Plate 8b is a photo-micrograph (X200) of an area of TK immuno-labelled body region of group 1. There appears to be moderate to low intensity DAB staining, of which the distinctly-stained cells include the parietal cells (arrow). There are a

Plate 7a: Photo-micrograph showing an H&E-stained antral section (X200) of histological group 1. Note the presence of some inflammatory cells in the lamina propria surrounding the glands. The cellular structures of the glands appear intact, and there is evidence of mucin production.

Plate 7b: This is an H&E photo-micrograph (X400) of group 1 body gastric glands. The tall mucous cells of the glands are clearly defined and there are few inflammatory cells present within the tissue

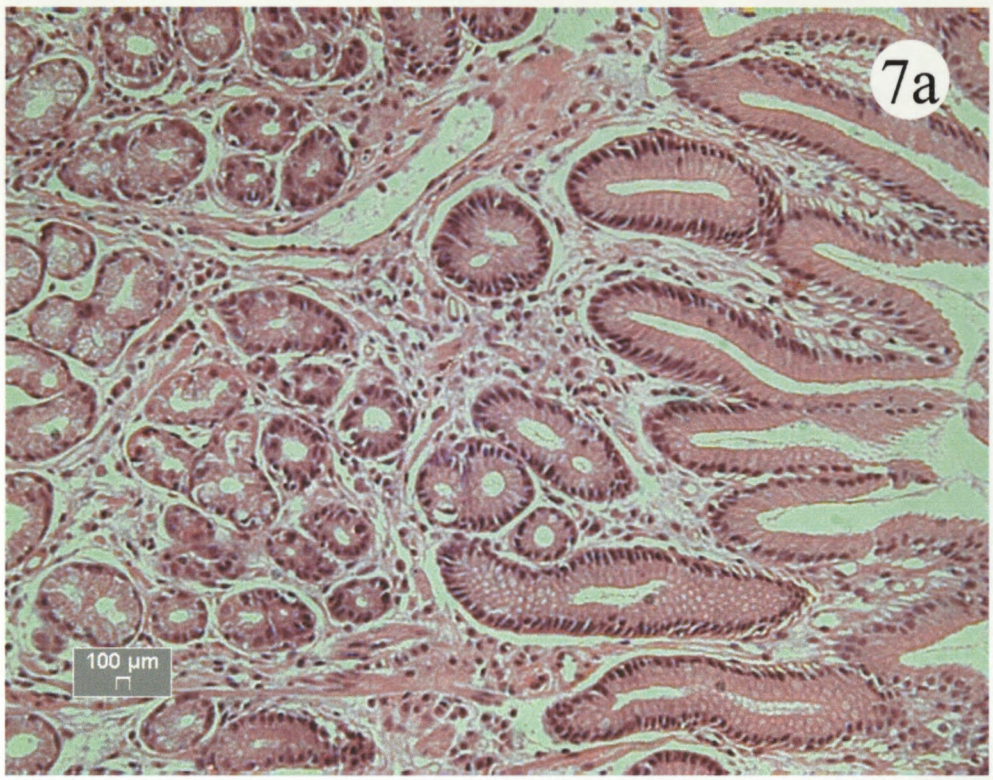
7a
100 µm

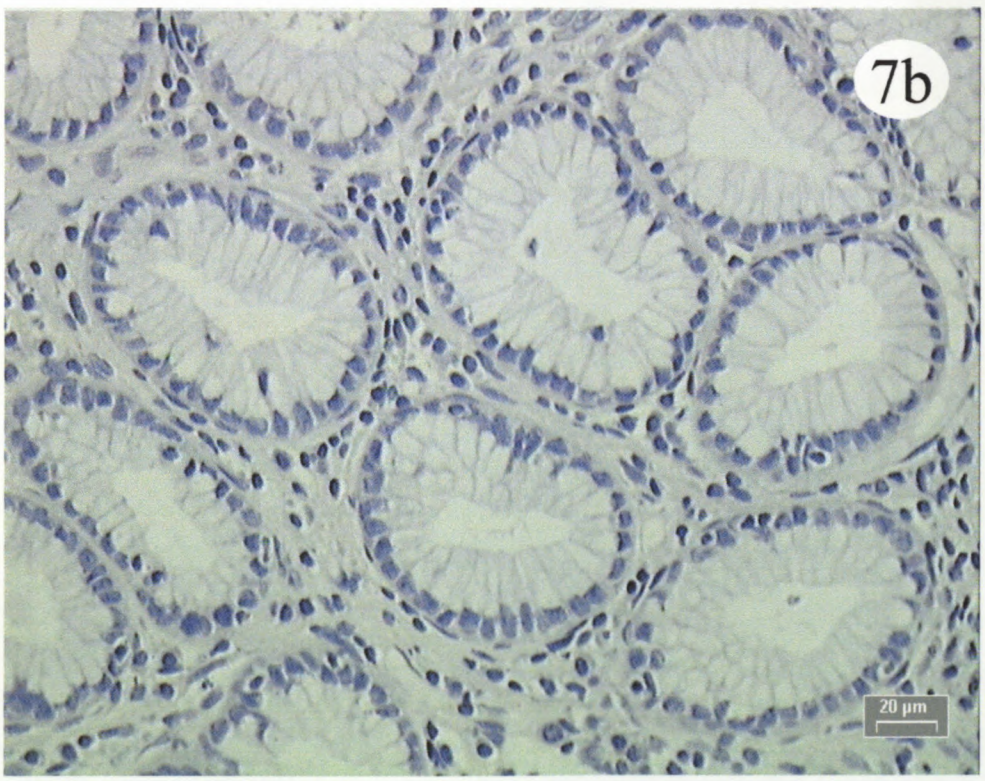
7b
20 µm

Plate 8a: This is a photo-micrograph (X200) of TK immuno-labelling on group 1 (normal control) antral tissue. The primary sites of localization are the parietal cells of the gastric glands (arrows). Label intensity is diffuse and does not occur within the connective tissue.

Plate 8b: This photo-micrograph (X200) shows TK localisation in the body region of group 1. Here, as in plate 2, there is specific labeling of the parietal cells (arrow). Chief cells do not label for the presence of TK.

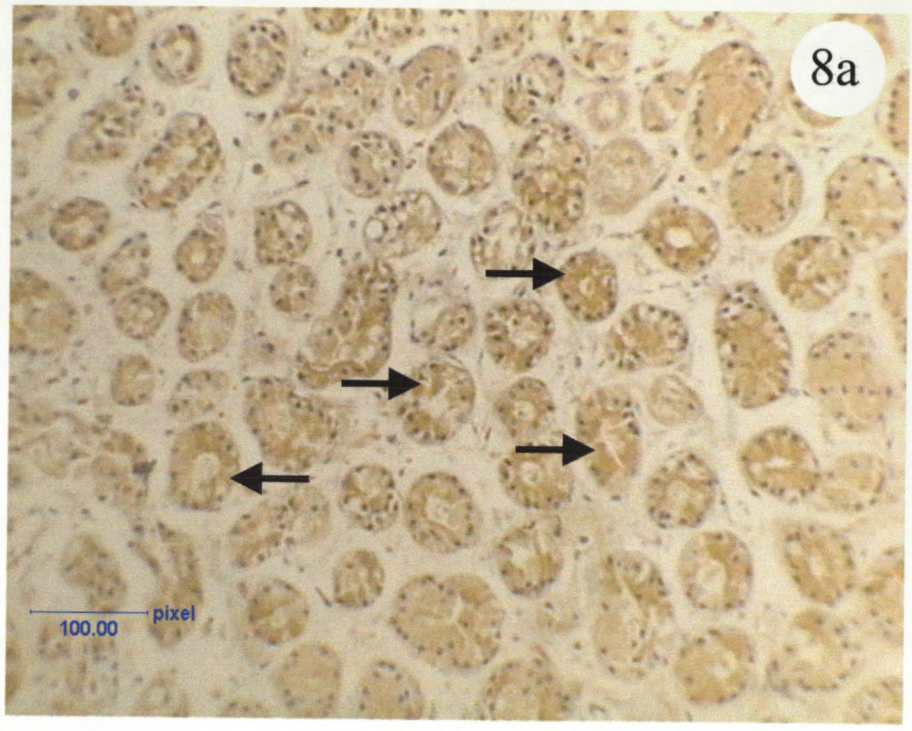
8a
100.00
pixel

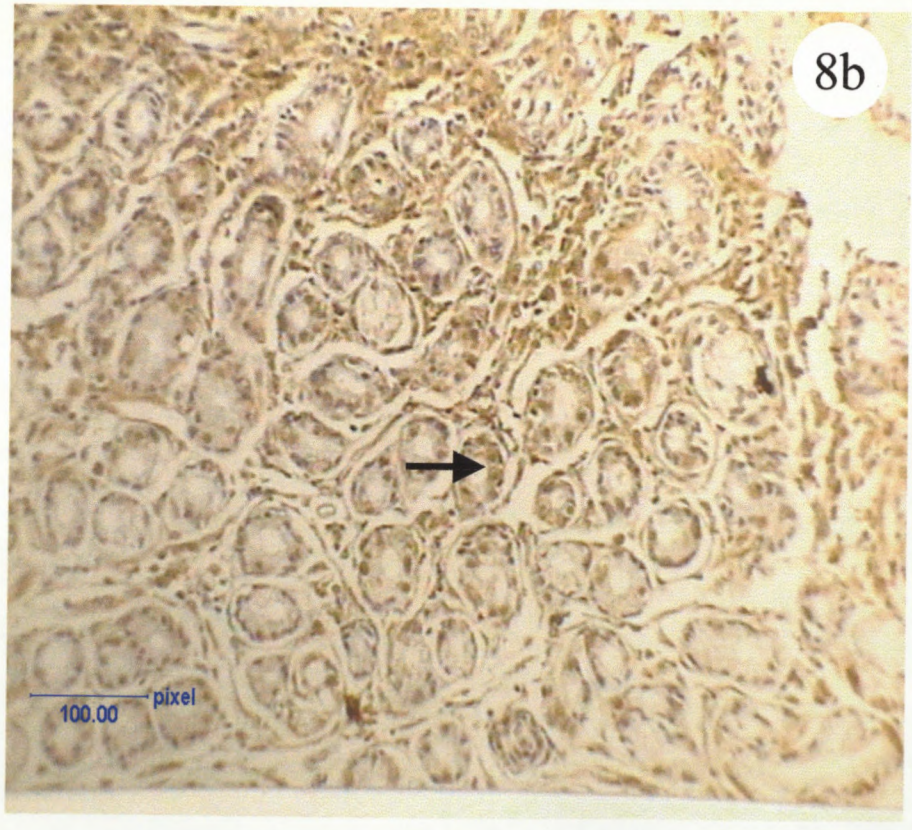
8b
100.00
pixel

few inflammatory cells present in the lamina propria, and these also are mildly positive for TK.

3.3.1.1.2 DAB staining in group 2

TK immuno-labelling in group 2 antrum is shown by plate 10a (X200). There is visually stronger labelling when compared to the normal group 1 (plate 8a). The parietal cells of the antrum (plate 10b, X1000) are much more clearly defined, and exhibit a distinct granular TK label (arrows).

The chief cells in this photo-micrograph show no positive label and neither do the stromal cells. Also note is that the nuclei show TK label. Plate 10c (X1000) exhibits TK labelling in the parietal cells (arrows). The granularity of the TK label is even more pronounced in this photo-micrograph. The mucus-secreting cells in the glands show no positive immuno-labelling and are structurally clear. There are a few inflammatory cells adjacent to the glandular structures that have taken up some of the DAB label, and show TK specificity.

Plate 11a (X200) illustrates TK immuno-localisation in the body area of group 2. The arrows show clearly the parietal cells that are labelled while the surrounding inflammatory cells are negative. There is also no label present in the chief cells and the epithelial cells. Plate 11b shows the body region at higher magnification (X1000) and intense label can be seen in the parietal cells (indicated by arrows). There is also TK label noted in the inflammatory cells (recognised by bipolar nuclei and being extra-glandular). The chief cells show no positivity (clear cells flanking labelled parietal cells in glands). Plate 11c demonstrates the deep glands

Plate 9a: This photomicrograph depicts an H&E section (X200) of antrum from mildly inflamed group 2. Note the presence of inflammatory cells (arrows) in the lamina propria between the glands, migrating towards the surface epithelia. Glandular structures still maintain their shape, regularity and form.

Figure 9b: This photo-micrograph is a X400 magnification of group 2 body tissue, showing the presence of a large number of inflammatory cells (arrows) in the connective tissue. Some inflammatory cells are beginning to infiltrate the glands, which will eventually lead to gland destruction.

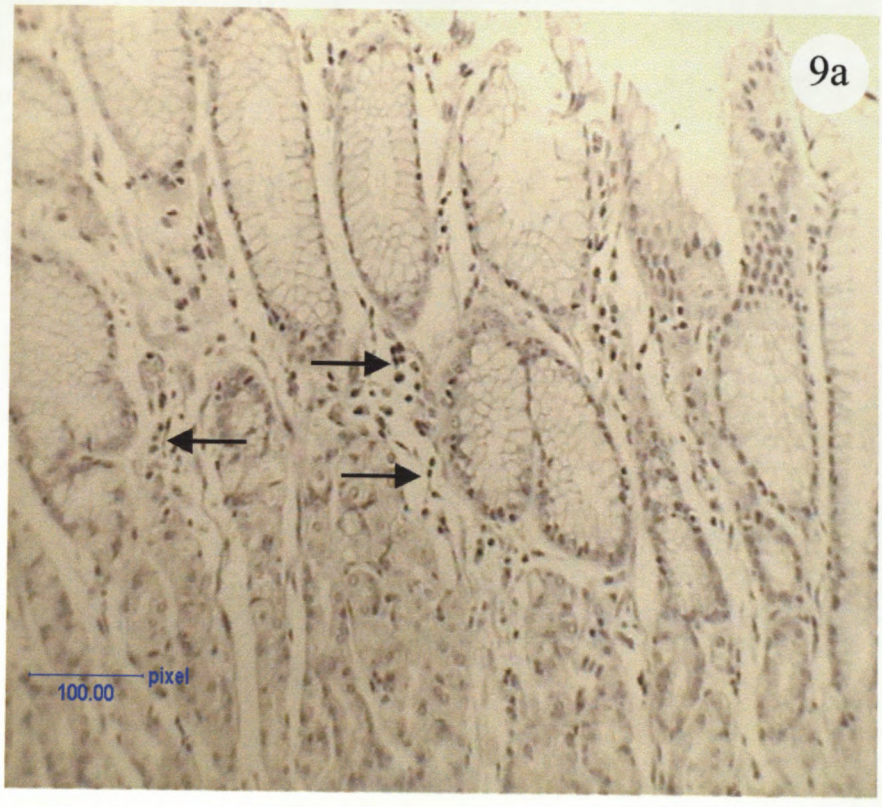
9a
100.00
pixel

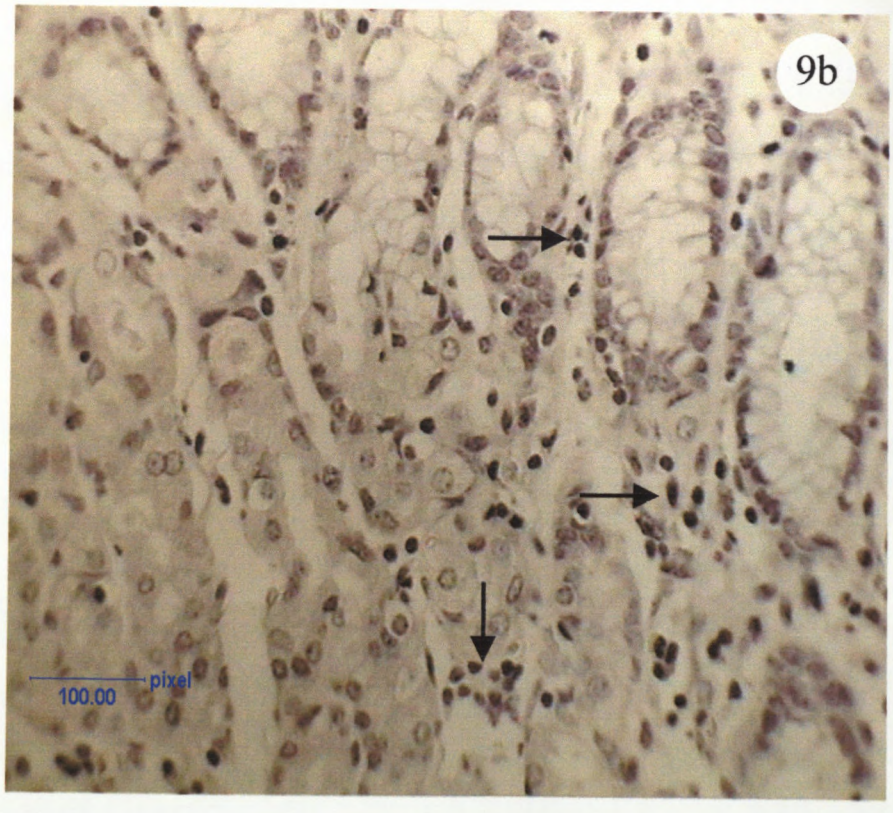
9b
100.00
pixel

Plate 10a Photo-micrograph (X200) of group 2 showing TK immuno-labelling in the antral glands. Parietal cells show specific DAB label (arrows).

Plate 10b: Photo-micrograph of antral deep crypts (X1000) of group 2 antrum showing specific TK immuno-labelling in the parietal glands (arrows) of the deep crypts. The chief cells show no label.

Plate 10c: This photo-micrograph (X1000) shows TK label in the crypt gland-parietal cells and inflammatory cells of deep antral mucosa. The oxyntic/chief cells do not show any TK label.

Plate 11a: Photo-micrograph (X200) of group 2 body tissue showing distinct and specific TK label in the parietal cells (arrows). Note the absence of label in the connective tissue and the mucous cells.

Plate 11b: Photo-micrograph (X1000) depicting strong TK DAB label in the parietal cells of the body glands. Feature to note is the specific staining of the parietal cells (arrows). Some interglandular inflammatory cells have also taken up TK.

Plate 11c: Photo-micrograph (X1000) showing intense granular TK-DAB immuno-localisation in the parietal cells (arrows) of the superficial body glands.

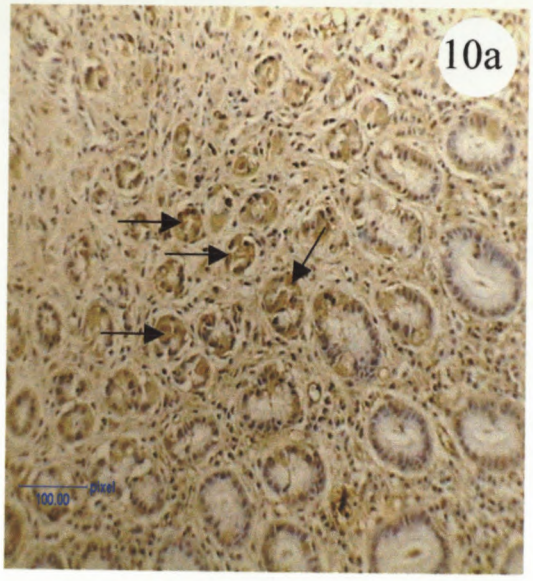
10a
100.00 pixel

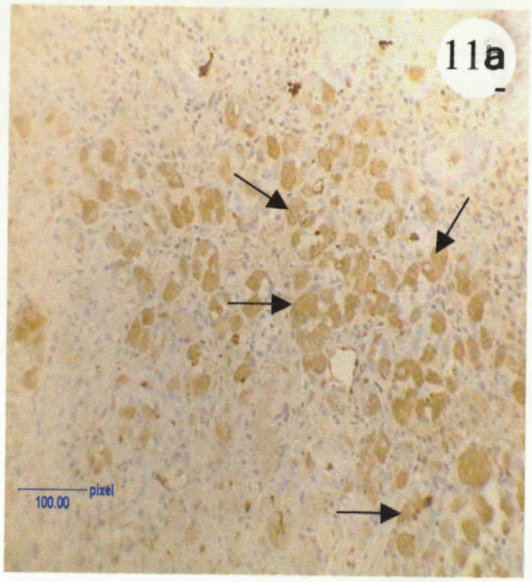
11a
100.00 pixel

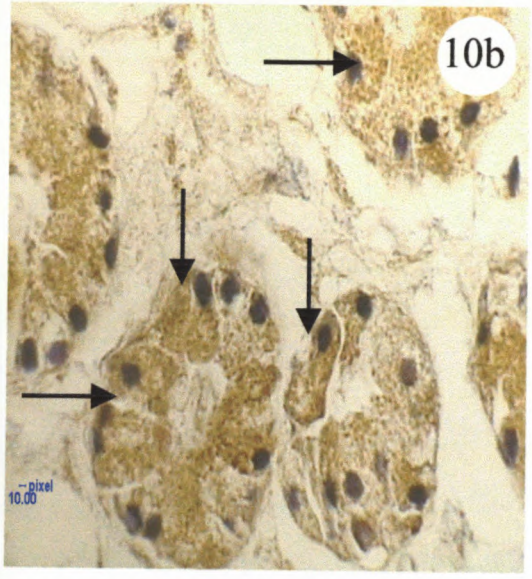
10b
10.00 pixel

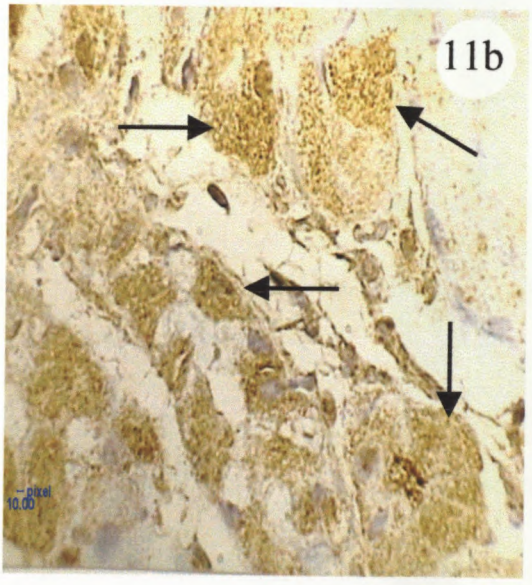
11b
10.00 pixel

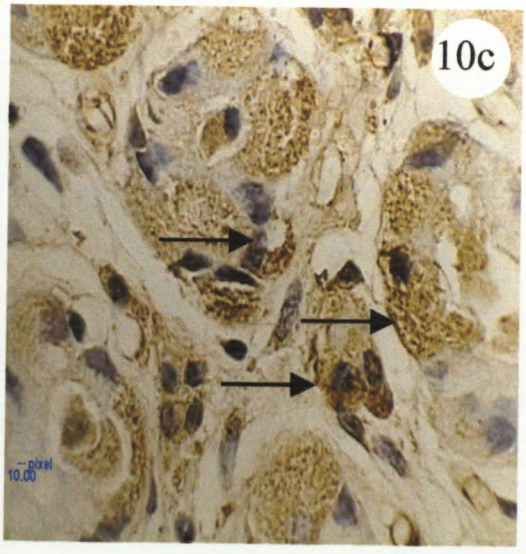
10c
10.00 pixel

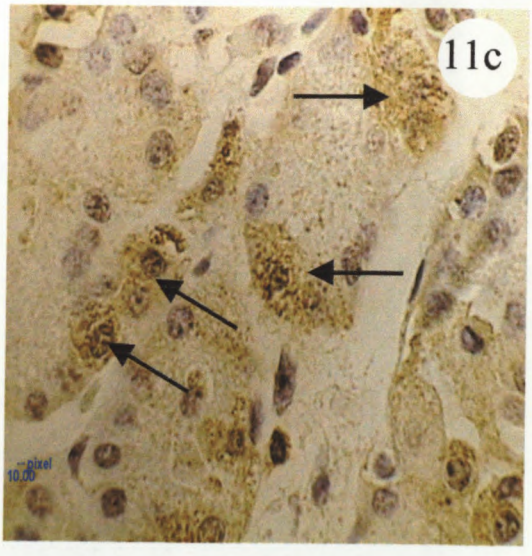
11c
10.00 pixel

of the body (X1000), and the arrows indicate intense TK immuno-label in the parietal cells. The epithelial cells lining the glands also show no label.

3.3.1.1.3 DAB staining in group 3

Plate 13a demonstrates TK immuno-labelling in the group 3 antrum (X1000). This plate is a definitive illustration of cryptitis, that is, inflammation of the crypt of a deep gland. As can be seen, the monocytes (neutrophils) have invaded the gland (arrow), infiltrated the bi-membrane, and are deposited in the lumen of the gland. The epithelial cells of the gland itself are not positive for TK, but the inflammatory cells surrounding it do show some TK label. A cross-section of the deep glands showing parietal cells (arrows) labelled with clear epithelial cells are shown in plate 13b (X1000). Plate 13c is another photo-micrograph depicting the deep antral glands (X1000). The epithelial cells with clear cytoplasm and large nuclei are negative while the larger, triangular parietal cells with basal nuclei (arrows) are immuno-positive.

Plates 14a, 14b, and 14c depict the body regions of group 3. Plate 14a (X200) shows a section of superficial glands and some cross-sectioned glands. As indicated by the arrows the parietal cells of the deeper glands show positive TK label. The inflammatory cells are negative, while some surface epithelial cells show TK immuno-positivity. Plate 14b is a higher magnification (X1000) of the body region of group 3. The TK staining (arrows) is shown to be very intense and granular in the body parietal cells. Plate 14c (X1000) shows large parietal

Plate 12a: Photo-micrograph (X200) of an H&E-stained antral tissue section of group 3. This image shows massive infiltration of the inflammatory cells (arrows) from the mucosa into the deep glandular area, extending into the superficial regions. This photograph is representative of active, chronic gastritis, which results in imminent tissue destruction, glandular atrophy and metaplasia.

Figure 12b: This is an H&E (X400) of group 3 body area. Shown are a large number of inflammatory cells present in the connective tissue. Also evident is the insinuation of the inflammatory cells into the glands, as depicted by the arrows. Tissue destruction is evident with glandular structures losing their form.

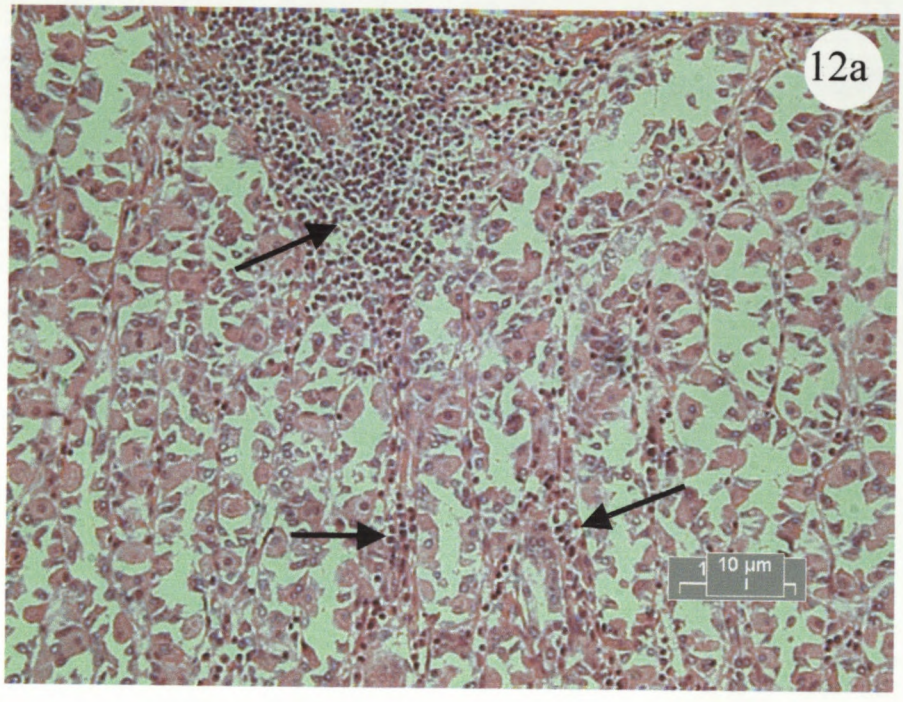
12a
10 µm

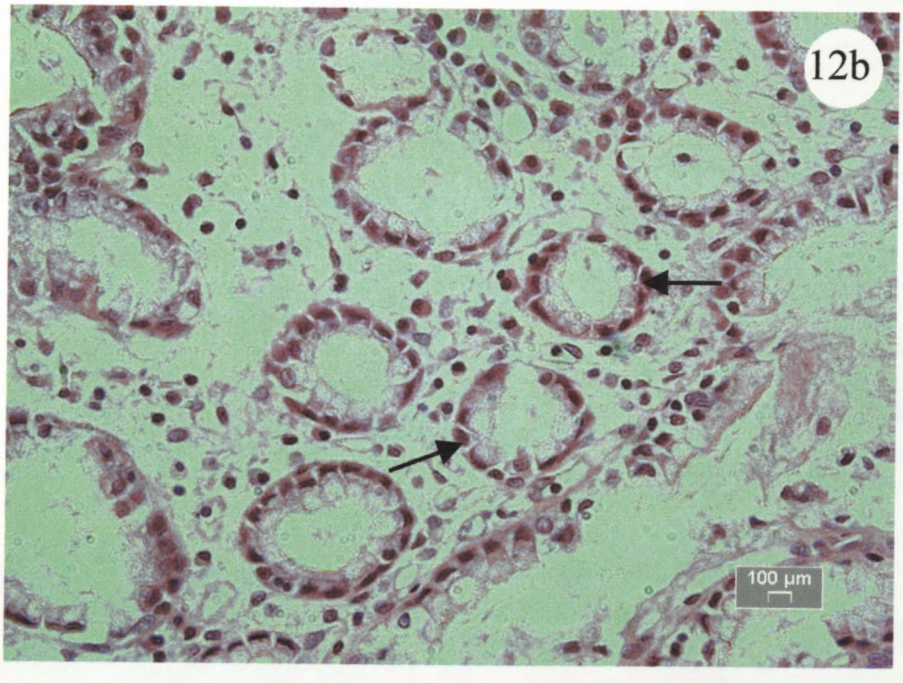
12b
100 µm

Plate 13a: This photo-micrograph (X1000) shows a definitive presentation of cryptitis in the antrum of group 3 gastric tissue. There are inflammatory cells present and the glandular bi-membrane (mucous cells) have been compromised. The arrow points to an inflammatory cell that is infiltrating the gland. In the lumen of the gland inflammatory cell-deposits are evident. In this image, TK immuno-label is shown in the inflammatory cells. The mucous cells show no specificity for TK.

Plate 13b: TK label is shown in the antral parietal cells (arrows) of group 3 in this photo-micrograph (X1000). The chief cells show no specificity for TK.

Plate 13c: This photo-micrograph (X1000) shows TK localisation in the parietal cells of group 3 antral superficial glands (arrows). Note the intense and granular effect of the DAB stain.

Plate 14a: Photo-micrograph (X200) illustrating TK immuno-label in the gastric body glands (arrows). There is a diffuse label over the entire glands and single-cell labeling is indistinctive. Inflammatory cells in the connective also show positive TK label.

Plate 14b: Photo-micrograph (X1000) of group 3 body tissue showing intense, granular TK immuno-localisation in the parietal cells (arrows) of the crypts of the deep glands. Inflammatory cells do not exhibit any TK label.

Plate 14c: High magnification (X1000) of deep glands of group 3 body tissue. Evident in this image is the clear and distinctive granular labeling of TK in the parietal cells (arrows). Also shown is destruction of the glands and the non-labelling of the inflammatory cells.

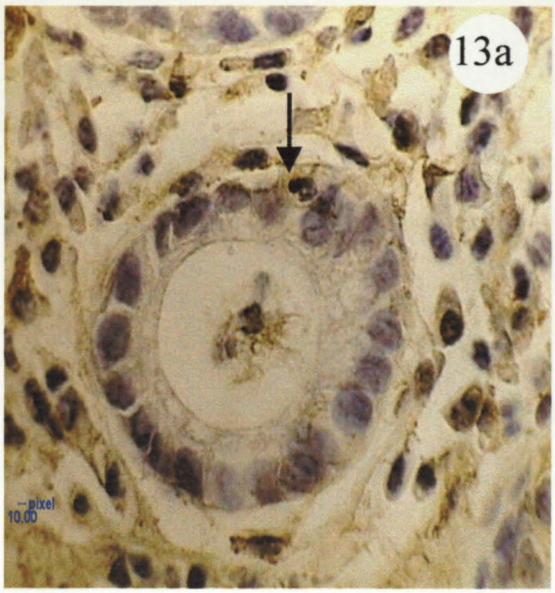
13a

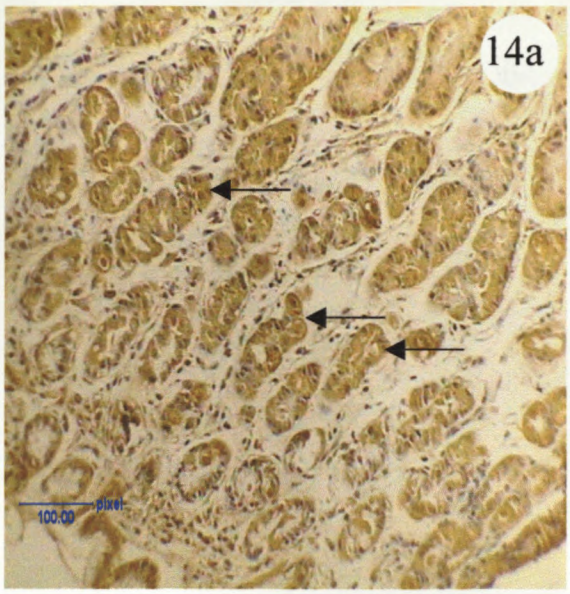
14a

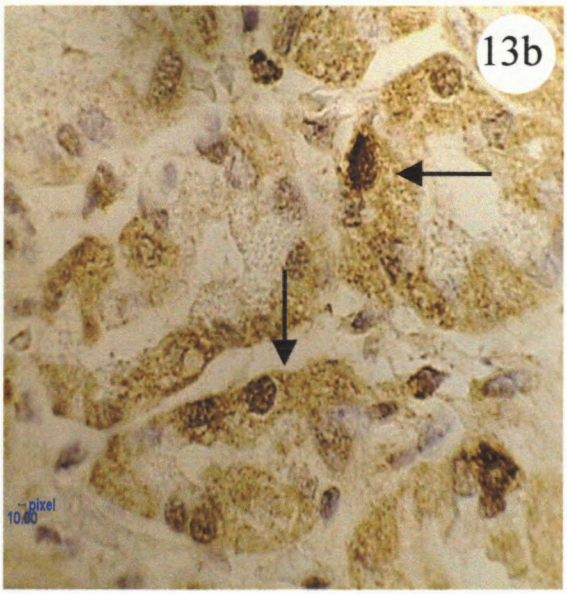
13b

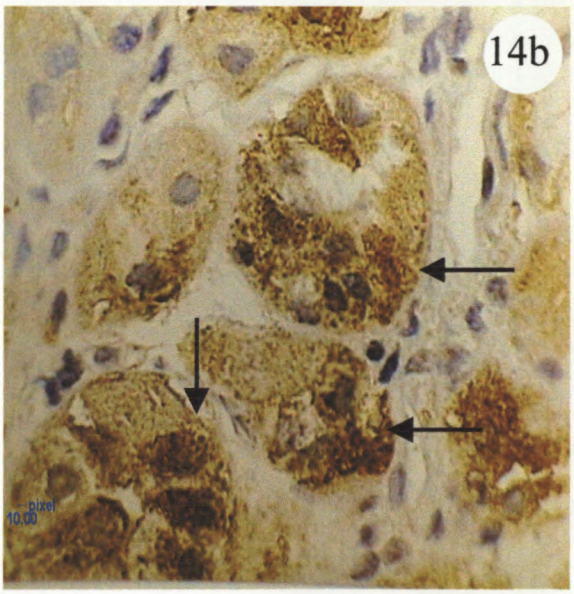
14b

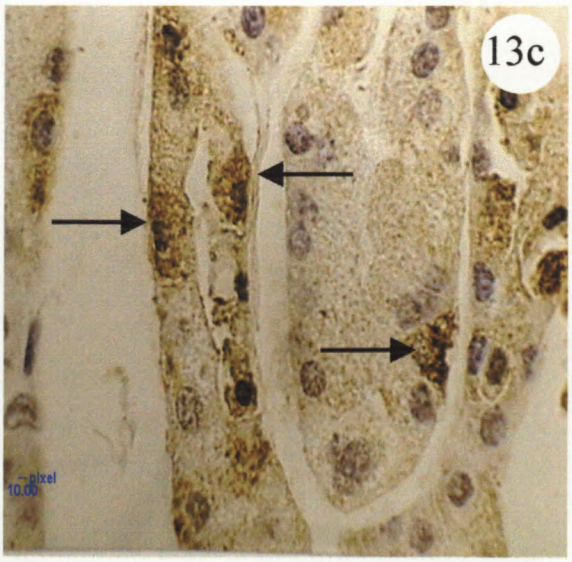
13c

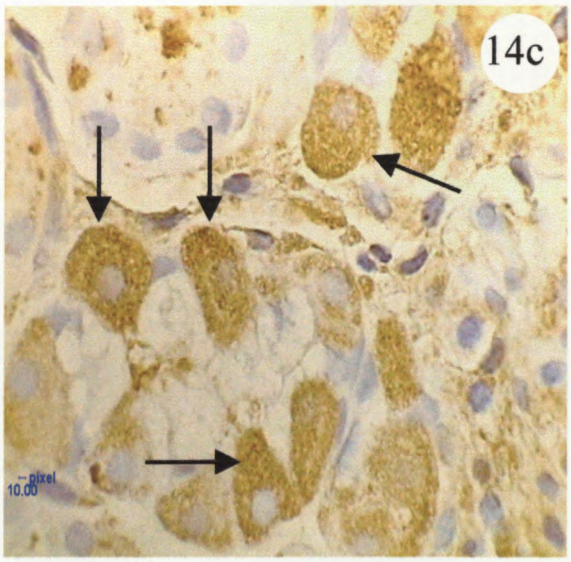
14c

cells labelled (arrows), smaller epithelial cells (small, round nuclei) negative and TK-positive inflammatory cells in surrounding tissue. This photo-micrograph also shows the destruction of the body glands, with glandular deformation and cellular structures being compromised.

Plate 15a is a photo-micrograph (X1000) depicting a section of deep glands being destroyed in the antrum of group 3. As can be seen, the parietal cells (indicated by arrows) are intensely stained for TK. Of particular interest are the mucous cells (cells in the deep glands with central, round nuclei and clear cytoplasm) which are also mildly labelled. The inflammatory cells present between the glands are also labelled. Plate 15b (X1000) is similar to plate 15a in that there are strongly labelled parietal cells in the deep glands

Plate 16a (X1000) shows TK immuno-label in the body area of group 3. The epithelial cell cytoplasm remains clear, but the nuclei (arrows) have taken up the DAB stain. There are some inflammatory cells present that have also stained positive. Plate 16b is a section of the deep glands. As illustrated by the arrows, TK immuno-label is found in the parietal cells, but not in the chief cells that flank the parietal cells in the glands.

3.3.1.1.4 DAB staining in group 4

Plate 18 (X200) shows TK immuno-labelling in the superficial antral region of group 4. As can be seen by the arrows, the parietal cells and the epithelial cells are negative. There are some inflammatory cells present that are TK positive.

Plate 15a: Photo-micrograph of the deep antral tissue of group 3 (X1000). TK label is seen, in detail, in the parietal cells (arrows). Inflammatory cells show no TK label.

Plate 15b: Superficial glands (X1000) of the antrum. Distinctive TK label (arrows) in the parietal cells. Mucous cells show no label.

Plate 16a: Photo-micrograph (X1000) of the body superficial gastric glands of group 3 showing TK immuno-label in the nuclei of the mucous cells (arrows). Inflammatory cells infiltrating the glands also display TK immuno-label.

Plate 16b: TK specific immuno-localisation in the parietal cells (arrows) of superficial body area (X1000). Mucous cells do not show any positivity for TK.

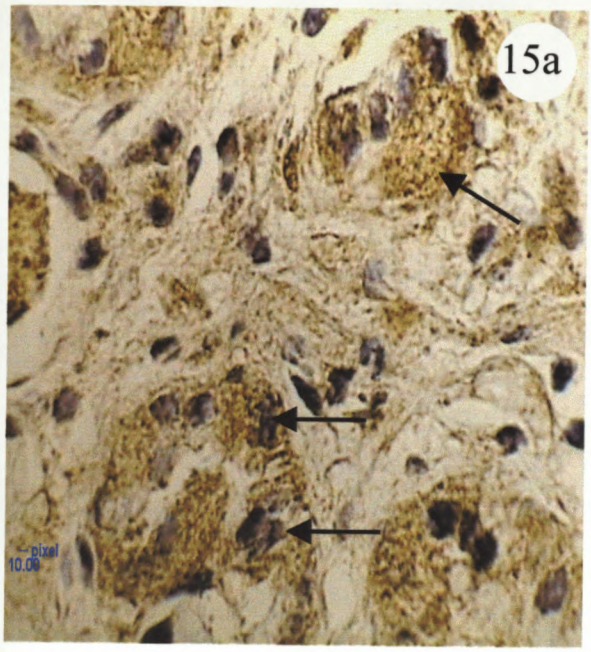
15a

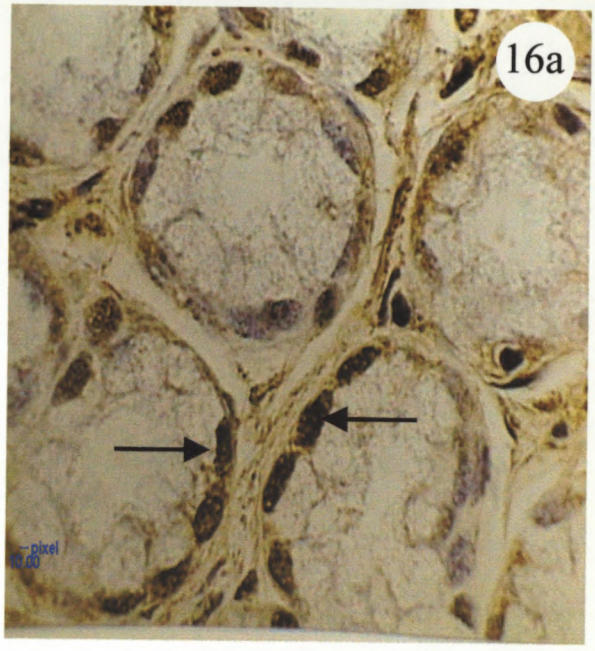
16a

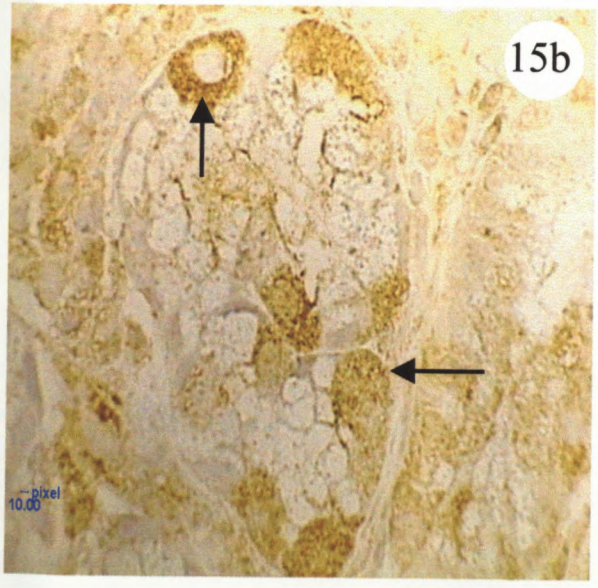
15b

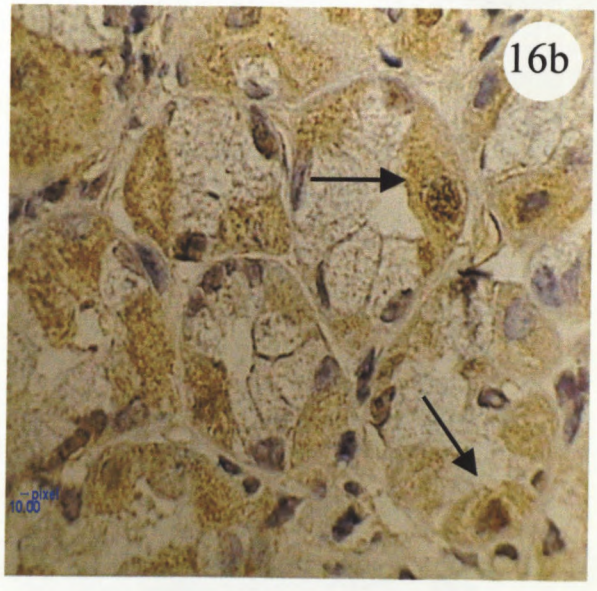
16b

Plate 17: Photo-micrograph (X1000) of an H&E-stained tissue section of group 4. There are a large number of inflammatory cells present in the surrounding connective tissue. Glands show metaplasic differentiation and have assumed a simple mucous type profile with large clear cytoplasm (arrow).

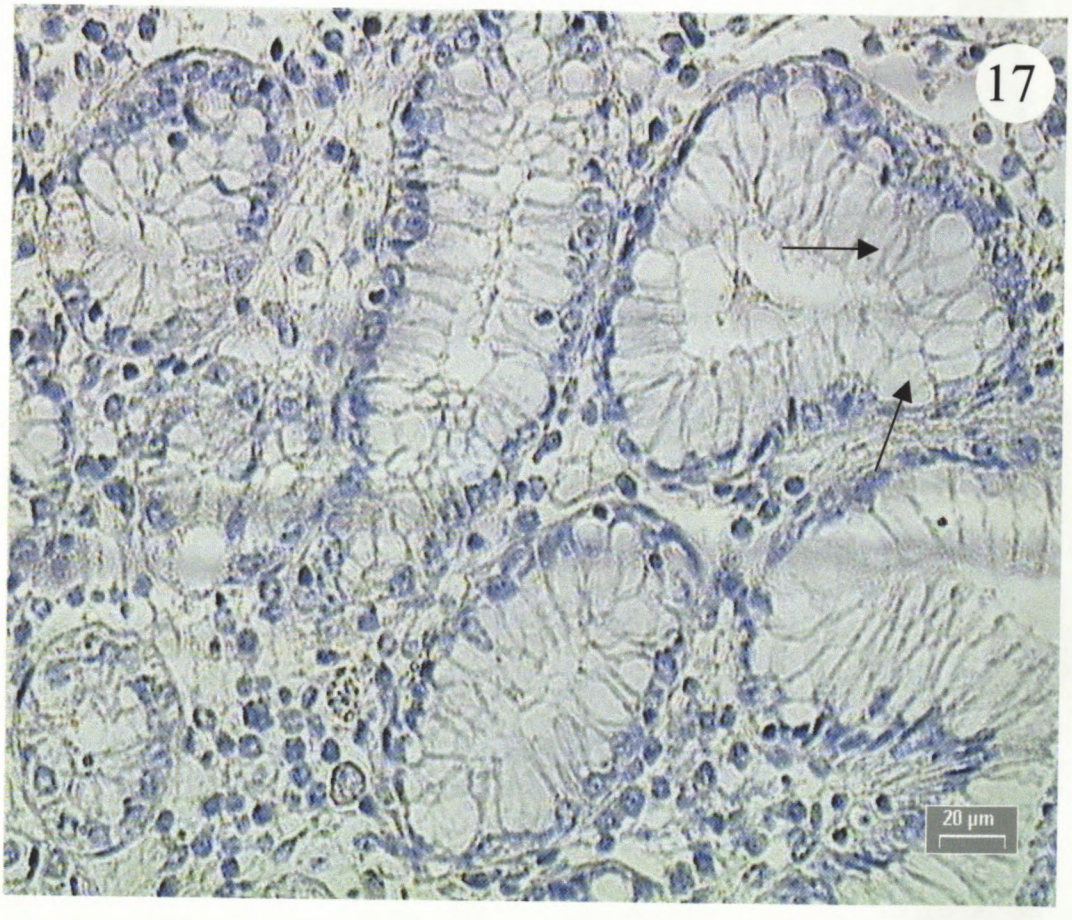
17
20 µm

Plate 18: Photo-micrograph (X200) of TK labeling in group 4 antral tissue. There is evidence of glandular destruction (arrows) and cells show no TK immuno-label. Inflammatory cells show some TK immuno-localisation.

Plate 19: This photo-micrograph (X1000) shows TK immuno-labelling in a parietal cell of a group 4 body gland (arrow). The chief cells exhibit no TK label, and there is evidence of tissue destruction.

Plate 20: Photo-micrograph (X400) of a method control for the DAB immunocytochemical labeling procedure. The primary TK antibody was replaced with PBS buffer, and all cellular processes show no specific TK label

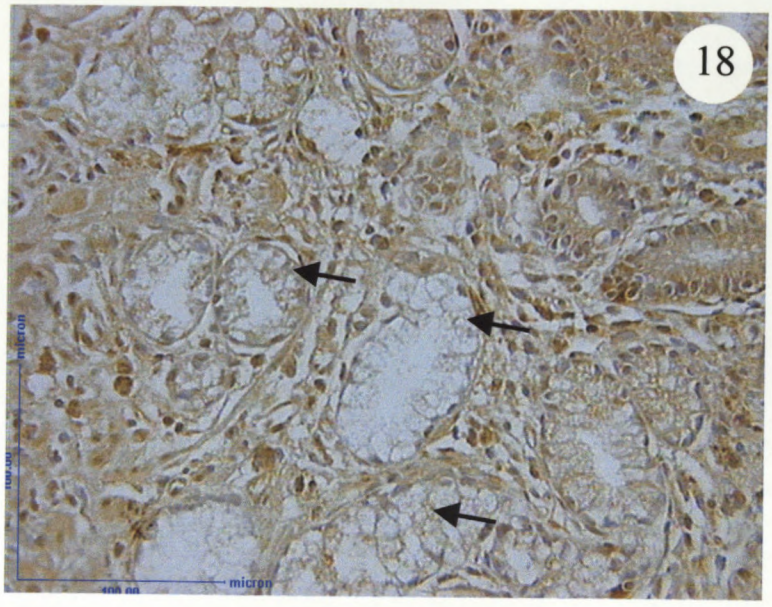
18
micron


19

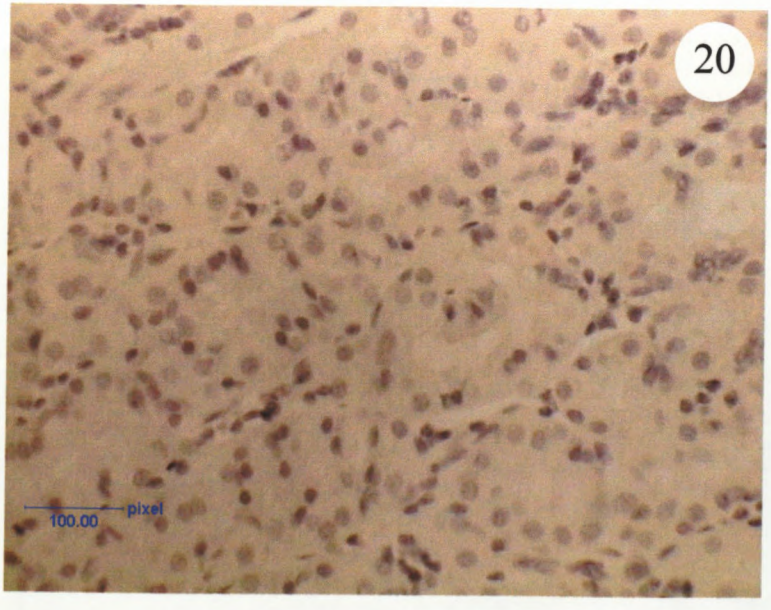
20
100.00
pixel

Plate 19 shows a parietal cell weakly labelled for TK in the deep body region of group 4. There is glandular destruction and the chief cells do not label positive.

Plate 20 depicts deep glands in the body region of group 4 (X400). This tissue section served as a method control for the immunocytochemistry labelling experiments (refer to section 2.4.4.4). The primary antibody, goat anti-human tissue kallikrein was replaced by buffer in the labelling protocol.

As can be seen the glands do not label for TK, that is, the parietal cells or the chief cells.

3.3.1.2 Image analysis of tissue kallikrein DAB immuno-localisation

3.3.1.2.1 Statistics of Image analysis for DAB immuno-precipitation

Analysis of the raw image data obtained for TK DAB immuno precipitation was done with use of the Kontron KS300 imaging system (Kontron GmbH, Germany) (refer to section 3.1.4). The intensity of labelling obtained for each group was calculated as intensity being represented as units of pixels per unit area examined (pixels/um^2). Table 11 tabulates the descriptive intensity of each group examined and is further divided into two histological antral and body regions. From table 11, the mean intensity of TK staining in the antrum decreases from group 1 (3.3 x 10^{-3} pixels/um^2) to group 4 (0.8 x 10^{-3} pixels/um^2). This represents a definite decrease in the mean staining intensity of TK as the disease state progresses from non-inflamed normal

control to severely inflamed. For the mean staining intensity of the body areas labelled with immuno-reactive TK, there appears to be a slight increase from group 1 (control, 4.10 x 10^{-3} pixels/um^2) to group 3 (moderate to severe inflammation, 5.7 x 10^{-3} pixels/um^2). The mean intensity of the body obtained for severely inflamed group 4 (0.0037 x 10^{-3} pixels/um^2) is lower than even the basal control group (4.10 x 10^{-3} pixels/um^2). There is no difference between the mean intensity of group 1 and group 2 body regions (4.10 x 10^{-3} pixels/um^2).

3.3.1.2.2 Comparison of staining intensity for TK DAB immuno-labelling of the antral regions between the histological groups

Table 12 represents an *inter-group t-test comparison* with *equal variance* between the antral areas between the histological groups. A p value < 0.05 was considered statistically significant. There was no significant difference established when group 1 was compared to group 2. This would be accounted for by the similar staining intensities obtained by image analysis (see section 3.3.1.2.1). When group 1 antrum was compared to group 3 antrum there was almost significant comparison factor (p = 0.08 ± 0.0023). The extremely significant factor was obtained by comparison of group 1 to group 4 (p = 0.004 ± 0.002). Comparison of group 2 versus group 4 showed significance also (0.003 ± 0.003) representing a reduction in staining intensity from group 2 versus group 4. The p value for comparison of group 3 to group 4 was 0.03 ± 0.0024. These results suggest a basal staining intensity in the mild inflamed antrum for TK, but as the disease progresses the staining intensity is markedly increased.

3.3.1.2.3 Comparison of staining intensity for TK DAB immuno-labelling between the body regions of the histological groups

Table 13 shows the comparison of groups with respect to staining intensity for TK. The comparison factor of significance shows only on comparison of group 3 body versus group 1 body (0.001 ± 0.0029). This represents the increase in TK staining intensity (see table 11) between the body area of the non-infected group 1 to the moderate to severely inflamed body of group 3.

Table 11 Single descriptive statistics (column) of various histological groups for DAB image analysis immuno-localisation

Group		Mean (pixels/μm^2 $x10^{-3}$)	Median (pixels/μm^2 $x10^{-3}$)	Range (pixels/μm^2 $x10^{-3}$)	SEM (±)
Group 1	Antrum	3.30	3.29	3.2 - 3.35	0.01
	Body	4.10	4.06	3.0 - 5.02	0.30
Group 2	Antrum	3.30	3.25	2.70 - 3.79	0.50
	Body	4.0	3.90	3.1 - 4.92	0.50
group 3	Antrum	2.10	1.89	1.40 - 3.76	0.30
	Body	5.70	3.03	0.60 - 26.60	2.70
Group 4	Antrum	0.8	0.825	0.7-0.99	0.2
	Body	0.0037	0.000368	0.0007-0.00668	0.0029

SEM : standard error of the mean
pixels : unit of measure of colour/light intensity

Table 12 **Intergroup comparison using t-test with equal variance (95% confidence interval, maximum) for Tissue Kallikrein DAB immuno-labelling between antral regions of the various histological groups**

Group	**Group 1** *antrum* ($p \pm$ 95% CI)	**Group 2** *antrum* ($p \pm$ 95% CI)	**Group 3** *antrum* ($p \pm$ 95% CI)
Group 1 *antrum* ($p \pm$ 95% CI)			
Group 2 *antrum* ($p \pm$ 95% CI)	0.94 ± 0.0023		
Group 3 *antrum* ($p \pm$ 95% CI)	0.08 ± 0.0027	0.15 ± 0.0024	
Group 4 *antrum* ($p \pm$ 95% CI)	0.004 ± 0.002	0.003 ± 0.003	0.03 ± 0.0024

95% CI (maximum) = 95% confidence interval
p value < 0.05 is not considered to be statistically

Table 13 **Intergroup comparison using t-test with equal variance (95% confidence interval, maximum) for Tissue Kallikrein DAB immuno-labelling between body regions of the various histological groups**

Group	**versus Group 1** *body* ($p \pm$ 95% CI)	**versus Group 2** *body* ($p \pm$ 95% CI)	**versus Group 3** *body* ($p \pm$ 95% CI)
Group 1 *body* ($p \pm$ 95% CI)			
Group 2 *body* ($p \pm$ 95% CI)	0.88 ± 0.0013		
Group 3 *body* ($p \pm$ 95% CI)	0.001 ± 0.0029	0.73 ± 0.0092	
Group 4 *body* ($p \pm$ 95% CI)	0.76 ± 0.0026	0.81 ± 0.0048	0.81 ± 0.01

95% C.I. (maximum) = 95% confidence interval
p value < 0.05 is not considered to be statistically significant

3.3.2 Immuno-fluorescence and confocal microscopy

3.3.2.1 Immunofluorescent localisation using FITC (fluorescein-isothiocyanate)

For immuno-fluorescence the target protein is probed with a specific antibody that is then conjugated to an anti-species FITC conjugate. This conjugate fluoresces at 525 nm and the fluorescent intensity has been captured and converted by confocal microscopy software to be presented as colour. Therefore, the intensity of the staining is represented by a segmented visible colour spectrum. The fluorescent photo-micrographs in this section are presented as colour images, each with a scale colour-bar. The colour of the immuno-labelling ,according to its position on the colour-bar, is a function of the intensity of the label (Refer to section 3.1.3).

3.3.2.1.1 Fluorescent immuno-localisation in group 1

Group 1 antral TK immuno-fluorescence is represented by plate 21 a to 21 d. Plate 21a shows label in the antral region of group 1, evident in the parietal cells (white arrows) and neck glandular regions. The general staining intensity is in the mid range, as can be gauged from the colour bar. Plate 21b shows antral glandular cells labelling in the basal-plane areas. Phase contrast diagram (not shown) indicates that the TK label is concentrated in the parietal cells (arrows) of the neck glands. The tall columnar-shaped superficial and neck mucous cells do not appear to label for TK. Plate 21c shows widespread label along the basal edge of the superficial glands. There is no TK labelling of the mucous cells. Interglandular areas (lamina propria) shows scattered labelling in the mid intensity range. Plate 21d depicts mid

Plate 21a: photo-micrograph showing fluorescent image of TK-FITC labeling in group 1 antrum. There is mild intensity staining in the parietal cells (arrows), and in some inflammatory cells.

Plate 21b: Fluorescent TK immuno-localisation in the superficial glands of the group 1 antrum. Medium staining intensity (reference colour-bar) is evident in the basement membranes of the mucous cells (arrows).

Plate 21c: This photo-micrograph shows TK label in the surface glands of the group 1 antral tissue. There is widespread diffuse labeling of the surface epithelia and mucous-secreting cells.

Plate 21d: Photo-micrograph showing fluorescent image of TK-FITC labeling in deep glands of group 1 antrum. Indicated by the arrows are labeled parietal cells. Staining intensity is in the medium range.

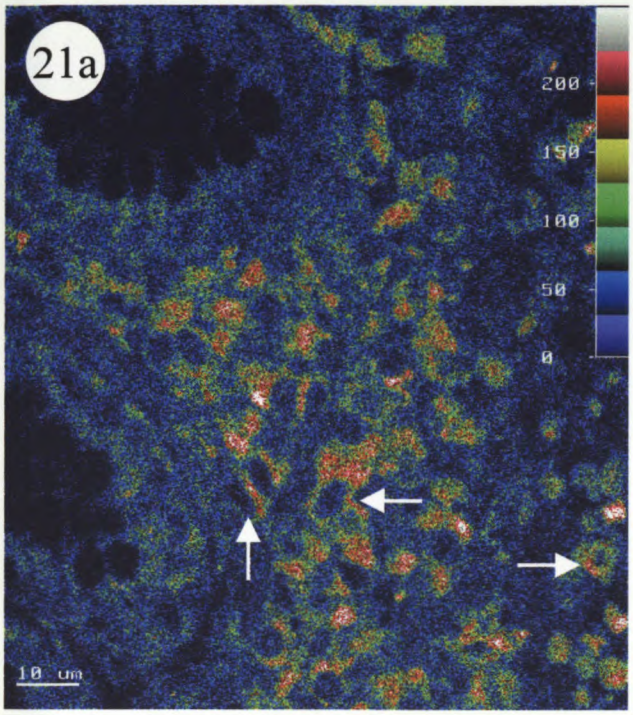
21a
200
150
100
50
0
10 um

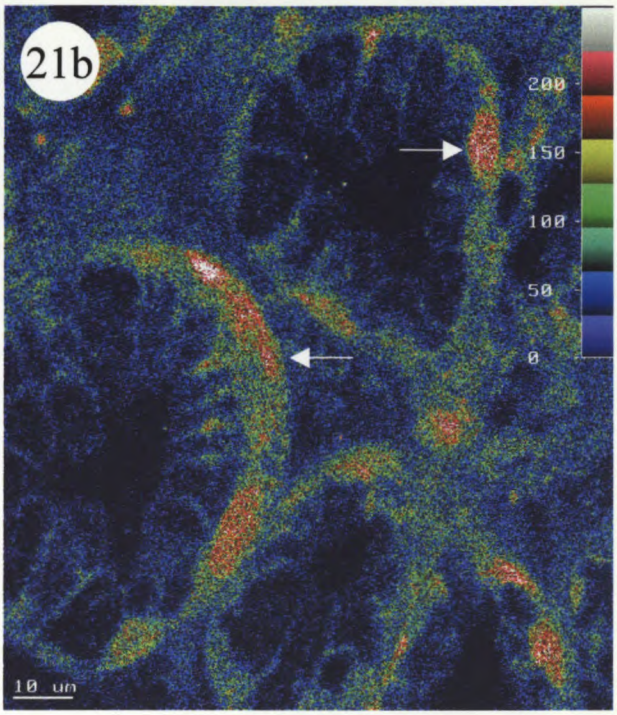
21b
200
150
100
50
0
10 um

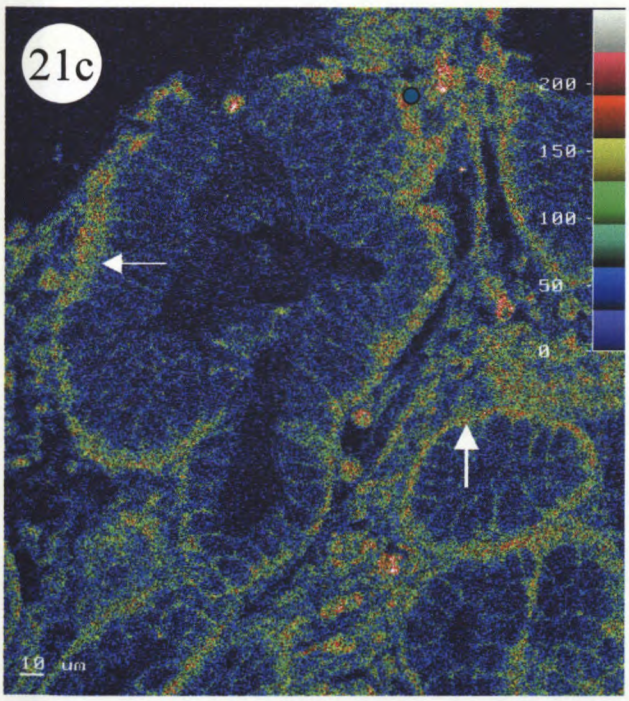
21c
200
150
100
50
0
10 um

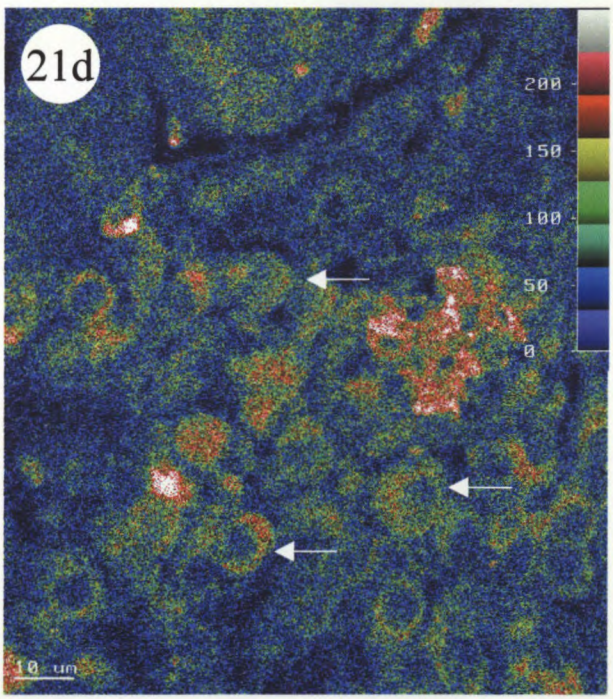
21d
200
150
100
50
0
10 um

to high intensity label in predominantly parietal cells in the deeper glands (arrows) of the normal antrum. Overall, the intensity of label in group 1 was in the mid-colour range

Plates 22a, b, and c are photo-micrographs of fluorescently-labelled body regions of group 1. Plate 22a depicts TK labelling in the deep glands, and visually the label seems to be in the mid to upper colour-bar region (refer to image analysis for exact quantification of intensity in this group in section 3.2.2.2). The arrows (white) point to labelled parietal cells, although the amount of label is not widespread. Plate 22b shows a similar area of the deep body glands, and again depicts label in the parietal cells (arrows). There is diffuse TK label spread over the deep glands and the visual intensity lies in the mid to upper reference range of the colour-bar. Plate 22c shows intense label over the glandular structures with high (white colour being a maximum reference point on the colour-bar) intensity label found particularly on the parietal cells (arrows).

Overall, for group 1 body and antrum, subjective visual detection of fluorescence intensity shows TK to be diffusely spread over the deep gland parietal cells, and over the basement membranes of the superficial and neck gland cells.

3.3.2.1.2 Fluorescent immuno-localisation in group 2

Plates 23a to 23d represent TK immunofluorescence in the antral area of the mildly-inflamed group 2. For group 2, TK immuno-label seems to be concentrated in the parietal cells of the antral regions probed (refer to arrows on plate 23a). Plate

Plate 22a: photo-micrograph showing fluorescent image of TK-FITC labeling in group 1 body. Arrows show label in some parietal cells. Visual intensity of label can be determined from the reference colour-bar showing intensity profile. Generally, the glands do not exhibit intense TK fluorescent labeling.

Plate 22b: photo-micrograph showing fluorescent image of TK-FITC labeling in group 1 body. Shown, by arrows, are the TK label in the parietal cells. There is some diffuse label over the glandular structures (indicated to be parietal cells on phase contrast, not shown).

Plate 22c: photo-micrograph showing fluorescent image of TK-FITC labeling in deep body glands, with diffuse staining patterns. The highest staining intensities were seen in the parietal cells (arrows).

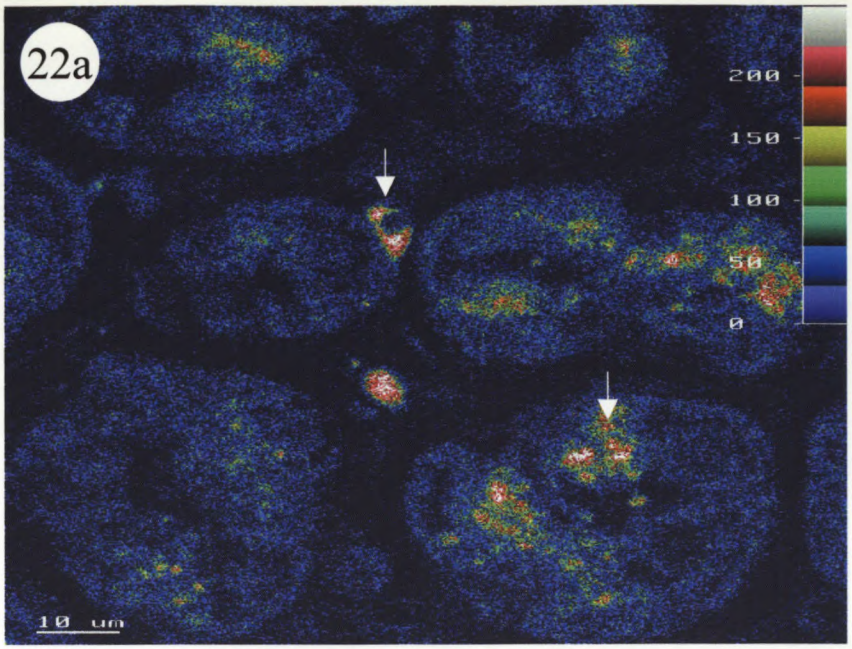
22a
200
150
100
50
0
10 um

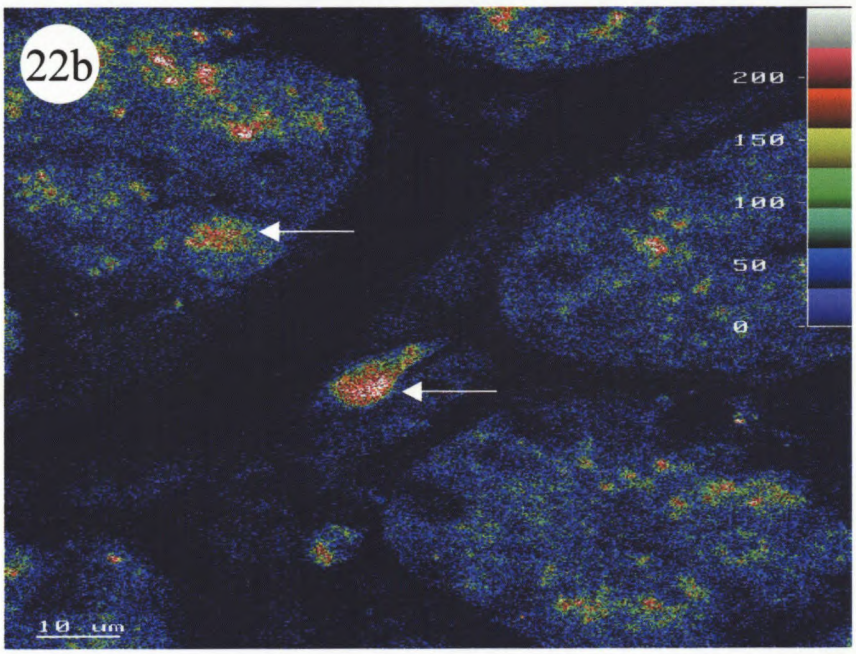
22b
200
150
100
50
0
10 um

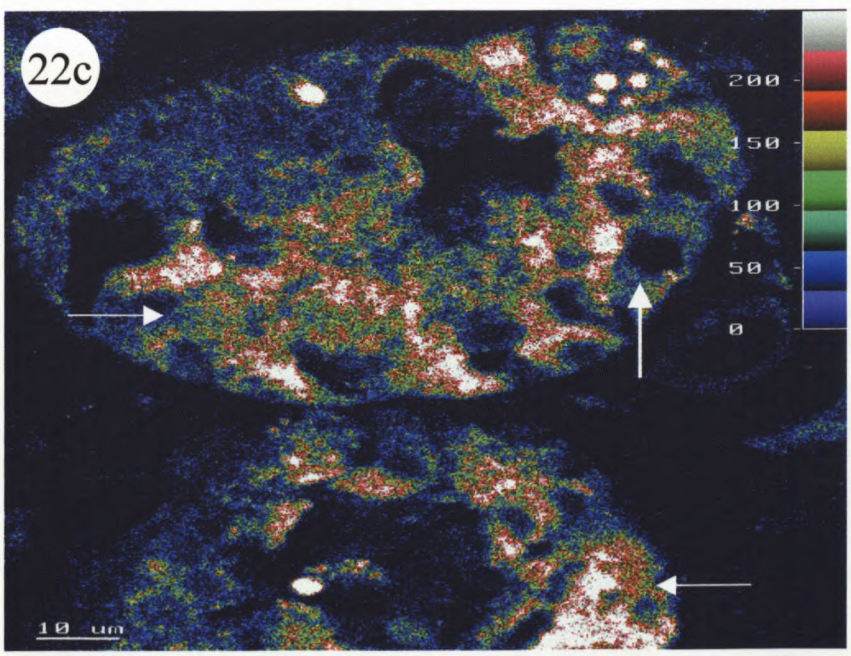
22c
200
150
100
50
0
10 um

Plate 23a: Photo-micrograph showing fluorescent image of TK-FITC labeling in group 2 antrum. Superficial tissue show label in the parietal cells (arrows) and in some of the inflammatory cells in the connective tissue.

Plate 23b: This photo-micrograph is a phase-contrast diagram of figure 17a. The phase diagrams are used to identify cellular and glandular structures. The arrows in figure 17a and figure 17b point to the same cells in the tissue, and this method is used to identify the cells that are immuno-labeled.

Plate 23c: In this photo-micrograph distinct fluorescent TK immuno-localisation is seen in the parietal cells of the deep antral glands (arrows). The chief cells and mucous cells do not show any TK specificity.

Plate 23d: Photo-micrograph showing fluorescent image of TK-FITC labeling in group 2 antrum. The TK label is spread diffusely over the deep glands and are of a medium intensity. From the corresponding phase diagrams (not shown), the label is predominantly on the parietal cells.

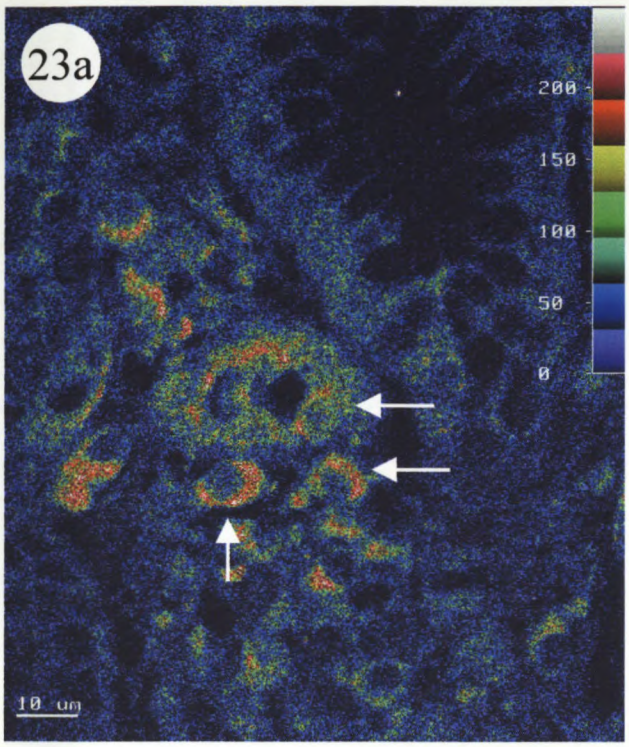
23a
200
150
100
50
0
10 um


23b

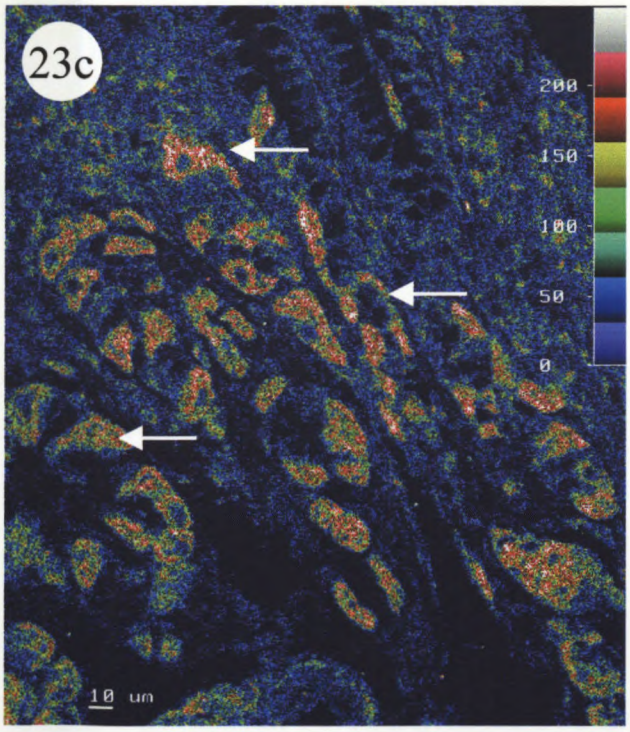
23c
200
150
100
50
0
10 um

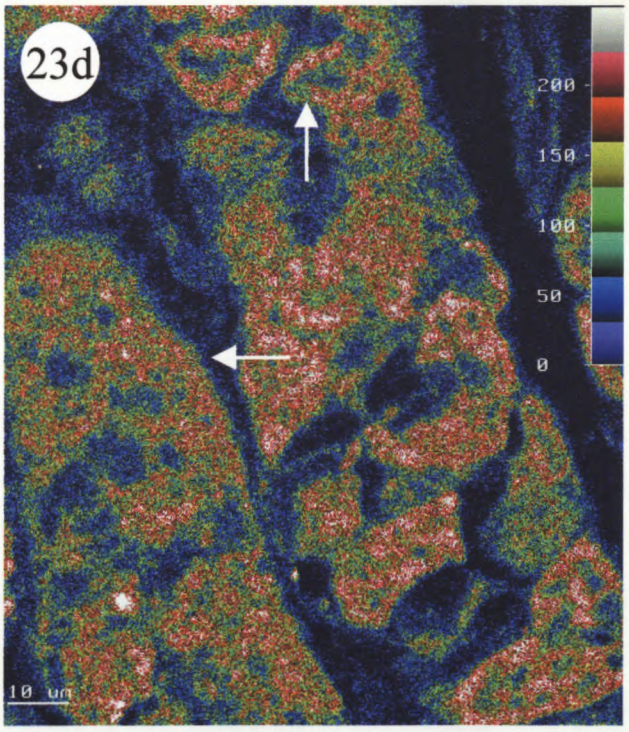
23d
200
150
100
50
0
10 um

23b is a black and white phase contrast image of plate 23a, and serves to illustrate structural details. As is evident, the arrows on both plate 23a and plate 23b point to the same cellular structures, parietal cells that are labelled. The adjacent gland in the photo-micrograph does not exhibit any label in the epithelial mucous cells. Plate 23c displays well-defined TK label (in the mid to upper reference colour-bar range) in a number of distinct parietal cells in deep antral glands (arrows). There is no label in the mucus-secreting cells or inter-glandular lamina propria. Plate 23d is a photo-micrograph showing diffuse (arrows) TK immuno-fluorescent label over deep glands. From the phase contrast image (not shown) most of the label is concentrated over the parietal cells.

Plates 24a to 24d depict immuno-fluorescent labelling of TK in the body region of group 2. Plate 24a shows significant and intense (according to colour bar) labelling of the deep glands. The intensity of label supersedes that of the deep glands of group 2 antral regions (refer to plate 23d). Plate 24b shows a region of deep crypts where distinct immuno-fluorescence is found in the parietal cells (arrows). There are also some inflammatory cells flanking the glands that exhibit fluorescence. There is a diffuse and increased (as compared to plate 23c) label in the parietal cells (arrows) of pate 24c. The intensity scale of this labelling is in the upper regions of the reference scale colour-bar. Plate 24d also shows (arrows) intense immuno-fluorescence in the deep glandular structures. The area of most intense label (indicated on phase contrast, not shown here) is on the parietal cells and on the basement membrane side of the glandular structures.

Plate 24a: Photo-micrograph showing fluorescent image of TK-FITC labeling in group 2 body. There is high intensity label (arrows) in the deep gland structures and parietal cells (from phase contrast, not shown).

Plate 24b: This photo-micrograph shows clearly, medium to high intensity TK immuno-label in the parietal cells of the deep glands of group 2 body tissue.

Plate 24c: Deep glands of group 2 body showing medium to high intensity (reference from colour scale-bar) immuno-localisation of TK in the parietal cells (arrows).

Plate 24d: High intensity TK label spread over the deep glands of group 2 body.

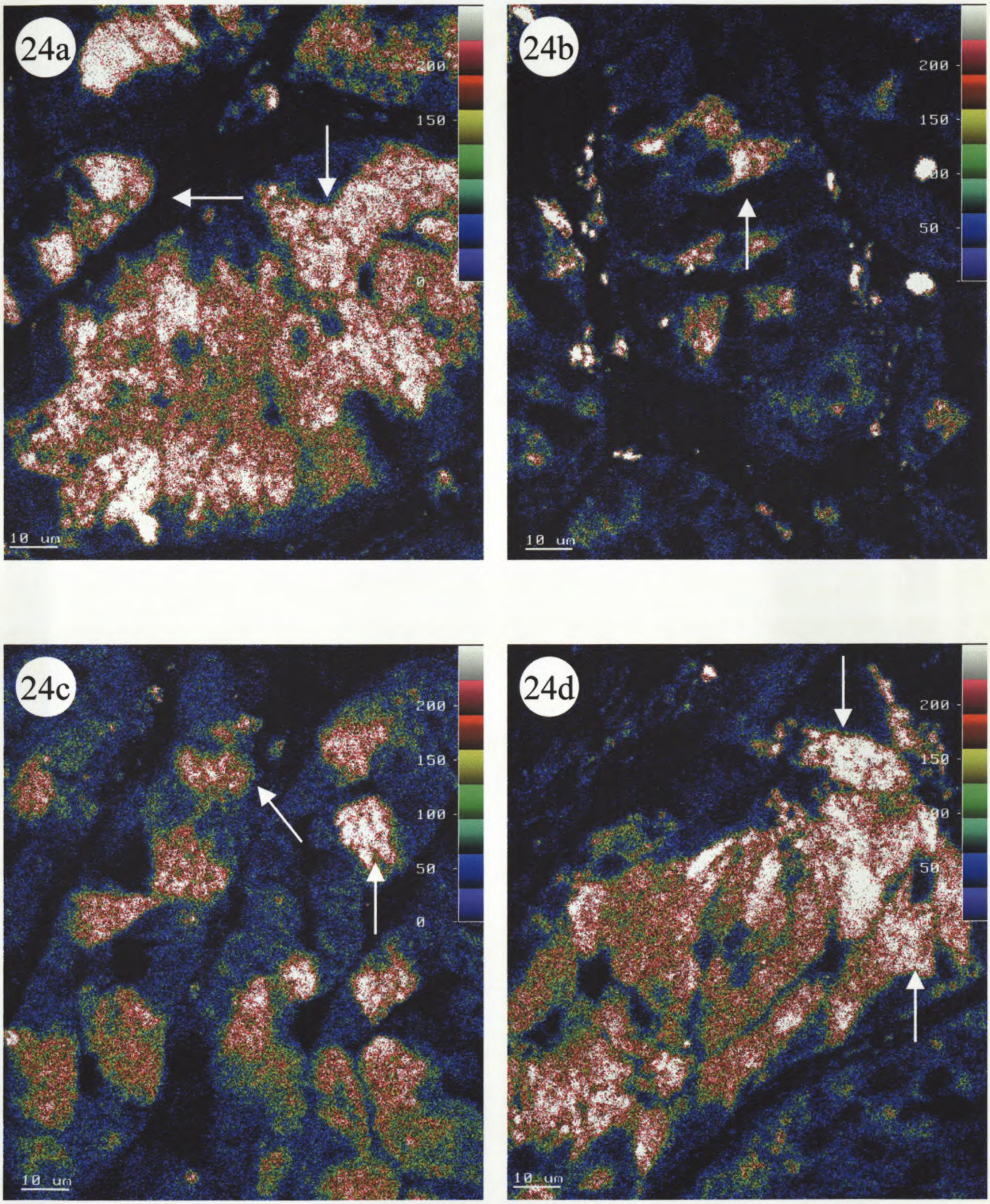
24a
200
150
0
10 um
24b
200
150
50
10 um
24c
200
150
100
50
0
10 um
24d
200
150
50
10 um

Generally for group 2, the labels seems to have increased (visually subjective, refer to image analysis for verification, section 3.2.2.2) in the deeper glands, and particularly the parietal cells. The mucous cells also appear to be exhibiting TK immuno-fluorescence.

3.3.2.1.3 Fluorescent immuno-localisation in group 3

Group 3 was the moderate to severely inflamed group. Plates 25a to 25f depict immuno-fluorescent photo-micrographs of the antral areas of this group. Plate 25a shows an area of deep glandular structures. Chief cells and mucous cells flank the parietal cells. Immuno-fluorescence is predominantly in the parietal cells (arrows). There are also some chief cells that exhibit immuno-label. The label is in the mid to upper intensity range (scale colour bar as reference). Plate 25b and 25c again depict typical sections of antral deep glands with the parietal cells (arrows) showing intense label. The chief cells and the mucous cells do not show TK presence. Plate 25d shows an antral area of crypt cells. The parietal cells forming the base of the pit show extremely intense immuno-fluorescence. Plate 25e is a photo-micrograph depicting TK label in the parietal cells (arrows). Plates 25d, 25d, and 25f all exhibit some degree of glandular destruction and atrophy.

Plates 26a to 26f represent photo-micrographs of TK immuno-labelled body regions of group 3. Plate 26a shows mid intensity label within the deep glandular

Plate 25a: Photo-micrograph showing fluorescent image of TK-FITC labeling in group 3 antrum. As indicated by the arrows there is distinct labeling in the parietal cells. There are also some inflammatory cells that exhibit TK label.

Plate 25b: TK fluorescent immuno-localisation in the superficial glands of group 3 antrum. Parietal cells (arrows) show predominant label in the mid to upper intensity range (reference intensity colour-bar).

Plate 25c: Fluorescent immuno-labelling for TK in the parietal cells (arrows) of the deep glands. Basement membrane labeling of some mucous cells is also seen.

Plate 25d: TK immuno-fluorescence is seen in the parietal cells (arrows) that have labeled intensely. Also noted is evidence of glandular destruction.

Plate 25e: Photo-micrograph of immuno-localisation of deep glands of group 3 antrum. Arrows point to strongly labeled parietal cells. There are also some chief cells (from phase diagram, not shown) that also exhibit immuno-label.

Plate 25f: This photo-micrograph shows glandular destruction in the antrum of group 3. TK label still predominates (arrows), and there is label seen in some of the simple mucous-type cells.

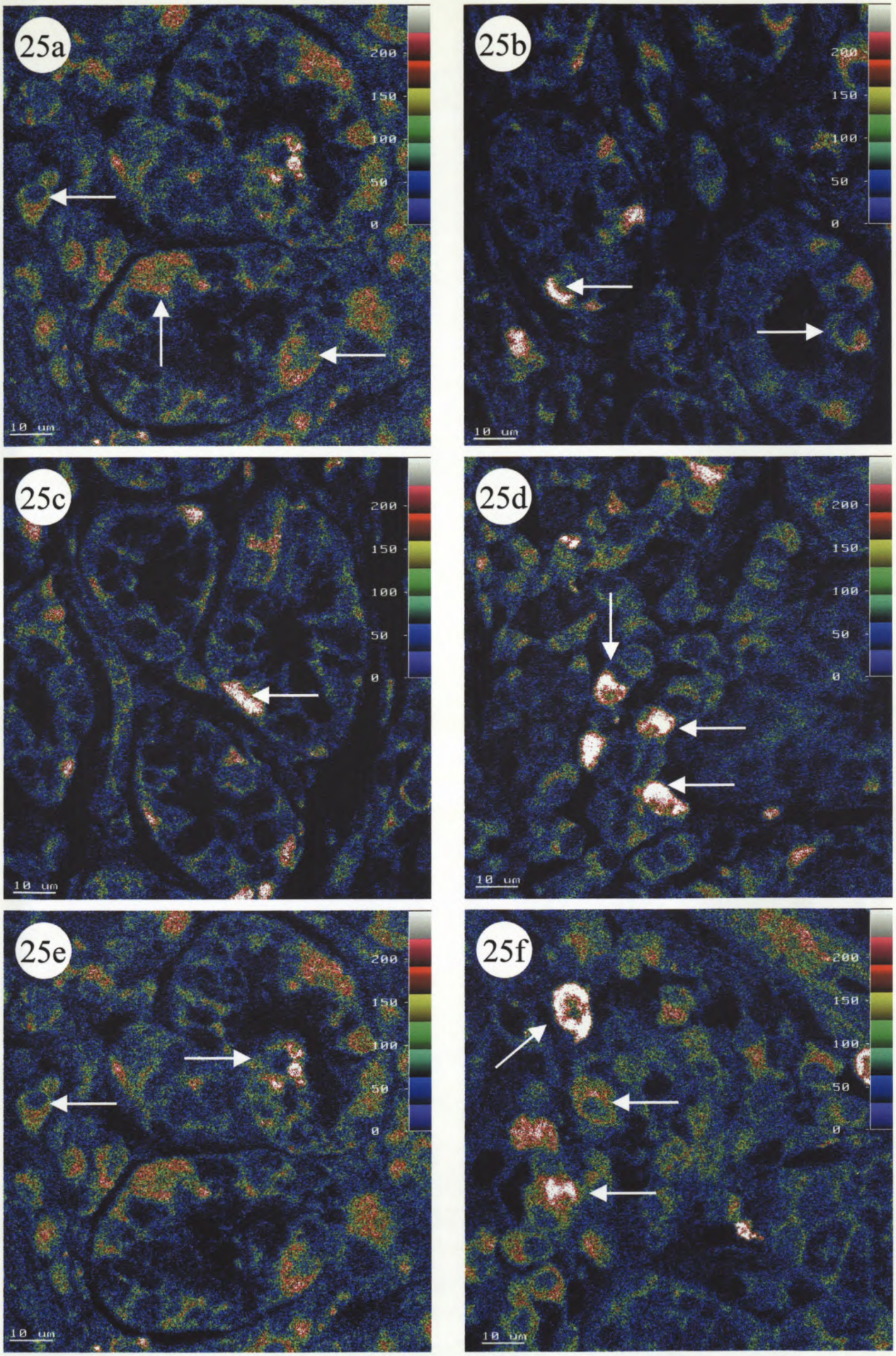
25a
25b
25c
25d
25e
25f
200
150
100
50
0
10 um

Plate 26a: Photo-micrograph showing fluorescent image of TK-FITC labeling in group 3 body. Arrows point to label in the parietal cells (phase contrast images, not shown). Diffuse labeling over deep glands are seen.

Plate 26b: This photo-micrograph indicates low intensity (from reference colour scale-bar), diffuse label over the deep glands (arrows). The tissue is indicative of glandular destruction and cellular structures are not well-defined.

Plate 26c: TK immuno-fluorescent labeling of the inflammatory cell (arrows) in the connective tissue surrounding superficial body glands. Simple mucous cells (indicative of metaplasia) do not label for TK.

Plate 26d: Photo-micrograph showing TK immuno-localisation on some inflammatory cells and also parietal cells (arrows). The simple mucous-type cells also show low intensity label.

Plate 26e: Strong immuno-fluorescence seen in the deep glands, covering it in its entirety. TK is widespread over the whole body glands and the connective tissue show no evidence of immuno-label.

Plate 26f: High intensity immuno-fluorescence is seen in the deep body glands of group 3. A few inflammatory cells do exhibit TK label.

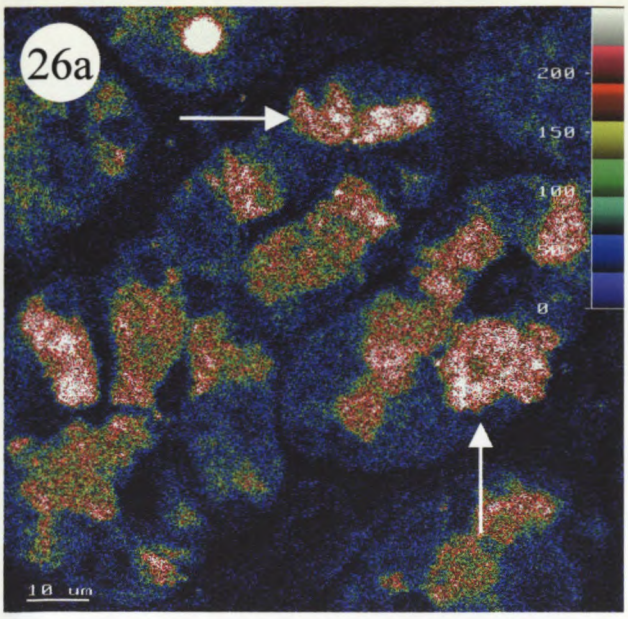
26a
200
150
100
50
0
10 um

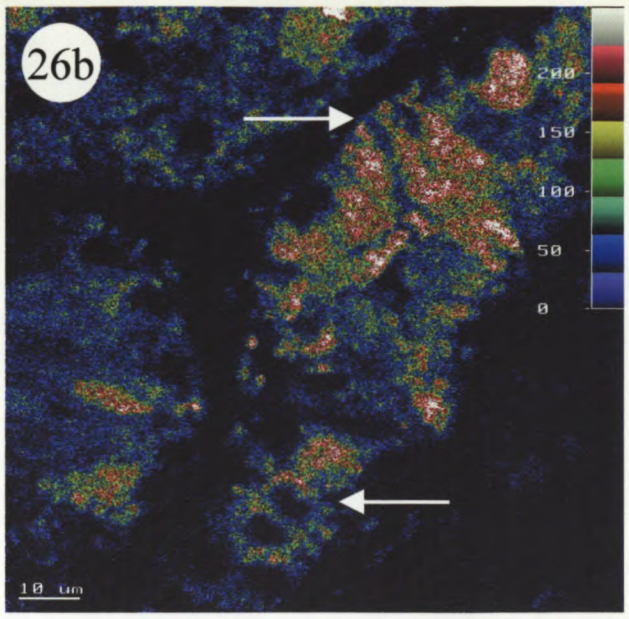
26b
200
150
100
50
0
10 um

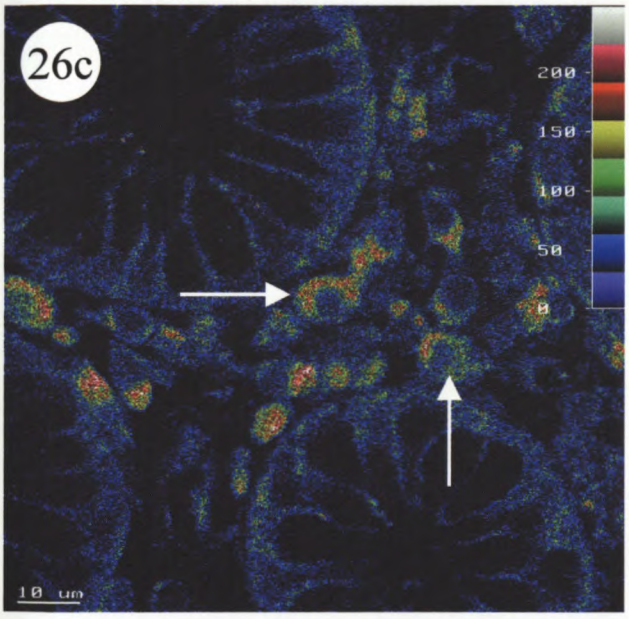
26c
200
150
100
50
0
10 um

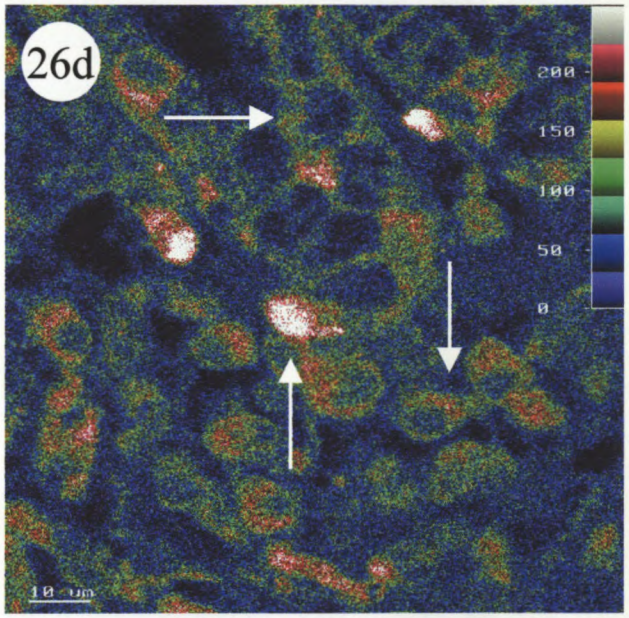
26d
200
150
100
50
0
10 um

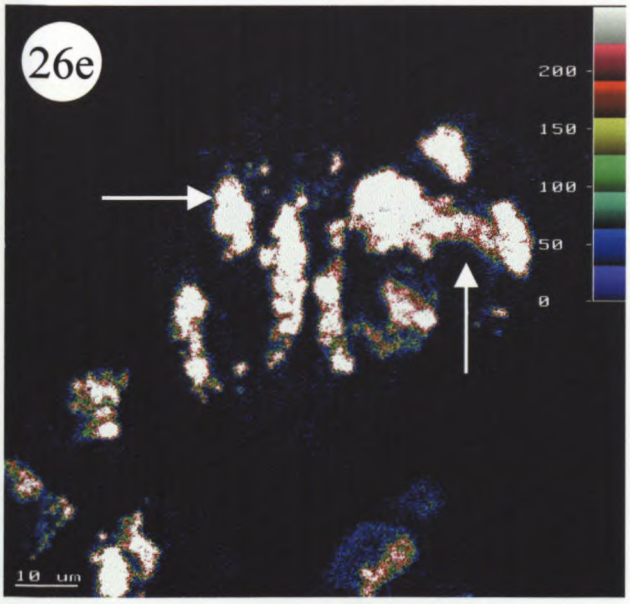
26e
200
150
100
50
0
10 um

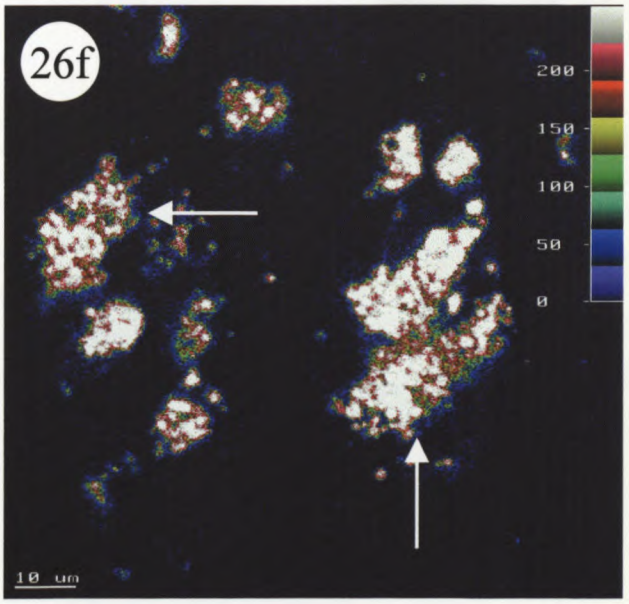
26f
200
150
100
50
0
10 um

structures. Arrows point to areas of intense label (these have been identified as parietal cells and some mucous cells on the phase contrast images, not shown here). Plate 26b shows TK in deep glands and a crypt structure (arrows). Label intensity is in the mid to upper region of the reference colour-bar scale. Plate 26c and 26d show glandular structures (parietal cells on phase contrast) that are distinctly labelled (arrows). Plate 26c also has glandular mucous cells that do not show any TK immuno-fluorescence. Plate 26e and 26f depict immuno-label over deep glandular structures that appear to be diffuse. Labelling is very intense (scale colour bar reference) even though it envelopes the structures.

For group 3, the TK immuno-label seems to have increased in visual intensity compared to group 1 and group 2. There are also more mucous cells showing specific labelling compared to that in the mild (group 1) and non-inflamed groups (group 2).

3.3.2.1.4 Fluorescent immuno-localisation in group 4

Group 4 antrum is represented by photo-micrographs shown in plates 27a to 27d. The labelling appears to occur diffusely over the surface epithelial structures and is of low intensity (scale colour bar reference). Plate 27a shows TK immuno-label on a superficial gland along the basement membrane region (arrows). There is low intensity label on cells containing large internal cytoplasmic spaces. These may be metaplasic cells of a simple epithelial origin. Plate 27b is a higher magnification of plate 27a. Here the label in the superficial structures can be seen in more detail. Plate 27c shows upper range label intensity of deep glandular structures in antral

Plate 27a: This photo-micrograph depicts TK immuno-localisation in group 4 antrum. Low intensity label (reference scale colour-bar) is concentrated over the surface glands (arrows) and particularly the simple mucous cells that have replaced the epithelia following metaplasia. Some inflammatory cells that are present also show TK immuno-localisation.

Plate 27b: This photo-micrograph is a higher magnification image of figure 21a. It shows the labeling over the cell membranes (arrows) of large simple mucous type-cells. There is no evidence of label in the cytoplasm.

Plate 27c: Strong immuno-labelling of two inflammatory cells in the deep glands of group 4 antrum.

Plate 27d: Distinctive TK immuno-fluorescence in the parietal cells (arrows), in the mid-intensity region.

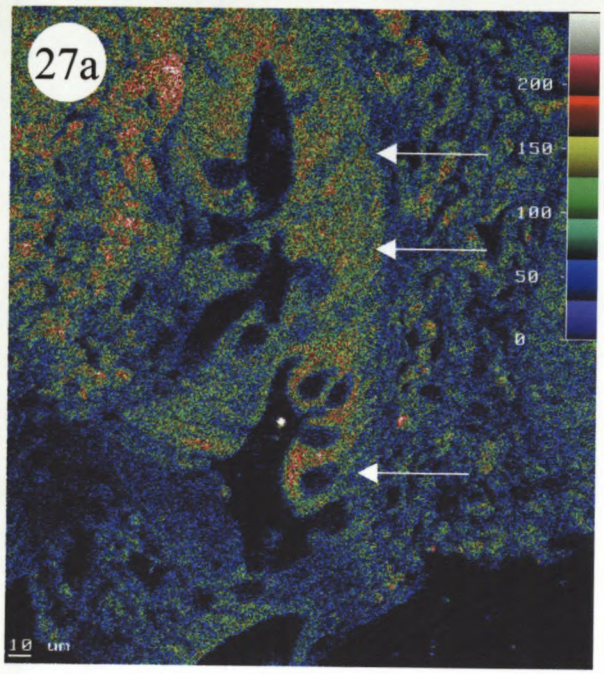
27a
200
150
100
50
0
10 um

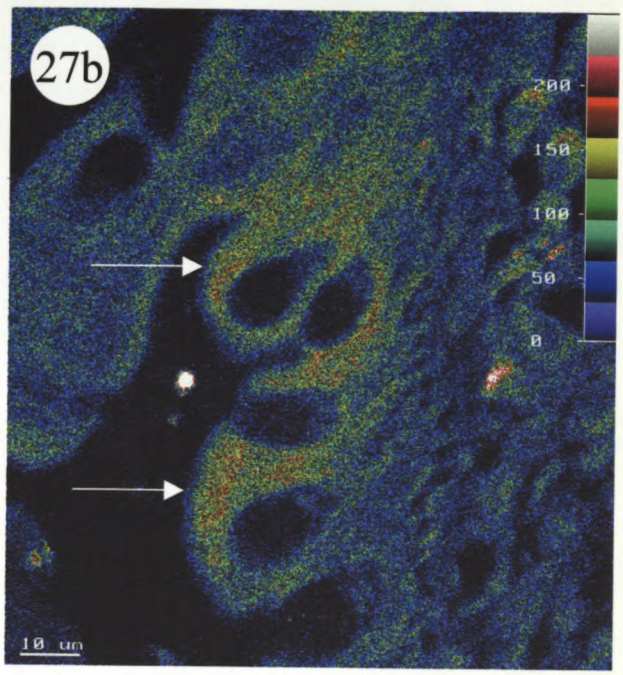
27b
200
150
100
50
0
10 um

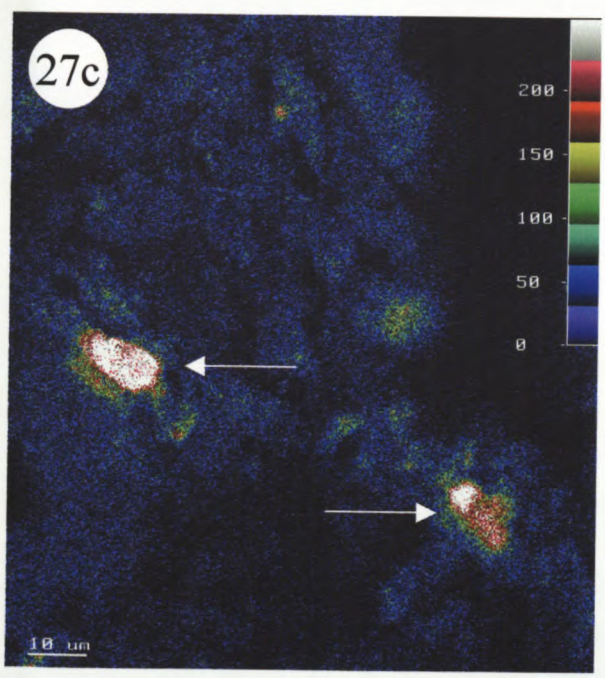
27c
200
150
100
50
0
10 um

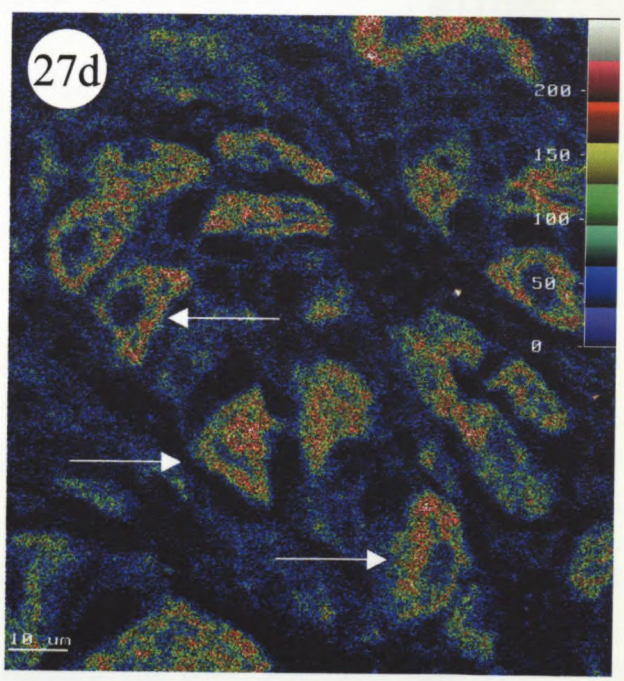
27d
200
150
100
50
0
10 um

tissue that are undergoing atrophy. Plate 27d shows distinct, yet diffuse and mid intensity label in the deep glands of the antrum.

Group 4 body regions show TK immuno-label visible along the basement membrane borders of the superficial glands as depicted by plate 28a. There is also evidence of structural damage to the glands and some inflammatory cells appear to be labelled. Plate 28b shows label spread along the superficial gland structure on the basal plane with a large vesicular structure also displaying immuno-label.

TK immuno-labelling of group 4 (severe inflammation) appears to be concentrated in the superficial areas. Large vesicle-like cells (probably metaplasic cells) also take up immuno-fluorescence.

3.3.2.2 Image analysis of fluorescent immuno-localisation

3.3.2.2.1 Statistics of Image analysis for FITC immuno precipitation

Table 14 displays the descriptive statistics (*t-test* of *equal variance*) of results of image analysis of fluorescent immuno-labelling for the various histological groups in the gastric antral region. The results have been manipulated to reflect the immuno-fluorescent intensity (in pixels/um^2) of two broad groups, that is, the glandular structures and the extra glandular cells. The mean intensity of label for the antral cells appear to increase from normal (1.09 ±0.084 pixels/um^2) to mild (2.40 ± 0.65 pixels/um^2) to moderate (3.10 ± 0.80 pixels/um^2) groups. Intensity of immuno-fluorescence tapers off slightly in group 4 antral cells (2.92 ± 0.66

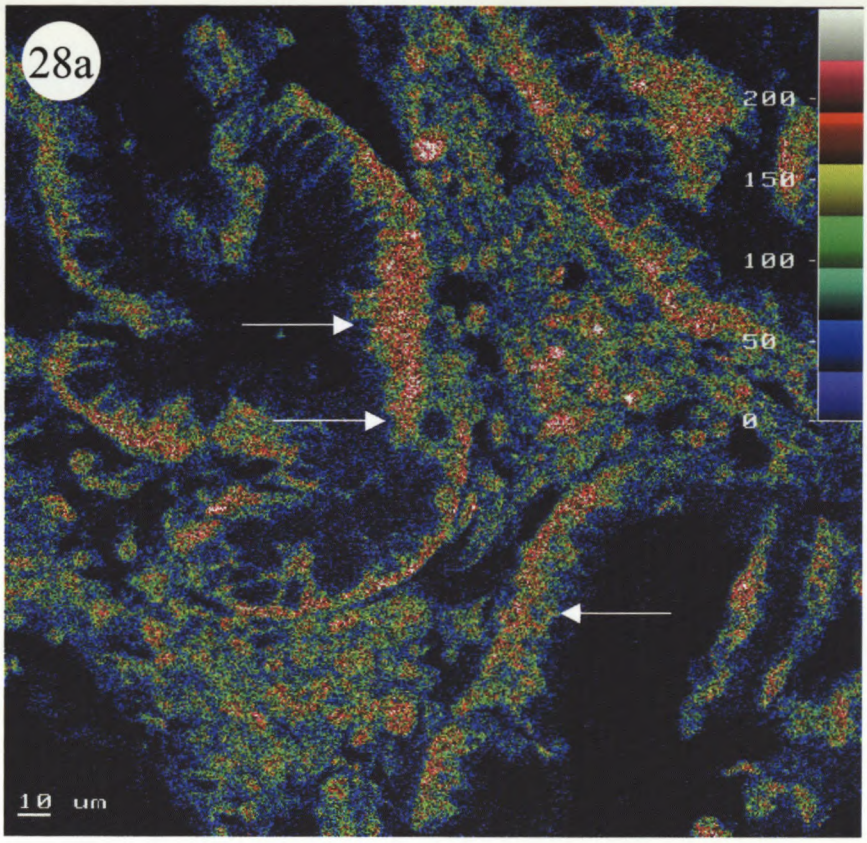
28a
200
150
100
50
0
10 um

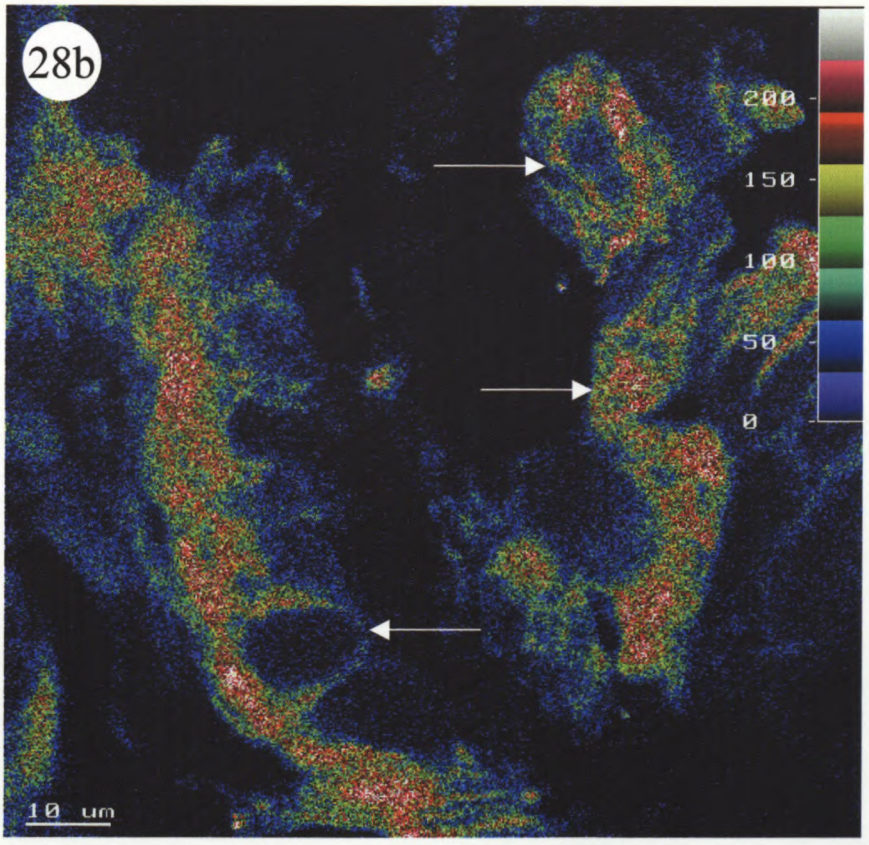
28b
200
150
100
50
0
10 um

Plate 28a: Photo-micrograph showing fluorescent image of TK-FITC labeling in group 4 body tissue. Arrows indicate label in the surface glands, in the basement membranes. Inflammatory cells in the connective tissue also exhibit medium intensity label.

Plate 28b: Higher magnification of surface glands, showing immuno-fluorescent TK label in the simple mucous-type cells that has replaced surface mucous epithelia by metaplasia.

pixels/um^2). The mean intensity of the glands for group 1 and group 2 antral glands plateau at 3.29 ± 1.84 pixels/um^2 and 3.29 ± 1.97 pixels/um^2, respectively. These mean intensity values fall by more than 60% to 1.04 ± 0.42 pixels/um^2 in group 3 glands. It is interesting to note that the mean intensity of group 4 glands is 3.14± 1.30 pixels/um^2.

Table 15 displays the single descriptive statistics of the results of image analysis of fluorescent immuno-labelling for the various histological groups in the gastric body regions. The mean intensity of group 1 cells in the gastric body is 3.05 ± 0.89 pixels/um^2. This indicates the basal level in a normal group. Group 2 cells reflect a similar mean intensity level, that is, 3.05 ± 1.37 pixels/um^2. The mean intensity, as the disease state progresses to moderate to severely inflamed group 3 cells is 3.02 ± 1.89 pixels/um^2. The severely inflamed group 4 exhibits a mean intensity value of 1.06 ± 0.19 pixels/um^2. This represents a dramatic loss of almost 60% of the mean intensity in the body cells from groups' 1,2, and 3 to group 4. Conversely, for the mean staining intensity of the body glands, there is a gradual decrease as the disease state progresses, that is, for group 1 < group 2 < group 3 < group 4, the results show 3.22 ± 2.09 pixels/um^2 < 1.98 ± 1.07 pixels/um^2 < 1.46 ± 0.71 pixels/um^2 < 1.06 ± 0.50 pixels/um^2 respectively.

3.3.2.2.2 Comparison of staining intensity for TK FITC immuno-labelling of the antral regions of the histological groups

Table 16 represents an inter-group comparison (using a *t-test* of *equal variance*) of image analysis of TK immunofluorescence between the antral regions of the

histological groups. The factor of significance was taken when a p value of 0.05 was obtained by comparison. Comparing mean staining intensity of group 1 versus group 2 antral cells, a value close to significance $p = 0.06 \pm 0.27$ was obtained. Group 1 antral cells versus group 3 antral cells yielded an even more significant difference, $p = 0.04 \pm 0.20$. Other inter-group comparisons from table 16 yielded no other significant comparisons.

3.3.2.2.3 Comparison of staining intensity for TK FITC immuno-labelling of the body regions of the histological groups

Table 17 represents an inter-group comparison (using a *t-test* of *equal variance*) to compare the results of image analysis of TK immunofluorescence between the body regions of the histological groups. The only significant value of comparison of mean immuno-fluorescent staining intensity obtained was between group 1 cells versus group 2 cells ($p = 0.01 \pm 0.4$). All other comparisons yielded no significant factors of comparison.

Table 14 ***Single descriptive statistics*** **(column) of fluorescent image analysis for antral immuno-localisation**

Group		Mean (pixels/μm^2 $x10^{-3}$)	Median (pixels/μm^2 $x10^{-3}$)	Range (pixels/μm^2 $x10^{-3}$)	SEM (±)
Group 1 antrum	cells	1.09	1.16	0.56 - 1.40	0.084
	glands	3.29	1.29	0.175 - 16.17	1.84
Group 2 antrum	cells	2.40	1.16	0.56 - 1.40	0.65
	glands	3.29	1.04	0.53 - 16.93	1.97
group 3 antrum	cells	3.10	2.77	0.38 - 7.99	0.80
	glands	1.04	0.67	0.071 - 4.07	0.42
Group 4 antrum	cells	2.92	2.76	0.54 - 5.34	0.66
	glands	3.14	1.84	1.09 - 12.29	1.30

SEM standard error of the mean
pixels unit of measure of colour/light intensity

Table 15 ***Single descriptive statistics*** **(column) of fluorescent image analysis for body immuno-localisation**

Group		Mean (pixels/μm^2 $x10^{-3}$)	Median (pixels/μm^2 $x10^{-3}$)	Range (pixels/μm^2 $x10^{-3}$)	SEM (±)
Group 1 body	cells	3.05	2.38	0.61 - 8.61	0.89
	glands	3.22	0.83	0.13 - 17.73	2.09
Group 2 body	cells	3.05	1.49	0.39 - 12.39	1.37
	glands	1.98	0.89	0.28 - 9.48	1.07
group 3 body	cells	3.02	0.78	0.10 - 16.10	1.89
	glands	1.46	0.76	0.013 - 6.39	0.71
Group 4 body	cells	1.09	1.28	0.17 - 1.81	0.19
	glands	1.06	0.65	0.07 - 4.73	0.50

SEM : standard error of the mean
Pixels : unit of measure of colour/light intensity

Table 16 **Intergroup comparison using *t-test* with *equal variance* of tissue kallikrein immuno-labelled antrum for fluorescent immuno-labelling image analysis**

group		Group 1 antrum		Group 2 antrum		Group 3 antrum	
	region	cells	glands	cells	glands	cells	glands
Group 2 antrum	*cells*	0.06 ± 0.27					
	glands		0.25 ± 6.29				
Group 3 antrum	*cells*	0.04 ± 0.02		0.9 ± 2.6			
	glands		0.97 ± 6.03		.0.36± 6.05		
Group4 antrum	*cells*	0.3 ± 2.1		0.97 ± 4.49		0.99 ± 4.53	
	glands		0.36 ± 6.05		0.32 ± 2.38		0.61 ± 1.34

Factors of comparison are given as $p \pm$ 95% CI
95% CI =95% confidence interval (maximum)

Table 17 **Intergroup comparison using *t-test* with *equal variance* of tissue kallikrein immuno-labelled body for fluorescent immuno-labelling image analysis**

group		Group 1 body		Group 2 body		Group 3 body	
	region	cells	glands	cells	glands	cells	glands
Group 2 body	*cells*	0.01 ± 0.4					
	glands		0.94 ± 5.23				
Group 3 body	*cells*	0.17 ± 0.99		0.93 ± 3.38			
	glands		0.56 ± 6.10		0.50 ± 4.78		
Group4 body	*cells*	0.98 ± 0.46		0.01 ± 3.31		0.18 ± 4.92	
	glands		0.29 ± 6.59		0.16 ± 5.06		0.54 ± 3.51

Factors of comparison are given as $p \pm$ 95% CI
95% CI =95% confidence interval (maximum)

CHAPTER 4

DISCUSSION

DISCUSSION

4.1 Discussion of the experimental results

4.1.1 The validity of results

The validity of any experimental result is governed by a number of procedures, most important of which are proper schedules and method controls. All the assays performed in this study, as outlined in chapter 2, were conducted using proper method controls, and had in place inter- and intra-assay variability limits that were designed to minimise errant results.

4.1.2 The variability of results

Variance of results in specific groups may have been due to a number of factors, least of which may reside in histological grading of the groups. The presentation of the disease histology itself may not be totally unrelated to Hp infection, and there is continuing debate as to the inflammatory response that Hp, found overlaying the superficial gastric cells, causes in the underlying gastric mucosa. The patient number (n = 23) for this study may have sufficed to elicit general conclusions about the Hp-TK relationship, but in order to achieve specific, statistical results, a larger patient base may be required. Also, the clinical procedure for obtaining gastric lavage fluid may also have to be called into question. The rapid wash-out of physiological saline, infused into the gastric lumen for a few minutes, may have not been of sufficient time to allow complete equilibration and uptake of all TK present on the surface of the gastric mucosa. One point, in favour of non-variance was that

the amidase assay buffer contained soybean trypsin inhibitor (SBTI) which would inhibit any non-tissue kallikrein serine-proteases. The general amidase assay buffer system of 0.02 M Tris-Cl (pH 8.0) is optimal for TK activity.

4.2 Tissue kallikrein in gastric mucosal tissue

The question as to whether tissue kallikrein was involved in the aetiology of gastritis was assessed in each of the four histological groups, differentiated on the basis of the severity of the disease. Another causal factor to consider was the presence of the infective bacterium *Helicobacter pylori*, clearly an initiator of gastritis. Therefore, the ensuing discussion will focus on the different experimental findings, and then integrate these to examine whether tissue kallikrein, through the formation of lysyl-bradykinin affects the cellular transformations observed in the inflamed gastric mucosa. Further, it presents an overview of the interactive relationship between tissue kallikrein and *Helicobacter pylori* in the cellular pathology seen in gastritis.

4.2.1 Enzymic activity of TK in gastric tissue

The amidase assay is a micro-assay used to determine the amount of functionally active tissue kallikrein, and is based on the cleavage of an arginyl bond on a synthetic substrate to release a chromophore. The sensitivity of the assay is obviously a function of the reliability, reproducibility and specificity of the assay. This study has demonstrated the presence of a basal amount (mean, *single descriptive statistics)* of enzymically active tissue kallikrein (as measured by amidase assay, Table 5) in a histological group that can be defined as *control* due to the fact that none of the individuals examined had Hp infection or

showed any evidence of Hp infection and minimal inflammatory activity cell activity (group 1). It has to be understood that the presence of inflammatory cells does not necessarily constitute an inflammatory episode. To the contrary, examination of group 1 (non-infected, non-inflamed group) H&E photo-micrographs (plates 4a, b and plates 7a, b) showed the presence of a few polymorphonuclear leucocytes (PMN's) in the connective tissue between glands. Since gastritis is predominantly antral-based, it was assumed that any inflammatory changes would initially occur in that region. The measurement of tissue kallikrein activity was considered to reflect and, more importantly, predict the status of inflammation in the antrum. The measurement of mean antral-tissue TK amidase activity did not change significantly since the amidase activity increased only slightly from 3.29 ng TK/ml protein ± 2.55 (group 1 to group 2, Table 5) to 3.47 ± 2.49 (p = 0.96 ± 9.8, Table 6). This trend could not be analysed fully since the activity values for the lavage fluid for group 3 and group 4 fell below the detection limit of the assay. One can speculate that TK amidase activity should have increased as the disease pathology became more pronounced. This result could be explained by supposing that as inflammation became more pronounced, more TK was produced, and subsequently released into the gastric lumen. Therefore, the measurable amount left in the tissue, as the disease worsened, was negligible.

A more significant result was the finding of TK activity in the body area (Table 5) which showed marked elevation from group 1 to group 4 (2.27 ng TK/ml protein ± 1.55 to 5.39 ± 5.38, p = 0.54 ± 11.15). One explanation could be that TK builds up in the mucosal tissue of the body tissue as the inflammation progresses. The histological delineation of the cell populations of the body indicates it to be a specialised region of predominantly parietal cells in which TK is primarily localised. The turnover of TK in the parietal cell probably

alters considerably as the dysfunction of glandular activity and atrophy set in. Another factor that may cause TK to increase is the elevated acid secretion from the parietal cells in inflamed stomach mucosa induced by Hp.

4.2.2 Enzymic activity of tissue kallikrein released by the gastric mucosal cells

The TK amidase activity of gastric lavage fluid (Table5) revealed that a trend of increased activity (p = 0.6 ± 177.45) as the initial inflammation (73.21 ng TK/ug protein ± 69.36) progressed, with a maximum having been reached in the moderate to severe inflammation state (130.71 ng TK/ug protein ± 14.11). The atrophic disease state (group 4) showed a decrease in TK activity of the gastric lavage fluid. Interpretation of these results suggests that as the mucosal inflammation increased, the amount of enzymically active TK released also increased. But when atrophy set in, with the majority of the parietal and mucous-producing cells in the antrum having been lost, the acid-producing ability of the glands would have declined. TK activity in group 4 (112.05 ng TK/ug protein ± 14.11) showed a significant reduction from the severely inflamed group 3 value.

4.3.1 Immuno-reactivity of tissue kallikrein released by the gastric mucosal cells

Measurement of tissue kallikrein by ELISA estimates the total TK, namely both tissue pro-kallikrein and activated tissue kallikrein. The amount of total TK in the gastric lavage fluid in group 1 (Table 9) was too low to be measured by the ELISA (sensitivity of the assay is from 20 ng TK/ml to 0.625 ng TK/ml). As the disease process increased from mild to moderate to severe, there was a concurrent increase in the amount of measurable TK in the lavage fluid. The difference in TK between group 2 and group 4 represented a

four-fold increase ($p = 0.01$). If the premise that the antral glands were also contributing to the secretion of TK is accepted, then the substantive amount of TK produced was being influenced by the antral disease pathology. The role of Hp in this paracrine release of TK is uncertain. It may be hypothesised that Hp does, through some undefined inflammation-inducing ability, stimulate hyperacidity in the gastric luminal exudate. The presence of Hp (highest in group 2, least in group 4 and none in group 1; refer to table 4) showed an inverse correlation with TK in the gastric lavage fluid. It is therefore possible that Hp proteases may cleave TK immuno-reactive epitopes of the enzyme, making it no longer measurable by ELISA.

The biopsy material usually contains 2 to 5 mg of tissue. As enzymic activity of tissue kallikrein was considered to be of greater significance, the measurements had to be restricted to amidase assay only.

4.3.2 Comparison of enzymic and immuno-reactive TK in gastric lavage fluid

The results for the gastric lavage fluid show similar trends for the determination of TK enzymic activity (Table 5) and total TK content (Table 9). Although it may be presumed that the amount of amidolytically active TK would be proportional to the total amount of immuno-reactive TK produced, the determinants for enzymic activity (namely, inhibitors and proteolytic hydrases) are different from determinants for immuno-reactivity (namely, epitopes in tertiary structure). It is, therefore, not surprising that inter-group comparison (Table 10) showed no correlation between the amidase assay and ELISA for the lavage fluid, suggesting that the ratio of enzymically-active TK compared to total TK did not stay proportional through the progression of inflammation, for the reasons enunciated above.

4.3.3 Comparison of TK enzymic activity in lavage fluid with that of tissue extracts

Comparing the individual groups to each other for amidase assays of tissue extracts and lavage fluid (Table 8) showed a statistical difference between all the groups compared, bar one. There was no statistical difference on comparison of the amidase assay between group 1 lavage fluid and group 1 tissue extracts. The statistical difference between group 2 (p = 0.02), group 3 (p = 0.06) and group 4 (p = 0.0003) indicated that as the disease progressed (that is, from group 1 to group 4), the amount of functionally active tissue kallikrein being produced in the tissue increased, and this caused the amount of functionally active tissue kallikrein released into the gastric lumen to increase. What needs to be remembered is that the secretory ability of the antrum was decreasing at the same time.

4.4 Gastric cellular localisation of tissue kallikrein

Tissue kallikrein was histochemically immuno-localised in the gastric biopsy specimens. As well as determining the gastric cellular orientation of TK in the gastric mucosa by light microscopy-based visual recording, digital images were captured and subjected to analysis by converting the light and fluorescent immuno-labelling to standard units of intensity to pixels per unit area.

4.4.1 Immuno-precipitation

4.4.1.1 Using conventional light microscopy techniques

Results from immuno-precipitation with diaminobenzidine (DAB) [plate 8 to plate 20] showed a common immuno-labelling trend. As the disease progressed, the visual intensity of label also increased. This result was unexpected as the results of TK amidase activity in the gastric tissue extracts did not show the same increasing trends. The main cellular localisation of TK was in the parietal cells for all groups, and for both antral and body regions. Sakai et al. (1997) have reported that immuno-reactive TK was found in the mucous granules of goblet cells in gastric regions showing metaplasia. This study also shows the presence of TK in metaplasic cells (Plate 18). Tissue kallikrein seems to be associated with gastric inflammation regardless of the degree of mucosal damage (and even normal mucosa), as is indicated by the immuno-labelling seen in all groups. Generally, in the control groups, most of the parietal cells and deep gland cells labelled, but as the inflammation progressed the mucous cells (both gastric and metaplasic type) and superficial epithelial cells also showed TK presence. One explanation for this may be that as parietal cells are lost, a concomitant induction of TK synthesis occurs in other cell types, particularly in regenerating cells. Such a re-synthesis of TK in differentiating and differentiated tissue suggests a physiological role in the regeneration and reconstruction of the gastric mucosa, either indirectly or through the formation of lysyl-bradykinin.

An interesting finding was that the intensity of immuno-labelling correlated with the presence of Hp. Furthermore, in the latter stages of gastritis (tending towards atrophy and metaplasia) the decrease in Hp also correlated with the decrease in TK (visually). Clearly, the question arises as to whether Hp releases products that stimulate the hKLK1 gene to transcribe more TK.

4.4.1.2 Image analysis of TK-DAB immuno-localisation

Image analysis of the DAB immuno-labelling produced somewhat interesting results (Table 11). The mean intensity of labelled cells in the antrum for the control group and the mildly inflamed group were similar (3.3×10^{-3} pixels/ $um^2 \pm 0.01$) suggesting little change in intra-cellular TK in early inflammation. Yet, the mean intensity decreased sharply in the latter stages of disease (group 4 = 0.8×10^{-3} pixels/$um^2 \pm 0.2$) and this difference ($p = 0.004 \pm 0.002$, Table 12) could suggest a tissue depletion of TK and/ or inactivation of the immuno-reactive protease possibly due to release of an inhibitor related to chronic gastritis pathophysiology. Another explanation could be that, as inflammation regresses due to tissue metaplasia and regeneration, TK switches from being an inflammatory mediator to being a physiological gastro-protective factor.

An altogether different trend was observed for the body area DAB immuno-labelling with mean intensity of group 1 (4.10 pixels/ $um^2 \pm 0.30$, Table 11) rising significantly in group 3 (5.70 pixels/ $um^2 \pm 2.7$, Table 11; $p = 0.001 \pm 0.0029$, Table 13), and then falling in group 4 (0.0037 pixels/ $um^2 \pm 0.0029$, Table 11). This sharp increase in TK immuno-presence may herald the modulatory role of

TK, with the concomitant formation of kinins by TK as the degree of inflammation progressed in severity. The decrease from the chronic group 3 to group 4 ($p = 0.03 \pm 0.0024$) signalled a reduction in inflammation as atrophy set in, and most of gastric functional activity, including endocrine regulation slowed down.

4.4.2 Immuno-fluorescence of TK in gastric tissue

4.4.2.1 Confocal immuno-fluorescent techniques

Fluorescein-isothiocyanate (FITC) was the fluorophore of choice used to immuno-label TK in the gastric tissue (indicated by Plates 21 to 28). In addition to viewing the labelled cells under a confocal microscope, digital images were captured and subjected to analysis. Visually, TK was seen to be sequestered in parietal cells and surface epithelia in the control groups, and this finding was regarded as being the basal appearance. As inflammation increased in the subsequent groups, so too did the level of TK immuno-fluorescence, affirming a role for TK in gastric inflammation. In the latter stages of inflammation TK tended to be localised in the superficial mucosal regions and metaplasic structures.

4.4.2.2 Image analysis of fluorescent immuno-localisation

Image analysis of fluorescent immuno-labelling was divided into two groups, namely, cells comprising the connective tissue and glands. The results of fluorescent image analysis (Table 15) show a gradual decrease in the intensity of

TK label in cells as the progression from group 1 (3.05 pixels/ um^2 ± 0.89) to group 4 (1.09 pixels/ um^2 ± 0.19) occurred. The intensity of labelling in the glandular structures showed the same gradual decrease as the disease state progressed (3.22 pixels/ um^2 ± 2.09 to 1.06 pixels/ um^2 ± 0.50). This finding served to reaffirm the supposition that as the disease progressed from mild to chronic to atrophy, the labelling in inflamed cells decreased in number reflecting the loss of labelled parietal cells of the glands. Metaplasic cells, that did not label as intensely, replaced the specialised cells, and the labelling profile was seen diffusely over the superficial mucosal tissue. The decrease from control group 1 antrum to group 4 antrum labelling (Table 16) showed a significant reduction (p = 0.3 ± 2.1). Concurrently, the number of Hp seen was reduced, and was virtually non-existent in group 4. Therefore, it is clear that as inflammation regressed, the number of Hp was reduced, and the staining intensity of TK was decreased. Comparison of the body regions (Table 17) also showed the same trend, but with exception that the difference between the group 1 glands and cells (p =0.29 ± 6.59 and p = 0.98 ± 0.46, respectively), and the group 4 glands and cells was not significant. This finding may indicate that the reduction in staining intensity per se was not of such great import as the difference between group 1 cells and group 2 cells of the body region (p = 0.01 ± 0.4).

4.5 Possible sequence of infectious and inflammatory events in gastritis

Previous reports of tissue kallikrein localisation found increased immuno-reactive TK in antral inflamed mucosa that was associated with Hp infection (Naidoo et al. 1997). Recent work on the kinin-generating potential of the gastric lavage fluid has been found to

increase with increasing severity of infection. This linear relationship also co-exists with the occurrence of Hp, excluding gastric atrophy (Naidoo et al. *in press*).

A summary of possible events that may occur during gastric inflammation and Hp infection has been outlined figure 11. The basal levels of TK observed in the control tissue may have a possible gastro-protective role, in the absence of inflammation. Hp may release certain stimulants that initiate the release, synthesis and/ or fracture of TK, and sets in motion a series of cellular and proteolytic events that leads to a chronic gastric inflammatory state. Autocrine stimulation by Hp products released, induce the parietal cells to (1) over-express gastric acid, and (2) possibly TK synthesis. In the absence of documented evidence, the induction of the hKLK1 gene at this stage is speculative. What has been shown by this study is that the amidase activity of TK, at the early phases of the inflammatory process, is increased in the gastric exudates. Further advances in tissue inflammation finally lead to atrophy and a reduction in acid-producing ability, together with a loss of the parietal cells and their TK-synthesis or storage capacity. This loss in gastric cell function and integrity is associated with Hp infection. Whether these events are merely coincidental is uncertain. Further, differentiation and tissue regeneration leads to simple metaplasic structures that replace the original gastric tissue. The low intensity, diffusely localised immuno-reactive TK observed in these cells and the superficial epithelia may signal a conversion of kallidin released by TK from a pro-inflammatory to a physiological role. This is the first study implicating Hp as a regulator of TK in gastric mucosal inflammation.

Tissue kallikrein is stable at pH 4.0. The question as to whether changes in luminal acidity produced by the Hp would affect the *in vivo* enzymic activity of TK is an interesting one.

However, since the optimal activity of TK is at pH 8.0, the enzymic activity of TK would be expected to be enhanced in severe Hp infection, at least in the chronic phases of the inflammatory response, which is the stage of increased acid production. The patient population studied was in the adult age group. The prevalence of childhood acquisition of Hp colonisation is at its highest in a developing country such as South Africa, where factors such poor socio-economic status would encourage early Hp infection. The progression from an asymptomatic, Hp-infected dyspeptic to a full-blown chronic sufferer is dependant on a number of factors, least of which is genetic and environmental. It stands to reason that the degree of infection has a direct relationship with the degree of inflammation. Whether Hp is required for the initial inflammation to begin, and then inflammation continues independently is not clear. Two patterns of *in vitro* inflammatory activation by Hp have been determined, one being slow and low-level and the other a rapid fast acting proliferation. The latter is most often isolated from patients with dyspepsia (Atherton 1996).

4.6 The role of proteases in inflammation

The question arises as to whether Hp proteases release TK from parietal cells and mucosal antral cells. As a first step, the effect of bacterial proteases on cell functions, in particular on gastric mucosal cells, will be discussed. All organisms depend on the availability of

However, since the optimal activity of TK is at pH 8.0, the enzymic activity of TK would be expected to be enhanced in severe Hp infection, at least in the chronic phases of the inflammatory response, which is the stage of increased acid production. The patient population studied was in the adult age group. The prevalence of childhood acquisition of Hp colonisation is at its highest in a developing country such as South Africa, where factors such poor socio-economic status would encourage early Hp infection. The progression from an asymptomatic, Hp-infected dyspeptic to a full-blown chronic sufferer is dependant on a number of factors, least of which is genetic and environmental. It stands to reason that the degree of infection has a direct relationship with the degree of inflammation. Whether Hp is required for the initial inflammation to begin, and then inflammation continues independently is not clear. Two patterns of *in vitro* inflammatory activation by Hp have been determined, one being slow and low-level and the other a rapid fast acting proliferation. The latter is most often isolated from patients with dyspepsia (Atherton 1996).

4.6 The role of proteases in inflammation

The question arises as to whether Hp proteases release TK from parietal cells and mucosal antral cells. As a first step, the effect of bacterial proteases on cell functions, in particular on gastric mucosal cells, will be discussed. All organisms depend on the availability of

Figure 11 Diagram depicting the possible sequence of events following infection with *Helicobacter pylori*. Hp releases factors that initiate inflammation, and stimulates autocrine release of TK from the parietal cells. TK in normal (non-inflamed) and metaplasic (post-atrophy) tissue is thought to have a gastro-protective role.

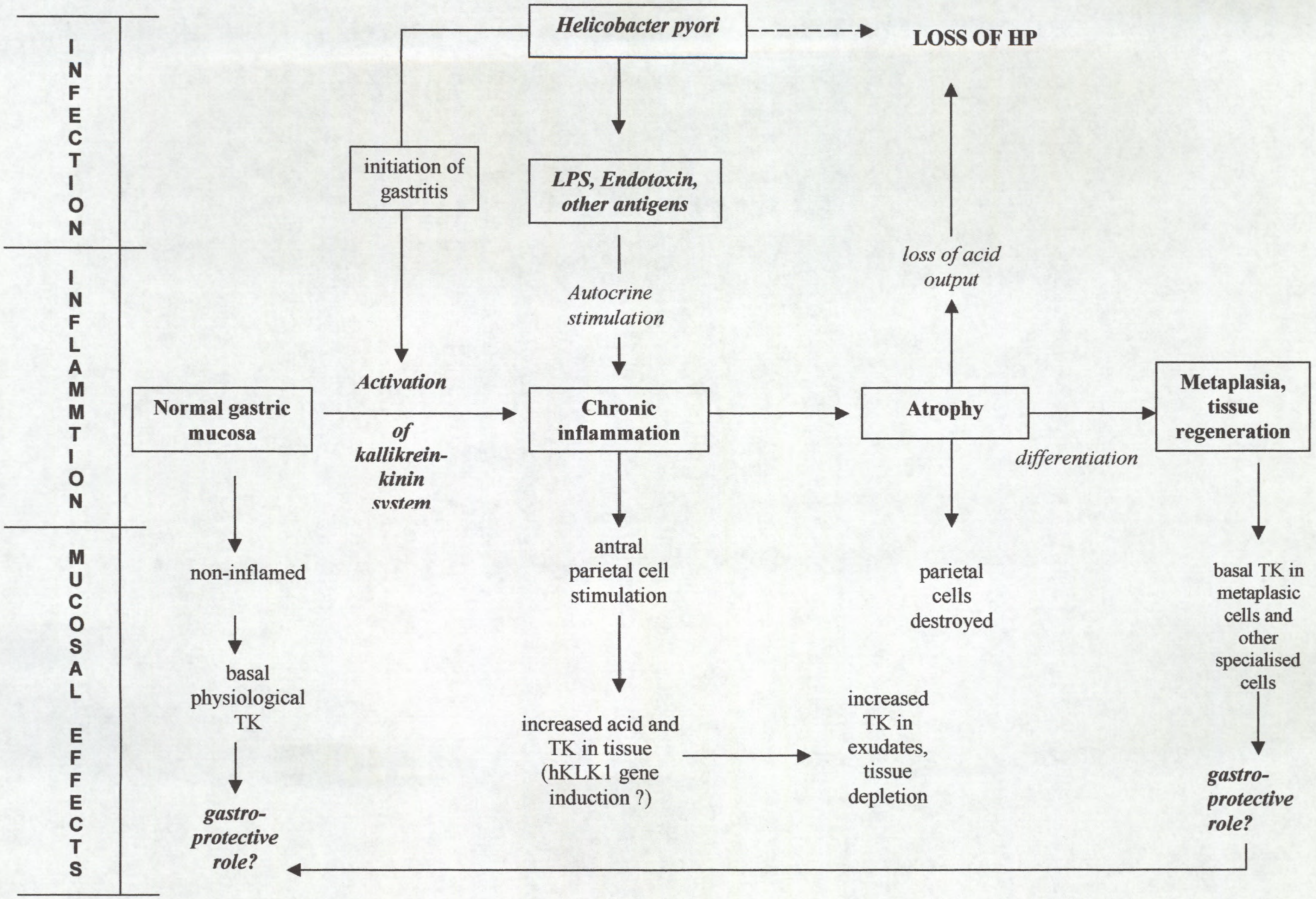
INFECTION
INFLAMMTION
MUCOSAL EFFECTS
Helicobacter pyori
LOSS OF HP
initiation of gastritis
LPS, Endotoxin, other antigens
Autocrine stimulation
loss of acid output
Activation of kallikrein-kinin system
Normal gastric mucosa
Chronic inflammation
Atrophy
differentiation
Metaplasia, tissue regeneration
non-inflamed
basal physiological TK
gastro-protective role?
antral parietal cell stimulation
increased acid and TK in tissue (hKLK1 gene induction ?)
increased TK in exudates, tissue depletion
parietal cells destroyed
basal TK in metaplasic cells and other specialised cells
gastro-protective role?

extra-cellular sources of nutrition for survival. Bacteria require nitrogen and/or carbon, and this is usually acquired by the enzymatic hydrolysis of extra-cellular biopolymers, by proteinases and glycosidases, into simple sugars or amino acids. This process plays a vital role during infection when bacterial proteases are virtually unregulated, and are detrimental to host proteins and proteinaceous structures (Travis et al. 1995). The primary effect of these bacterial proteases, especially with asaccharolytic bacteria like *Helicobacter pylori,* is to provide a continuous source of amino acids for growth and survival.

In addition, many of the bacterial proteases excreted into host's cellular environment produce many pathogenic potentials that range from activation of sensory nerve-fibre terminal that cause pain and oedema due to the opening of capillary gap junctions, symptoms that are associated with septicaemia (Maeda and Yamamoto 1996). One of the classic actions of non-specific microbial proteases is the direct digestion and liquefaction of host tissues. Host-derived proteolytic action is involved, to some extent, in tissue destruction caused by all bacterial infections, including that of Hp. Proteases released by bacteria from neutrophils at sites of inflammation, and indirectly through the action of microbial proteases themselves on latent connective-tissue-degrading-metallo-proteinases derived from fibroblasts, causes injury to cell membranes and disruption of cell function. (Sorsa et al. 1992). It has also been reported that certain bacteria may even evade the immune system by inactivating the complement cascade, and secreting enzymes that specifically degrade IgG (Molla et al. 1986, Kilian et al. 1988, Prokesova et al. 1992).

Many enteric bacteria inhabit a mucosal environment rich in nutrition, and thus may not need to utilise their own proteases to recruit growth factors. These bacteria proliferate because of the actions of endogenous gastric proteinases that produce their nutritional

requirements. However, without their protease potential, the entero-bacteria were found to have minimal pathogenic effect (Matsumoto et al. 1996).

Work by Sakai (1990) has demonstrated the immuno-localisation of tissue kallikrein in gastric tissue exhibiting intestinal metaplasia and goblet cells in patients with chronic gastritis. Work by the Russian group of Vizir (1981) found that the kinin system is activated in peptic ulcer diseases.

Work by the Fuller group (1989) has demonstrated, by mRNA *in situ* hybridisation, that TK is found, and indeed synthesised in the body of the rat stomach. Their results also show that the antrum did not produce amidolytically-active TK in the rat. Studies by Schachter et al. (1983) have immuno-localised TK in the goblet cells of the human colon, and they suggest a gastro-protective role for TK. Clearly, further molecular studies are required to precisely determine the gastric cell types that synthesise TK, and that the presence of TK in the lavage fluid and tissue extracts does not arise from the exocrine salivary and pancreatic secretions. Also, there is a need to functionally determine the basal physiological function (non inflammatory) of TK in the human stomach.

4.7 Regulation of the serine protease, tissue kallikrein by bacterial proteases

One of the major bacterial proteases released from gram negative bacteria is lipopolysaccharide (LPS). Muschel et al. (1964) showed that LPS has the capacity to activate serum complement without the participation of the initial complement cascade components. Morrison and Kline (1977) demonstrated that the *lipid A* portion of bacterial

LPS is responsible for the classical contact activation pathway, and that the polysaccharide region of the bacterium is responsible for the properdin pathway activation.

Bacterial proteases are responsible also for the activation of other tissue-damaging host protease zymogens. It has been established that fibroblasts, various cancerous cell types and macrophages excrete proenzymes such as urokinase-type plasminogen activators, matrix metallo-proteases and stromelysins (Matsumoto et al. 1992, Conese and Blasi 1995, Nargase et al. 1990). These tissue-derived zymogens are activated by bacterial proteases (Uitto et al. 1989). Activation of tissue pro-kallikrein to kallikrein causes the degradation of tissue matrix and facilitates bacterial migration and translocation. Also, activation of tissue kallikrein (see figure 6) leads to the formation of the inflammatory vasoactive peptides, kinins (section 1.4.3)

Endotoxin, a major component of the bacterial cell wall, interacts with inflammatory cells, releasing endogenous mediators such as cytokines, hydrolases, peptidases, prostaglandins, and amines that contribute to the pathophysiology of septic shock (Morrison and Ryan 1987, Beutler et al. 1987). Ingestion studies with normal human volunteers indicated that administration of bacterial endotoxin caused an increase in BK generation (Kimball et al. 1972). De la Cadena et al. (1993) also found that injection of endotoxin produced a decrease in plasma Factor XI, while there was an increase in the circulating kallikrein-α_2 macroglobulin complexes. Molla et al. (1989) demonstrated that certain bacteria with 56 kD serratial-like proteases generated BK, irrespective of whether pre-kallikrein and/or Hageman factor were activated. Bacterial cell wall fractions (LPS and lipid A from *E. coli*, techoic acid and peptidoglycan from *S. aureus*) produces kallikrein-like amidolytic activity in a mixture of prekallikrein, Hageman factor and H- kininogen (Kalter et al. 1983).

It is also interesting to note that through the passage of time selective pressure on the Hp bacterium may have forced the organism to devolve into a more resilient (considering the vigorous humoral and immune response mounted against it), less virulent form in order to enjoy a more commensal relation with its human host in its well-suited ecological niche. What also has to be taken into account is that about 60% of all Hp strains tested are non-toxigenic. In fact, recent studies by Ishihara et al. (1997) have demonstrated that oral bacteria produce bacteriocin-like inhibitory proteins that prevent Hp from colonising the oral cavity. Blaser (1997) has also claimed that mass Hp-eradication programmes may be premature since not enough is known about the organism, and there may exist strains that could be beneficial to man. One of these benefits may be the protective effect of hyperacidity against ingested pathogens and intestinal micro-flora endeavouring to colonise the gastric mucosa. Therefore, what is clear is that a relationship does exist between Hp and the regulation of tissue kallikrein in gastric inflammation, but the nature of which is still too ambiguous to unequivocally define.

Many clinical trials have been performed to determine the efficacy of drug treatment regimens for non-ulcer dyspepsia associated with Hp infection. The more recently introduced drugs for the treatment of dyspepsia are the proton-pump inhibitors. Of particular relevance is the localisation of TK in parietal cell, which specifically produces gastic acid using the H_2-ATPase pump. Therefore the current treatment of choice, for most physicians, is triple therapy with an H_2 proton-pump inhibitor, bismuth salt derivatives and an antibacterial. This type of treatment has proved highly effective in eradication (90-94%) of Hp associated inflammation. As long as the triple therapy is prescribed remission of the Hp-induced gastritis continues. The important outcome of this study is that kinin antagonists may play an important therapeutic role in dyspepsia.

CHAPTER 5

CONCLUSIONS

]

CONCLUSIONS

The relevance of gastric disease therapy is of major financial proportions, since remedies for this type of disease are the number one income-generating drugs in the world. The degree of colonisation world-wide makes Hp-associated gastric disease a significant socio eocomic woe.

From the findings of this study, it may be concluded that the expression of enzymically active TK in the antral inflamed gastric tissue is not affected by disease pathology. The body regions, forming the vast acid-producing region of the stomach, of the inflamed tissue showed an increase in the amount of functionally active TK, and this suggests a plausible role of the parietal cells in the gastric disease.

Total TK measurement in gastric antral tissue shows a depletion of TK as the disease condition progresses, and this would indicate a glandular exudation into the lumen. This exocytosis is confirmed by the increase in TK amidase activity in the lavage fluid from a chronic inflamed stomach.

In the inflamed stomach, we find no correlation between the amount of TK released into the lumen to the amount of enzymically active TK contained therein. It is thought that the presence of Hp has an inhibitory action on functionally active TK in gastric luminal fluid.

It also appears that Hp stimulates hyperacidity in the gastric lumen, a condition the bacterium is found to thrive in, as inflammation becomes increasingly severe. The atrophy

of gastric tissue effectively destroys this acid-secreting environment, and therefore a non-ideal environment eventually sees a disappearance of Hp.

We may also speculate that the role of TK as a basal level in the normal stomach has a gastro-protective role. This would effectively change, with the onset of inflammation induced by Hp antigens, to a pro-inflammatory role. We see this basal TK level return with regression of disease (atrophy) and disappearance of Hp, reaffirming the former suggestion.

To ensure complete eradication of the inflammation and the presence Hp, this study establishes the need for a kinin antagonist to be coupled to the existing H_2 receptor antagonist and anti-bacterial treatments.

REFERENCES

Abelous, J. E. and E. Bardier. 1909. Les substances hypotensives de l'urine humaine normale. C. R. Soc. Biol. **66**: 511-512.

Al Moagel, M.A.. Evans, D.G. and Abdulghani, M.E. 1990. Prevalence of *Helicobacter* (formerly *Campylobacter*) *pylori* infection in Saudi Arabia, and comparison of those with and without upper gastrointestinal symptoms. Am. J. Gastroenterol. **85**:944-948.

Amundson, E., J. Putter. 1979. Methods for the determination of glandular kallikrein by means of a chromogenic tripeptide substrate. Advances in Experimental Medicine and Biology 120A: 83-95.

Atherton, G.D., Fossi, S., Lind, T and Bell, G. 1996. Efficacy and tolerability of a short term low dose triple therapy for eradication of *Helicobcater pylori*. Gastroenterol. **104**: A40-48.

Bayer, E.A. and Wilchik, M. 1974. The use avidin-biotin in immunoassays. Methods Enzymol. **34**: 365-371.

Beaubien, G., Rosinski-Chupin, I., Mattei, M.G., Mbikay, M., Chretien, M. and Seidah, N.G. 1991. Gene structure and chromosomal localisation of plasma kallikrein." Biochemistry **30**: 1628-1635.

Beutler, B. and Cerami, A. 1987. Cachetin: more than a tumour necrosis factor. N. Engl. J. Med. **316: 379-384.**

Bhoola, K.D and Schachter, M. 1960 Some properties of kallidin, bradykinin and wasp venom kinin. In: M. Schachter, ed. Polypeptides which affect smooth muscles and blood vessels. Oxford: Pergamon Press, 1960: 232-246.

Bhoola, K.D., Elson, C.J., Dieppe, P.A. 1992b. Kinins-key mediators in inflammatory arthritis. British Journal of Rheumatology **31**: 509-518.

Bhoola, K.D., Figueroa, C.D., Worthy, K. 1992a. Bioregulation of kinins: kallikreins, kininogens and kininases. Pharmacological Reviews **44**(1): 1-80.

Bizzozero, G. 1893 Ueber de schauchformigen drusen des magendarmkanals und die bezeihungan ihres epithels zu dem oberflachenepithel der schleimhaut. Arch. Mikr. Anast. **42**: 82.

Blaser, M.J. 1990. Helicobacter pylori and the pathogenesis of gastroduodenal inflammation. J Infect. Dis. **161**: 626-633.

Blaser, M.J. 1997. Not all helicobacter strains are created equal: should all be eliminated. Lancet **349**: 1020-1022.

Bode, G., Malfertheiner, P., Lehnhardt, G., Nilius, M. and Dischuneit, H. 1993 Ultrastructural localisation of urease of Helicobacter Pylori. Med. Microbiol. Immunol. **182**: 233-242.

Bode, W., Chen, Z., Barrels, K., Kutzbach, C., Schmidt-Kastner, G. and Bartunik, H. 1983. Refined 2A X-ray crystal structure of porcine pancreatic kallikrein A, a specific trypsin-like serine protease. J Mol. Biol. **165**: 237-282.

Boissonnas, R.A., Guttmann, S.T. and Jaquenoud, P.A. 1960. Synthesis and biological activity of peptides related to bradykinin. Experimentia **16**: 326.

Bond, J.S. and Beynon, R.J. 1995. The astacin family of metallopeptadases. Prot. Sci. **4**: 1247-1261.

Bradford M.M. 1976. A rapid and sensitive method for quantitation of microgram quantity of protein utilising the principal of protein dye binding. Anal. Biochem. **72**: 248-254.

Brenner, M., Doerfler, M.E., Danner. R.I., Reilly, J.M., Weiderman, M.M. and Parrillo, J.E. 1997. Determination of direct myocardial contractile effects of eicasanoids, endotoxin, tumour necrosis factor and other mediators using a newly developed quantititative cellular contractility assay. Clin. Res. **35**: 78A.

Brown,J.F., Whittle, B.J.R. and Hanson, P.J. 1992. Bradykinin stimulates PGE_2 release in cell fractions isolated from the rat gastric mucosa via the B_1 receptor. Biochem. Soc. Trans. **20**:276S.

Butt, S.K., Dawson, L.G. and Hall, J.M. 1995. Bradykinin B_1 receptors in the rabbit urinary bladder: Induction of responses, smooth muscle contraction, and phosphatidylinisitol hydrolysis. Br. J. Pharmacol. **114**: 612-617.

Cahill, R.J., Sant, S., Hamilton, H. and Beattie, S. 1988. *Helicobacter pylori* and increased cell proliferation: a risk for cancer. Gastroenterol. **104**: 1032.

Carretero, O.A. and Scicli, A.G. 1988. Kinins paracrine hormone. Kidney International **34** (suppl. 26): S52-S59.

Carretero,O.A. and Scicli, A.G. 1980 The renal kallikrein kinin system. American J Physiol. **238**: F247-255.

Chahine, R., Adam., A., Yamaguchi, N., Gaspo, R., Regoli, D. and Nadeau, R. 1993. Protective effects of bradykinin on the ischaemic heart: implication of the B_1 receptor. Br. J. Pharmacol. **108**:318-322.

Chao, J., Chai, K.X., Chen, L.M., Xiong, W., Chao, S., Woodley-Miller, C., Wang, L.X., Lu, H.S. and Chao, L. 1990. Tissue kallikrein-binding protein is a serpin. I. Purification, characterisation and distribution in normotensive and spontaneously hypotensive rats. J. Biol. Chem. **265**: 16394-16401.

Chung D.W., Fujikawa, K., McMullen, B.A. and Davie, E.W. 1986. Human plasma prekallikrein, a zymogen to a serine protease that contains poor tandem repeats. Biochemistry **25**: 2410-2417.

Citran, D., Malaty, H.M. and Evans, D.G. 1994. Epidemiology of *Helicobacter pylori* in an asymptomatic population in the United States. Gastroenterol. **100**: 1495-1501.

Collins, J.S.A. 1992. Role of *Helicobacter pylori* in gastritis and duodenitis in man. Agents Actions. c47-c49.

Colman, R.W., Wachtfogel, Y.T., Kucich, U., Weinbaum, G., Hahn, S., Pixley, R.A., Scott, C.F., de Agostini, A., Burger, D. and Schapira, M. 1985. Effect of cleavage of the heavy chain of human plasma kallikrein on its functional properties. Blood **65** (2): 311-318.

Conese, M. and Blasi, F. 1995. Urokinase/urokinase receptor system: Internalisation/degradation of urokinase serpin complex: mechanism and regulation. Biol. Chem. Hoppe-Seyler. **376**: 143-155.

Cotran RS, Kumar V and Robbins SL. The gastrointestinal tract. In: Robbins Pathologic Basis of Disease. 5ed. Philadelphia: W.B. Saunders, 1994: 767-783.

Crabtree, J.E., Shallcross, T.M., Heatley, R.V. and Wyatt, J.I. 1991. Mucosal tumour necrosis factor alpha and interleukin 6 in patients with *Helicobacter pylori*-associated gastritis. Gut **32**: 1473-1477.

Cruwys, S.C., Garret, N.E., Perkins, M.N., Blake, D.R. and Kidd, B.L. 1994. The role of bradykinin B_1 receptors in the maintenance of intra-articular plasma extravasation in chronic antigen-induced arthritis. Br. J. Pharmacol. **113**: 940-944.

DeLa Cadena, R.A., Suffredini, A.F., Page, J.D., Pixley, R.A., Kaufman, N., Parillo, J.E. and Colman, R.W. 1993. Activation of kallikrein-kinin system after endotoxin administration to normal human volunteers. Blood. **81**: 3313-3317.

Dixon, M.F. *Helicobacter pylori* and acid peptic disease. In Axon, A.T.R. ed. *Helicobcater pylori*, its role in gastrointestinal disease. London. Science Press,1994: 18-34

Doenges, J.L. 1939. Spirochetes in the gastric glands of *Macacus rhesus* and of man without related disease. Arch Pathol. Lab. Med. **27**: 469-477.

Dunn, B., Sung., C.C., Taylor, N.S. and Fox, J.G. 1991. Purification and characterisation of helicobacter mustelae urease Infect. Immunol. **59**: 3343-3345.

Dunn, B.E,., Campbell, G.P., Perez-Perez, G.I. and Blaser, M.J. 1990. Purification and characterisation of urease from *Helicobacter Pylori*. J. Biol. Chem. **265**: 9464-9469.

Dunn, B.E. 1993. "Pathogenic mechanisms of *Helicobacter pylori*. Gastroenterol. Clin. North Am. **22**: 43-57.

Eaton, K.A., Dewhirst, F.E., Radin, M.J., Foz, J.G., Paster, B.J., Krakowka, S. and Morgan, D.R. 1991. *Helicobacter acinonyx* sp. Nov. isolated from cheetahs with gastritis. Int. J. Cyst. Bacterial. **43**: 99-106.

Eaton, K.A., Morgan D.R. and Krakowka, S. 1989. *Campylobacter pylori* virulence factors in gnotobiotic piglets. Infect. Immun. **57**: 1119-1125.

Eaton, K.A., Morgan, D.R., Brooks, C. and Krakowka, S. 1991. Essential role of urease in the pathogenesis of gastritis induced by *Helicobacter pylori* in gnotobiotic piglets" Infect. Immunol. **59**: 2470-2475.

Eisen, V.. Some recent developments in kinin formation. In: Haberland GL, Rohan, JW , Blümel G P, eds. Kininogenases, F.K. Schattaeur Verlag, 1975: 3-9.

Elliot, D.F., Horton, E.W. and Lewis, G.P. 1960. Actions of pure bradykinin. J. Physiol. **153**: 473-477.

El-Omar, E.M., Penman, I.D., Ardill, J.E.S. and Chittajallu, R.S. 1995. *Helicobacter pylori* infections and abnormalities of acid secretion in patients with duodenal ulcer disease. Gastroenterology **103** (9): 681-691.

Emödy L., Carlsson, Å, Ljungh Å. and Wadström, T. 1988. Mannose-resistant haemagglutination by *Campylobacter pylori*. J. Inf. Dis. **20**: 353-354.

Engstrand, I., Scheynius, A., Pahlson, C., Grimelius, L., Schwan, A. and Gustavsson, S. 1989. Association of *Campylobacter pylori* with induced expression of class II transplant antigens on gastric epithelial cells. Infect. Immunol. **57**: 827-832.

Engvall, E and Perlmann, P. 1971. Enzyme-linked immunosorbant assay (ELISA). Quantititative assay of immunoglobulin G. Immunochem. **8** (9): 871-874.

Evans, B.A., Yun, Z.X., Close, J.A., Tregear, G.W., Kitumura, N., Nakanishi, S., Callen, D.F., Baker, E., Hyland, V.J., Sutherland, G.R. and Richards, R.I. 1988. Structure and chromosomal localisation of the human renal kallikrein gene. Biochemistry. **27**: 3124-3129.

Evans, D.G., Evans, D.J. and Graham, D.Y. 1992. Adherence and internalisation of *Helicobacter pylori* by HEp-2 cells. Gastroenterol. **102**: 15557-1567.

Evans, D.G., Evans, D.J., Moulds, J.J. and Graham, D.Y. 1988. N-acetylneuraminyllactose-binding fibrillar heamgglutinin of *Campylobacter pylori*: a putative colonisation factor antigen. Infect. Immun. **56**: 2896-2906.

Farber, J.L. The gastrointestinal tract. In: Rubin, E. ed. Essential Pathology. Philadelphia: J.B. Lippincott, 1995: 354-365.

Farmer, S.G., Burch, R.M., Meeker, S.A. and Wilkins, D.E. 1988. Evidence for a pulmonary B_3 bradykinin receptor. Mol. Pharm. **36**: 1-8.

Ferrero, R.L. and Lee, A. 1991. The importance of urease in acid protection for the gastric colonising bacteria *Helicobacter pylori* and *Helicobacter felis sp.* nov. Microb. Ecol. Health. Dis. **4**: 121-134.

Fiedler F, Enzymology of glandular kallikreins. In: Erdos E G, ed. Handbook of experimental Pharmacology Supplement: Bradykinin, Kallidin and Kallikrein. New York: Springer-Verlag, 1979: (23) 103-161.

Figueroa, C. D. and MacIver, A.G. et al. 1989. Identification of a tissue kallikrein in human polymorphonuclear leucocytes. British Journal of Haematology. **72**: 321-328.

Figueroa, C.D., Gonzalez, C.B., Grigoriev, S., Abd Alla, S., Haasemann, M., Jarnagin, K. and Muller Esterl, W. 1995. Probing for a bradykinin B2 receptor in rat kidney by anti-peptide and anti-ligand antibodies. J. Histochem. Cytochem. **43**: 137-148.

Fraser, A.G., Prewett, E.J. and Pounder, R.E. 1992. Twenty-four hour hyperpepsinogaemia in Helicobacter pylori-positive subjects is abolished by the eradication of the infection. Aliment. Pharmacol. Ther. **6**: 389-394.

Freedburg, A.S. and Barron, L.E. 1940. The presence of spirochaetes in human gastric mucosa. Am. J. Dig. Dis. 7: 443-445.

Freston, J.W. 1994. pH and Hp: *H. pylori* infection and peptic ulcer disease. Highlights from : Infections in Medicine. **4**: 3-6.

Frey E.K., Traut, H., Werle, E., Vogel., R. and Zickgraf-Rüde, G., Trautschold, I. Das kallikrein-kinin system und seine inhibitoren. Stuttgartl: Enke, 1968.

Frey, E.K. and Kraut, H. 1928. Ein neues kreislaufhormon und seine wirking. Naunyn Schmiedebergs Arch. Pharmak. **133**:1-56.

Frey, E.K. and Werle, E. 1933. Kallikrein im inneren und äußeren pankreassekret. Klein. Wochenschr. **12**: 600-601.

Frey, E.K., Kraut, H., Werle, E. Kallikrein padutin. Stuttgart: Enke, 1950.

Fuller, P.J. and Funder, J.W. 1986. The cellular physiology of glandular kallikrein. Kidney International. **29**: 953-964.

Fuller, P.J., Verity, K., Matheson, B.A. and, Clements, J.A. 1989. Kallikrein gene expression in the rat gastrointestinal tract. Biochem. J. **264**: 133-136.

Girolami, P., Alhenc-Gelas, F., Dos Reis, M.L., Bascands, J.L., Suc, J.M., Corvol, P. and Menard, J. 1986. Hydrolysis of high molecular weight kininogen by purified rat urinary kallikrein; identification of bradykinin as the kininogen formed. Adv. Exp. Med. Biol. **198A**: 137-145.

Goodwin, C.S. and Worsley, B.W. 1993. Microbiology of *Helicobacter pylori*. Gastroenterol. Clin. N. Am. **22**: 5-19.

Goodwin, C.S., Blincow, E., Peterson, G., Sanderson, C., Cheng, W., Marshall, B., Warren, J.R. and McCulloch, R. 1987. Enzyme-linked immunosorbent assay for *Campylobacter pyloridis*: Correlation with presence of *C. pyloridis* in the gastric mucosa. J. Inf. Dis. **155(3):** 488-494.

Goodwin, C.S., Mendall, M.M. and Northfield, T.C. 1997. Helicobacter pylori infection. Lancet **349**: 265-269.

Graham, D.Y., Klein, P.D. and Opekun, A.R. Boutton TW. 1988. Effect of age on the frequency of active *Campylobacter pylori* infection diagnosed by the [^{13}C] urea breath test in normal subjects and patients with peptic ulcer disease. J. Inf. Dis. **157 (4):** 777-780.

Graham, D.Y., Opekun, A., Lew, G.M., et al. 1990. Ablation of exaggerated meal-stimulated gastrin release in duodenal ulcer patients after clearance of *Helicobacter (campylobacter) pylori* infection. Am. J. Gastroenterol. **85**: 394-398.

Greenbaum, L.M. and Sherman, R. 1962. Studies on catheptic carboxypeptidase. J. Biol. Chem. 237: 1082-1085.

Griffin, J.H. and Cochrane, C.G. 1976. Mechanisms for the involvement of high molecular weight kininogen in surface-dependant reactions of Hageman factor. Proc. natl. Acad. Sci. USA. **73** (8): 2554-2558.

Guimaraes, J.A., Borges, D.R., Prado, E.S. and Prado, J.L. 1973. Kinin-converting aminopeptidase from human serum. Biochem. Pharmacol. **22**: 3157-3172.

Guyton AC. Secretory functions of the alimentary canal. In: Human Physiology and mechanisms of Disease, 5ed. Philadelphia: W.B. Saunders, 1992: 487-493

Hall JM, Morton IKM.. Pharmacology of kinin receptors. In: Farmer S G. ed The Kinin System. San Diego: Academic Press, 1997: 10

Hall JM, Morton IKM.. The pharmacology and immunopharmacology of kinin receptors. In: Farmer S G. The Kinin System. San Diego: Academic Press, 1997: 9-32.

Halter, F., Hurlimann, S. and Inauen, W. 1992. Pathophysiology and clinical relevance of *Helicobacter pylori.* Yale J. Biol. Med. **65**: 625-638.

Hanson, L-E., Engstrand, L., Nyren, O., Evans, D.J., Lindgren, A., Bergstrom, R., Andersson, B., Athlin, L., Bendtson, Q., Tracz, P. 1993. *Helicobacter pylori* infection: Independent risk factor of adenocarcinoma. Gastroenterology. **105(4):** 1099-1103.

Hasan, A.A.K., Cines, D.B., Ngaiza, J.R., Jaffe, E.A. and Schmaier, A.H. 1995. A high molecular weight kininogen is exclusively membrane bound on endothelial cells to influence activation of vascular endothelial cells. Blood **85**: 3134-3143.

Hatz, R.A., Brooks, W.P., Kramling, H.J. and Enders, G. 1992. Stomach immunology and *Helicobacter pylori* infection. Curr. Sci. **8**: 993-1001

Hawtin, P.R., Stacey, A.R. and Newell, D.G. 1990. Investigation of the structure and localisation of the urease of *Helicobacter pylori* using monoclonal antibodies. J. Gen. Microbiol. **136**: 1995-2000.

Hazell, S.L., Lee, A., Brady, L. and Hennessy, W. 1996. *Campylobacter pyloris* and gastritis; association with intercellular spaces and adaptation to an environment of

mucus as important factors in colonisation of the gastric epithelium. J. Infect. Dis. **153**: 658-663.

Hemalatha, S.G., Drumm, B. and Sherman, P. 1991. Adherence of *Helicobacter pylori* to human gastric epithelial cells *in vitro*. J. Med. Microbiol. **35**: 197-202.

Hess, J.F., Borkowski, J.A., Young, G.S., Strader, C.D. and Ransom, R.W. 1992 Cloning and pharmacological characterisation of a human bradykinin (BK-2) receptor. Biochem Biophys. Res. Commun. **184**: 260-268.

Ishihara, K., Miura, T., Kimizuka, R., Ebihara, Y., Mizuno, Y. and Okuda, K. 1997. Oral bacteria inhibit *Helicobacter pylori* growth. FEMS Microbiology Letters **152**: 355-361.

Jaques, R. and Schachter, M. 1954. The presence of histamine, 5-hydroxytryptamine and a potent slow-contracting substance in wasp venom. British Journal of Pharmacology **9**: 53.

Johnstone, A. and Thorpe, R. Immunohistochemistry in practice. Oxford. Blackwell Scientific Publications, 1982: 44-47.

Kalter, E.S., van Dijk, W.C., Timmerman, A., Verhoef, J. and Bouma, B.N. 1983. Activation of purified human plasma prekallikrein triggered by cell wall fractions of *Eschericia coli* and *Staphylococcus aureus*. J. Inf. Dis. **148**: 682-691.

Kaplan, A.P., Kay, A.B., Austen, K.F. 1972. A prealbumin activator of prekallikrein. III. Appearance of chemotactic activity for human neutrophil by the conversion of human prekallikrein to kallikrein. J. Exp. Med. **135**: 81.

Kaufman, S.H., Schoel, E.B., Wand-Wurttenberger, A., Steinhoff, U., Munk, M.E. and Koga, T. 1990. T cells, stress proteins, and the pathogenesis of mycobacterial infections. Curr. Top. Microbiol. Immunol. **155**: 125-141.

Kawano, S., Tsujii, M., Tsuji, S., Takei, Y., Masuda, E., Bing, pH 1993 Effects of ammonia on *Helicobacter pylori*-associated gastric disease. Eur. J. Gastroenterol. Hepatol. **5**: S29-S33.

Kellerman, J., Thelen, C., Lottspeich, F., Henschen, A., Vogel, R., Muller-Esterl, W. 1987. Arrangement of the disulphide bridges in human low-M_r kininogen. J. Biol. Chem. **247**: 15-21.

Kendall, C., Ionescu-Matiu, I. and Dreesman, G.R. 1983. Utilisation of the biotin/avidin system to amplify the sensitivity of the enzyme-linked immunosorbent assay (ELISA). Journal of Immunological Methods. **56**: 3329-339

Kerbiriou, D.M., Bouma, B.N. and Griffin, J.H. 1980. Immunochemical studies of human high molecular weight kininogen and of its complexes with plasma prekallikrein or kallikrein. J. Biol. Chem. **255**: 3952-3958.

Kilian, M., Mestecky, J. and Russel, M. 1988. Defence mechanisms involving Fc-independant functions of immunoglobulins and their subversion by bacterial immunoglobulin A proteases. Microbiol. Rev. **52**: 296-303

Kimball, H.R., Melmon, K.L. and Wolff, S.M., 1972. Endotoxin-induced kinin production in man. Proc. Soc. Exp. Biol. Med. **139**: 307-312.

Kirchner, T., Melber, A., Fischback, W., Heilmann, K. and Muller-Hermelink, H. 1990. Immunohistological patterns of the local immune response in *Helicobacter pylori* gastritis. In Malfertner, P., Ditschunit, H. Eds. *Helicobacter pylori*, gastritis and peptic ulcer. Berlin. Springer-Verlag, 1990, 213-222.

Kitamura, N., Kitagawa, H., Fushima, D., Takagaki, Y., Miyata, T., Nakanishi, S. 1985. Structural organistaion of the human kininogen gene and a model for its evolution. J. Biol. Chem. **260**: 8610-8617.

Kraut, H., Frey, E.K. and Werle, E. 1930. Der nachweis eines kreislaufhormons in der pankreasdrüse. Z. Physiol. Chem. **189**: 97.

Kraut, H., Frey, E.K. and Werle, E. 1933. Über den nachweis und das vorkommen des kallikreins im blut. Z. Physiol. Chem. **222**: 73.

Kraut, H., Frey, E.K., Werle, E. 1930. Über die inaktivierung des kallikreins. Hoppe-Seylers Z. Physiol. Chem. **192**: 1-21

Kraut, J. 1971. Serine proteases: structure and mechanisms of catalysis. Ann. Rev. Biochem. **4: 331-358.**

Kumar V, Cotran RS, Robbins SL. The oral cavity and the gastrointestinal tract. In: Basic Pathology. 6ed. Philadelphia: W.B. Saunders, 1997: 482-489.

Laine, L., Lewin, D.L., Naritoku, W. and Cohen,. H. 1997. Prospective comparison of H&E, Giemsa and Genta stains for the diagnosis of *Helicobacter pylori*. Gastrointestinal Endoscopy. **45**: 463-467.

Lauren, P. 1965. The two histological main types of gastric carcinoma: diffuse and so-called intestinal type-carcinoma. Acta Pathol. Microbiol. Scand. **64**: 31-49.

Lee, A. 1991. Spiral organisms: what are they?. Scand. J. Gastroenterol. 26 suppl **187**:9-22.

Lee, A. 1998. The *Helicobacter pylori* genome- new insights into pathogenesis and therapeutics. New. Engl. J. Med. **338**: 832.

Leeson, T.S. and Leeson, C.R. Histology (4ed) Philadelphia: W.B. Saunders, 1981: 350-367.

Leunk, R.D., Ferguson, M.A., Morgan, D.R., Low, D.E. and Simor, A.E. 1990 Antibody to cytotoxin in infection by *Helicobacter pylori*. J. Clin. Microbiol. **28**: 1181-1184.

Lin, F. -K., Lin, C.H., Chou, C.C., Chen, K., Lu, H.S., Bacheller, W., Herrera, C., Jones, T., Chao, J. and Chao, L., 1993. Molecular cloning and sequence analysis of the monkey and human tissue kallikrein genes. Biochim. Biophys. Acta **1173**: 325-328.

Lingwood, C.A., Law, H., Pellizzari, A., Sherman P., Drumm, B., (1989) "Gastric gylycerolipid as a receptor for *Campylobacter pylori*" Lancet, 340:239.

Ljunggren, Ö. and Lerner U.H. 1990. Evidence for BK_1 bradykinin receptor-mediated prostaglandin formation in osteoblasts and subsequent enhancement of bone resorption. Br. J. Pharmacol. **101**: 382-386.

MacDonald, R.J., Margolius, H.S. and Erdos, E.G. 1988. Molecular biology of tissue kallikrein. Biochem J. **253**: 313-321.

Maeda, H. and Yamamoto, T. 1996. Pathogenic mechanisms induced by microbial proteases in microbial infections. Biol. Chem. Hoppe-Seyler **377**: 217-226.

Mahan, L.C. and Burch, R.M. 1990. Functional expression of B_2 bradykinin receptors from balb/ c cell mRNA *Xenopus* oocyte. Mol. Pharmacol. **37**: 785-789.

Mai, U.E.H., Perez-Perez, G.I., Allen, J.B., Wahl, S.M., Blaser, M.J. and Smith, P.D. 1992. Surface proteins from *Helicobacter pylori* exhibit chemotactic activity for human leukocytes and are present in gastric mucosa. J. Exp. Med. **175**: 517-525.

Malaty HM, Mitchell HM and Graham DY. Epidemiology of *Helicobacter pylori* infection In: Axon A.T.R (ed). *Helicobacter pylori*, its role in gastrointestinal disease. London: Science Press, 1994: 1-10.

Malaty, H.M., Evans, D.G., Evans and D.J. 1992. *Helicobacter pylori* in Hispanics: comparison with blacks and whites of similar age and socioeconomic class Gastroenterology **103**: 813-816.

Malaty, H.M., Graham, D.Y. and Klein, P.D. 1991. Transmission of *Helicobacter pylori* infection. Studies in families of healthy individuals. Scand. J. Gastroenterol., **26**: 927-932.

Malfertheiner, P.J., Dominguez-Munoz, E., Heckenmuller, H., Neubrand, M., Fischer, H.-P. and Sauerbach, T. 1996. Modified rapid urease test for detection of *Helicobacter pylori* infection. Eur. J. Gastroenterol. Hepatol. **8**:53-56.

Mandle, R., Jr. and Kaplan, A.P. 1977. Hageman factor substrates. II. Human plasma prekallikrein. Mechanism of activation by Hageman factor and participation in Hageman factor dependant fibrinolysis. J. Biol. Chem. **252**: 6097-6104.

Mandle, R., Jr., Colman, R.W. and Kaplan, A.P. 1976. Identification of prekallikrein and HMW-kininogen as a circulating complex in human plasma. Proc Natl. Acad. Sci. USA **73**: 4179-4183.

Marceau, F. 1995. Kinin B_1 receptors: a review" Immunopharmacology **30**: 1-26.

Marceau, F., Lussier, A., Regoli, D. and Giroud, J.P. 1983. Pharmacology of kinins: their relevance to tissue injury and inflammation. Gen. Pharmacol. **14**: 209-229.

Marsh, K.A. and Hill, S.J. 1994. Des-arg^9-bradykinin-induced increases in calcium ion concentration in single bovine tracheal smooth muscle cells. Br. J. Pharmacol. **112**: 934-938.

Marshall, B.J. and Warren., J.R. 1984. Unidentified curved bacilli in the stomach of patients with gastritis and peptic ulceration" Lancet (i): 1311-1315.

Mason, A.J., Evans, B.A., Cox, D.R., Shine, J. and Richards, R.I. 1983. Structure of mouse kallikrein gene family suggests a role in specific processing of biologically active peptides. Nature. **303**: 300-307.

Matsumoto, K., Miyagawa, S., Okamura, R. and Maeda, H. 1996. Productyion of the protease in experimental *Serratia* keratitus in guinea pigs, and spreading in the tissue. An immunohistochemical study. Curr. Eye Res. *in press.*

Matsumoto, K., Shams, N.B.K., Hanninen, L.A. and Kenyon, K.R. 1992. Proteolytic activation of cornela matrix metalloproteinse by *Pseudomas aeruginosa* elastase. Curr. Eye. Res. **11**: 1105-1109.

McEachern, A.E., Shelton, E.R., Bhakta, S., Obernolte, R., Bach, C., Zuppan, P., Fujisaki, J., Aldrich, R.W. and Jarnagin, K. 1991. Expression cloning of a rat B_2 receptor. Biochem. **88**: 7724-7728.

McGowan, C.C., Clover, T.L. and Blaser, M.J. 1996. Helicobacter and gastric acid: biological and therapeutic implications. Gastroenterology **110**: 926-938.

McIntyre, P., Phillips, E., Skidmore, E., Brown, M. and Webb, M. 1993. Cloned murine bradykinin receptor exhibits a mixed B_1 and B_2 pharmacological selectivity. Mol. Pharmacol. **44**: 346-355.

Megraud, F. 1994. Toxic factors of *Helicobacter pylori*. Eur. J. Gastroenterol. Hepatol. **6** (suppl.1): s5-s10.

Megraud, J. 1991. Epidemiology of *Helicobacter pylori* infection. Gastroenterol. Clin. North Am. **22**: 73-88.

Mendall, M.A., Goggin, P.M. and Molineaux, M. 1992. Childhood living conditions and *Helicobacter pylori* seropositivity in adult life. Lancet **339**: 896-897.

Miller, N.M., Sathar, M.A., Naran, A.D., Van den Ende, J., Simjee, A.E. and Manion, G. 1991. Evaluation of various laboratory techniques to diagnose *Helicobacter pylori* in patients with upper gastro-intestinal tract symptoms. S. A. M. J. **80:** 575-578.

Mitchel, H.M., Bohane, T.D. and Berkowicz, J. 1987. Antibody to Campylobacter pylori in families of index children with gastrontestinal illness due to C. pylori. [letter] Lancet **2**: 681-682.

Mobley, H.L.T. and Hausinger, R.P. 1989. Microbial ureases: significance, regulation and molecular characterisation. Micronbiol. Rev. **53**: 85-105.

Mobley, H.L.T., Hu, L.-T. and Foxall, P.A. 1991. *Helicobacter pylori* urease: Properties and role in pathogenesis. Scand. J. Gastroenterol. suppl. **187**: 39-46.

Molla, A., Matsumoto, K., Otamada, I., Katsuki, T. and Maeda, H. 1986. Degradation of protease inhibitors, immunoglobulin and other serum proteins by *Serratia* protease and its toxicity to fibroblasts in culture. Infect. Immunol. 53: 522-529.

Molla, A., Yamamoto, T., Akaike, T., Miyoshi, S. and Maeda, H. 1989. Activation of hageman factor and prekallikrein and generation of kinin by various microbial proteinases. J. Biol. Chem. **264**: 10589-10594.

Morris, A. and Nicholson, G. 1987. Ingestion of *Campylobacter pyloridis* causes gastritis and raises fasting pH. Am. J. Gastroenterol. **82**: 192-199.

Morrison, D.C. and Kline, L.F. 1977. Activation of the classical and properdin pathways of complement by bacterial lipopolysaccharides (LPS). J. Immunol. **118**: 362-368.

Morrison, D.C. and Ryan, J.L. 1987. Endotoxin and disease mechanisms. Ann. Rev. Med. **38**: 417-421.

Muller-Esterl, W. 1989. Kininogen, kinins and kinships. Thromb. Haemost. **61**: 2-6.

Muller-Esterl. W., Iwanaaga, S. and Nakanishi, S. 1986. Kininogens revisited. TIBS **11**:336-339.

Murray, S.R., Chao, J., Lin, F.and Chao, L. 1990. Kallikrein multigene families and the regulation of their expression. Journal of Cardiovascular Pharmacology. **15** (suppl.): S7-S15.

Muschel, L.H., Schmoker, K. and Webb, P.M. 1964. Anticomplementary action of endotoxin. Proc. Soc. Exp. Biol. Med. **117**: 639-642.

Nagase, H., Enghild, J.J., Suzuki, K. and Salvesen G. 1990. Stepwise activation mechanism of the precursor of matrix metalloproteinase 3 (stromelysin) by proteinases and (4-amino-phenyl) mercuric acetate. Biochem. **29**: 5783-5789.

Naidoo, S., Ramsaroop, R., Bhoola, R. and Bhoola, K.D. 1997. The evaluation of tissue kallikrein in *Helicobacter pylori*-associated gastric ulcer disease. Immunopharm. **36**: 263-269.

Naidoo, S., Ramsaroop, R., Bhoola, R.L. and Bhoola, K.D. 1999. Correlation of kinin-generating activity tissue kallikrein to *Helicobacter pylori* associated gastric infection. Immunopharm. *In press.*

Neurath H. The diversity of protoelytic enzymes. In: Beynon R J, Bond J S, eds. Proteolytic Enzymes - A Practical Approach. Oxford: Oxford University Press 1989: 1-13.,

Newell, D.G. 1991. Virulence factors of *Helicobacter pylori*. Scand. J. Gastroenterol. **26** suppl 187: 31-38.

Nilsson, B. 1990. Enzyme-linked immunoadsorbent assays. Current Opinion in Immunology. **2**: 898-904.

Nitsch, R.M., Kim, C. and Growdon, J.H. 1998. Vasodepressin and bradykinin regulate secretory processing of the amyloid precursor of Alzheimer's Disease. Neurochemical Research **23** (5): 807-814.

Okamoto, H. and Greenbaum, L.M. 1983. Isolation and structure of T-kinin. Biochem. Biophys. Res. Commun. **112**: 701-708.

Overlack, A., Scicli, A.G. and Carretero, O.A. 1983. Intestinal absorption of glandular kallikrein in the rat. Am. J. Physiol. **244B**: G689-G694.

Papinin, E., Debernard, M., Bugnoli, M., Milia, E., Rappuoli, R. and Montecucco, C. 1993. Cell-vacuolisation induced by *Helicobacter pylori* – inhibition by bafilomycin A1, bafilomycin-B1, bafilomycin-C1 and bafilomycin-D. FEMS Microbiol. Lett. **113**:155-160.

Peek, R.M. and Blaser M.J. 1996. Pathophysiology of *Helicobacter pylori*-induced gastritis and peptic ulcer disease. Am. J. Med. **102**: 200-207.

Perez-Perez, G.I., Bhat, N., Gaensbauer, J., Taylor, D., Kuipers, E.J., Zhang, L., You, W-C. and Blaser, M.J. 1996. Country-specific constancy by age in cagA proportions of *H. pylori* infections. Gut **39** (suppl 2): A83.

Perkins, M.N., Campbell, E. and Dray, A. 1993. Anti-nociceptive activity of the bradykinin B_1 and B_2 receptor antagonists des-arg^9,[Leu^8]-BK and Hoe 140, in two models of persistent hyperalgesia in rats. Pain **53**: 191-197.

Peterson, E.M. 1981. ELISA: A tool for the clinical microbiologist. American Journal of Medical Technology. **47** (11): 905-908.

Phull, P.S., Gower, J.D. and Price A.B. 1993. γ-tocopherol (vitamin E) antioxidant levels in chronic gastritis; correlation with mucosal neutrophil infiltration. Gut. **34**: S34.

Piotrowski, J., Morita, M., Slomiany, A. and Slomiany, B.L. 1992. Inhibition of gastric mucosal laminin receptor by *Helicobacter pylori* lipopolysaccharide. Effect of ebrotidine. Biochem. Int. **271**: 131-138.

Pisano J J. Chemistry and biology of the kallikrein kinin system. In: Proteases and biological control., Reich E, Rifkin D B, Shaw E, eds. New York: Cold Spring harbour Laboratory, 1975: 199-222,.

Powers, C.A. 1986. Trypsin-like, partial characterisation, and distribution of kallikrein-like and thrombin-like proteases in the neurointermediate lobe of the rat pituitary. J Neurochem. **47**: 145-153.

Pribram, H. and Hernheiser, G. 1920. Zur Kentnnis der adialysblen bestandteile des menschenharnes. Biochem. Z. **111**:30

Prokesova, L., Potuznikova, B., Potempka, J., ZXikan, J., Radl, J., Hachova, L., Baran, K., Porwit-Bobr, Z and John, C. 1992. Immunol. Lett. **31**: 259-266.

Rahman, M.M,. Identification and functional importance of kallikrein in inflammatory joint disease. PhD. University of Bristol. UK, 1994: 69-78.

Rang, H.P. and Urban, L. 1995. New molecules in analgesia. British J. Anaesth. **75**: 145-156.

Rappin, J.P. 1881. Contra l'etude de bacterium de la bouche a l'etat normal. Quoted by Breed, R.S., Murray, E.G.D., Hitchens, A.P., Bergeys manual of determinative bacteriology. 6th ed. Williams and Wilkins Co. Baltimore, p68

Regoli, D. and Barabe, J. 1980. Pharmacology of kinins and related kinins. Pharmacol. Rev. **32**: 1-46.

Regoli, D., Barabe, J. and Park, W.K. 1977. Receptors for bradykinin in the rat aortae. Can. J. Physiol. Pharmacol. **55**: 855-867.

Regoli, D., Marceau, F. and Barabe, J. 1978. *De novo* formation of vascular receptors for kinin. Can. J. Physiol. Pharmacol. **56**: 674-677.

Regoli, D., Marceau, F. and Lavigne, J. 1981. Induction of B1 receptors for kinin in the rabbit by a bacterial lipopolysaccharide. Eur. J. Pharmacol. **71**: 105-115.

Regoli, D., Rhaleb, N.-E., Tousignant, C., Nantel, F., Jukic, D. and Drapeau, G. 1991. New highly potent bradykinin B_2 receptor antagonists. Agents Actions **34**: 138-141.

Revak, S.D., Cochrane, C.G. and Griffin, J.H. 1977. The binding and cleavage characteristics of human Hageman factor during contact activation. A comparison of normal plasma with plasmas deficient in factor XI, prekallikrein or high molecular weight kininogen. J. Clin. Invest. **59**: 1159-1167.

Riddel, R.H. 1991. *Helicobacter pylori*- some what., why, and how morphologic issues. Scand. J. Gastroenterol. **26** (suppl 187): 78-84.

Robert, R.A. and Gulick, W.J. 1989. Bradykinin receptor number and sensitivity to ligand stimulation of mitogenesis by expression of mutant *ras* oncogene. J. Cell Sci. **94**: 527-535.

Rocha e Silva, M., Beraldo, W.T. and Rosenfeld, G. 1949. Bradykinin, a hypotensive and smooth muscle stimulating factor released from plasma globulins by snake venoms and by trypsin. American Journal of Physiology **156**: 261

Rodell, T.C., Naidoo, Y.and Bhoola, K.D. 1995 Role of kinins in inflammatory responses. Prospects for drug therapy. Clin. Immunother. **3**(5): 1995.

Sachs, G., Zeng, N. and Prinz, C. 1997. Physiology of isolated gastric endocrine cells. Ann. Rev. Physiol. **59**: 243-256.

Sakai, T. 1990. Role of tissue kallikrein in chronic gastritis. Nip. Shok. Gabb. Zash. **87** (8) 1653-1661.

Sakai, T., Otsuka, S., Kizuki, K. and Moriya, H. 1997. Significance of kallikrein in chronic atrophic gastritis. Adv. Exp. Med. Biol. **247B**: 657-661.

Sakamoto, W., Satoh, F., Gotoh, K. and Uehara, S. 1987. Ile-Ser-bradykinin (T-kinin) and Met-Ile-Ser-bradykinin are released from T-kininogen by an acid protease of granulomatous tissue in rats. FEBS Lett. 219: 437-440.

Salomon, H. 1896. Ueber das spirillum des saugetiermagens und sen verhalten zu den belegzellen. Zentralbl. Bakteriol. **19**: 422-441.

Salvesen, G., Parkes, C., Abrahamson, M., Grubb, A. and Barret, A.J. 1986. Human low-M_r kininogen contains three copies of a cystatin sequence that are divergent in structure and in inhibitory activity for cysteine proteinases. Biochem. J. **234**: 429-434.

Sambrook, J., Fritsch, E. and Maniatus, T. Molecular cloning. A laboratory manual. Cold Spring Harbor. Cold Spring Harbor Laboratory Press, 1989: 6.3-7.2.

Sato, F. and Nakasawo, S. 1988. Mechanism of kinin release from human low molecular-mass-kininogen by the synergistic action of human plasma kallikrein and leukocyte elastase. Biol. Chem. Hoppe Seyler **369**: 1009-1017.

Sawada, S. and Dickinson, C.J. 1997. The G cell. Annual Rev. Physiol. **59**: 273-298.

Schachter, M., B. Maranda, et al. 1978. Localisation of glandular kallikrein in the coagulating and submandibular glands of the guinea-pig. Journal of Histochemistry and Cytochemistry **26**: 318-321.

Schacter, M. and Thain, E.M. 1954. Chemical and pharmacological properties of the potent, slow-contracting substance (kinin) in wasp venom. British Journal of Pharmacology **9**: 352.

Schacter, M., (1980) "Kallikreins (kininogenases)- a group of serine proteases with bioregulatory actions" Pharmacol. Rev., 31:1.

Schacter, M., Longridge, D.J., Wheeler, G.D., Mehta, J.G., and Uchida, Y. 1986. J. Histochem Cytochem.. **34**: 927-934."

Schacter, M., Peret, M.W., Billing, A.G. and Wheeler, G.D. 1983. Immunolocalisation of the protease kallikrein in the colon. J. Histochem. Cytochem. **31**(11): 1255-1260.

Schapira, M., Scott, C.F. and Colman, R.W. 1982. Contribution of plasma kallikrein protease inhibitors to the inactivation of kallikrein in plasma. J. Clin. Invest. **69**: 465.

Schmaier, A.H., Bradford, H., Silver, L.D., Farber, A., Scott, C.F. and Colman, R.W. 1986. High molecular eight kininogen is an inhibitor of platelet calpain. J. Clin. Invest. **77**: 1565-1573.

Schmaier, A.H., Kou, A., Lundberg, D., Murray, S. and Cines, D.B. 1988 Expression of high molecular weight kininogen on human umbilical vein endothelial cells. J. Biol. Chem. **263**: 16327-16333.

Schmaier, A.H., Smith, P.M., Purdon, A.D., White, J.G. and Colman, R.W. 1986 High molecular weight kininogen. Localisation in the unstimulated and activated platelet and activation by a platelet calpain(s). Blood **67**: 119-130.

Segal, E.D., Shon, J. and Tompkins, L.S. 1992. Characterisation of Helicobacter pylori urease mutants. Infect. Immun. **60**: 1883-1889.

Seidah, N.G., Sawyer, N., Hamelin, J., Mion, P., Beaubien, G., Brachpapa, L., Rochemont, J., Mbikay, M. and Chretien, M. 1990. Mouse plasma kallikrein: CDNA structure,

enzyme characterisation and comparison of protein and mRNA levels among species. DNA Cell Biol. **9**: 737-748.

Shi, S.-R., Key, M.E. and Kalra, K.L. 1991. Antigen retrieval in formalin-fixed, paraffin-embedded tissues: An enhancement method for immunohistochemical staining based on microwave oven heating of tissue sections. Journal of Histochemistry and Cytochemistry **39**(6): 741-748.

Simson, J. A. V. and Condon, J. 1988. Immunocytochemical localisation of a kallikrein-like serine protease (esterase A) in rat salivary glands. Anatomical Record **221**: 475-481.

Skidgel R A. Basic science aspects of angiotensin-converting enzyme and its inhibitors. In: Gwarthmey JK, Briggs G M, Allen P D, eds. Heart failure; basic science and clinical aspects, New York: Marcel Dekker, 1993: 399-427.

Slomiany B L., Murty V L N., Piotrowski J., Slomiany A. Gastroprotective agents in mucosal defence against *Helicobacter pylori*: Gen. Pharmac.: Elsevier Sci. Ltd, 1994.

Slomiany, B.L. and Slomiany, A. 1991. Role of mucus in gastric mucosal protection. J. Physiol. Pharmac. **42**: 147-161.

Smoot, D.T., Mobley, H.L.T., Chippendale, G.R. and Lewison, J.F. 1990. *Helicobacter pylori* urease activity is toxic to human gastric epithelial cells. Infect. Immun. **58**: 1992-1994.

Snider, R.M. and Richelson, E. 1984. Bradykinin receptor mediated cyclic GMP formation in a nerve cell population (murine neuroblastoma, clone NIE 115). J. Neurochem. **43**: 1749-1754.

Sorsa, T., Ingman, T., Suomalainen, K., Haapasalo, M., Konttinen, Y.T., Lindy, O., Saari, H. and Uitto, V.J. 1992. Identification of proteases from periodontopathogenic bacteria as activators of latent human neutrophils and fibroblast type callagenases. Infection and Immunity. **60** (11): 4491-4495.

Stark, R.M., Greenman, J. and Millar, M.R. 1995. Physiology and biochemistry of H*elicobacter pylori*. Br. J. Biomed. Sc. **52**: 282-290.

Steer, H.W. 1975. Ultrastructure of cell migration through the gastric epithelium and its relationship to bacteria. J. Clin. Path. **28**: 639-646.

Steer, H.W. and Collin-Jones, D.G. 1975. Mucosal changes in gastric ulceration and their response to carbenoxolone sodium. Gut **16**: 590-597.

Stevens, A., Lowe, J.S. Alimentary canal. In: Human Histology, 2ed, Barcelona: Mosby,1997.

Stewart, J.M. and Vavrek, R.J. 1987. Bradykinin competitive antagonists: designs and activities. Adv. Biosc. **65**: 73-80.

Stockbruegger, R.W., Cotton, P.B., Eugenides, G.N., Bartholomew, B.A., Hill and M.J., Walters, C.L. (982. Intragastric nitrates, nitrosamines, and bacterial overgrowth during cimetidine treatment " Gut **23**: 1048-1054.

Takada, Y., Skidgel, R.A. and Erdos, E.G. 1985. Purification of human prokallikrein. Identification of the site of activation by the metalloproteinase thermolysin. Biochem J. **232**: 851-858.

Takada, Y., Skidgel, R.A. and Erdos, E.G. 1986. Purification of human urinary prekallikrein. Identification of the site of activation by the metalloproteinase thermolysin. Biochem. J. **232**: 851-858.

Takagaki, Y., Kitamura, N. and Nakanishi, S. 1985. Cloning and sequence analysis of cDNAs for human high molecular weight and low molecular weight kininogen. J. Biol. Chem. **260**: 8601-8609.

Tiffany, C.W. and Burch, R.M. 1989. Bradykinin stimulates tumour necrosis factor and interleukin-1 release from macrophages. FEBS Lett. **247**: 189-192.

Tokamasu, T., Ueno, A. and Oh-ishi, S. 1995. A hypotensive response induced by Des-arg^9-bradykinin in Young/Brown Norway rats pretreated with endotoxin. Uer. J. Pharmacol. **274**; 225-228.

Tompkins D S. Survival and growth of Campylobacter pylori. In: Rathbone B J, Heathley R A, eds. *Campylobacter pylori* and gastrodoudenal disease. Oxford: Blackwell Scientific Publications, 1989:24-30.

Travis, J., Potempa, J. and Maeda, H. 1995. Are bacterial proteinases pathogenic factors? Trends in Microbiology **3**(10): 405-407.

Tricottet, V., Bruneval, P., Vire, O. and Camilleri, J.P. 1986. Campylobacter-like organisms and surface epithelial abnormalities in active, chronic gastritis in humans: an ultrastructural study. Ultrastruc. Pathol. **10**: 113-122.

Uchida, K., Niinobe, M., Kato, H. and Fuji, S. 1980. Purification and properties of rat stomach kallikrein. Biochim. Biophys. Acta **614**: 501-501.

Uetsuji, S., Yamamura, M., Yamamoto, M., Uchida, K., Kushiro, H., Kodama, J. and Fujii, S. 1982. Agents Actions, suppl 9: 137-141.

Uitto, V.-J., Larjava, H., Heino, J. and Sorsa, T. 1989. A protease of *Bacteroides gingivaslis*degrades cell surface and matrix glycoproteins of cultured gingival fibroblasts and induces secretion of collagenase and plasminogen activator. Infect. Immunol. **57**: 213-218.

Underwood J C E. Alimentary system. In: General Systemic Pathology, 2ed,New York: Churchill Livingstone, , 1996: 410-422.

Van der Graaf, F., Tans, G., Bouma, B.M. and Griffin, J.H. 1982. Isolation and functional properties of the heavy and light chains of human plasma kallikrein. J. Biol. Chem. **257**: 14300-14305.

Van Deuren, M., Dofferhoff, A.S.M. and Van Der Meer, J.W.M. 1992. Cytokines and the response to infections. J. Pathol. **168**: 349-356.

Vizir, A.D and Kraidashenko, O.V. 1981. Blood kinins in diseases of the abdominal organs. Vestn-Khir. **127** (8): 33-35.

Vogel, R., Assfalg-Machleidt, I., Esterl, A., Machleidt, W. and Muller-Esterl, W. 1988. Proteinase-sensitive regions in the heavy chain of low molecular kininogen map to the inter domain junctions. J. Biol. Chem. **263**: 12661-12668.

Voller, A., Bartlett, A. and Bidwell, D.E. 1978. Enzyme immunoassays with special reference to ELISA techniques. Journal of Clinical Pathology. **31**: 507-520.

Wallace, J.L. 1991. Possible mechanisms and mediators of gastritis associated with *Helicobacter pylori* infection. Scand. J. Gastroenterol. **26** (suppl. 187): 65-70.

Ward P E, Metabolism of bradykinin and bradykinin analogues In: Burch R M, ed. Bradykinin Antagonists: Basic and Clinical Applications. New York: Marcel Dekker Publishing Corp, 1991: 147.

Wenzel H R, Beckman J, Mehlich A, Schnabel E, Tschesche H. Semisynthetic conversion of the bovine trypsin inhibitor (kunitz) into an efficient leukocyte-elastase inhibitor by

specific valine for lysine substitution in the reactive site. In: Woelter W, Bayer E, Ovchinnikov Y A, Ivanov V T, eds. Chemistry of Peptides and proteins. Berlin : Walter de Gruyter and Co., 1986: vol 3.

Werle, E. 1934. Über die anaktivierung des kallikreins. Biochem. Z. **273**: 291.

Werle, E. 1936. Über kallikreinaus blut. Biochem. Z. **287**:235.

Werle, E. and Berek, U. 1948. Zur kenntnis des kallikreins. Angew Chem. **60A**: 53.

Werle, E., Gõtze, W. and Keppler, E. 1937. Über die wirkung des kallikreins auf den isolierten darm und über eine neue darmkontrahierende substanz. Biochem. Z. **289**: 217.

Woodbury, R.G., Gruzenski, G.M. and Lagunoff, G. 1978. Immunofluorescent localisation of a serine protease in rat small intestine. Proc. Natl. Acad. Sci. USA. **75**: 2785.

Worthy, K., Figueroa, C.D., Dieppe, P.A. and Bhoola, K.D. 1990. Kallikreins and kinins: mediators in inflammatory joint disease. Int. J. Exp. Path. **71**: 587-601.

Xiang, Z., Bugnoli, M., Ponzetto, A. 1993. Detection in an enzyme immunoassay of an immune response to a recombinant fragment of the 128-kilodalton protein (CagA) of *Helicobacter pylori*. Eur. J. Clin. Microbiol. Infect. Dis. **12**: 739-745.

Xu, J.-K., Goodwin, C.S., Cooper, M. and Robinson, J. 1990. Intracellular vacuolisation caused by the urease of *Helicobacter pylori*. J. Clin. Pathol. **161**: 1302-1304.

Yamada, K. and Erdos, E.G. 1982. The Renal- Kinin system. Kidney International. **22**: 331-337.

APPENDICES

APPENDIX 1

PATIENT CONSENT FORMS

INFORMATION TO PATIENTS

Introduction

We would like you to take part in a dyspepsia research study. You can also ask any question at any time. If you decide you do not want to take part, this will make no difference whatsoever to the quality of the treatment you will receive. If, however, you do decide to take part, then we will ask you to do everything you can to follow all the instructions given to you.

Clinical Investigation

From your symptoms and the clinical examination it seems that there is inflammation of the mucosal lining of your stomach. To confirm this impression I will pass a flexible tube into your stomach. This procedure is called endoscopy, and it will allow me to examine the lining of your stomach and duodenum. Furthermore, I will take biopsies. The purpose of the biopsy is to test whether you have an infection in your stomach which is caused by a particular bacterium called *Helicobacter pylori.* The infection causes histological changes produced by substances called kinins that are responsible for the pain and dyspepsia. This knowledge may help us to propose a new type of treatment for inflammation of the stomach mucosa.

You are free to refuse to have an endoscopic examination, and your refusal will in no way affect my care for you as a patient.

PATIENT CONSENT FORM

Study Title : Are kinins implicated in dyspepsia?

City : Durban, South Africa

I,(Name).....,
hereby consent to the following Procedure and/ or Treatment being conducted on myself or the person indicated in below:

I acknowledge that I have been informed by:

(Name).....,
concerning the possible advantages and possible adverse effects which may result from the above-mentioned procedure and/or treatment and of the ways in which it is different from the conventional procedure and/ or treatment.

I,. (Name).....,
hereby acknowledge that I understand and accept the "Information to Patients" leaflet handed to me in connection with this trial.

3 **I agree that the above procedure and/or treatment will be carried out and/or supervised by**
(Name),.....

4 **I acknowledge that I understand the contents of this form, including the information provided in the "Information to Patients" leaflet and as the subject**
freely consent to the above procedure and/or treatment being conducted on me

5 **I am aware that I may withdraw my consent at any time without prejudice to further care.**

Signed: _____ Date:
Subject

Signed: _____ Date:
Witness

Signed: _____ Date:
Researcher

APPENDIX 2

PATIENT DATA FORMS

PATIENT DATA FORM

Title- ***Are kinins implicated in dyspepsia*** ?

NUMBER: Date- Time-

Name Age Male/female Ethnic group

Address

Home Telephone Work Telephone

Referring Practitioner: Dr

Symptoms:

Smoking- Y/N Alcohol Y/N occasional/moderate

Pain- burning Y/N cramps Y/N duration

Nausea Y/N Vomiting- Y/N Haematensis- Y/N

Abdominal distension- Y/N Bloating- Y/N

Constipation- Y/N Diarrhoea- Y/N Dysphagia- Y/N

Past History:

Peptic Ulcer- Y/N Abdominal surgery- Y/N

Clinical Examination:

Blood pressure- diabetes- Y/N

Medication:

Previous-

Current-

INVESTIGATION:

Endoscopy-

Hernia- H/N Oesophagitis- 1 2 3 4

Gastritis- local/general Erosions- Y/N

Ulcer- duodenal Y/N Gastric Y/N Other pathology-

CONCLUSIONS

Normal *Gastritis (Hp+ Hp-)* *Ulcers (Hp+ Hp-)*

BUFFERS

AND

REAGENTS

1. Reagents for Sample Collection, Processing, Dissection, Embedding Storage and Histological staining

- Sterile normal saline (physiological saline) (0.9% NaCl, pH 7, Sabax)
- 5% formal saline (41% formaldehyde / 0.9% NaCl, 1:8 v/v)
- Absolute ethanol (99% ethanol, analytical grade; Saarchem, SA)
- Xylene (analytical grade; Saarchem, SA)
- Mayer's Haematoxylin (Sigma, St. Louis)
- Eosin (Sigma, St. Louis)
- Poly-L-lysine (Sigma, St. Louis) - dilute 1:10 in distilled water in plastic-ware and store at 4°C for 3 months
- TK cocktail 40 mM Tris-Cl, pH 8 - dissolve 4.8 g Trizma base (Sigma, St. Louis) in 800 ml distilled water, adjust pH to 8.0 with HCl and adjust volume to 1 l.
- Giemsa Stain (Sigma, St. Louis)
- Acetic acid (analytical grade; Saarchem, SA)

2 Reagents for Isolation of IgG from serum

- Diethylaminoethyl sephadex (DEAE A-25, Sigma, St. Louis) - 50 ml wet settled volume.
- 14% Sodium sulphate - dissolve 0.14 g anhydrous Na_2SO_4 (analytical grade; Saarchem, SA) in 1 ml serum
- 0.07 M Sodium phosphate pH 6.3 - dissolve 54.6 g NaH_2PO_4 (analytical grade; Saarchem, SA) in 5 l distilled water

3 Reagents for Enzymic assay (Amidolytic microassay)

- Amidase buffer (0.2 M Tris-HCl, pH 8.2) - dissolve 24.22 g Trizma base (Sigma, St. Louis) in 800 ml distilled water, adjust pH to 8.0 with HCl and adjust volume to 1 l.

- Assay buffer - dissolve 300 ug SBTI (Sigma, St. Louis) and 375 mg EDTA (Saarchem) in 1 ml amidase buffer.
- 1.5 mM S2266 Solution - dissolve 25 mg S2266 (Chromogenix, Sweden) in 28 ml distilled water
- SBTI/Bacitracin - dissolve 1.47 g SBTI (Sigma, St. Louis; 2720units/mg) and 40 mg Bacitracin (Sigma, St. Louis) in 1 ml Amidase buffer

4 Reagents and Immunochemicals for TK ELISA

- Coating buffer ($Na_2CO_3/NaHCO_3$, pH 9.6) - dissolve 1.59 g Na_2CO_3 and 2.93 g $NaHCO_3$ in 1 l distilled water
- Substrate buffer (5 mM $MgCl_2$/10% Diethanolamine, pH 9.8) - dissolve 0.10163 g $MgCl_2$ in 80 ml distilled water, add 10 ml Diethanolamine (Sigma, St. Louis), adjust pH to 9.8 with HCl and make up to 100 ml with distilled water
- 0.01M PBS, pH 7.2 - dissolve 1 PBS tablet (Sigma, St. Louis) in 200 ml distilled water
- 5% Milk protein blocker - dissolve 5g Country Pasteur fat free milk powder (Nutritional Foods, SA) in 100 ml PBS. Make fresh.
- 0.01M PBS/ 0.5%Tween - dilute 100 ul Tween 20 (Sigma, St. Louis) in 200 ml 0.01M PBS
- Human Urinary Kallikrein (HUK, Calbiochem, USA) - dissolve 1 mg HUK in 833 ml physiological saline. Store 200 ul aliquots at -20°C
- Goat anti-human TK IgG (30 ng/ml)
- Rabbit anti-human TK IgG (25 ng/ml)
- Anti-rabbit IgG alkaline phosphatase (Sigma, St. Louis)
- Disodium paranitrophenyl phosphate substrate (pNPP, 5 mg tablets, Sigma, St. Louis) - dissolve 1 tablet in 5 ml substrate buffer. Make fresh and use within 90 min.